



18th European Conference on Solid State Chemistry

Book of Abstracts
Programme
List of Participant
Author Index

Editor: Tomáš Wágner



University
of Pardubice
Faculty
of Chemical Technology

July 9–12, 2023 | Prague | CR

ORGANIZED BY



IN COOPERATION WITH



SUPPORTED BY





18th European Conference on Solid State Chemistry

Editor: **Tomáš Wágner**

Book of Abstracts
Programme
List of Participants
Author Index



University
of Pardubice
Faculty
of Chemical Technology

July 9–12, 2023 | Prague | CR

Edited by: Tomáš Wágner

Published by University of Pardubice, Studentska 95, 532 10 Pardubice, Czech Republic

Copyright © 2023 by University of Pardubice

Cover Design © 2023 by Dana Husníková

Typo © 2023 by Dana Husníková

Redaction © 2023 by Darina Bouzková

ISBN 978-80-7560-466-8

International Advisory Board

Antoine Maignan (*Lab. CRISMAT, Caen, France*) Chair
Sylvie Begin-Collin (*University of Strasbourg, France*)
Evgeny V. Antipov (*Moscow State Univ. Russia*)
José M. Gonzales-Calbet (*University Complutense, Madrid, Spain*)
Helmer Fjellvag (*University of Oslo, Norway*)
Sven Lidin (*University of Lund, Sweden*)
Jürg Hulliger (*University of Bern, Switzerland*)
Matthew Rosseinsky (*University of Liverpool, UK*)
Tony West (*University of Sheffield, UK*)
Barbara Albert (*TU Darmstadt, Germany*)
Wolfgang Schnick (*LMU Muenchen, Germany*)
Stafvan Tendeloo (*University of Antwerp, Belgium*)
Tomas Wagner (*University of Pardubice, Czech Republic*)

EuChemS Solid State Chemistry Division delegates

Hubert Huppertz (*Innsbruck, Austria*)
Tomas Wagner (*Pardubice, Czech Republic*)
Antoine Maignan (*Caen, France*)
Olivier Mentré (*Lille, France*)
Claus Feldmann (*Karlsruhe, Germany*)
Klaus Müller-Buschbaum (*Stuttgart, Germany*)
Miklós Zrinyi (*Budapest, Hungary*)
Meital Reches (*Jerusalem, Israel*)
Salvatore Coluccia (*Torino, Italy*)
Filipe Alexandre Almeida Paz (*Aviero, Portugal*)
Andrei Shevelkov (*Moscow, Russia*)
Milan Drabik (*Dubravská, Slovakia*)
Mirela Dragomir (*Ljubljana, Slovenia*)
Flaviano Garcia-Alvarado (*Madrid, Spain*)
Sven Lidin (*Lund, Sweden*)
Greta Patzke (*Zurich, Switzerland*)
John Paul Attfield (*Edinburgh, United Kingdom*)

Organising Committee

Barbara Albert – **chair** (*Technical University Darmstadt*)
Tomas Wagner – **organizer** (*University of Pardubice*)
David Sedmidubský – **co-organizer** (*University of Chemistry and Technology, Prague*)
M. Vlček, B. Frumarová, M. Krbal, J. Orava, L. Střížík, M. Fraenkl, V. Prokop, T. Netolický,
R. Přiklopilová, D. Bouzková, L. Sedláčková, V. Wágnerová

Contents

Contents	4
Preface	15
General Information	16
Part I	
PROGRAMME	
Programme	21
Part II	
PLENARY LECTURES	
Metal-organic frameworks for sustainable separations and reactions: A computational perspective	
J. Jiang	36
Solid-state batteries – at the edge between Solid State Chemistry and Materials Science	
J. Janek	37
Fast cation conductivity in complex metal halides & hydrides; Prospects for solid state electrolytes	
D. H. Gregory	38
Phase change optical memory materials: Why are alloys of Ge, Sb, and Te almost the only materials of choice?	
R. O. Jones	39
New possibilities <i>in situ</i> and <i>ex situ</i> crystal structure determination based upon 3D ED	
R. Poppe, D. Vandemeulebroucke, M. Quintelier, A. Hazijadeh, S. Rahimi, S. Gholam, M. Batuk, J. Hadermann	40
Exploring new transition metal nitride materials	
A. Fuytes	41
Part III	
INVITED LECTURES	
Designer’s metal-organic materials and interfaces through ALD/MLD	
M. Karppinen	44
Exploring model catalysts through the integration of in-situ near-ambient pressure XPS and STM	
P. Matvija, M. Vorokhta, F. Pehálek, S. Oveysipoor, L. Piliai, T.N. Dinhová, B. Šmíd, I. Matolínová	45
Prediction of electrical conductivity of porous composites using 3D equivalent electronic circuit network model. Solid oxides fuel cell electrode case study	
D. Budáč, V. Miloš, M. Carda, M. Paidar, K. Bouzek	46

Synthesis-dependent structure-property relationships of quantum materials

L. Clark, J. N. Graham, J. R. Stewart, J. A. Cooley, M. Songvilay, G. Confalonieri, D. Fortes,
P. Manuel, A. R. Wildes 47

Probing fuel cell catalysts degradation under simulated operational environment by advanced in situ techniques

I. Khalakhan 48

Discovery of quantum materials by combining chemical and physical design principles

F. O. von Rohr 49

Chalcogenide glasses and fibers for photonic applications in the infrared

J.-L. Adam, J. Trolès, C. Boussard-Plédel, X.H. Zhang 50

Polymorphism and magnetic properties in high pressure A-site manganites

E. Solana-Madruga 51

In-situ characterization of gas-solid interfaces by near-ambient pressure X-ray photoelectron spectroscopy

M. Vorokhta, L. Piliai, T.N. Dinhová, P. Matvija, I. Matolinová 52

Bias-free graphene-based in situ TEM observation of electrode materials for batteries

J. Y. Cheong, J. H. Chang 53

Investigating the catalytic potential of iron-doped calcium titanate: a study of oxide vacancy structures and microstructures

M. Amano Patino, M. Ibrahim, N. Frederich, H. Kaper, M. Ceretti, W. Paulus 54

Compositionally complex alloys for the hydrogen society

M. Sahlberg 55

Mineral-inspired sulphides for thermoelectric energy harvesting

A.V. Powell 56

Reaction mechanisms in molten salts for the design of solid-state materials at the nanoscale

D. Portehault, F. Igoa Saldaña, E. de Rolland Dalon, M. Baron, A. Ghoridi, A. Séné, E. Defoy,
Y. Song, P.-O. Autran, D. Thiaudière 57

Nanostructured thin-film catalysts for hydrogen production via PEM water electrolysis

P. Kůš, T. Hrbek, H. Nedumkulam, M. Mirolo, I. Martens, J. Drnec, I. Matolinová 58

Part IV**LECTURES****Negative linear compressibility of the hybrid perovskite $[\text{C}(\text{NH}_2)_3]\text{Er}(\text{HCO}_2)_2(\text{C}_2\text{O}_4)$**

T. J. Hitchings, A. B. Cairns, D. Allen, P. J. Saines 60

Complex modulations of the crystal structure of functional oxides with perovskite-related structure

S. García-Martín, R. Marín-Gamero, E. Urones-Garrote, X. Martínez de Irujo-Labalde 61

Perovskite-type RbNbO_3 as a high-pressure polymorphism

A. Yamamoto, K. Murase, K. Sugiyama, T. Kawamata 62

Chemical and physical pressure effects on structural and magnetic properties of R_2CuTiO_6 perovskite series with R ranging from La to Lu

L. Sederholm, A. Yamamoto, M. Karpinen 63

Critical current density of $\text{Li}_6\text{PS}_5\text{Cl}$ powder pellets and processed films

A. Tron, A. Beutl 64

Quantum spin liquids in cation ordered perovskites	
M. J. Milton, P. Manuel, J. P. Attfield	65
Lithium transport mechanisms characterised by ssNMR and ToF-SIMS in hybrid electrolytes for solid-state batteries	
T. Meyer, T. Gutel, M. Bardet, H. Manzanarez, E. De Vito	66
Packings of sphere packings - a new path to solid state ionic conductors?	
M. Petrik, W. Hornfeck	67
Growth of metal oxide film electrodes for electrochemical capacitor by electrospray deposition	
M. P. Chavhan	68
New tungsten bronzes via electrochemical intercalation	
B. Rasche, I. Neumann, Y. Chen, M. Yang	69
Composition-activity-stability relationship in Pt-Au alloys for oxygen reduction reaction	
X. X. Xie, V. Briega-Martos, R. Farris, M. Vorokhta, T. Skála, I. Matolínová, K. M. Neyman, S. Cherevko, I. Khalakhan	70
Metal-insulator transitions in hollandite vanadate and chromate	
M. Isobe, P. Puphal, H. Takagi	71
Fluoridoargentates(II) as potential analogues to superconducting cuprates	
M. Dragomir, M. Belak Vivod, M. Lozinšek, Z. Jagličić, G. King	72
FeMn₃Ge₂Sn₇O₁₆: a “partial” spin-liquid candidate with a perfectly isotropic 2-D Kagomé Lattice	
C. D. Ling, M. C. Allison, S. Wurmehl, B. Büchner, J. L. Vella, T. Söhnel, S. A. Bräuninger, H.-H. Klauss	73
Hidden orders in 2D van der Waals materials: The example of magnetic crossover in the mixed-anion compound CrSBr	
S. A. López-Paz, Z. Guguchia, V. Y. Pomjakushin, C. Witteveen, A. Cervellino, H. Luetkens, N. Casati, A. F. Morpurgo, F. O. von Rohr	74
Solid-state synthesis of carbon-coated lithium vanadate Li₃VO₄- as anodes for High-Performance Li-ion Capacitors	
S. Lonkar, C. Busa	75
Elucidating catalytic performance of a family of low-valent metal nitrides for the hydrogen evolution reaction from water	
A. Y. Ganin, Y. Sun, O. Guseynikova, Y. Zhou, N. López	76
Understanding the performance of high-power niobium oxide based Li ion battery materials	
A. Green, E. Driscoll, P. Slater	77
Supraparticles as identifiers or temperature indicators with spectral magnetic readout	
S. Müssig, J. Reichstein, S. Wintzheimer, K. Mandel	78
Crystal and electronic structure of the lanthanide dibismuthides REBi₂ (RE = La, Ce, Pr, Nd, Sm)	
A. Ovchinnikov, M. Ruck	79
New nickel-based lithium rich layered/disordered rock salt cathode materials for lithium-ion batteries	
B. Dong, J. Castells-Gil, P. Zhu, L. Driscoll, P. Allan, E. Kendrick, P. Slater	80
Operando investigation of Ir-Ru-based catalyst for Proton Exchange Membrane Water Electrolysis	
T. Hrbek, P. Kůš, M. G. Rodriguez, H. Nedumkulam, M. Mirolo, J. Drnec, V. Matolín, I. Matolínová ...	81

The influence of Al and Ga doping on the chemical and electrochemical cycling of T-LiFeO₂ S. Mahato, X. M. De Irujo Labalde, S. Booth, M. Hayward	82
Designing new lithium layered oxides from sodium layered oxides to stabilize oxygen redox M. Guignard, V. Saïbi, L. Castro, I. Sugiyama, C. Delmas	83
Sodium insertion into TiO₂ hollandite: structural and electrochemical study F. García-Alvarado, A. Duarte, P. Díaz-Carrasco, A. Kuhn, A. Basa	84
Structural evolution of layered H₂V₃O₈ high-capacity cathode material for lithium-ion batteries during lithium intercalation A. Kuhn, J. C. Pérez-Flores, M. Hoelzel, V. Díez-Gómez, I. Sobrados, J. Sanz, F. García-Alvarado	85
Evidence for a disorder-induced spin liquid in the tuneable spin ladder-chain system Ba₂CuTe_{1-x}W_xO₆ (0 ≤ x ≤ 0.3) O. Mustonen, C. Pughe, A. Gibbs, A. Yaresko, P. Baker, L. Mangin-Thro, H. C. Walker, E. J. Cussen	86
Structural variations of the magnetic topological insulators Mn_{1+x}Sb_{2-2x/3}Te₄ E. Kochetkova, O. Renier, A. Isaeva, M. Sahoo, L.T. Corredor	87
2D-Metals with locked charge density wave, in the novel layered monophosphate tungsten bronzes [Ba(PO₄)₂]WmO₃m³ H. Nimoh, R. Glaum, A. Cano, A. M. Arévalo-López, O. Mentré	88
Experimental investigation of magnetic dilution effect on the frustrated quantum antiferromagnet SrCu₂(BO₃)₂ L. Šibav, G. King, Z. Jagličić, M. Koblar, M. Otoničar, D. Arčon, M. Dragomir	89
Magnetic structures of Dirac nodal-line semimetals LnSbTe I. Plokhikh	90
Light-induced surface microstructures on Ge-As-S glasses E. Samsonova, P. Kutálek, E. Černošková, P. Knotek, J. Schwarz	91
Locking any magnetization by freezing of magnetic domains in a transient soft to super-hard magnet O. Mentré, B. Leclercq, A. Pautrat, A. M. Arevalo-Lopez, S. petit, V. Stolyarov	92
Er³⁺-doped TeO₂-ZnO-La₂O₃ optical glasses J. Suský, S. Šlang, L. Beneš, B. Frumarová, R. Svoboda, T. Wágner, L. Stržik	93
Structural analyses and properties of complex sulphides in the Cr-Sn-S system F. Guiot, V. Dorcet, E. Guilmeau, B. Malaman, T. Schweitzer, P. Lemoine, C. Prestipino	94
Holmium-doped TeO₂-ZnO-La₂O₃ tellurite glasses for photonics applications and fibre optics J. Hrabovsky, F. Desevedavy, L. Strizik, J. Oswald, L. Nowak, T. Wagner, F. Smektala, M. Veis	95
Gold(I)-thiolate coordination polymers as transparent glasses and cyclic phase-changing materials S. Vaidya, O. Veselska, Z. Fan, A. Zhadan, A. Fateeva, P. Bordet, S. Horike, A. Demessence	96
Tuning the metallic glasses properties via ultrafast heating/cooling J. Orava, Y. H. Sun, I. Kaban	97
Cation ordered doping of ferrite perovskites: influence on redox behavior, magnetism, and mixed ionic electronic conductivity A. J. Brown, O. Wagstaff, A. Manjón-Sanz, H. Brand, M. Avdeev, I. Evans, C. D. Ling	98

Understanding the texture degree on zinc aluminate Nd, Ce sub-micrometer films by screen printing for NIR emitting applications	
R. E. Rojas-Hernandez, F. Rubio-Marcos, J. F. Fernandez, I. Hussainova.....	99
Many body localisation in $\text{CeMnAsO}_{1-x}\text{Fx}$?	
A. C. McLaughlin, G. Lawrence, S. Simpson, E. J. Wildman	100
V-V dimerization in MnVO_3 ilmenite low-pressure polymorph: Crystal and magnetic structures and properties	
A. M. Arévalo-López, D. Khalyavin, O. Mentré	101
Multifunctional coordination polymers for fluorescent sensing of VOCs and hazardous ions from contaminated water	
K. A. Siddiqui	102
Structural investigation of new Li ion containing oxides using combined diffraction and NMR and EXAFS spectroscopy	
F. N. Sayed, Q. Jacquet, P. Groszewicz, S. P. Emge, P. C. M. M. Magusin, C. O'Keefe, S. Dey, C. Kocer, A. Morris, C. P. Grey	103
Theoretical insights into the monolayer adsorption and characterization of HB238 merocyanine on $\text{Ag}(100)$ surface	
R. Tomar, A. Kny, M. Sokolowski, T. Bredow	104
Understanding the synthetic reliability of NaxMnO_2 and similar layered phases	
J. Beecham-Lonsdale, D. C. Arnold, S. Ramos-Perez	105
X-ray photoelectron spectroscopy: a key tool for assessment of 2D molybdenum dichalcogenides synthesized by ALD	
J. Rodriguez-Pereira, R. Zazpe, J. Charvot, F. Bures, J.M. Macak	106
Charge density refinement on inorganic crystals using electron diffraction	
E. Yörük, A. Suresh, P. Brázda, M. K. Cabaj L. Palatinus	107
Chemistry at the nanoscale: AFM meets IR spectroscopy	
J. Horák	108
CeScSi-type intermetallics: Modulation of magnetic properties through light elements insertion and catalysis of ammonia	
E. Gaudin, K. Alabd, C. Croisé, F. Can, X. Courtois, N. Bion, A. Villesuzanne, S. Tencé	109
Analysis of ground particle behavior in wet ball milling by DEM-CFD simulation	
K. Kushimoto, J. Kano	110
Optomagnetic composites by combination of strong magnetic and luminescent components	
K. Müller-Buschbaum, M. Seuffert, T. Wehner1	111
Exploring structure-property correlations in the frustrated layered material, $\text{Mn}_2\text{Mo}_3\text{O}_8$	
D. C. Arnold, H. L. McPhillips, S. Ramos	112
Developments in high-pressure growth of rare earth nickelates single crystals	
D. J. Gawryluk	113
Tuning physicochemical properties in $\text{TbMgNi}_{4-x}\text{Cox}(\text{H,D})_2$ system	
V. Shtender	114
Magnetic properties controlled by short-range structural and spin order in layered materials	
J. D. Bocarsly, S. E. Dutton, C. P. Grey	115

Crystal growth of new uranium and transuranic phases via high temperature solution and mild hydrothermal methods: Exploration of new materials as potential nuclear waste forms	
H.-C. zur Loye, T. K. Deason, A. T. Hines, H. Tisdale, T. M. Besmann, J. Amoroso, D. P. DiPrete	116
<i>In-situ</i> XRD and PDF investigation of battery fluoride materials MF_{3,3}H₂O (M = Fe, Cr) in controlled atmosphere: accessing new phases with controlled chemistry	
G. Nénert, L. Ding, K. Forsberg, C. V. Colin	117
A facile preparation of Y₂O₂S nanoparticles through sulfidation under a CS₂ atmosphere	
Y. Kanazawa, M. Matsubara, R. Ohsuga, A. Muramatsu, K. Domen, K. Kanie	118
Mechanochemical process to prepare amorphous oxides precursor with isomorphous substitution of Si(IV) by heteroatoms and successive hydrothermal synthesis to crystallize zeolites	
A. Muramatsu, H. Kobayashi, G. Tanaka, M. Yabushita, R. Osuga, K. Ninomiya, M. Matsubara, S. Maki, M. Nishibori, K. Kanie	119
Alkali shuffling in honeycomb layered oxides	
E. Mumba-Mpanga, R. Berthelot	120
Inorganic materials synthesis in ultra-alkaline hydroflux	
H. He, Y. Li, R. Albrecht, M. Ruck	121
Anion redox as a means to derive layered manganese oxychalcogenides with exotic intergrowth structures	
S. Giri, S. Sasaki, S. Cassidy, S. Dey, G. Cibir, C. Grey, S. Clarke	122
Quadrature frequency resolved spectroscopy on green upconversion photoluminescence in GeGa(As)S:Er³⁺ chalcogenide glasses	
L. Strizik, T. Aoki, V. Prokop, J. Hrabovsky, T. Wagner	123
TESCAN's Analytical Solutions for Lithium-Ion Battery Research	
J. Honč, T. Šamořil, J. Dluhoř, T. Sui, X. Yao	124
Local structure and high-performance catalysts	
X. Xing, Q. Li	125
Defect engineering: Eu³⁺ emission enhancement via induced local distortion	
S. C. S. Lemos, M. Assis, L. Gracia, L. K. Ribeiro, A. F. Gouveia, Y. G. Galvão, E. Cordoncillo, R. C. Lima, E. Longo, J. Andrés	126
Urinary oxidative stress sensor based on zinc oxide nanorods	
A. Ejaz, D. Gibson, C. Garcia Nuñez	127
Tecto-borosulfates—syntheses, structures, and properties	
E. Turgunbajew, P. Netzsch, M. Hämmer, G. Buchner, H. A. Höppe	128
Crystal structures of new phosphidosilicates and its homologues	
D. Johrendt, A. Haffner, V. Weippert, J. Aicher, K. Witthaut	129
Exploring trirutile materials as a platform for energy storage	
E. Djafri, D. Arnold, O. Mentré	130
Understanding the formation mechanism of intermetallic nanoparticles in polyol processes	
M. Smuda, J. Ströh, N. Pienack, A. Khadiev, H. Terraschke, M. Ruck, T. Doert	131
Structural trends and ion diffusion mechanisms in the postspinel-type NaFe_{1-x}Ru_{1-x}O₄ system	
L. Benincasa, M. Duttine, M. Suchomel, M. Guignard	132
Base-metal nanoparticles as reactants at room temperature	
C. Feldmann	133

Functionalization of chalcogenide IR photonic sensor by polymer membrane for the purpose of detecting aromatic hydrocarbon pollutants in water	
M. Vrazel, R. K. Ismail, M. Baillieul, P. Nemeec, P. Loulergue, A. Szymczyk, K. Boukerma, R. Courson, A. Hammouti, L. Bodiou, J. Charrier, T. Halenkovic, M. Bouska, V. Nazabal	134
Soft chemistry of layered titanium and vanadium oxytellurides	
N. D. Kelly, S. J. Clarke	135
Thermal transformations and cation redistribution on $A_2B_2O_6$ oxides	
K. Ji, E. Solana-Madruga, M. A. Patino, Y. Shimakawa, J. P. Attfield	136
Photoluminescence properties of nanocrystalline multicomponent garnet $Gd_3Sc_xGa_{5-x}O_{12}$ doped with Er^{3+}	
T. Netolicky, L. Benes, S. Slang, B. Frumarova, J. Oswald, T. Wagner	137
Borosulfates – silicate analogue anions with the potential to stabilize polycations	
J. Bruns	138
Characterisation of Rh^{4+} oxides, an unusual case of pyrochlore stabilisation under high pressure, high temperature synthesis conditions	
S. D. Injac, B. Mullens, F. Denis Romero, M. Avdeev, C. Barnett, A. K. L. Yuen, B. J. Kennedy, Y. Shimakawa	139
Alkali metal oxide mercurides with isolated mercuride anions	
L. Nusser, S. Feldl, C. Hoch	140
Synthesis and characterization of a novel oxychloride, $SrTe_2FeO_6Cl$	
J. A. Sannes, B. Gonano, Ø. S. Fjellvåg, S. Kumar, O. Nilsen, M. Valldor	141
The absence of expected paramagnetic behavior in $Ba_6Fe_2Te_3S_7$	
E. H. Frøen, P. Adler, M. Valldor	142
Oxides as Pt catchment materials in the ammonia oxidation process - methodology and mechanistic insight	
J. Hessevik, A. S. Fjellvåg, O. Iveland, C. S. Carlsen, H. Sønsteby, T. By, J. Skjelstad, D. Waller, H. Fjellvåg, A. O. Sjøstad	143
Probing for dynamics in a strongly frustrated magnet	
L. Kubíčková, A. K. Weber, M. Panthöfer, A. Möller	144
Chemical pressure driving phase transition and morphology in Eu^{3+}-doped KY_3F_{10}: An experimental and theoretical insight	
P. Serna-Gallén, S. C. S. Lemos, L. Gracia, E. O. Gomes, H. Beltrán-Mir, E. Cordoncillo, J. Andrés ...	145

Part V

POSTERS

Nitridooxorhenate and -technetate anions $[MO_3N]_2^-$ (M = Tc, Re) from reactions in highly alkaline media	
D. Badea, E. Strub, J. Bruns	148
Ternary Alkali metal Thallides ATl (A = K/Rb, Cs/Rb)	
V. F. Schwinghammer, S. Gärtner	149
Solution combustion synthesis of thermodynamically metastable oxide-phosphates with rutile- and anatase-related structures	
S. Früchtnicht, M. Weber, R. Glaum	150

Ferroelectric Properties on $\text{Ba}_{0.975}\text{Ln}_{0.017}(\text{Zr}_x\text{Ti}_{0.95-x})\text{Sn}_{0.05}\text{O}_3$ Materials	
K. Taibi, S. Zemouri-Smail, A. Lahmar	151
Electrocrystallisation of Ternary Amalgams	
D. Kraut, C. Hoch	152
Cs_2O as a strong oxidiser - A new synthetic route towards oxometalates	
I. Zaytseva, C. Hoch	153
Novel representatives of the structure type $\text{Na}_7\text{RbT}_{14}$ with the lighter homologue Indium	
M. Janesch, S. Gärtner	154
High-pressure Synthesis of Alkaline Metal Niobates with Tetragonal Tungsten Bronze-type Structure	
K. Murase, T. Sato, A. Yamamoto, K. Sugiyama	155
Anion Redox in Lithium Main-group Metal Oxides	
Z. Chen, S. Mahato, X. M. De Irujo Labalde, M. Hayward	156
Synthesis and characterisation of lanthanum zirconate as a candidate filler material for polymer derived ceramic coatings	
P. N. Moghaddam, M. Parchovianský, I. Parchovianská, A. Pakseresht	157
Investigation of structure and luminescence properties of bismuth-based coordination polymers with N-donor ligands	
K. V. Borysova, J. R. Sorg, E. A. Mikhalyova, K. Müller-Buschbaum	158
Tin-Boroxines-Based Inorganic-Organic Macrocycles: Synthesis, Characterization and Hydrophobicity	
M. Novák, M. Bouška, Š. Podzimek, R. Jambor	159
High-Pressure Synthesis of SmSi_3	
T. Neziraj, S. Wirth, Y. Grin, U. Schwarz	160
Mixed-metal monophosphate tungsten bronzes containing divalent transition metal ions (MII: Fe, Co, Ni) and tungsten(VI)	
L. K. Aymans, R. Glaum	161
Amino acid crystals as high-performance, eco-friendly structural health monitors	
K. Hari, S. Bhattacharya, S. Guerin	162
High temperature magnetic ordering in new quadruple perovskites $\text{Sr}_4\text{NaM}_3\text{O}_{12}$ (M = Ru and Os)	
G. S. Thakur, T. Doert, T. Hansen, E. Osmic, W. Schnelle, T. Herrmannsdörfer, M. Ruck	163
Effect of concentration of conductive polymers in zinc-pigmented epoxy-ester based anticorrosive coatings	
Y. Raycha, M. Kohl, A. Kalendová	164
Oligothiophene Dendron-Modified CdS Nanoparticles and Their Optical Properties	
A. Yoshida, R. Nozawa, Y. Sakagami, M. Matsubara, A. Mori, A. Muramatsu, K. Kanie	165
Synthesis and characterization of glass and crystalline compositions in the $(\text{Na}_2\text{Se})_x(\text{As}_2\text{Se}_3)_{1-x}$ chalcogenide system	
A. Sammoury, M. Kassem, M. Bokova, T. Hamieh, J. Toufaily, E. Bychkov	166
Influence of twill fabric topography on bloodstain pattern shape	
S. Brnada, A. Kalazic	167

Assessing the local structure and quantifying defects in $\text{Ca}_4\text{Fe}_9\text{O}_{17}$ combining STEM and FAULTS	
J. Oró-Solé, J. Serrano-Sevillano, J. Gázquez, C. Frontera, A. P. Black, M. Casas-Cabanas, M. Rosa Palacín	168
Resonant Properties of Polycrystalline Biomolecular Assemblies	
T. E. Ryan, S. Guerin	169
Polysulfide in-situ characterization with 3D electron diffraction for Lithium-Sulfur batteries	
S. Rahimi, A. Hajizadeh, J. Hadermann	170
<i>In-situ</i> 3D ED to study the structural transformation of NMC during electrochemical reactions	
A. Hajizadeh, S. Rahimi, J. Hadermann	171
Bloodstain pattern analysis using shape descriptors	
A. Kalazic, S. Brnada	172
The effects of alkali metal intercalation on the structure and superconductivity of Niobium Selenide	
K. Steele, S. J. Clarke	173
Discovery of superconductivity in Nb_4SiSb_2 with a V_4SiSb_2-type structure and implications of interstitial doping on its physical properties	
M. D. Balestra, O. Atanov, O. Blacque, R. Lefèvre, Y. H. Ng, R. Lortz, F. O. von Rohr	174
Selective ion transport of catalytic hybrid aerofilm Li-S batteries	
C. Senthil, S.S. Kim, H.S. Kim, J.W. Hong, H.Y. Jung	175
Solid-state electrolytes for Na-ion batteries: exploring the synergy between metal-organic frameworks and ionic liquids	
A. Mirandona-Olaeta, E. Goikolea, S. Lanceros-Mendez, A. Fidalgo-Marijuan, I. Ruiz de Larramendi ..	176
Understanding Fe-cation migration in $\text{LiFe}_{2-x}\text{In}_x\text{SbO}_6$ Cathode Materials	
X. Martinez de Irujo-Labalde, S. Mahato, M. Hayward	177
Synthesis of Low-Pt-Based Electrocatalyst Derived from Porous MOF-808(Zr)-NH_2 Nanoparticles Towards Oxygen Reduction Reaction	
T. M. Pham, J. Kim	178
Upcycling Lithium Titanate (LTO) Anodes into the Next Generation of High Power Ti Doped Nb_2O_5 Anodes (TNO).	
A. J. Green, E. H. Driscoll, P. R. Slater	179
Investigation of electrochemical properties of Zn-ion batteries based on ZnMo_6S_8 cathodes	
Y. Wang, A. Y. Ganin	180
Crystal chemistry of Argyrodite type Li-ion conductors	
D. Shanbhag, J. Auvergniot, V. Viallet, C. Masquelier	181
Boosting the electrochemical performance of TNO anode material through structural and compositional modifications	
E. García-González, A. Solana-Bello, F. García-Alvarado	182
Fe-substituted LiTi_2O_4 ramsdellite as electrode material in lithium batteries	
P. Díaz-Carrasco, A. Kuhn, N. Menéndez, F. García-Alvarado	183
Fabrication and characterization of Cu, Zn-doped $\text{Li}_4\text{Ti}_5\text{O}_{12}$ anode nanomaterials for energy conversion applications	
J. Dhairat, B. A. Albiss, A. Bozeya	184

Alloy Nanowire Arrays With Controlled Compositions Templated by Block Copolymers O. Burg, R. Shenhar	185
Local Structure Insight into Hydrogen Evolution Reaction with Bimetal Nanocatalysts Q. Li, X. Xing	186
Impact of Surfactant-Assisted Downsizing to Luminescent nanoMOFs on Morphological and Photophysical Properties M. Maxeiner, L. Wittig, A. Sedykh, T. Kasper, K. Müller Buschbaum	187
Hydrophobic materials based on heteroboroxines R. Jambor, M. Srb, M. Novák	188
Preparation of GeTe nanoparticles by low temperature synthetic method M. Bouška, Y. Milasheuskaya, R. Jambor, P. Němec	189
High-spin vs low-spin Ni²⁺ ions in highly distended octahedral environments: Sr₂NiO₂Cu₂Se₂, Sr₂NiO₂Cu₂S₂ and the solid solution Sr₂NiO₂Cu₂(Se_{1-x}S_x)₂ R. D. Smyth, J. N. Blandy, Z. Yu, S. Liu, C. V. Topping, S. J. Cassidy, C. F. Smura, D. N. Woodruff, P. Manuel, C. L. Bull, N. P. Funnell, J. E. McGrady, S. J. Clarke	190
Complex magnetic ordering of the mixed-valent layered oxychalcogenides Ca₂Fe_{2.6}O₃S_(2-x)Se_(x) (x = 0, 0.5, 1, 1.5) A. Gillette, B. Sheath, S. J. Clarke	191
Tuning magnetism and superconductivity in transition metal chalcogenides as a function of composition L. Taskesen, S. J. Clarke	192
Lattice Dynamics of Cs₂[Mo₂O₇]*CsX (X = Cl, Br, I) A. K. Weber, K. Denisova, P. Lemmens, A. Möller	193
Novel Oxochloridoselenites(IV) with Cuban-derived Structural Motives M. A. Bonnin, C. Feldmann	194
Wurtzite-Type Be₂PN₃ - a new and hard-type material G. Krach, M. Pointner, K. Witthaut, W. Schnick	195
Ionic-liquid-based synthesis of Ge₃N₄ nanoparticles F. Jung, C. Feldmann	196
Structural Influence of Lone Pairs in GeP₂N₄, a Germanium(II) Nitridophosphate S. J. Ambach, C. Somers, T. de Boer, L. Eisenburger, A. Moewes, W. Schnick	197
Ca₅AsSb(NH)₂ – a cation-deficient Antiperovskite with A-site ordering T. Chau, S. Rudel, D. Han, F. Wolf, T. Bein, H. Ebert, W. Schnick	198
Morin transition in beta-Fe₂SeO N. Qureshi, R. Morrow, S. Eltoukhy, V. Grinenko, Y. A. Onykienko, D. S. Inosov, M. Valldor	199
Electron-Electron and Electron-Phonon Interactions in van-der-Waals compounds: MOX, M = Sc, Ti, V, Fe and X = Cl, Br F. Predelli, F. Büscher, P. Lemmens, V. P. Gnezdilov, Yu. G. Pashkevich, T. N. Shevtsova, S. Berinskat, A. Möller	200
Intercalation chemistry of excitonic insulator candidate Ta₂NiSe₅ P. A. Hyde, J. Cen, S. J. Cassidy, N. H. Rees, P. Holdship, R. I. Smit, D. O. Scanlo, S. J. Clarke	201
Functionalisation of CaAl₂O₄:Eu²⁺, Nd³⁺ phosphors with Fe₃O₄ magnetic nanoparticles S. T. Tsantis, G. Kastinaki, V. Zaspalis, C. Sarafidis, C. Chatzidoukas, S. N. Yannopoulos	202

Transition metal doping strategy for the reversible anion redox process
A. Wang, Z. Chen, M. Hayward 203

Part VI

LIST OF PARTICIPANTS

List of participants 205

Part VII

AUTHOR INDEX

Author index 211

PREFACE

Dear Colleagues,

The Steering Committee postponed the ECSSC in Prague in August 2021 to July 2023 due to the pandemic still prevalent and severe travel restrictions. To avoid full disruptions of the 2021 ECSSC sequence and as a reminder of the taste of the current event in Prague the Steering Committee also unanimously arranged the conference as a virtual online (ZOOM program) one day meeting e.g., August 16 or June 28, 2021, with 4 invited speakers.

Now, it is with pleasure that we welcome you for the 18th European Conference on Solid State Chemistry (ECSSC 2023) held in Prague, Czech Republic, on July 9 – 12, 2023.

Solid state research and topic of the ECSSC 2023 are a combination of chemistry, physics, crystallography, and engineering that aims at synthesis, design, and evolution of solid functional materials with extended structures and interesting chemical or physical properties. As systems, this includes ceramics, heterogeneous catalysts, electrode, and battery materials, semi- and superconductors, photocatalysts, sensors, pigments, luminescent substances and much more. Recently, especially materials for better energy efficiency are amongst the most investigated systems. Also, the question of resources and renewables has become prominent for materials research.

Solid materials are often inorganic chemicals (like oxides, chalcogenides, silicates, halides, borides, intermetallics), but the methods and models that are used for characterization, analysis and description of the substances come from physical chemistry, physics, or crystallography. Synthetic methods include molecular and ceramic routes. An increasing role is attributed to theory both for prediction and understanding as well as for modelling and tuning of materials.

We hope you are going to enjoy your stay in Prague now.

Barbara Albert – chairperson (*Technical University Darmstadt*)

Tomáš Wágner – organizer of 18 the ECSSC2023 (*University of Pardubice*)

David Sedmidubský – co-organizer (*University of Chemistry and Technology, Prague*)

Paul Attfield – Solid State Chemistry division of EuChemS, (*University of Edinburg, Edinburgh*)

GENERAL INFORMATION

Conference venue

The conference will take place in the Břevnov monastery in Prague, the first male monastery in Bohemia, founded in 993. It is a monastery in the Benedictine tradition.

The Benedictine monks follow the rule of Saint Benedict, a rule of their community which Saint Benedict of Nursia wrote down for them in the sixth century. The way of life of this order is expressed in the maxim „To pray and to work“. The community of monks prays and works again in the monastery.

The representative halls of the prelate's residence are hired for cultural and various public or private events.

Address

Benediktinské arcidiecéze sv. Vojtěcha a sv. Markéty,
Markétská 1/28, 169 00 Praha 6-Břevnov
GPS: 50°5'4", 14°21'25"

Conference language

The conference language is English. Simultaneous translation will not be provided.

Conference office and on-site registration

The Conference office in the conference venue will be open for registration and information:

Sunday, July 9, 2023	13:00 – 19:00
Monday, July 10, 2023	8:00 – 12:00
Tuesday, July 11, 2023	8:30 – 12:00
Wednesday, July 12, 2023	8:30 – 12:00

Conference Opening

The conference will officially begin on Sunday, July 9, 2023, at 16:00 with Plenary Lecture presented by Prof. J. Jiang (National University of Singapore) followed by a series of invited lectures and contributed lectures.

All participants are cordially invited to a Welcome Drink, which will be served at 18:00.

Student Award

All student poster contributions are automatically included in the Student Award contest. The best student's contribution will be awarded by a valuable price.

Students not wishing to participate are kindly asked to inform the Organising committee at the registration desk upon arrival.

Contacts

Prof. Tomas Wagner

Department of General and Inorganic Chemistry
Faculty of Chemical Technology
and Center of Materials and Nanotechnologies
University of Pardubice
Cs. Legii sq. 565,532 10 Pardubice
Czech Republic

phone +(420) 466 037 144,

fax +(420) 466 037 311

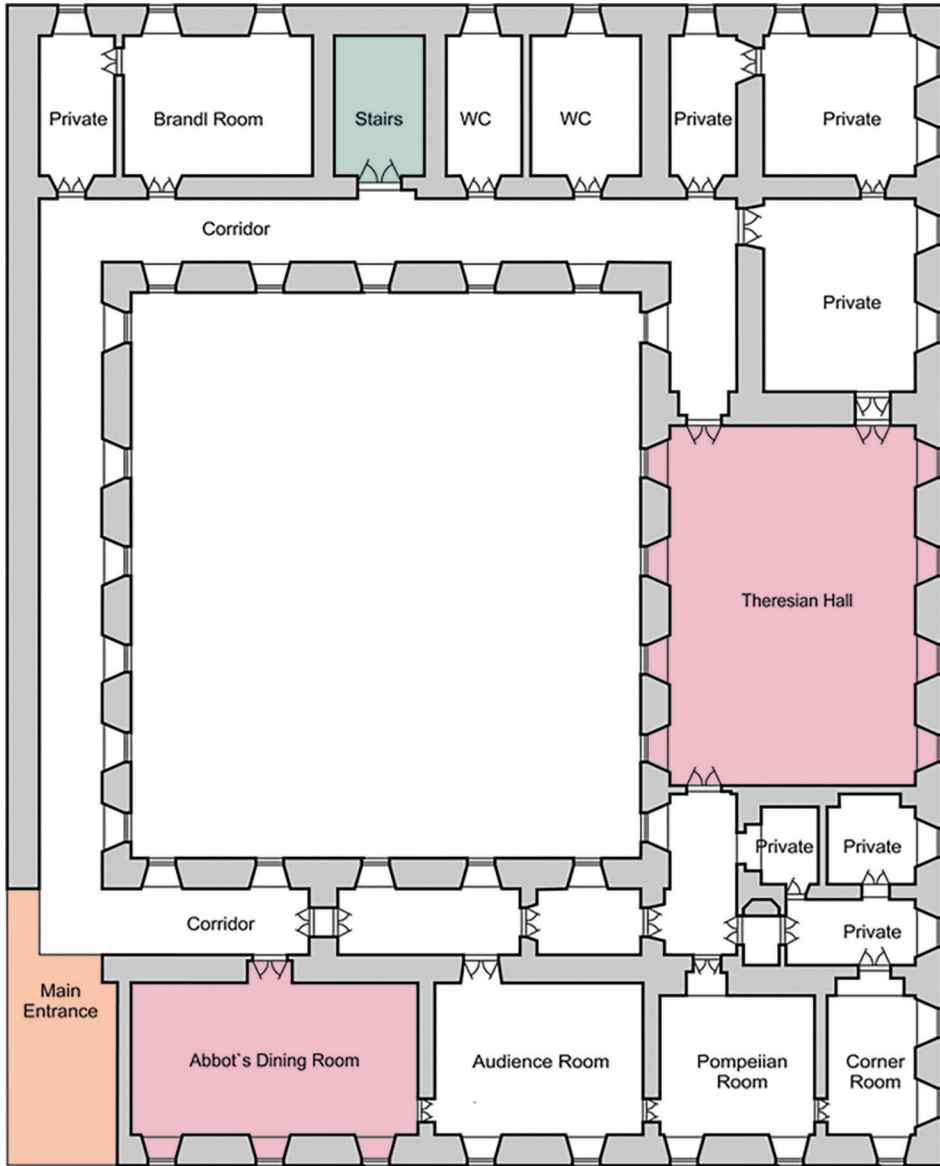
e-mail: Tomas.Wagner@upce.cz

www.ecssc18.com

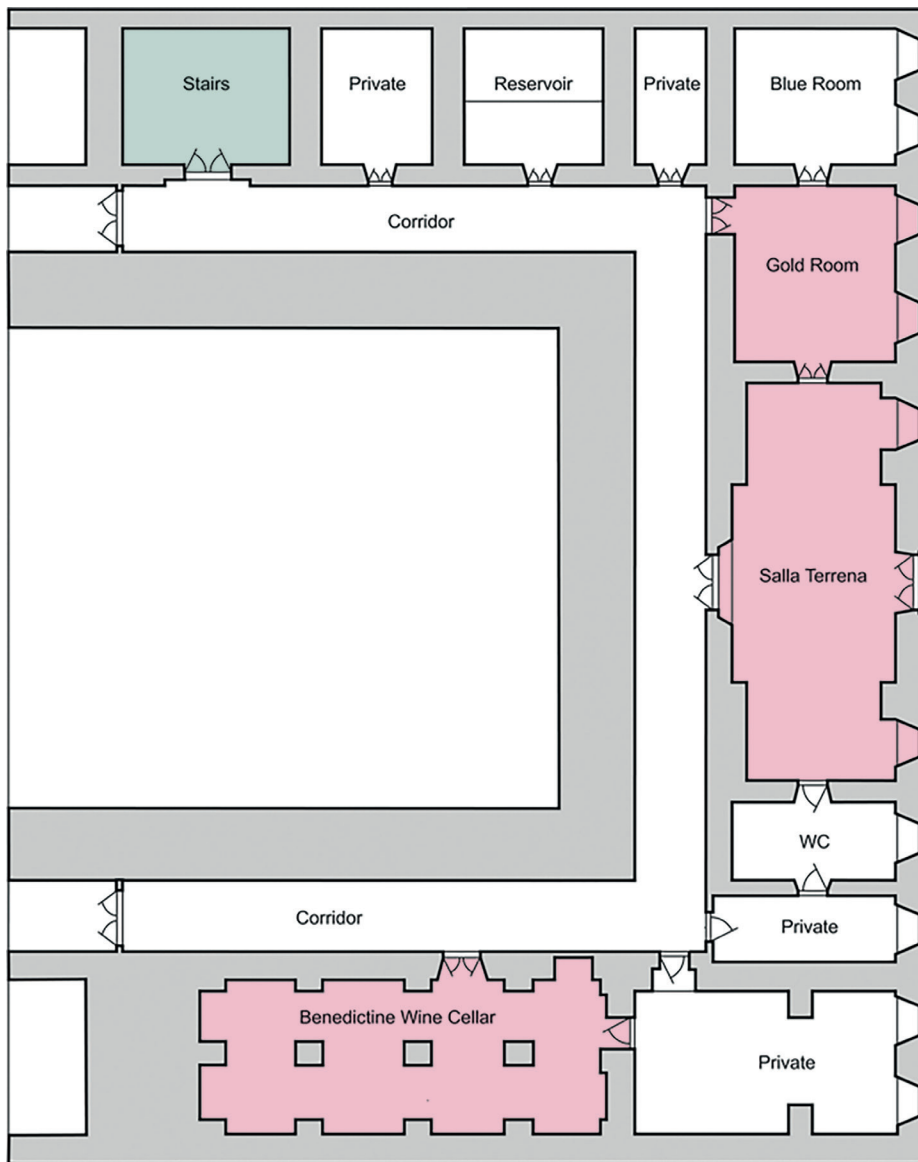
info@ecssc18.com



The 1st floor – Registration desk, Scientific Programme, Exhibitors,
Coffee breaks



Ground floor – Lunches



Part I

PROGRAMME

18th European
Conference
on Solid State
Chemistry

SUNDAY, JULY 9, 2023

13:00–19:00	REGISTRATION	
16:00–16:20	OPENING SESSION Tomas Wagner, Barbara Albert, Paul Attfield, David Sedmidubský	<i>Chairperson:</i> David Sedmidubský
16:20–17:00	Metal-organic frameworks for sustainable separations and reactions: A computational perspective J. Jiang	PL 01
17:00–17:30	Designer's metal-organic materials and interfaces through ALD/MLD M. Karppinen	IL 01
17:30–18:00	Exploring model catalysts through the integration of in-situ near-ambient pressure XPS and STM P. Matvija, M. Vorokhta, F. Pchálek, S. Oveysipoor, L. Piliai, T. N. Dinhová, B. Šmíd, I. Matolínová	IL 02
18:00–18:30	WELCOME DRINK	

		<i>Chairperson:</i> Tomas Wagner
18:30–18:50	Negative linear compressibility of the hybrid perovskite $[C(NH_2)_3]Er(HCO_2)_2(C_2O_4)$ T. J. Hitchings, A. B. Cairns, D. Allen, P. J. Saines	L 01
18:50–19:10	Complex modulations of the crystal structure of functional oxides with perovskite-related structure S. García-Martín, R. Marín-Gamero, E. Urones-Garrote, X. Martínez de Irujo-Labalde	L 02
19:10–19:30	Perovskite-type $RbNbO_3$ as a high-pressure polymorphism A. Yamamoto, K. Murase, K. Sugiyama, T. Kawamata	L 03
19:30–19:50	Chemical and physical pressure effects on structural and magnetic properties of R_2CuTiO_6 perovskite series with R ranging from La to Lu L. Sederholm, A. Yamamoto, M. Karppinen	L 04

MONDAY, JULY 10, 2023

8:00–12:00	REGISTRATION	
		<i>Chairperson:</i> Barbara Albert
9:00–9:40	Solid-state batteries – at the edge between Solid State Chemistry and Materials Science J. Janek	PL 02

SESSION I		<i>Chairperson: Duncan H. Gregory</i>
9:40–10:10	Prediction of electrical conductivity of porous composites using 3D equivalent electronic circuit network model. Solid oxides fuel cell electrode case study D. Budáč, V. Miloš, M. Carda, M. Paidar, K. Bouzek	IL 03
10:10–10:30	Critical current density of Li₆PS₅Cl powder pellets and processed films A. Tron, A. Beutl	L 05

SESSION II		<i>Chairperson: Ivan Khalakhan</i>
9:40–10:10	Synthesis-dependent structure-property relationships of quantum materials L. Clark, J. N. Graham, J. R. Stewart, J. A. Cooley, M. Songvilay, G. Confalonieri, D. Fortes, P. Manuel, A. R. Wildes	IL 04
10:10–10:30	Quantum spin liquids in cation ordered perovskites M. J. Milton, P. Manuel, J. P. Attfield	L 06
10:30–11:00	Coffee Break	

SESSION I		<i>Chairperson: Maarit Karppinen</i>
11:00–11:20	Lithium transport mechanisms characterised by ssNMR andToF-SIMS in hybrid electrolytes for solid-state batteries T. Meyer, T. Gutel, M. Bardet, H. Manzanarez, E. De Vito	L 07
11:20–11:40	Packings of sphere packings - a new path to solid state ionic conductors? M. Petrik, W. Hornfeck	L 08
11:40–12:00	Growth of metal oxide film electrodes for electrochemical capacitor by electrospray deposition M. P. Chavhan	L 09
12:00–12:20	New tungsten bronzes via electrochemical intercalation B. Rasche, I. Neumann, Y. Chen, M. Yang	L 10
12:20–12:40	Composition-activity-stability relationship in Pt-Au alloys for oxygen reduction reaction X. X. Xie, V. Briega-Martos, R. Farris, M. Vorokhta, T. Skála, I. Matolinová, K. M. Neyman, S. Cherevko, I. Khalakhan	L 11

SESSION II		<i>Chairperson: Lucy Clark</i>
11:00–11:20	Metal-insulator transitions in hollandite vanadate and chromate M. Isobe, P. Puphal, H. Takagi	L 12
11:20–11:40	Fluoridoargentates(II) as potential analogues to superconducting cuprates M. Dragomir, M. Belak Vivod, M. Lozinšek, Z. Jagličić, G. King	L 13
11:40–12:00	FeMn₂Ge₂Sn₂O₁₆: a “partial” spin-liquid candidate with a perfectly isotropic 2-D Kagomé Lattice C. D. Ling, M. C. Allison, S. Wurmehl, B. Büchner, J. L. Vella, T. Söhnel, S. A. Bräuninger, H.-H. Klauss	L 14
12:00–12:20	Hidden orders in 2D van der Waals materials: The example of magnetic crossover in the mixed-anion compound CrSBr S. A. López-Paz, Z. Guguchia, V. Y. Pomjakushin, C. Witteveen, A. Cervellino, H. Luetkens, N. Casati, A. F. Morpurgo, F. O. von Rohr	L 15
12:20–12:40	Solid-state synthesis of carbon-coated lithium vanadate Li₃VO₄ as anodes for High-Performance Li-ion Capacitors S. Lonkar, C. Busa	L 16
12:40–13:40	Lunch	

	<i>Chairperson: Jürgen Janek</i>	
13:40–14:20	Fast cation conductivity in complex metal halides & hydrides; Prospects for solid state electrolytes <u>D. H. Gregory</u>	PL 03

	SESSION I <i>Chairperson: Peter Matvija</i>	
14:20–14:50	Probing fuel cell catalysts degradation under simulated operational environment by advanced in situ techniques <u>I. Khalakhan</u>	IL 05
14:50–15:10	Elucidating catalytic performance of a family of low-valent metal nitrides for the hydrogen evolution reaction from water <u>A. Y. Ganin</u> , Y. Sun, O. Guselnikova, Y. Zhou, N. López	L 17
15:10–15:30	Understanding the performance of high power niobium oxide based Li ion battery materials A. Green, E. Driscoll, <u>P. Slater</u>	L 18

	SESSION II <i>Chairperson: Karel Bouzek</i>	
14:20–14:50	Discovery of quantum materials by combining chemical and physical design principles <u>F. O. von Rohr</u>	IL 06
14:50–15:10	Supraparticles as identifiers or temperature indicators with spectral magnetic read-out <u>S. Müssig</u> , J. Reichstein, S. Wintzheimer, K. Mandel	L 19
15:10–15:30	Crystal and electronic structure of the lanthanide dibismuthides REBi₂ (RE = La, Ce, Pr, Nd, Sm) <u>A. Ovchinnikov</u> , M. Ruck	L 20
15:30–16:00	Coffee Break	

	SESSION I <i>Chairperson: Fabian von Rohr</i>	
16:00–16:20	New nickel-based lithium rich layered/disordered rock salt cathode materials for lithium ion batteries <u>B. Dong</u> , J. Castells-Gil, P. Zhu, L. Driscoll, P. Allan, E. Kendrick, P. Slater	L 21
16:20–16:40	Operando investigation of Ir-Ru-based catalyst for Proton Exchange Membrane Water Electrolysis <u>T. Hrbek</u> , P. Kúš, M. G. Rodriguez, H. Nedumkulam, M. Mirolo, J. Drnec, V. Matolín, I. Matolínová	L 22
16:40–17:00	The influence of Al and Ga doping on the chemical and electrochemical cycling of T-LiFeO₂ <u>S. Mahato</u> , X. M. De Irujo Labalde, S. Booth, M. Hayward	L 23
17:00–17:20	Designing new lithium layered oxides from sodium layered oxides to stabilize oxygen redox <u>M. Guignard</u> , V. Saïbi, L. Castro, I. Sugiyama, C. Delmas	L 24
17:20–17:40	Sodium insertion into TiO₂ hollandite: structural and electrochemical study <u>F. García-Alvarado</u> , A. Duarte, P. Díaz-Carrasco, A. Kuhn, A. Basa	L 25
17:40–18:00	Structural evolution of layered H₂V₃O₈ high-capacity cathode material for lithium-ion batteries during lithium intercalation <u>A. Kuhn</u> , J. C. Pérez-Flores, M. Hoelzel, V. Diez-Gómez, I. Sobrados, J. Sanz, F. García-Alvarado	L 26

SESSION II		<i>Chairperson: Jianwen Jiang</i>	
16:00–16:20	Evidence for a disorder-induced spin liquid in the tuneable spin ladder-chain system $\text{Ba}_2\text{CuTe}_{1-x}\text{W}_x\text{O}_6$ ($0 \leq x \leq 0.3$) <i>O. Mustonen, C. Pughe, A. Gibbs, A. Yaresko, P. Baker, L. Mangin-Thro, H. C. Walker, E. J. Cussen</i>		L 27
16:20–16:40	Structural variations of the magnetic topological insulators $\text{Mn}_{1+x}\text{Sb}_{2-2x/3}\text{Te}_4$ <i>E. Kochetkova, O. Renier, A. Isaeva, M. Sahoo, L. T. Corredor</i>		L 28
16:40–17:00	2D-Metals with locked charge density wave, in the novel layered monophosphate tungsten bronzes $[\text{Ba}(\text{PO}_4)_2]\text{WmO}_3\text{m}^{-3}$ <i>H. Nimoh, R. Glaum, A. Cano, A. M. Arévalo-López, O. Mentré</i>		L 29
17:00–17:20	Experimental investigation of magnetic dilution effect on the frustrated quantum antiferromagnet $\text{SrCu}_2(\text{BO}_3)_2$ <i>L. Šibav, G. King, Z. Jagličić, M. Koblar, M. Otoničar, D. Arčon, M. Dragomir</i>		L 30
17:20–17:40	Magnetic structures of Dirac nodal-line semimetals LnSbTe <i>I. Plokhikh</i>		L 31

POSTER SESSION I			
18:00–20:00	Nitridooxorhenate and -technetate anions $[\text{MO}_3\text{N}]_2^-$ (M = Tc, Re) from reactions in highly alkaline media <i>D. Badea, E. Strub, J. Bruns</i>		P 01
	Ternary Alkali metal Thallides ATl (A = K/Rb, Cs/Rb) <i>V. F. Schwinghammer, S. Gärtner</i>		P 02
	Solution combustion synthesis of thermodynamically metastable oxide-phosphates with rutile- and anatase-related structures <i>S. Früchticht, M. Weber, R. Glaum</i>		P 03
	Ferroelectric Properties on $\text{Ba}_{0.975}\text{Ln}_{0.017}$ ($\text{ZrxTi}_{0.95-x}$) $\text{Sn}_{0.05}\text{O}_3$ Materials <i>K. Taibi, S. Zemouri-Smail, A. Lahmar</i>		P 04
	Electrocrystallisation of Ternary Amalgams <i>D. Kraut, C. Hoch</i>		P 05
	Cs_2O as a strong oxidiser - A new synthetic route towards oxometalates <i>I. Žaytseva, C. Hoch</i>		P 06
	Novel representatives of the structure type $\text{Na}_7\text{RbT}_{14}$ with the lighter homologue Indium <i>M. Janesch, S. Gärtner</i>		P 07
	High-pressure Synthesis of Alkaline Metal Niobates with Tetragonal Tungsten Bronze-type Structure <i>K. Murase, T. Sato, A. Yamamoto, K. Sugiyama</i>		P 08
	Anion Redox in Lithium Main-group Metal Oxides <i>Z. Chen, S. Mahato, X. M. De Irujo Labalde, M. Hayward</i>		P 09
	Synthesis and characterisation of lanthanum zirconate as a candidate filler material for polymer derived ceramic coatings <i>P. N. Moghaddam, M. Parchovianský, I. Parchovianská, A. Pakseresht</i>		P 10
	Investigation of structure and luminescence properties of bismuth-based coordination polymers with N-donor ligands <i>K. V. Borysova, J. R. Sorg, E. A. Mikhalyova, K. Müller-Buschbaum</i>		P 11
	Tin-Boroxines-Based Inorganic-Organic Macrocycles: Synthesis, Characterization and Hydrophobicity <i>M. Novák, M. Bouška, Š. Podzimek, R. Jambor</i>		P 12
	High-Pressure Synthesis of SmSi_3 <i>T. Neziraj, S. Wirth, Y. Grin, U. Schwarz</i>		P 13

	Mixed-metal monophosphate tungsten bronzes containing divalent transition metal ions (MII: Fe, Co, Ni) and tungsten(VI) <u>L. K. Aymans, R. Glaum</u>	P 14
	Amino acid crystals as high-performance, eco-friendly structural health monitors <u>K. Hari, S. Bhattacharya, S. Guerin</u>	P 15
	High temperature magnetic ordering in new quadruple perovskites $\text{Sr}_4\text{NaM}_3\text{O}_{12}$ (M = Ru and Os) <u>G. S. Thakur, T. Doert, T. Hansen, E. Osmic, W. Schnelle, T. Herrmannsdörfer, M. Ruck</u>	P 16
	Effect of concentration of conductive polymers in zinc-pigmented epoxy-ester based anticorrosive coatings <u>Y. Raycha, M. Kohl, A. Kalendová</u>	P 17
	Oligothiophene Dendron-Modified CdS Nanoparticles and Their Optical Properties <u>A. Yoshida, R. Nozawa, Y. Sakagami, M. Matsubara, A. Mori, A. Muramatsu, K. Kanie</u>	P 18
	Synthesis and characterization of glass and crystalline compositions in the $(\text{Na}_2\text{Se})_x(\text{As}_2\text{Se}_3)_{1-x}$ chalcogenide system <u>A. Sammoury, M. Kassem, M. Bokova, T. Hamieh, J. Toufaily, E. Bychkov</u>	P 19
	Influence of twill fabric topography on bloodstain pattern shape <u>S. Brnada, A. Kalazic</u>	P 20
	Assessing the local structure and quantifying defects in $\text{Ca}_4\text{Fe}_3\text{O}_{17}$ combining STEM and FAULTS <u>J. Oró-Solé, J. Serrano-Sevillano, J. Gázquez, C. Frontera, A. P. Black, M. Casas-Cabanas, M. Rosa Palacín</u>	P 21
	Resonant Properties of Polycrystalline Biomolecular Assemblies <u>T. E. Ryan, S. Guerin</u>	P 22
	Polysulfide in-situ characterization with 3D electron diffraction for Lithium-Sulfur batteries <u>S. Rahimi, A. Hajizadeh, J. Hadermann</u>	P 23
	<i>In-situ</i> 3D ED to study the structural transformation of NMC during electrochemical reactions <u>A. Hajizadeh, S. Rahimi, J. Hadermann</u>	P 24
	Bloodstain pattern analysis using shape descriptors <u>A. Kalazic, S. Brnada</u>	P 25
	The effects of alkali metal intercalation on the structure and superconductivity of Niobium Selenide <u>K. Steele, S. J. Clarke</u>	P 26
	Discovery of superconductivity in Nb_4SiSb_2 with a V_4SiSb_2-type structure and implications of interstitial doping on its physical properties <u>M. D. Balestra, O. Atanov, O. Blacque, R. Lefèvre, Y. H. Ng, R. Lortz, F. O. von Rohr</u>	P 27

TUESDAY, JULY 11, 2023

		<i>Chairperson: Spyros Yannopoulos</i>	
9:00–9:40	Phase change optical memory materials: Why are alloys of Ge, Sb, and Te almost the only materials of choice? <u>R. O. Jones</u>		PL 04
	SESSION I	<i>Chairperson: Jiří Orava</i>	
9:40–10:10	Chalcogenide glasses and fibers for photonic applications in the infrared <u>J.-L. Adam</u> , J. Trolès, C. Boussard-Plédel, X. H. Zhang		IL 07
10:10–10:30	Light-induced surface microstructures on Ge-As-S glasses <u>E. Samsonova</u> , P. Kutálek, E. Černošková, P. Knotek, J. Schwarz		L 32
	SESSION II	<i>Chairperson: Joke Hadermann</i>	
9:40–10:10	Polymorphism and magnetic properties in high pressure A-site manganites <u>E. Solana-Madruga</u>		IL 08
10:10–10:30	Locking any magnetization by freezing of magnetic domains in a transient soft to super-hard magnet <u>O. Mentré</u> , B. Leclercq, A. Pautrat, A. M. Arevalo-Lopez, S. petit, V. Stolyarov		L 33
10:30–11:00	Coffee Break		
	SESSION I	<i>Chairperson: Miroslav Vlček</i>	
11:00–11:20	Er³⁺-doped TeO₂-ZnO-La₂O₃ optical glasses <u>J. Suský</u> , S. Šlang, L. Beneš, B. Frumarová, R. Svoboda, T. Wágner, L. Strižík		L 34
11:20–11:40	Structural analyses and properties of complex sulphides in the Cr-Sn-S system <u>F. Guiot</u> , V. Dorcet, E. Guilmeau, B. Malaman, T. Schweitzer, P. Lemoine, C. Prestipino		L 35
11:40–12:00	Holmium-doped TeO₂-ZnO-La₂O₃ tellurite glasses for photonics applications and fibre optics <u>J. Hrabovsky</u> , F. Desevedavy, L. Strizik, J. Oswald, L. Nowak, T. Wagner, F. Smektala, M. Veis		L 36
12:00–12:20	Gold(I)-thiolate coordination polymers as transparent glasses and cyclic phase-changing materials <u>S. Vaidya</u> , O. Veselska, Z. Fan, A. Zhadan, A. Fateeva, P. Bordet, S. Horike, A. Demessence		L 37
12:20–12:40	Tuning the metallic glasses properties via ultrafast heating/cooling <u>J. Orava</u> , Y. H. Sun, I. Kaban		L 38

SESSION II		<i>Chairperson:</i> Elena Solana-Madruga
11:00–11:20	Cation ordered doping of ferrite perovskites: influence on redox behaviour, magnetism, and mixed ionic electronic conductivity <u>A. J. Brown</u> , O. Wagstaff, A. Manjón-Sanz, H. Brand, M. Avdeev, I. Evans, C. D. Ling	L 39
11:20–11:40	Understanding the texture degree on zinc aluminate Nd, Ce sub-micrometer films by screen printing for NIR emitting applications <u>R. E. Rojas-Hernandez</u> , F. Rubio-Marcos, J. F. Fernandez, I. Hussainova	L 40
11:40–12:00	Many body localisation in $\text{CeMnAsO}_{1-x}\text{Fx}$? <u>A. C. McLaughlin</u> , G. Lawrence, S. Simpson, E. J. Wildman	L 41
12:00–12:20	V-V dimerization in MnVO_3 ilmenite low-pressure polymorph: Crystal and magnetic structures and properties <u>A. M. Arévalo-López</u> , D. Khalyavin, O. Mentré	L 42
12:20–12:40	Multifunctional coordination polymers for fluorescent sensing of VOCs and hazardous ions from contaminated water <u>K. A. Siddiqui</u>	L 43
12:40–13:40	Lunch	

		<i>Chairperson:</i> Paul Attfield
13:40–14:20	New possibilities in <i>in situ</i> and <i>ex situ</i> crystal structure determination based upon 3D ED R. Poppe, D. Vandemeulebroucke, M. Quintelier, A. Hazijadeh, S. Rahimi, S. Gholam, M. Batuk, <u>J. Hadermann</u>	PL 05

SESSION I		<i>Chairperson:</i> Olivier Mentré
14:20–14:50	<i>In-situ</i> characterization of gas-solid interfaces by near-ambient pressure X-ray photoelectron spectroscopy <u>M. Vorokhta</u> , L. Piliiai, T.N. Dinhová, P. Matvija, I. Matolinová	IL 09
14:50–15:20	Bias-free graphene-based <i>in situ</i> TEM observation of electrode materials for batteries <u>J. Y. Cheong</u> , J. H. Chang	IL 10
15:20–15:40	Structural investigation of new Li ion containing oxides using combined diffraction and NMR and EXAFS spectroscopy <u>F. N. Sayed</u> , Q. Jacquet, P. Groszewicz, S. P. Emge, P. C. M. M. Magusin, C. O'Keefe, S. Dey, C. Kocer, A. Morris, C. P. Grey	L 44

SESSION II		<i>Chairperson:</i> Klaus Müller-Buschbaum
14:20–14:50	Investigating the catalytic potential of iron-doped calcium titanate: a study of oxide vacancy structures and microstructures <u>M. Amano Patino</u> , M. Ibrahim, N. Frederich, H. Kaper, M. Ceretti, W. Paulus	IL 11
14:50–15:10	Theoretical insights into the monolayer adsorption and characterization of HB238 merocyanine on $\text{Ag}(100)$ surface <u>R. Tomar</u> , A. Kny, M. Sokolowski, T. Bredow	L 45
15:10–15:30	Understanding the synthetic reliability of Na_xMnO_2 and similar layered phases <u>J. Beecham-Lonsdale</u> , D. C. Arnold, S. Ramos-Perez	L 46
15:30–16:00	Coffee Break	

SESSION I		<i>Chairperson:</i> Claus Feldmann
16:00–16:20	X-ray photoelectron spectroscopy: a key tool for assessment of 2D molybdenum dichalcogenides synthesized by ALD <u>J. Rodriguez-Pereira, R. Zazpe, J. Charvot, F. Bures, J.M. Macak</u>	L 47
16:20–16:40	Charge density refinement on inorganic crystals using electron diffraction <u>E. Yörüük, A. Suresh, P. Brázda, M. K. Cabaj L. Palatinus</u>	L 48
16:40–17:00	Chemistry at the nanoscale: AFM meets IR spectroscopy <u>J. Horák</u>	L 49
17:00–17:20	CeScSi-type intermetallics: Modulation of magnetic properties through light elements insertion and catalysis of ammonia <u>E. Gaudin, K. Alabd, C. Croisé, F. Can, X. Courtois, N. Bion, A. Villesuzanne, S. Tencé</u>	L 50
17:20–17:40	Analysis of ground particle behavior in wet ball milling by DEM-CFD simulation <u>K. Kushimoto, J. Kano</u>	L 51

SESSION II		<i>Chairperson:</i> Helmer Fjellvag
16:00–16:20	Optomagnetic composites by combination of strong magnetic and luminescent components <u>K. Müller-Buschbaum, M. Seuffert, T. Wehner</u>	L 52
16:20–16:40	Exploring structure-property correlations in the frustrated layered material, $Mn_2Mo_3O_8$ <u>D. C. Arnold, H. L. McPhillips, S. Ramos</u>	L 53
16:40–17:00	Developments in high-pressure growth of rare earth nickelates single crystals <u>D. J. Gawryluk</u>	L 54
17:00–17:20	Tuning physicochemical properties in $TbMgNi_{4-x}Co_x-(H,D)_2$ system <u>V. Shtender</u>	L 55
17:20–17:40	Magnetic properties controlled by short-range structural and spin order in layered materials <u>J. D. Bocarsly, S. E. Dutton, C. P. Grey</u>	L 56

18:00–20:00	POSTER SESSION II	
	Selective ion transport of catalytic hybrid aerofilm Li-S batteries C. Senthil, S. S. Kim, H. S. Kim, J. W. Hong, <u>H. Y. Jung</u>	P 28
	Solid-state electrolytes for Na-ion batteries: exploring the synergy between metal-organic frameworks and ionic liquids A. Mirandona-Olaeta, E. Goikolea, S. Lanceros-Mendez, A. Fidalgo-Marijuan, <u>I. Ruiz de Larramendi</u>	P 29
	Understanding Fe-cation migration in $\text{LiF}_{e_{2-x}\text{In}_x\text{SbO}_6}$ Cathode Materials X. Martinez de Irujo-Labalde, <u>S. Mahato</u> , M. Hayward	P 30
	Synthesis of Low-Pt-Based Electrocatalyst Derived from Porous MOF-808(Zr)-NH_2 Nanoparticles Towards Oxygen Reduction Reaction T. M. Pham, <u>J. Kim</u>	P 31
	Upcycling Lithium Titanate (LTO) Anodes into the Next Generation of High Power Ti Doped Nb_2O_5 Anodes (TNO) <u>A. J. Green</u> , E. H. Driscoll, P. R. Slater	P 32
	Investigation of electrochemical properties of Zn-ion batteries based on ZnMo_6S_8 cathodes <u>Y. Wang</u> , A. Y. Ganin	P 33
	Crystal chemistry of Argyrodite type Li-ion conductors <u>D. Shanbhag</u> , J. Auvergniot, V. Viallet, C. Masquelier	P 34
	Boosting the electrochemical performance of TNO anode material through structural and compositional modifications <u>E. García-González</u> , A. Solana-Bello, F. García-Alvarado	P 35
	Fe-substituted LiTi_2O_4 ramsdellite as electrode material in lithium batteries P. Díaz-Carrasco, <u>A. Kuhn</u> , N. Menéndez, F. Garcia-Alvarado	P 36
	Fabrication and characterization of Cu, Zn-doped $\text{Li}_4\text{Ti}_5\text{O}_{12}$ anode nanomaterials for energy conversion applications J. Dhairat, <u>B. A. Albiss</u> , A. Bozeya	P 37
	Alloy Nanowire Arrays With Controlled Compositions Templated by Block Copolymers <u>O. Burg</u> , R. Shenhar	P 38
	Local Structure Insight into Hydrogen Evolution Reaction with Bimetal Nanocatalysts Q. Li, <u>X. Xing</u>	P 39
	Impact of Surfactant-Assisted Downsizing to Luminescent nanoMOFs on Morphological and Photophysical Properties <u>M. Maxeiner</u> , L. Wittig, A. Sedykh, T. Kasper, K. Müller-Buschbaum	P 40
	Hydrophobic materials based on heteroboroxines <u>R. Jambor</u> , M. Srb, M. Novák	P 41
	Preparation of GeTe nanoparticles by low temperature synthetic method <u>M. Bouška</u> , Y. Milasheuskaya, R. Jambor, P. Němec	P 42
	High-spin vs low-spin Ni^{2+} ions in highly distended octahedral environments: $\text{Sr}_2\text{NiO}_2\text{Cu}_2\text{Se}_2$, $\text{Sr}_2\text{NiO}_2\text{Cu}_2\text{S}_2$ and the solid solution $\text{Sr}_2\text{NiO}_2\text{Cu}_2(\text{Se}_{1-x}\text{S}_x)_2$ <u>R. D. Smyth</u> , J. N. Blandy, Z. Yu, S. Liu, C. V. Topping, S. J. Cassidy, C. F. Smura, D. N. Woodruff, P. Manuel, C. L. Bull, N. P. Funnell, J. E. McGrady, S. J. Clarke	P 43
	Complex magnetic ordering of the mixed-valent layered oxychalcogenides $\text{Ca}_2\text{Fe}_{2-6x}\text{O}_3\text{S}(2-x)\text{Se}(x)$ ($x = 0, 0.5, 1, 1.5$) <u>A. Gillette</u> , B. Sheath, S. J. Clarke	P 44
	Tuning magnetism and superconductivity in transition metal chalcogenides as a function of composition <u>L. Taskesen</u> , S. J. Clarke	P 45
	Lattice Dynamics of $\text{Cs}_2[\text{Mo}_2\text{O}_7] \cdot \text{CsX}$ ($X = \text{Cl}, \text{Br}, \text{I}$) <u>A. K. Weber</u> , K. Denisova, P. Lemmens, A. Möller	P 46

	Novel Oxochloridoselenites(IV) with Cuban-derived Structural Motives <u>M. A. Bonnin</u> , C. Feldmann	P 47
	Wurtzite-Type Be₂PN₃ - a new and hard-type material G. Krach, M. Pointner, K. Witthaut, W. Schnick	P 48
	Ionic-liquid-based synthesis of Ge₃N₄ nanoparticles F. Jung, C. Feldmann	P 49
	Structural Influence of Lone Pairs in GeP₂N₄, a Germanium(II) Nitridophosphate <u>S. J. Ambach</u> , C. Somers, T. de Boer, L. Eisenburger, A. Moewes, W. Schnick	P 50
	Ca₅AsSb(NH)₂ – a cation-deficient Antiperovskite with A-site ordering <u>T. Chau</u> , S. Rudel, D. Han, F. Wolf, T. Bein, H. Ebert, W. Schnick	P 51
	Morin transition in beta-Fe₂SeO N. Qureshi, R. Morrow, S. Eltoukhy, V. Grinenko, Y. A. Onykienko, D. S. Inosov, <u>M. Valldor</u>	P 52
	Electron-Electron and Electron-Phonon Interactions in van-der-Waals compounds: MO_x, M = Sc, Ti, V, Fe and X = Cl, Br F. Predelli, F. Büscher, <u>P. Lemmens</u> , V. P. Gnezdilov, Y. G. Pashkevich, T. N. Shevtsova, S. Berinskat, A. Möller	P 53
	Intercalation chemistry of excitonic insulator candidate Ta₂NiSe₅ <u>P. A. Hyde</u> , J. Cen, S. J. Cassidy, N. H. Rees, P. Holdship, R. I. Smit, D. O. Scanlo, S. J. Clarke	P 54
	Functionalisation of CaA₁₂O₄:Eu²⁺, Nd³⁺ phosphors with Fe₃O₄ magnetic nanoparticles S. T. Tsantis, G. Kastrinaki, V. Zaspalis, C. Sarafidis, C. Chatzidoukas, <u>S. N. Yannopoulos</u>	P 55
	Transition metal doping strategy for the reversible anion redox process <u>A. Wang</u> , Z. Chen, M. Hayward	P 56

WEDNESDAY, JULY 12, 2023

	<i>Chairperson: Robert Jones</i>	
9:00–9:40	Exploring new transition metal nitride materials <u>A. Fuertes</u>	PL 06
	<i>Chairperson: Midori Amano Patino</i>	
9:40–10:10	Compositionally complex alloys for the hydrogen society <u>M. Sahlberg</u>	IL 12
10:10–10:30	Crystal growth of new uranium and transuranic phases via high temperature solution and mild hydrothermal methods: Exploration of new materials as potential nuclear waste forms <u>H.-C. zur Loye</u> , T. K. Deason, A. T. Hines, H. Tisdale, T. M. Besmann, J. Amoroso, D. P. DiPrete	L 57
	<i>Chairperson: Jean-Luc Adam</i>	
9:40–10:10	Mineral-inspired sulphides for thermoelectric energy harvesting <u>A.V. Powell</u>	IL 13
10:10–10:30	<i>In-situ</i> XRD and PDF investigation of battery fluoride materials $MF_{3.3}H_2O$ (M = Fe, Cr) in controlled atmosphere: accessing new phases with controlled chemistry <u>G. Nénerl</u> , L. Ding, K. Forsberg, C. V. Colin	L 58
10:30–11:00	Coffee Break	
	<i>Chairperson: Amparo Fuertes</i>	
11:00–11:20	A facile preparation of Y_2O_3S nanoparticles through sulfidation under a CS_2 atmosphere <u>Y. Kanazawa</u> , M. Matsubara, R. Ohsuga, A. Muramatsu, K. Domen, K. Kanie	L 59
11:20–11:40	Mechanochemical process to prepare amorphous oxides precursor with isomorphous substitution of Si(IV) by heteroatoms and successive hydrothermal synthesis to crystalize zeolites <u>A. Muramatsu</u> , H. Kobayashi, G. Tanaka, M. Yabushita, R. Osuga, K. Ninomiya, M. Matsubara, S. Maki, M. Nishibori, K. Kanie	L 60
11:40–12:00	Alkali shuffling in honeycomb layered oxides <u>E. Mumba-Mpanga</u> , R. Berthelot	L 61
12:00–12:20	Inorganic materials synthesis in ultra-alkaline hydroflux H. He, Y. Li, R. Albrecht, <u>M. Ruck</u>	L 62
12:20–12:40	Anion redox as a means to derive layered manganese oxychalcogenides with exotic intergrowth structures <u>S. Giri</u> , S. Sasaki, S. Cassidy, S. Dey, G. Cibin, C. Grey, S. Clarke	L 63

	SESSION II	<i>Chairperson: Flaviano Garcia-Alvarado</i>	
11:00–11:20	Quadrature frequency resolved spectroscopy on green upconversion photoluminescence in GeGa(As)S:Er³⁺ CHALCOGENIDE GLASSES <i>L. Strizik, T. Aoki, V. Prokop, J. Hrabovsky, T. Wagner</i>		L 64
11:20–11:40	TESCAN's Analytical Solutions for Lithium-Ion Battery Research <i>J. Honč, T. Šamořil, J. Dluhoř, T. Sui, X. Yao</i>		L 65
11:40–12:00	Local structure and high performance catalysts <i>X. Xing, Q. Li</i>		L 66
12:00–12:20	Defect engineering: Eu³⁺ emission enhancement via induced local distortion <i>S. C. S. Lemos, M. Assis, L. Gracia, L. K. Ribeiro, A. F. Gouveia, Y. G. Galvão, E. Cordoncillo, R. C. Lima, E. Longo, J. Andrés</i>		L 67
12:20–12:40	Urinary oxidative stress sensor based on zinc oxide nanorods <i>A. Ejaz, D. Gibson, C. Garcia Nuñez</i>		L 68
12:40–13:40	Lunch		

	SESSION I	<i>Chairperson: Anthony V. Powell</i>	
13:40–14:10	Reaction mechanisms in molten salts for the design of solid-state materials at the nanoscale <i>D. Portehault, F. Igoa Saldaña, E. de Rolland Dalon, M. Baron, A. Ghoridi, A. Séné, E. Defoy, Y. Song, P.-O. Autran, D. Thiaudière</i>		IL 14
14:10–14:30	Tecto-borosulfates–syntheses, structures and properties <i>E. Turgunbajew, P. Netzsch, M. Hämmer, G. Buchner, H. A. Höppe</i>		L 69
14:30–14:50	Crystal structures of new phosphosilicates and its homologues <i>D. Johrendt, A. Haffner, V. Weippert, J. Aicher, K. Witthaut</i>		L 70
14:50–15:10	Exploring trirutile materials as a platform for energy storage <i>E. Djafri, D. Arnold, O. Mentré</i>		L 71
15:10–15:30	Understanding the formation mechanism of intermetallic nanoparticles in polyol processes <i>M. Smuda, J. Ströh, N. Pienack, A. Khadiev, H. Terraschke, M. Ruck, T. Doert</i>		L 72

	SESSION II	<i>Chairperson: Mirela Dragomir</i>	
13:40–14:10	Nanostructured thin-film catalysts for hydrogen production via PEM water electrolysis <i>P. Kúř, T. Hrbek, H. Nedumkulam, M. Mirolo, I. Martens, J. Drnec, I. Matolínová</i>		IL 15
14:10–14:30	Structural trends and ion diffusion mechanisms in the postspinel-type NaFe_{1-x}Ru_{1-x}O₄ system <i>L. Benincasa, M. Duttine, M. Suchomel, M. Guignard</i>		L 73
14:30–14:50	Base-metal nanoparticles as reactants at room temperature <i>C. Feldmann</i>		L 74
14:50–15:10	Functionalization of chalcogenide IR photonic sensor by polymer membrane for the purpose of detecting aromatic hydrocarbon pollutants in water <i>M. Vrazel, R. K. Ismail, M. Baillieul, P. Nemeč, P. Loulergue, A. Szymczyk, K. Boukerma, R. Courson, A. Hammouti, L. Bodiou, J. Charrier, T. Halenkovic, M. Bouska, V. Nazabal</i>		L 75
15:10–15:30	Soft chemistry of layered titanium and vanadium oxytellurides <i>N. D. Kelly, S. J. Clarke</i>		L 76
15:30–16:00	Coffee Break		

SESSION I		<i>Chairperson: Peter Kúš</i>
16:00–16:20	Thermal transformations and cation redistribution on $A_2B_2O_6$ oxides <u>K. Ji</u> , E. Solana-Madruga, M. A. Patino, Y. Shimakawa, J. P. Attfield	L 77
16:20–16:40	Photoluminescence properties of nanocrystalline multicomponent garnet $Gd_3Sc_xGa_{5-x}O_{12}$ doped with Er^{3+} <u>T. Netolický</u> , L. Benes, S. Slang, B. Frumarova, J. Oswald, T. Wagner	L 78
16:40–17:00	Borosulfates – silicate analogue anions with the potential to stabilize polycations <u>J. Bruns</u>	L 79
17:00–17:20	Characterisation of Rh^{4+} oxides, an unusual case of pyrochlore stabilisation under high pressure, high temperature synthesis conditions S. D. Injac, B. Mullens, F. Denis Romero, M. Avdeev, C. Barnett, A. K. L. Yuen, B. J. Kennedy, Y. Shimakawa	L 80
17:20–17:40	Alkali metal oxide mercurides with isolated mercuride anions L. Nusser, S. Feldl, <u>C. Hoch</u>	L 81

SESSION II		<i>Chairperson: Jun Young Cheong</i>
16:00–16:20	Synthesis and characterization of a novel oxychloride, $SrTe_2FeO_6Cl$ <u>J. A. Sannes</u> , B. Gonano, Ø. S. Fjellvåg, S. Kumar, O. Nilsen, M. Valldor	L 82
16:20–16:40	The absence of expected paramagnetic behavior in $Ba_6Fe_2Te_3S_7$ <u>E. H. Frøen</u> , P. Adler, M. Valldor	L 83
16:40–17:00	Oxides as Pt catchment materials in the ammonia oxidation process - methodology and mechanistic insight <u>J. Hessevåg</u> , A. S. Fjellvåg, O. Iveland, C. S. Carlsen, H. Sønsteby, T. By, J. Skjelstad, D. Waller, H. Fjellvåg, A. O. Sjøstad	L 84
17:00–17:20	Probing for dynamics in a strongly frustrated magnet <u>L. Kubičková</u> , A. K. Weber, M. Panthöfer, A. Möller	L 85
17:20–17:40	Chemical pressure driving phase transition and morphology in Eu^{3+}-doped KY_3F_{10}: An experimental and theoretical insight <u>P. Serna-Gallén</u> , S. C. S. Lemos, L. Gracia, E. O. Gomes, H. Beltrán-Mir, E. Cordoncillo, J. Andrés	L 86
17:40–18:00	CLOSING CEREMONY Tomas Wagner	

Part II

PLENARY LECTURES

18th European
Conference
on Solid State
Chemistry

Metal-organic frameworks for sustainable separations and reactions: a computational perspective

J. Jiang*

Department of Chemical and Biomolecular Engineering, National University of Singapore, Singapore

* The corresponding author e-mail: chejj@nus.edu.sg

Keywords: metal-organic frameworks; nanoporous materials; separations; reactions; computations

Metal-organic frameworks (MOFs) are a unique class of solid-state nanoporous materials and have received tremendous interest over the last two decades. The nearly unlimited variations of metal clusters and organic linkers allow the pore sizes, volumes and functionalities of MOFs to be readily tailored in a rational manner. Consequently, MOFs provide a wealth of opportunities for molecular engineering of nanoporous materials and have been considered as versatile candidates for many important potential applications. Nevertheless, the number of MOFs synthesized to date is extremely large, thus experimental testing alone is economically expensive and practically infeasible. With rapidly growing computational resources, computational methods have become indispensable to characterize, screen and design MOFs. In this presentation, I will give an overview of recent computational studies on MOFs for chemical separations and reactions, such as carbon capture, biofuel purification, water desalination, CO₂ conversion. It will be demonstrated that computations at an atomic/molecular level can secure the quantitative interpretation of experimental observations, provide microscopic insight from bottom-up, and facilitate the development of new MOFs.

References

- [1] R. Krishna, K. W. Yang, K. Hashem, J. W. Jiang,* “Metallated porphyrinic metal-organic frameworks for CO₂ conversion to HCOOH: a computational screening and mechanistic study”, *Molecular Catalysis*, **527**, 112407 (2022).
- [2] H. J. Tang, J. W. Jiang,* “In silico screening and design strategies of ethane-selective metal-organic frameworks for ethane/ethylene separation”, *AIChE Journal*, **67**, e17025 (2021).
- [3] K. W. Yang, J. W. Jiang,* “Transforming CO₂ into Methanol with N-Heterocyclic Carbene-Stabilized Coinage Metal Hydrides Immobilised in a Metal–Organic Framework UiO-68”, *ACS Applied Materials & Interfaces*, **13**, 58723-58736 (2021).
- [4] A. Nalaparaju, J. W. Jiang,* “Metal-Organic Frameworks for Liquid Phase Applications”, *Advanced Science*, **8**, 2003143 (2021).
- [5] J. W. Jiang,* “Computational Screening of Metal-Organic Frameworks for CO₂ Capture”, *Current Opinion in Green and Sustainable Chemistry*, **16**, 57-64 (2019).
- [6] Metal-Organic Frameworks: Materials Modeling toward Potential Engineering Applications, J. W. Jiang (ed), Pan Stanford Publishing Pte. Ltd. (2015).

Solid-state batteries – at the edge between Solid State Chemistry and Materials Science

PL02

J. Janek^{1,2}¹ Institute of Physical Chemistry & Center for Materials Research, Justus Liebig University, 35392 Giessen Germany² Batteries and Electrochemistry Laboratory (BELLA), Institute of Nanotechnology, Karlsruhe Institute of Technology, 76344 Eggenstein-Leopoldshafen, Germany* *The corresponding author e-mail:* juergen.janek@pc.jlug.de**Keywords:** solid electrolytes; mixed conductors; intercalation compounds; electrochemistry; ion conduction

Since about a decade, solid-state batteries (SSB) experience fast rising interest as potential electrochemical energy storage device. In SSB, the flammable organic electrolyte is replaced by a solid electrolyte, which may enable the use of high-capacity metal anodes and can lead to safe high-energy batteries.

In this lecture, the requirements for different cell components (active electrode materials, solid electrolytes, separators) will be presented and discussed from the materials perspective. All components typically require a combination of various chemical and physical properties, and successful “design” of new materials requires in-depth knowledge of solid-state chemistry, electrochemistry and physics. It is a major aim of this lecture to highlight the solid-state chemical concepts that are necessary ingredients.

The lecture will focus on three major subjects that are key to the development of solid-state batteries. Firstly, solid electrolytes will be discussed that may enter into successful SSB concepts. Secondly, cathode active materials will be discussed as these typically limit the capacity of alkali bases batteries. Third, the chemo-mechanics of SSBs will be introduced as a critical issue with respect to long-term stability of SSBs.

While lithium-based batteries will form the major part of the lecture, the current rise of sodium-based solid-state batteries will also be commented.

References

- [1] J. Janek and W. Zeier, *Nat. Energy*, **1**, 16141(1–4), (2016)
- [2] P. Minnmann, et int., J. Janek, *Adv. Ener. Mater.*, **12**, 2201425(1–18), (2022)

Acknowledgments

The author acknowledges financial support by Federal Ministry of Education and Research (BMBF, Cluster of Competence FESTBATT, project 03XP0431).

Fast cation conductivity in Complex Metal Halides & Hydrides; prospects for solid state electrolytes

D. H. Gregory*

¹ University of Glasgow, School of Chemistry, Joseph Black Building, Glasgow G12 8QQ, UK

Tel: +44 (0)1413308128;

* The corresponding author e-mail: Duncan.Gregory@glasgow.ac.uk

Keywords: synthesis; structure; lithium; conductivity; batteries

Many of the most ubiquitous materials in Li-ion batteries are oxides. Nevertheless, some of the best performing materials contain elements from elsewhere in the periodic table (e.g. chalcogenides, pnictides). Although halide salts have long been employed as electrolytes in solution or in the molten state, there are few examples of halides as solid-state ionic conductors and until recently, still less in terms of hydrides.

This contribution focuses principally on the possibilities for designing fast Li-ion conducting (pseudo-)halides as potential solid state electrolytes. In switching the materials design emphasis from cations to anions, it will be shown how both static and dynamic disorder might be exploited to enhance Li-ion transport and how diffusion pathways might be modified in terms of anion geometry and electronegativity (e.g. **Figure 1**). Synthesis can be challenging, but mechanochemistry and other “soft” chemical approaches, can provide a means to access such materials, while facilitating nanostructuring and generating defects.

This contribution covers several exemplar systems of promising hydride and halide cation conductors, including Li-ion conductors such as $\text{Li}(\text{BH}_4)_2\text{X}$, LiAlX_4 and $\text{LiCe}(\text{BH}_4)_3\text{X}$; $\text{X} = \text{Cl}, \text{Br}, \text{I}$, among others. In each case a raft of techniques including neutron diffraction and muon spin relaxation spectroscopy have been fundamental in elucidating the structure-property relationships in these systems. A complementary combination of experiment and computational calculations are beginning to shed light on the mechanisms for ionic conduction in these families of non-oxide materials (e.g. **Fig. 1**) and their prospects as solid state electrolytes will be evaluated.

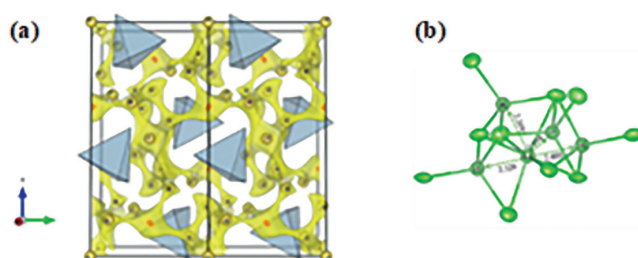


Figure 1: (a) BVSE map showing Li^+ migration pathways in a (100) projection of the LiAlI_4 structure. Filled tetrahedra represent $[\text{AlI}_4]^-$ cations. (b) Immediate environment around the octahedral Li site in LiAlI_4 , showing the positions of nearby interstitial sites.

References

- [1] I. Cascallana-Matias, D. A. Keen, E. J. Cussen, D. H. Gregory, *Chem. Mater.*, **27**, 7780-7787 (2015)
- [2] N. Flores-González, N. Minafra, G. Dewald, H. Reardon, R. I. Smith, S. Adams, W. G. Zeier, D. H. Gregory, *ACS Mater. Lett.*, **3**, 652-657 (2021)
- [3] N. Flores-González, M. López, N. Minafra, J. Bohnenberger, F. Viñes, S. Rudić, I. Krossing, W. G. Zeier, F. Illas, D. H. Gregory, *J. Mater. Chem. A*, **10**, 13467-13475 (2022)

Phase change optical memory materials: Why are alloys of Ge, Sb, and Te almost the only materials of choice?

R. O. Jones¹

¹ Forschungszentrum Jülich, Peter-Grünberg-Institut PGI-1, D-52425 Jülich, Germany

* *The corresponding author e-mail: r.jones@fz-juelich.de*

Keywords: phase change materials; chemical bonding; Ge/Sb/Te alloys; electron-rich multicentre bonding; “metavalent” bonding

Phase change memory materials (PCM) exhibit extremely rapid (nanoseconds) and reversible crystallization of amorphous nano dots in very thin polycrystalline layers. The phase changes are usually triggered by voltage or laser pulses of appropriate duration and intensity, and the nature of the metastable states can be determined by measuring the electrical resistivity or optical reflectivity. They are the basis of optical memories, including DVD-RW and Blu-ray Disc. These remarkable properties are matched by the remarkably few materials that have the desired properties; almost all contain Sb and/or Te, and the commercially most successful are alloys of Ge, Sb, and Te. I shall discuss two views of the reasons. One [1] notes that these materials have approximately five valence electrons per atom, which favours rock salt structures that are found to be essential to successful PCM, the other [2] insists that the chemical bond in these materials is new and fundamentally different from commonly accepted “covalent”, „metallic“, and “ionic” bonding and deserves a distinct name, “metavalent”. Is it possible to use either to find improved PCM?

References

- [1] R. O. Jones, *Phys. Rev. B*, **101**, 024103 (2020)
- [2] M. Wuttig, C.-F. Schön, et al., *Adv. Mater.* (2023, in press) DOI: 10.1002/adma.202208485

New possibilities in *in situ* and *ex situ* crystal structure determination based upon 3D ED

R. Poppe¹, D. Vandemeulebroucke¹, M. Quintelier¹, A. Hazijadeh¹, S. Rahimi¹, S. Gholam¹, M. Batuk¹, J. Hadermann¹

¹ EMAT, Department of Physics, University of Antwerp, Belgium

* The corresponding author e-mail: joke.hadermann@uantwerpen.be

Keywords: *in situ*; 3DED; diffuse scattering; redox; perovskite; electrochemistry; solid-gas reaction

Whereas 3DED is by now well established for solving and refining structures of particles with a size down to a few ten nanometres, its application to non-single-crystal particles is only starting to be explored. However, particles that underwent a reaction are often multiphased, or have defects or short-range order, thus this is an important route to develop. When the reactions have taken place *ex situ*, the particles can be studied by conventional TEM, which can show the different phases, short range order and defects directly on the images and diffraction patterns but cannot analyze their presence quantitatively. Moreover, when the reactions are performed with *in situ* TEM, high resolution imaging and in zone patterns of powder particles are not possible due to only a single rotation axis of the *in-situ* holders (thus the particles cannot be oriented in-zone). We will demonstrate that for such *in situ* TEM experiments not only the crystal structure, but also the parameters of the short range order and defects [1] and the volume ratios of the phases [2] can be now determined using 3DED data and we will discuss our *in situ* 3DED experiments on the solid-gas redox reactions of perovskite based materials [3] and electrochemical redox reactions of battery materials [4].

References

- [1] R. Poppe, D. Vandemeulebroucke, R.B. Neder, J. Hadermann, *IUCrJ*, **9**,695–704, (2022)
- [2] M. Quintelier, T. Perkisas, R. Poppe, M. Batuk, M. Hendrickx, J. Hadermann, *Symmetry*, **13**, 1989 (2021)
- [3] M. Batuk, D. Vandemeulebroucke, M. Ceretti, W. Paulus, *J Mater Chem A*, **11**, 213–220 (2023)
- [4] O. M. Karakulina, A. Demortière, W. Dachraoui, A. M. Abakumov, J. Hadermann, *Nano Lett.*, **18**, 6286–6291 (2018)

Acknowledgments

Financial support is acknowledged from FWO I003218N, G035619N and G040116N, University of Antwerp BOF TOP 38689 and the European Commission NanED Grant number 956099. We acknowledge the Hercules fund 'Direct electron detector for soft matter TEM' from Flemish Government for the purchase of the K2 DED. The computational resources and services used in this work were provided by the HPC core facility CalcUA of the Universiteit Antwerpen, and VSC (Flemish Supercomputer Center).

Exploring new transition metal nitride materials

PL06

A. Fuertes

Institut de Ciència de Materials de Barcelona (CSIC), Campus UAB, 08193 Bellaterra, Spain

* The corresponding author e-mail: amparo.fuertes@icmab.es

Keywords: nitrides; oxynitrides; spinels; perovskites; anion order; electronic properties

The introduction of nitrogen in transition metal oxides involves changes in the electronic structure affecting the physical properties. The lower electronegativity and higher polarizability of nitrogen compared to oxygen increases the bond covalency, decreasing the interelectronic repulsion. The larger electrical charge of nitride anion increases the crystal field splitting and the polarization, and allows the stabilization of structures with new cation compositions and properties. [1-3] This lecture will present recent results on transition metal nitride compounds with new structure types and electronic properties.

Pseudocubic perovskite oxynitrides ABO_2N or $ABON_2$ derived from the Pm-3m aristo-type (A=rare earth, alkaline earth metal; B = transition metal) are important materials that show high permittivities, visible-light photocatalytic activity and colossal magnetoresistance among other properties.^[3] $BaWON_2$ is the first example of a hexagonal perovskite oxynitride, formed by sequences of cubic and hexagonal close packed AX_3 layers where anions are in sharing corners and faces of the octahedra respectively. It crystallizes in the 6H polytype with the non-centrosymmetric space group $P6_3mc$. The anion order, together with second order Jahn-Teller effect of W^{6+} cations and electrostatic repulsions along the sharing faces of the octahedra, induce high distortions in the tungsten coordination, leading a polar structure and a large dielectric permittivity. [4]

There is only a limited number of spinel nitrides and their discovery is relatively recent compared with the oxide analogues. $MnTa_2N_4$ is the first ternary nitride spinel containing only transition metals, and one of the few examples of nitrides with this structure type. It is a normal spinel with total order of Mn^{2+} and Ta^{5+} cations in the tetrahedral and octahedral sites respectively. [5] The nitride anions reinforce the superexchange magnetic interactions in the tetrahedral sublattice and modulate the direct magnetic exchange between the Mn^{2+} cations. This produces a strong magnetic frustration that is enhanced with respect to the analogous spinels $MnAl_2O_4$ and $MnSc_2S_4$, formed by tetrahedral Mn^{2+} cations and a non-magnetic cation in the octahedral sites.

References

- [1] A. Fuertes, *Mater. Hor.*, 2, 453–461 (2015)
- [2] A. Fuertes, *Prog. Solid State Chem.*, 51, 63–70 (2018)
- [3] A. Fuertes, *APL Materials*, 8, 020903 (2020)
- [4] J. Oró-Solé, I. Fina, C. Frontera, J. Gázquez, C. Ritter, M. Cunqueiro, P. Loza-Alvarez, S. Conejeros, P. Alemany, E. Canadell, J. Fontcuberta and A. Fuertes, *Angew. Chem. Int. Ed.*, 59, 18395–18399 (2020)
- [5] R. Trocoli, C. Frontera, J. Oró-Solé, C. Ritter, P. Alemany, E. Canadell, M. R. Palacín, J. Fontcuberta and A. Fuertes, *Chem. Mat.*, 34, 6098–6107 (2022)

Part III

INVITED LECTURES

18th European
Conference
on Solid State
Chemistry

Designer's metal-organic materials and interfaces through ALD/MLD

M. Karppinen¹

¹ Department of Chemistry and Materials Science, Aalto University, FI-00076 Espoo, Finland

* *The corresponding author e-mail:* maarit.karppinen@aalto.fi

Keywords: metal-organic framework; inorganic-organic superstructure; atomic/molecular layer deposition; thin film; energy conversion and storage

Atomic layer deposition (ALD) of high-quality inorganic thin films has been one of the cornerstones of microelectronics already for decades, while its counterpart for organic thin films, i.e. molecular layer deposition (MLD), remained nearly un-exploited for long. In recent years, the hybrid of these two techniques, i.e. ALD/MLD, has been strongly emerging as a state-of-the-art route for novel designer's metal-organic thin-film materials.

Currently, the ALD/MLD literature comprises ca. 300 original papers covering processes for most of the alkali and alkaline earth metals, 3d transition metals, and lanthanides as the metal component and a variety of aliphatic, aromatic and natural organic components [1]. Excitingly, some of these processes yield in-situ crystalline and porous metal organic framework (MOF) structures [2]. Another attractive aspect is that many of the metal-organics realized through ALD/MLD are fundamentally new materials, difficult if not impossible to access through conventional synthesis. Moreover, since both ALD and MLD cycles are modular, they can be combined into any arbitrary precursor cycling pattern to grow elaborated superstructures with functional interfaces to introduce multiple and even mutually contradicting properties into a single material.

In this presentation, my intension is to: (i) shortly introduce the breath of the ALD/MLD processes developed, (ii) address the advantages of fabricating the MOF-like metal-organic materials and inorganic-organic interfaces in a layer-by-layer manner through gas-phase synthesis, and (iii) highlight some promising ALD/MLD materials for their application potential in rechargeable batteries, magnetics, and light-conversion materials. My material highlights include artificial lithium-organic-carbonate SEI (solid-electrolyte interphase) coating layers and electroactive lithium-organic MOF-like components for Li-ion battery [3], ϵ - Fe_2O_3 :azobenzene superlattice structures for photo-switchable magnetic films [4,5], and organic-component-sensitized multi-lanthanide-organic films for flexible white-light emitting thin-film phosphors [6].

References

- [1] J. Multia, M. Karppinen, *Adv. Mater. Interfaces* 2022, 202200210 (2022).
- [2] J. Multia, D. Kravchenko, V. Rubio-Giménez, A. Philip, R. Ameloot, M. Karppinen, *ACS Appl. Nano Mater.* 6, 827 (2023).
- [3] M. Madadi, J. Heiska, J. Multia, M. Karppinen, *ACS Appl. Mater. Interfaces* 13, 56793 (2021).
- [4] T. Jussila, A. Philip, J. Linden, M. Karppinen, *Adv. Eng. Mater.* 25, 2201262 (2023).
- [5] A. Philip, Y. Zhou, G. C. Tewari, S. van Dijken, M. Karppinen, *J. Mater. Chem. C* 10, 294 (2022).
- [6] A. Ghazy, M. Lastusaari, M. Karppinen, submitted (2023).

Exploring model catalysts through the integration of *in-situ* Near-Ambient Pressure XPS and STM

P. Matvija¹, M. Vorokhta¹, F. Pchálek¹, S. Oveysipoor¹, L. Piliai¹, T.N. Dinhová¹, B. Šmíd¹, I. Matolínová¹

¹ Department of Surface and Plasma Science, Faculty of Mathematics and Physics, Charles University, V Holešovičkách 2, 180 00 Prague, Czech Republic

* The corresponding author e-mail: peter.matvija@mff.cuni.cz

Keywords: NAP-STM; NAP-XPS; *in-situ*/operando study; cerium oxide; iron oxide; mixed reducible oxides; low-temperature CO oxidation

The study of catalytic reactions has long been a topic of interest in the field of chemistry and materials science. In recent years, advancements in analytical techniques have allowed for more in-depth studies of catalysts at the atomic level in operando conditions. By studying catalysts in real-time, in their native environment, we can gain a deeper understanding of the underlying mechanisms that drive catalytic reactions. In this presentation, we will highlight the benefits of combining *in-situ* near-ambient pressure X-ray photoelectron spectroscopy (NAP-XPS) and near-ambient pressure scanning tunneling microscopy (NAP-STM). The integration of XPS and STM provides a unique combination of surface analytical techniques that can be used to probe both the electronic and geometric structures of model catalytically active surfaces at elevated temperature and pressure up to a millibar range.

In our laboratory at the Department of Surface and Plasma Science of Charles University we operate a combined apparatus that comprises NAP-STM/AFM, NAP-XPS/USP, *in-situ* electrochemical cell and other surface science techniques. To showcase the use of the system we will present the study of the room-temperature CO oxidation on the Au clusters supported by the epitaxial CeO₂(111) layers, epitaxial FeO_x/CeO₂(111) layers and intermixed CeFe_xO_y layers. The Au/CeO₂ system exhibits significant chemical and morphological changes upon exposure to 1 mbar of the mixture of CO and O₂ at room temperature. At the same conditions, the active Au clusters on epitaxial and intermixed Ce-Fe oxide layers are more stable. Moreover, introduction of Fe increases low temperature diffusivity of oxygen vacancies in the CeO_x-FeO_x interface. Both of these factors contribute to the increased catalytic activity of Au supported by the Ce-Fe oxides compared to the single-component Ce oxide.

References

- [1] O. Bezkrovnyi, M. Vorokhta et al., *J. Mater. Chem. A*, **10**, 16675–16684 (2022)
- [2] L. Piliai, P. Matvija, et al., *ACS Appl. Mater. Interfaces*, **14**, 56280–56289 (2022)

Acknowledgments

This work was supported by the Czech Science Foundation (GAČR 20-13573S).

Prediction of electrical conductivity of porous composites using 3D equivalent electronic circuit network model. Solid oxides fuel cell electrode case study

D. Budáč, V. Miloš, M. Carda, M. Paidar, K. Bouzek*

Department of Inorganic Technology, University of Chemistry and Technology, Prague, Technická 5, 16628 Prague 6, Czech Republic;

* *The corresponding author e-mail: bouzekk@vscht.cz*

Keywords: composite electronic conductor; electronic conductivity prediction; equivalent electronic circuit network; material percolation; impedance response simulation

Multiphase electric charge conductors composed of materials with various properties are widely utilized in technical, as well as research practice. These composite materials include porous electrodes and other components utilized mainly in the fuel cell and battery technologies. In this study, a novel equivalent electronic circuit (EEC) network model is presented allowing for accurate prediction of the electrical properties of such materials without time-consuming experimental determination. The distinct attribute of this EEC network model is the fact, it requires only easily obtainable data as input parameters: phase composition, porosity and bulk electrical conductivity of individual constituents. The model generates a large number of cubic artificial specimens based on random distribution of individual phases according to the input composition. Each of the generated specimens is substituted with corresponding EEC network. The EEC networks are solved using the Kirchhoff's laws resulting in impedance response simulation for composite conductivity value prediction. Unlike similar models, the EEC network model is able to account for morphological phenomena such as tortuosity, for more than two present phases in the system and for the interface phenomena. The EEC network model was validated using the lanthanum strontium manganite mixed with yttria-stabilized zirconia. Excellent agreement between the experimentally determined and calculated electrical conductivity for the sample porosity of 0 to 60% was obtained. The phenomena observed were explained in terms of percolation theory and proven by microscopic observations.

Due to its variability, the EEC network model can be suitable for a wide range of practical applications. This approach has thus high potential to save enormous amount of experimental effort, while maintaining sufficient accuracy, when designing corresponding multiphase electrode structures.

Acknowledgments

This work was supported by the Technology Agency of the Czech Republic (TK04030143).

Synthesis-dependent structure-property relationships of quantum materials

L. Clark^{1*}, J. N. Graham^{1,2}, J. R. Stewart³, J. A. Cooley⁴, M. Songvilay⁵, G. Confalonieri⁶, D. Fortes³, P. Manuel³, A. R. Wildes²

¹ School of Chemistry, University of Birmingham; UK ² Institut Laue-Langevin, France;

³ ISIS Neutron and Muon Source, U;

⁴ California State University, Fullerton, USA;

⁵ Institute Néel, Franc; ⁶ European Synchrotron Radiation Facility, France

* The corresponding author e-mail: l.m.clark@bham.ac.uk

Keywords: quantum materials; structure-property relationships; magnetism; diffraction; PDF analysis; neutron magnetic diffuse scattering

Quantum ($S \leq 1$) magnets with frustrated magnetic interactions are predicted to give rise to a rich variety of exotic quantum materials properties. This includes novel quasiparticle excitations that could be manipulated to pave the way to a new form of topologically-protected quantum computing [1]. However, the complexity of quantum materials often makes characterising the exact nature of their exotic properties extremely challenging. For instance, in frustrated quantum magnets, the degeneracy of possible magnetic ground states stemming from the competition of magnetic interactions means that the experimentally observed properties are extremely sensitive to any defects or disorder in the underlying materials structure, which can vary from sample to sample depending on the synthesis method used [2,3]. This in turn poses challenges for the development of our theoretical understanding of quantum materials, and ultimately limits our current ability to design and synthesise new quantum materials with properties tailored towards specific applications [4].

In this talk, I will discuss our recent efforts to explore the synthesis-structure-property relationships of the frustrated $S = \frac{1}{2}$ spinel, ZnV_2O_4 . Previous studies of this material—which contains a pyrochlore network of antiferromagnetically coupled V^{3+} ions—reveal that the structural and magnetic ground states are sample dependent, ranging from a tetragonally distorted classical antiferromagnet to a cubic and highly frustrated spin glass [5-8]. I will present two samples of ZnV_2O_4 , one prepared via a conventional solid-state synthesis method and the other via a novel rapid microwave-assisted route. I will show how these two different synthesis routes distinctly impact the evolution of the chemical and magnetic behaviour of ZnV_2O_4 through a combination of high-resolution powder neutron and synchrotron X-ray diffraction, magnetometry, and X-ray PDF and diffuse neutron scattering measurements. In doing so, I will demonstrate the potential for rapid microwave-assisted synthesis as an appealing high-throughput approach to high-quality inorganic quantum materials discovery.

References

- [1] C. Broholm *et al.*, *Science* **367**, 6475 (2020).
- [2] D. F. Bowman *et al.*, *Nat. Commun.* **10**, 637 (2019).
- [3] K. Tustain *et al.*, *Chem. Mater.* **33**, 9638 (2021).
- [4] D. N. Basov *et al.*, *Nat. Mater.* **16**, 1077 (2017).
- [5] Y. Ueda *et al.*, *J. Phys. Soc. Jpn.* **66**, 778 (1997).
- [6] M. Reehuis *et al.*, *Eur. Phys. J. B* **35**, 311 (2003).
- [7] S. Ebbinghaus *et al.*, *J. Alloys Compd.* **370**, 75 (2005).
- [8] A. J. Browne and J. P. Attfield, *Phys. Rev. B* **101**, 0241122 (2020).

Probing fuel cell catalysts degradation under simulated operational environment by advanced in situ techniques

I. Khalakhan

Department of Surface and Plasma Science, Faculty of Mathematics and Physics,
Charles University, Prague, Czech Republic

* The corresponding author e-mail: khalakhan@gmail.com

Keywords: fuel cells; cathode catalyst; degradation; dealloying; Ostwald ripening; coalescence

Platinum-3d transition metal bimetallic alloys have been extensively investigated in recent years as a cost-effective alternative to expensive monometallic Pt cathode catalysts for proton-exchange membrane fuel cells (PEMFCs) [1].

Nonetheless, such alloys exhibit reduced stability under the corrosive environment of the cathode. The degradation of fuel cell catalysts during its operation is a complex process involving an interplay between multiple mechanisms such as dissolution of both platinum and transition metal, Ostwald ripening, coalescence and carbon support corrosion, which ultimately leads to PEMFC performance deterioration [2,3]. It is thus essential to describe the entire chain of interconnected degradation mechanisms in order to formulate a comprehensive model of catalyst degradation. This is a prerequisite for proposing corresponding mitigation strategies that may result in a more robust catalyst. With the rising of state-of-the-art *in situ* techniques that allow direct analysis of catalysts during operation, the above goal has received increasing attention from researchers.

This work highlights our recent results on the time-resolved degradation of bimetallic fuel cell catalysts under simulated operational conditions obtained using *in situ* electrochemical atomic force microscopy, *in situ* grazing incidence small angle X-ray scattering, and electrochemical scanning flow cell with online detection by inductively coupled plasma mass spectrometry.

References

- [1] J. Greeley, I. E. L. Stephens, A. S. Bondarenko, T. P. Johansson, H. A. Hansen, T. F. Jaramillo, J. Rossmeisl, I. Chorkendorff, J. K. Nørskov, *Nat. Chem.*, **1**, 552–556 (2009)
- [2] J. C. Meier, C. Galeano, I. Katsounaros, J. Witte, H. J. Bongard, A. A. Topalov, C. Baldizzone, S. Mezzavilla, F. Schüth, K. J. J. Mayrhofer, *Beilstein J. Nanotechnol.*, **5**, 44–67 (2014)
- [3] M. Bogar, Y. Yakovlev, D. Sandbeck, S. Cherevko, I. Matolínová, H. Amenitsch, I. Khalakhan, *ACS Catal.*, **11**, 11360–11370 (2021)

Acknowledgments

This work was supported by the Czech Science Foundation (22-03643S).

Discovery of quantum materials by combining chemical and physical design principles

F. O. von Rohr^{1*}

¹ Department of Quantum Matter Physics, University of Geneva, CH-1211 Geneva, Switzerland

* *The corresponding author e-mail:* fabian.vonrohr@unige.ch

Keywords: quantum materials, superconductivity, magnetism, TMDs, HEAs

The discovery of materials with tailored properties has, time and again, proven to be a crucial stimulus for technological advancement and, by implication, of societal progress. Currently, advancement in the development of many technologically relevant materials is reaching a point of stagnation. The consensus in the scientific and industrial communities is that we need to develop new device paradigms based on new materials to overcome this impasse. Quantum materials, in particular, are widely considered to have a key role in the development of such next-generation technologies that will meet the urgent technological demands of our society. Our research aims at establishing a general experimental platform for realizing new quantum materials. In this presentation, I will discuss some of our recent results regarding the discovery and characterization of new quantum materials. Specifically, our current work on (i) the heavy-fermion ferromagnet $\text{CeZn}_{2-\delta}\text{Ge}_2$, (ii) the unconventional scaling of the superfluid density with the critical temperature in layered transition metal dichalcogenides, and (iii) the remarkably robust superconducting properties of high-entropy alloys, will be presented. This work is at the intersection of condensed-matter physics and materials synthesis, and as I will discuss here, a special emphasis on the combination of physical and chemical concepts is extremely important for developing these new quantum materials.

Chalcogenide glasses and fibers for photonic applications in the infrared

J.-L. Adam, J. Trolès, C. Boussard-Plédel, X. H. Zhang

Univ Rennes, CNRS, ISCR (Institut des Sciences Chimiques de Rennes) - UMR 6226,
Campus de Beaulieu, F-35000 Rennes, France

* *The corresponding author:* jean-luc.adam@univ-rennes1.fr

Keywords: infrared; microstructured optical fibers; optical sensors; optical non-linearity; 3D-printing

Vitreous materials composed of chalcogen elements (S, Se, Te) show broad transparency windows that span from the visible up to 12-15 μm , depending on their compositions. This is due to the lower phonon energies of chalcogenides, which are also responsible for enhanced luminescence of rare-earth ions embedded in such matrices. In addition, chalcogenide glasses contain large polarisable atoms and external lone electron pairs that induce exceptional non-linear properties. These unique properties, combined with a good ability of chalcogenide glasses to be obtained in the form of bulk optics, optical fibers or channel waveguides, open the way to a large range of applications like thermal imaging, infrared light generation, or infrared optical sensing.

The presentation will illustrate the great affinity of chalcogenide glasses for infrared photonics through the latest results in two challenging topics. First, chalcogenide microstructured optical fibers, with enhanced non-linearities, for the generation of mid-IR supercontinuum will be addressed [1-3], with new developments on microstructured fibers obtained from preforms made by 3D-printing [4]. The second topic will deal with infrared optical sensors based on chalcogenide fibers for *in situ* and real-time identification of chemical species, with a focus on *in operando* tracking of the chemistry evolution in Li-ion batteries [5].

References

- [1] U. Møller, Y. Yu, I. Kubat, C. R. Petersen, X. Gai, L. Brilland, D. Méchin, C. Caillaud, J. Trolès, B. Luther-Davies, and O. Bang, *Optics Exp.* **23**, 3282–3291 (2015)
- [2] C. Caillaud, C. Gilles, L. Provino, L. Brilland, T. Jouan, S. Ferre, M. Carras, M. Brun, D. Méchin, J.-L. Adam, and J. Trolès, *Optics Exp.* **24**, 7977–7986 (2016)
- [3] M. Meneghetti, C. Caillaud, R. Chahal, E. Galdo, L. Brilland, J.-L. Adam, J. Trolès, *J. Non-Cryst. Solids* **503-504**, 84–88 (2019)
- [4] J. Carcreff, F. Cheviré, R. Lebullenger, A. Gautier, R. Chahal, J.-L. Adam, L. Calvez, L. Brilland, D. Le Coq, E. Galdo, G. Renversez, J. Trolès, *Crystals* **11**, 228 (2021)
- [5] C. Gervillié, C. Boussard, J. Huang, L. A. Blanquer, S. Boles, X. H. Zhang, J. L. Adam, J. M. Tarascon, *Nature Energy*, <https://doi.org/10.1038/s41560-022-01141-3> (2022)

Polymorphism and magnetic properties in high pressure A-site manganites

E. Solana-Madruga¹

¹ Universidad Complutense de Madrid, Avda. Complutense, sn, 28040, Madrid, Spain

* *The corresponding author e-mail: elsolana@ucm.es*

Keywords: high pressure; magnetic frustration; polymorphism; functional materials; neutron diffraction

ABO₃ oxides have proven to accommodate a wide variety of chemical compositions, to crystallise with several structures in competition and to develop diverse physical properties, being intensively studied in the search for new functional materials. Among them, the use of high-pressure and high-temperature (HPHT) synthesis techniques allows the stabilisation of the small Mn²⁺ cation in the larger A site, giving rise to the so-called A-site manganites [1] Some of the most exciting A-site manganites are spintronic (e.g. perovskite MnVO₃-II) [2] or multiferroic (e.g. LiNbO₃-type MnTiO₃-II) [3] materials.

Mixing different cations into the A and/or B sites induces cation order and further magnetic complexity. Recent studies on high pressure Mn₂BB'O₆ compounds have evidenced the accessibility to new structural derivatives, as the double double perovskite structures (DDPv) [4] or triple perovskites (TPv) with 1:2 order of the B-site cations [5]. The possibility to tune both structure and properties as a function of the chemical composition has also been observed, for instance in the Mn_{3-x}Co_xTeO₆ DPv – Ni₃TeO₆-type solid solutions [6].

High pressure Mn₂BB'O₆ oxides are known with compositional distribution of oxidation states 1+/7+, 2+/6+ and 3+/5+ over the B/B' sites. Surprisingly, polymorphism has only been found for compounds with B' d⁰/d¹⁰ cations up to date, suggesting accessibility to new compounds. A representative example, for instance, would be the comparison between the magnetoresistant Mn₂Fe³⁺Re⁵⁺O₆, [7] the frustrated Mn₂Mn²⁺Re⁶⁺O₆ [8] and the polymorphic Mn₂Li⁺Re⁷⁺O₆ [9].

Perspectives arising from this revision suggest many new unknown polymorphs may be found for A-site manganites under HPHT conditions, such as hexagonal perovskites, layered or oxygen deficient perovskite phases, unknown cation ordered derivatives of the parent corundum structure or further compositions with mixed anions, among many others. The already success on finding new materials with a variety of properties and compositions advocates to continue the search on this prolific playground of HPHT A-site manganites where many new compounds are envisaged.

References

- [1] E. Solana-Madruga, A. M. Arévalo-López, *Journal Solid State Chem.*, **315**, 123470 (2022)
- [2] M. Markkula *et al.*, *Phys. Rev. B* **84**, 94450 (2011)
- [3] A. M. Arévalo-López, J.P. Attfield, *Phys. Rev. B*, **88**, 104416 (2013)
- [4] E. Solana-Madruga *et al.* *Angew. Chem. Int. Ed.*, **55**, 9340–9344 (2016)
- [5] E. Solana-Madruga, *et al.* *Chem. Commun.*, **57**, 8441–8444 (2021)
- [6] E. Solana-Madruga *et al.* *Chem. Commun.*, **57**, 2511–2514 (2021)
- [7] A. M. Arévalo-López *et al.* *Angew. Chem. Int. Ed.*, **54**, 12074–12077 (2015)
- [8] A. M. Arévalo-López *et al.* *Chem. Commun.*, **52**, 5558–5560 (2016)
- [9] E. Solana-Madruga *et al.* *J. Mater. Chem. C*, **10**, 4336–4341 (2022)

In-situ characterization of gas-solid interfaces by near-ambient pressure X-ray photoelectron spectroscopy

M. Vorokhta¹, L. Piliai¹, T. N. Dinová¹, P. Matvija¹, I. Matolinová¹

¹ Department of Surface and Plasma Science, Faculty of Mathematics and Physics, Charles University, V Holešovičkách 2, 180 00 Prague, Czech Republic

* The corresponding author e-mail: vorokhtm@mbox.troja.mff.cuni.cz

Keywords: *in-situ/operando* study; ceria-based catalyst; low-temperature CO oxidation; propane oxidation; metal oxide gas sensor; gas sensing mechanism

A new laboratory for *in-situ/operando* studies of a gas-solid interface was recently built at the Department of Surface and Plasma Science of Charles University. The primary experimental technique in this laboratory is Near-Ambient Pressure X-ray Photoelectron Spectroscopy (NAP-XPS) which allows the chemical analysis of the surface of solid material, in the presence of a gas or vapor, at pressures in the mbar range. Information on the chemical state of surface atoms and the presence of adsorbate during exposure to gases is crucial in the field of heterogeneous catalysis to understand the mechanisms of chemical reactions and to optimize the composition of catalysts. Another area where NAP-XPS can be applied includes studying gas sensing mechanisms of gas.

In this work, we would like to report our recent results from the *in-situ* study of important industrial chemical reactions on the surface of ceria-based catalysts. To demonstrate the technique's capability and the importance of *in-situ* studies, we present the results from the study of low-temperature CO oxidation on the model Au/CeO₂(111) thin film catalyst and oxidation of propane and other large hydrocarbon molecules over a nanostructured Ru/CeO₂ powder-like catalyst. It is demonstrated that the Au/CeO₂ catalyst undergoes substantial chemical and morphological changes in CO oxidation operational conditions already at room temperature. At the same time, the hydrocarbon oxidation over Ru/CeO₂ revealed ruthenium oxidation into the volatile RuO₄, leading to its homogeneous redispersion inside the powder catalyst and increased catalytic activity.

Besides studies on ceria-based catalysts, we established a methodology that included XPS analysis of the sensor surface and measurements of its electrical resistance while controllably exposing it to different gases at high temperatures. The developed method was applied for studying ethanol and NO₂ (reducing and oxidizing agents) mechanisms on several nanostructured chemiresistors (SnO₂, Cu₂O, ZnO, and Zn-phthalocyanine-based ones). The information on the chemical state of surface atoms and the accumulation of different adsorbates during the detection process brought new insight into the existing theories of gas sensing.

References

- [1] O. Bezakrovny, M. Vorokhta et al., *J. Mater. Chem. A*, **10**, 16675–16684 (2022)
- [2] L. Piliai, P. Matvija, et al., *ACS Appl. Mater. Interfaces*, **14**, 56280–56289 (2022)
- [3] P. Hozák, M. Vorokhta, et al., *J. Phys. Chem. C*, **123**, 29739–29749 (2019)
- [4] M. Vorokhta, I. Khalakhan, et al., *Surf. Sci.*, **677**, 284–290 (2018)

Acknowledgments

This work was supported by the Czech Science Foundation (GAČR 20-13573S).

Bias-free graphene-based *in situ* TEM observation of electrode materials for batteries

IL10

J. Y. Cheong^{1*}, J. H. Chang²

¹ Bavarian Center for Battery Technology (BayBatt) and Department of Chemistry, University of Bayreuth, Universitätsstraße 30, 95447 Bayreuth, Germany;

² Department of Materials Science and Engineering, Korea Advanced Institute of Science and Technology, 291 Daehak-ro, Yuseong-gu, Daejeon, 305-701 Republic of Korea

* The corresponding author e-mail: Jun.Cheong@uni-bayreuth.de

Keywords: *in situ* TEM; graphene; liquid; solid; electrode

Real-time observation on the electrode materials during the electrochemical reaction is crucial to gain insights and knowledge on the advanced materials engineering for next-generation and advanced electrode materials. Amongst various *in situ* analytical tools, *in situ* TEM offers great advantage due to its multifunctional characterizations in (i) morphology and (ii) crystal structures & chemical state [1]. Since the initial work in *Science* to employ *in situ* TEM analysis to observe the dynamical changes that takes place in the electrode [2], a number of great works have been carried out on various electrode materials ranging from anode to cathode materials applied in lithium-ion batteries, solid state batteries, and metal-air batteries [3-5]. Conventional *in situ* TEM platform can be classified into two categories: i) solid-state *in situ* TEM method and ii) SiN_x-window based *in situ* TEM method. The former has a limitation in that it does resemble the liquid electrolyte environment that actual battery is in, while the latter has limitation in the high resolution imaging due to the thickness of SiN_x window. Moreover, both of these methods employ specialized TEM holder, which is costly and complicated. In this presentation, we would like to present an alternative *in situ* TEM platform that ensures both high resolution and bias-free *in situ* TEM platform based on graphene, which is facile to be implemented on the conventional TEM grid. The research progress and results will be discussed more in detail.

References

- [1] X. H. Liu, J. Y. Huang, *Energy Environ. Sci.*, **4**, 3844–3860 (2011)
- [2] J. Y. Huang, L. Zhong, C. M. Wang, J. P. Sullivan, S. X. Mao, N. S. Hudak, X. H. Liu, A. Subramanian, H. Fan, L. Qi, A. Kushima, J. Li, *Science*, **330**, 1515–1520 (2010)
- [3] Q. Su, J. Xie, J. Zhang, Y. Zhong, G. Du, B. Xu, *ACS Appl. Mater. Interfaces* **6**, 3016–3022 (2014)
- [4] Z. Wang, D. Santhanagopalan, W. Zhang, F. Wang, H. L. Xin, K. He, J. Li, N. Dudney, Y. S. Meng, *Nano Lett.* **16**, 3760–3767 (2016)
- [5] S. Han, C. Cai, F. Yang, Y. Zhu, Q. Sun, Y. G. Zhu, H. Li, H. Wang, Y. Shao-Horn, X. Sun, M. Gu, *ACS Nano* **14**, 3699–3677 (2020)

Acknowledgments

This work was supported by the funding from the Bavarian Center for Battery Technology (Baybatt) and the National Research Foundation of Korea grant (NRF-2017H1A2A1042006-Global Ph.D. Fellowship Program)).

Investigating the catalytic potential of iron-doped calcium titanate: a study of oxygen vacancy structures and microstructures

M. Amano Patino^{1*}, M. Ibrahim², N. Frederich², H. Kaper², M. Ceretti¹, W. Paulus¹

¹ ICGM, Univ. Montpellier, CNRS, ENSCM, Montpellier 34293, France;

² Saint-Gobain Research Provence, Cavaillon 84306, France

* The corresponding author e-mail: midori.amano-patino@umontpellier.fr

Keywords: perovskite materials; structural characterisation; oxygen vacancies; microstructure; catalytic activity

The presence of vacancies in the oxygen ion lattices of metal oxide materials profoundly affects their charge transport properties. In ABO_3 perovskites (where A and B are metal cations and O are oxygen ions), partially substituting B cations with lower valence ones (B') creates oxygen vacancies (**Fig. 1**). How such vacancies arrange in the structure affects the charge-carrier concentration and the materials' electronic band structure. [1,2] Here, we study $\text{Ca}(\text{Ti}_{1-x}\text{Fe}_x)\text{O}_{3-\delta}$ perovskite compounds, where $\text{Fe}^{3+/4+}$ cations substitute a fraction of the Ti^{4+} , yielding a deficiency δ in the oxygen stoichiometry.

Compositions of $\text{Ca}(\text{Ti}_{1-x}\text{Fe}_x)\text{O}_{3-\delta}$ with $x = 0.1-0.4$ are found to exhibit mixed ionic and electronic conductivity at surprisingly low temperatures. [3,4] Such promising charge transport properties, stability in reducing atmospheres, abundant component elements, and low toxicity make these materials ideal for electrochemical applications. [5] For example, they could be an alternative to CeO_2 -based materials in the heterogeneous catalysis of CO oxidation. However, relating the oxygen stoichiometry and distribution of oxygen vacancies with their charge transport properties remains a significant challenge.

Here we present our results from the preparation and thorough characterisation of the $\text{Ca}(\text{Ti}_{1-x}\text{Fe}_x)\text{O}_{3-\delta}$ ($x = 0.1-0.4$) materials. We discuss their catalytic activity toward CO oxidation and investigate their crystal structure, oxygen vacancy structure and microstructure in relation to their properties.

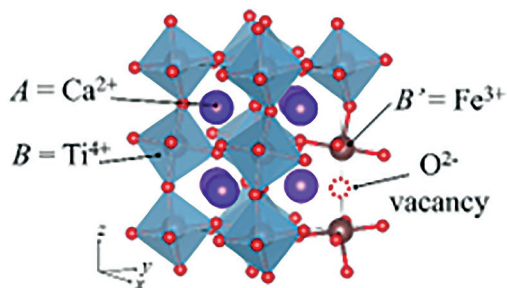


Fig. 1: Representation of the CaTiO_3 perovskite where vacancies can be produced by replacing Ti^{4+} with Fe^{3+} .

References

- [1] C. H. Park and D. J. Chadi, *Phys. Rev. B*, **57**, 13961–13964 (1998)
- [2] H. Cai, et al., *ACS Appl. Energy Mater.*, **5**, 11122–11132 (2022)
- [3] F. M. Figueiredo, et al. *Solid State Ionics*, **156**, 371–381 (2003)
- [4] M. Delporte, et al., *Inorganic Chemistry*, **61**, 15432–15443 (2022)
- [5] F. M. Figueiredo, et al., *Journal of Membrane Science*, **236**, 73–80 (2004)

Acknowledgments

This work is funded by the DESCARTES Project-ANR-20-CE08-0033.

Compositionally complex alloys for the hydrogen society

IL12

M. Sahlberg¹

¹ Department of Chemistry - Ångström Laboratory, Uppsala University, Sweden

* The corresponding author e-mail: martin.sahlberg@kemi.uu.se

Keywords: metal hydrides; neutron scattering; compositionally complex alloys; machine learning; materials design

Only two decades after their discovery, compositionally complex alloys or “high entropy alloys” (HEAs) have made great impact in science. Several materials, inspired by the results on metallic alloys have lately been introduced, e.g. nitrides and oxides. These alloys have been shown to have unique properties like exceptional tensile strength, hydrogen storage capacity, magneto-caloric effect etc. Many of these unique properties are believed to originate from the distorted structure leading to a high internal strain in HEAs. The research is focused on developing an understanding of structure-property relations in compositionally complex alloys and its potential for developing even higher performing alloys.

The research covers synthesis and evaluation of compositionally complex alloys as advanced materials, with emphasis on physical properties. This includes predicting materials properties, designing new compounds, determining internal strain, optimizing microstructure, advanced characterization etc. During this lecture, I will give a general introduction to high entropy alloys in the hydrogen society, followed by a discussion of recent results [1-2]. Focus will be on the use of X-ray and neutron scattering for the characterization.

References

- [1] G. Ek, M. M. Nygård, A. F. Pavan, J. Montero, P. F. Henry, M. H. Sørby, M. Witman, V. Stavila, C. Zlotca, B. C. Hauback, M. Sahlberg. *Inorg. Chem.* **60**, 1124–1132 (2021).
- [2] M. Witman, G. Ek, S. Ling, J. Chames, S. Agarwal, J. Chuan-Chi Wong, M. Allendorf, M. Sahlberg, V. Stavila. *Chemistry of Materials*, **33**, (2021)

Mineral-inspired sulphides for thermoelectric energy harvesting

A. V. Powell^{1,*}

¹ Department of Chemistry, University of Reading, Reading RG6 6DX, UK

* *The corresponding author e-mail: a.v.powell@reading.ac.uk*

Keywords: sulphides; thermoelectric; transport properties; bornite; chalcopyrite; kesterite

Thermoelectric (TE) devices, comprising an array of *n*- and *p*-type semiconductors, offer the unique capability to convert otherwise waste heat, directly into useful electrical energy. Device efficiency is dependent on the performance of the constituent *n*- and *p*-type materials, embodied in a figure-of-merit, $ZT = S^2\sigma T/\kappa$, where *S*, σ and κ are the Seebeck coefficient, electrical and thermal conductivity respectively. Our work focuses on mixed-metal sulphides for TE applications. The greater ($\times 10^5$) abundance of sulphur compared to that of tellurium, on which commercial Bi₂Te₃-based devices are based, makes sulphide-based devices attractive candidates for large-scale implementation of TE technology. Metal sulphides also show less degradation than Bi₂Te₃ at temperatures of much of the industrial waste heat. The polarizability of the sulphide anion also promotes cation mobility that can result in phonon-liquid electron-crystal (PLEC) behaviour that significantly reduces the thermal conductivity.

Here, recent investigations of synthetic analogues of sulphide minerals containing Earth-abundant elements will be described. This encompasses the use of chemical substitution to enhance the TE properties of a range of *p*-type materials related to tetrahedrite (Cu₁₂Sb₄S₁₃), bornite (Cu₅FeS₄) and kesterite/stannite (Cu₂ABS₄). Figures of merit in excess of $ZT = 0.5$ have been achieved at temperatures ($373 \leq T/K \leq 673$) relevant to energy harvesting from industrial waste heat, with those of substituted bornites reaching $ZT = 0.9$ at 550 K.

A significant barrier to the construction of an all-sulphide TE device is the inferior performance of *n*-type sulphides compared to their *p*-type counterparts. We have sought to address this, through a comprehensive investigation of chalcopyrite (CuFeS₂) related materials, containing the same tetrahedral CuS₄ building unit present in the high-performance binary copper sulphides. The presence of a second (Fe) cation suppresses the Cu-ion mobility that is responsible both for the high performance and the instability under operating conditions of the binary phases. We have sought to exploit substitution with high-valence cations, including Sn⁴⁺, Ge⁴⁺ and Cr³⁺, at copper and iron sites, to effect significant enhancements in charge-carrier concentration. While this has led to enhancement of TE properties by more than a factor of four over that of the parent phase, the substituted materials show an unexpected degree of complexity. Application of a range of state-of-the-art characterization and computational techniques reveals that this includes the formation of micro precipitates of substituent-rich phases, charge-localization through the formation of small polarons and changes in local structure. These results suggest an unexpected richness to composition-structure-property relations in *n*-type chalcopyrites and suggest future strategies for the development of *n*-type sulphides with enhanced performance.

Reaction mechanisms in molten salts for the design of solid-state materials at the nanoscale

IL14

D. Portehault¹, F. Igoa Saldaña^{1,2}, E. de Rolland Dalon¹, M. Baron¹, A. Ghoridi¹, A. Séné¹, E. Defoy¹, Y. Song¹, P.-O. Autran,³ D. Thiaudière⁴

¹ Laboratoire de chimie de la matière condensée de Paris, Sorbonne Université, CNRS, Paris, France;

² Institut de Minéralogie, de Physique des Matériaux et de Cosmochimie, Sorbonne Université, CNRS, MNHN, IRD Paris, France;

³ European Synchrotron Radiation Facility (ESRF), Grenoble, France;

⁴ Synchrotron SOLEIL, Gif-sur-Yvette, France

* *The corresponding author e-mail:* david.portehault@sorbonne-universite.fr

Keywords: molten salts; nanomaterials; borides; silicides; synthesis mechanisms; *in situ*; nanoparticles

Inorganic molten salts are non-volatile liquids stable at high temperatures, often up to 1000 °C and beyond. Performing chemical reactions in inorganic molten salts is a way to trigger reactivity in liquids at temperatures that usually pertain to solid-state reactions. This enables syntheses of unprecedented materials: new compounds, like oxychalcogenides, [1] and nano-objects of strongly covalent materials, like metal borides or silicides. [2-5] In most cases, the reaction mechanisms at play in molten salts are unknown, so that the key parameters enabling to tune reaction pathways and for instance phase selection are unidentified. Hence, it is increasingly important to shed light on crystallization pathways into inorganic molten salts.

In this talk, we will show how to tune the reactivity of nanoparticles in molten salts to deliver new nanomaterials of special interest for electrocatalysis applied to H₂ production from water and CO₂ reduction. We will especially focus on compounds of transition metals with boron and silicon [2,3] to demonstrate how new nanomaterials can be designed in molten salts, and we will discuss how synchrotron radiation, especially *in situ* X-ray diffraction and *in situ* X-ray absorption spectroscopy, unveil complex nucleation, growth and crystallization pathways in high temperature liquids.

References

- [1] X. Zhou, V. S. Chaitanya Kolluru, W. Xu, L. Wang, T. Chang, Y.-S. Chen, L. Yu, J. Wen, M. K. Y. Chan, D. Y. Chung, M. G. Kanatzidis *Nature*, **612**, 72-77 (2022)
- [2] D. Portehault, I. Gómez-Recio, M. A. Baron, V. Musumeci, C. Aymonier, V. Rouchon, Y. Le Godec, *Chem. Soc. Rev.*, **51**, 4828 (2022)
- [3] Y. Song, S. Casale, A. Miche, D. Montero, C. Laberty-Robert, D. Portehault, *J. Mater. Chem. A*, **10**, 1350 (2022)
- [4] G. Gouget, D. Bregiroux, R. Grosjean, D. Montero, S. Maier, F. Gascoin, C. Sanchez, D. Portehault, *Chem. Mater.*, **33**, 2099-2109 (2021)
- [5] F. Igoa Saldaña, E. Defoy, D. Janisch, G. Rousse, P.-O. Autran, A. Ghoridi, A. Séné, M. Baron, L. Suescun, Y. Le Godec, D. Portehault, *Inorg. Chem.*, **62**, 2073 (2023)

Acknowledgments

This work is supported by the European Research Council (ERC) Consolidator Grant GENESIS under the European Union's Horizon 2020 research and innovation programme (grant agreement n° 864850).

Nanostructured thin-film catalysts for hydrogen production via PEM water electrolysis

P. Kúš¹, T. Hrbek¹, H. Nedumkulam¹, M. Mirolo², I. Martens², J. Drnec², I. Matolínová¹

¹ Charles University, Faculty of Mathematics and Physics, Department of Surface and Plasma Science, V Holešovičkách 2, 180 00 Prague 8, Czech Republic

² European Synchrotron Radiation Facility, 71, avenue des Martyrs, CS 40220, 38043 Grenoble Cedex 9, France

* The corresponding author e-mail: peter.kus@mff.cuni.cz

Keywords: hydrogen; PEM water electrolysis; thin-film catalyst; magnetron sputtering; oxygen evolution reaction

Our society is progressively leaning towards utilization of renewable sources of energy. Moreover, recent conflict in Ukraine and consequent sanctions against Russia which affect the global gas trade further underline the necessity of a self-sustainable, less import-dependent energy policy. In this regard, the concept of the so-called Hydrogen Economy proves to be very promising. For its successful implementation, the efficiently working proton exchange membrane water electrolyzers (PEM-WEs) are essential. PEM-WEs use electrical power to drive electrochemical water splitting into hydrogen and oxygen. One of the top research priorities in this field is a significant reduction of noble metal dependence, predominantly on anode, through systematic studies of new materials. This talk will cover different approaches on how to improve the performance and durability of PEM-WE not only by employing new catalysts but also by modifying the membrane/catalyst interface. We will be focusing on magnetron sputtering as it is a very dependable, cost-effective, and industrially scalable method for depositing thin-film multielement catalysts and is also capable of enlarging the surface of PEM by so-called sputter-etching process. Finally, we will introduce several recent methods for operando analysis of membrane electrode assemblies within PEM-WE single cells which have potential to shed more light on complicated activity-stability relationship of novel catalytic materials.

References

- [1] T. Hrbek, P. Kúš, Y. Kosto, M. G. Rodríguez, I. Matolínová, *J. Power Sources*, **556**, 232375 (2023)
- [2] T. Hrbek, P. Kúš, T. Košutová, K. Veltruská, T. N. Dinhová, M. Dopita, V. Matolín, I. Matolínová, *Int. J. Hydrog. Energy*, **47** (49), 21033–21043 (2022)
- [3] T. Hrbek, P. Kúš, Y. Yakovlev, J. Nováková, Y. Lobko, I. Khalakhan, V. Matolín, I. Matolínová, *Int. J. Hydrog. Energy*, **45** (41), 20776–20786 (2020)

Acknowledgments

This work was supported by the Grant Agency of Charles University in Prague (GAUK No. 336922) and the project Mobility 8J23FR025.

Part IV

LECTURES

18th European
Conference
on Solid State
Chemistry

Negative linear compressibility of the hybrid perovskite $[\text{C}(\text{NH}_2)_3]\text{Er}(\text{HCO}_2)_2(\text{C}_2\text{O}_4)$

T. J. Hitchings¹, A. B. Cairns², D. Allen³, P. J. Saines¹

¹ School of Chemistry and Forensic Science, University of Kent, Canterbury, Kent, CT2 7NH, UK;

² Department of Materials, Imperial College London, South Kensington Campus, London, SW7 2AZ, UK;

³ Diamond Light Source Ltd., Harwell Science and Innovation Campus, Didcot, Oxfordshire, UK.

* The corresponding author e-mail: tjh55@kent.ac.uk

Keywords: hybrids, perovskite; high-pressure; crystallography; lanthanides

All solid-state systems should experience a decrease in crystal cell volume with applied hydrostatic pressure. This is due to the relationship of volume and pressure to Gibbs free energy being inversely proportional to each other. The overall cell volume must decrease to minimise the increase in Gibbs free energy. Some materials, however, exhibit the odd property known as negative linear compressibility (NLC), an expansion along one axis at the expense of a larger contraction in the perpendicular dimensions. Hybrid framework materials consist of metal nodes bridged by organic linkers and form a range of topologies with flexible mechanical properties, leading to more than 20 examples exhibiting NLC behaviour due to their mechanically flexible structures. [1,2] Frameworks with short linkers lack substantial porosity but have large enough voids to incorporate small organic cations, generating systems that are analogues of the ABX_3 inorganic perovskites. Such hybrid perovskites have been predicted to exhibit NLC, but to date, no hybrid perovskites have been found to have NLC experimentally [3,4]

A small family of hybrid perovskites, $[\text{A}]\text{Er}(\text{HCO}_2)_2(\text{C}_2\text{O}_4)$ where $[\text{A}]^+ = [\text{C}(\text{NH}_2)_3]^+$ and $[\text{C}(\text{NH}_2)_3]^+$ featuring monovalent and divalent organic linkers has recently been made. [5,6] These phases crystallise in the orthorhombic and monoclinic systems and exhibit negative thermal expansion. A recent variable pressure experiment on these hybrid perovskites found that $[\text{C}(\text{NH}_2)_3]\text{Er}(\text{HCO}_2)_2(\text{C}_2\text{O}_4)$ exhibited NLC behaviour, the first hybrid perovskite to do so. The isostructural $[(\text{CH}_3)_2\text{NH}_2]\text{Er}(\text{HCO}_2)_2(\text{C}_2\text{O}_4)$ system, however, did not exhibit NLC behaviour, instead undergoing a phase transition at moderately applied hydrostatic pressure. A comparison of these phases and their wine-rack-like structures allow the system requirements for NLC in them to be determined and used to further understand these strange behaviours.

References

- [1] Q. Zeng, K. Wang and B. Zou, *Langmuir*, **38**, 9031–9036 (2022)
- [2] A. B. Cairns and A. L. Goodwin, *Phys. Chem. Chem. Phys.*, **17**, 20449–20465 (2015)
- [3] Z. Yang, *et al.*, *Philos. Trans. R. Soc. A Math. Phys. Eng. Sci.*, **377**, 20180227 (2019)
- [4] P. S. Ghosh and I. Ponomareva, *J. Phys. Chem. Lett.*, **12**, 7560–7565 (2021)
- [5] L. G. Burley, *et al.*, *Dalt. Trans.*, **50**, 5437–5441 (2021)
- [6] L. G. Burley, *et al.*, *Eur. J. Inorg. Chem.*, **2021**, 3806–3811 (2021)

Acknowledgments

This work was supported by the EPSRC (EP/R011524/1) and Diamond Light Source.

Complex modulations of the crystal structure of functional oxides with perovskite-related structure

S. García-Martín^{1*}, R. Marín-Gamero¹, E. Urones-Garrote¹, X. Martínez de Irujo-Labalde²

¹ Inorganic Chemistry Department, Faculty of Chemistry, Complutense University, 28040 Madrid, Spain;

² Inorganic Chemistry Laboratory, Department of Chemistry, University of Oxford, Oxford OX1 3QR, United Kingdom.

* The corresponding author e-mail: sgmartin@uclm.es

Keywords: perovskite-type oxides; crystal structure determination; STEM and EELS with atomic resolution; magnetic properties; electrochemical properties

The compositional diversity of substitutional derivatives of ABO_3 perovskites is a testament to the flexibility of this crystal structure to accommodate different kinds of atoms within the A- or/and B-sublattice. Ordering at both A and B sites is a common mechanism to accommodate cations with different radii and/or oxidation states in the structure. In addition to atomic ordering, the perovskite structure admits a wide range of non-stoichiometry, not only in the anion sublattice but also within the A-sublattice. The non-stoichiometry is intimately related to the oxidation states of the B atoms. Therefore, both atomic ordering and non-stoichiometry highly impact the electronic structure of the perovskite-type oxides and consequently, their electric and magnetic properties.

We present in here the study of the crystal structure and properties of $Gd_{0.8-x}Ba_{0.8}Ca_{0.4+x}Fe_{2-y}M_yO_{6-\delta}$ layered perovskites with $M = Co, Ni$. We have used transmission electron microscopy methods with atomic resolution to solve the crystal structure [1-3]. The Ca-content highly affects the layered ordering of the atoms with the A positions. Substitution of Fe by Co or Ni results on partial ordering of the B atoms and modification of their coordination environment. The modulation of the crystal structure affects the oxygen content and location of anion vacancies leading to different superstructures with the corresponding impact on the electric, magnetic and electrochemical properties of the materials [1-4].

References

- [1] X. Martínez De Irujo-Labalde, D. Muñoz-Gil, E. Urones-Garrote, D. Ávila-Brandé, S. García-Martín, *J. Mater. Chem. A*, **4** (26), 10241–10247 (2016)
- [2] X. Martínez de Irujo-Labalde, M. Goto, E. Urones-Garrote, U. Amador, C. Ritter, M. E. Amano-Patino, A. Koedtrud, Z. Tan, Y. Shimakawa, S. García-Martín, *Chem. Mater.*, **31**, 5993–6000 (2019)
- [3] R. Marín-Gamero, X. Martínez de Irujo-Labalde, E. Urones-Garrote, S. García-Martín, *Inorg. Chem.*, **59**, 5529–5537 (2020)
- [4] X. Martínez de Irujo-Labalde, U. Amador, C. Ritter, M. Goto, M. E. Amano-Patino, Y. Shimakawa, S. García-Martín, *Inorg. Chem.*, **60**, 8027–8034 (2021)

Acknowledgments

This work was supported by the MICINN/AEI/10.13039/501100011033 funding the Project PID2019-106662RB-C44.

Perovskite-type RbNbO_3 as a High-pressure Polymorphism

A. Yamamoto^{1*}, K. Murase¹, K. Sugiyama², T. Kawamata²

¹ College of Eng. Shibaura Ins. Tech., 337-8570, Ohmiya, Japan;

² Ins. Mat. Res., Tohoku Univ., 980-8501, Sendai, Japan

* The corresponding author e-mail: ayako@shibaura-it.ac.jp

Keywords: perovskite; ferroelectrics; high-pressure phase; structural phase transition; thermal stability

A polymorphism of perovskite-type RbNbO_3 was obtained by a pressure-induced phase transition (Fig. 1). The high-temperature and high-pressure treatment effectively compacted the size of the relatively large alkaline ion, Rb^+ . The crystal structure refined by the single crystal X-ray analysis revealed that the distortion type of high-pressure phase (HPP)- RbNbO_3 is same as that of ferroelectric BaTiO_3 and KNbO_3 with an orthorhombic cell of space group $Amm2$. HPP- RbNbO_3 shows ferroelectricity at room temperature, proved by the second harmonic generation (SHG). The new perovskite-type niobate has the potential to high-performance functional-materials such as ferroelectrics, piezoelectrics, and optical devices.

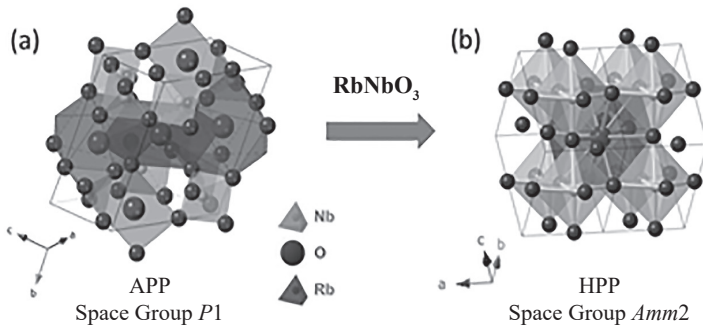


Figure 1: Phase transition of RbNbO_3 from ambient-pressure phase (APP) to high-pressure phase (HPP) with perovskite-type

Temperature-dependent structural phase transition of HPP- RbNbO_3 from an orthorhombic cell to a tetragonal one was observed similar to the transition of KNbO_3 [1] in high-temperature powder XRD patterns. Structural detail, ferroelectric property, and thermal stability of HPP- RbNbO_3 will be discussed in the presentation.

References

- [1] S. L. Skjærvø et al. Thermal evolution of the crystal structure and phase transitions of KNbO_3 . R. Soc. open sci. 5: 180368.

Acknowledgments

We thank Prof. Nobuyuki Inaguma of Gakusyuin University, Japan, for the SHG measurement. This work was supported by the Kazuchika Okura Memorial Foundation, Japan, and GIMRT program (202112-RDKGE-0008) of Institute of Materials Research, Tohoku University, Japan.

Chemical and physical pressure effects on structural and magnetic properties of $R_2\text{CuTiO}_6$ perovskite series with R ranging from La to Lu

L. Sederholm¹, A. Yamamoto², M. Karppinen¹

¹ Department of Chemistry and Materials Science, Aalto University, FI-00076 Espoo, Finland;

² Innovative Global Program, College of Eng. Shibaura Ins. Tech., 337-8570 Ohmiya, Japan

* The corresponding author e-mail: linda.sederholm@aalto.fi

Keywords: high-pressure effects; phase transformation; double perovskite; JT distortion

Double perovskite type oxides $A_2B'B''O_6$ with $3d$ transition metals at the B-site have attracted research attention for their potential magnetic properties [1]. Especially, the rare-earth element (R) based systems present a useful research platform for investigations of magnetic interactions and chemical ordering of the B-site as a function of the size of the R constituent. The $R_2\text{CuTiO}_6$ series with the Cu(II)/Ti(IV) B-site composition is particularly interesting as it combines a strongly Jahn-Teller active d^9 configuration known to promote B-site ordering, and a species completely lacking in d -electrons.

In conventional solid-state synthesis, only the larger R members of the series [La-Gd] form the perovskite structure, while the smaller R constituents induce the formation of phases with hexagonal symmetry [2]. However, through a high-pressure (HP) heat treatment (4 GPa, 1000 °C) these hexagonal phases can be converted to distorted perovskite-type structure [3]. Most interestingly, we observed signs of the very unusual, layered ordering of B-site cations for the thus HP-converted Y_2CuTiO_6 perovskite [4].

We discuss the chemical and physical pressure effects on the structural and magnetic properties of the $R_2\text{CuTiO}_6$ perovskite series within a wide R constituent range from Lu to La.

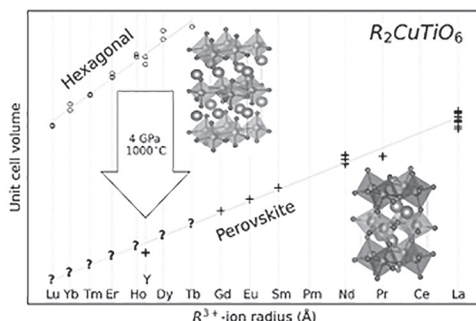


Figure: $R_2\text{CuTiO}_6$ compounds with hexagonal symmetry are expected to be converted to distorted perovskite-type structure under extreme pressure, following a linear correlation between unit cell volume and R -ion radius. [2]

References:

- [1] S. Vasala and M. Karppinen, $A_2B'B''O_6$ perovskites: A review, *Progress in Solid State Chemistry* **43**, 1 (2015).
- [2] N. Floros, J. T. Rijssenbeek, A. B. Martinson, K. R. Poeppelmeier, Structural study of $A_2\text{CuTiO}_6$ ($A = \text{Tb} - \text{Lu}$) compounds, *Solid State Sciences* **4** (2002) 1495–1498.
- [3] T. Tiittanen and M. Karppinen, Structure evolution upon chemical and physical pressure in $(\text{Sr}_{1-x}\text{Ba}_x)_2\text{FeSbO}_6$, *Journal of Solid State Chemistry* **246**, 245-251 (2017)
- [4] L. Sederholm, T. Tiittanen and M. Karppinen, High-pressure stabilisation of $R = \text{Y}$ member of $R_2\text{CuTiO}_6$ double perovskite series, *Journal of Solid State Chemistry* **317**, 123646 (2023).

Critical current density of $\text{Li}_6\text{PS}_5\text{Cl}$ powder pellets and processed films

A. Tron¹, A. Beutl¹

¹ AIT Austrian Institute of Technology GmbH, Center for Low-Emission Transport, Battery Technologies, Giefinggasse 2, 1210 Vienna, Austria;

* The corresponding author e-mail: artur.tron@ait.ac.at; +43 664 88904356

Keywords: argyrodite; $\text{Li}_6\text{PS}_5\text{Cl}$; critical current density; all-solid-state; lithium metal

All-solid-state batteries are regarded as one of the more promising technologies to improve safety and performance of current energy storage solutions. Especially the envisioned use of a metallic lithium anode could increase the energy density significantly. Li dendrite formation and the corresponding risk of internally shorting the battery cell is expected to be fully inhibited by using a thin, solid electrolyte sheet with high shear modulus [1].

Sulfide-electrolytes, especially the argyrodite family ($\text{Li}_6\text{PS}_5\text{X}$, X = Cl, Br) have attracted much attention for use in all-solid-state lithium batteries due to their high ionic conductivity ($> 1 \text{ mS cm}^{-1}$, RT) and feasible processability [2]. Although they also offer high mechanical stability [3], lithium dendrite growth remains an issue for cells employing this material. Especially, thin sheets prepared by combination of the electrolyte powder with a suitable binder suffer from a decrease in the electrochemical and mechanical performance.

Thus, the practicality of sulfide-electrolytes for use in battery cells with relevant power output is still a matter of debate. One key parameter to evaluate this materials class in more detail is the critical current density, i.e. the maximum current that can be applied to a battery cell without excessive Li dendrite formation. It is frequently determined in literature, however, due to the non-standard evaluation, the obtained data often lacks comparability and meaning (e.g. too low areal capacities are used, limiting conditions are not clarified). Many parameters which have a significant impact on the obtained critical current density are not controlled or reported [4].

Therefore, we conducted a series of systematic investigations on the critical current density of pressed $\text{Li}_6\text{PS}_5\text{Cl}$ powder pellets as well as processed films. First, the influences of the measurement procedure (step vs. continuous), cell setup (casing, Li source), and sample geometry (thickness, diameter) on the obtained critical current densities were determined. Then, powder pellets and films were tested using a set of optimized parameters. Thus, the practicality and limits of the $\text{Li}_6\text{PS}_5\text{Cl}$ solid-electrolyte for use in battery cells has been evaluated.

References

- [1] X. Ke, Y. Wang, G. Ren, *Energy Storage Materials*, **26**, 313–324 (2020)
- [2] C. Yu, F. Zhao, J. Luo, L. Zhang, X. Sun, *Nano Energy*, **83**, 105858 (2021)
- [3] D. K. Singh, A. Henss, B. Mogwitz, A. Gautam, J. Horn, T. Krauskopf, S. Burkhardt, J. Sann, F. H. Richter, J. Janek, *Cell Reports Physical Science*, **3**, 101043 (2022)
- [4] Y. Lu, C.-Z. Zhao, H. Yuan, X.-B. Cheng, J.-Q. Huang, Q. Zhang, *Adv. Funct. Mater.*, **31**, 2009925 (2021)

Acknowledgments

This project has received funding from the European Union's Horizon 2020 research and innovation program under Grant Agreement No. 875028 (SUBLIME Project).

Quantum spin liquids in cation ordered perovskites

L06

M. J. Milton¹, P. Manuel², J. P. Attfield¹

¹ School of Chemistry, University of Edinburgh, Edinburgh EH9 3JZ, UK;

² ISIS Facility, Rutherford Appleton Laboratory, Harwell Oxford, Didcot OX11 0QX, UK

* The corresponding author e-mail: m.j.milton@sms.ed.ac.uk

Keywords: perovskite; quantum material; quantum spin liquid; metal oxides; high pressure

Quantum spin liquids (QSL) are an elusive, highly nontrivial state of matter that are expected to display a variety of novel and exotic properties such as spin fractionalisation and long range entanglement. QSL are predicted to arise in low dimensional magnetic materials that have high degrees of frustration and small spin quantum number values, theoretically allowing for quantum fluctuations to persist at zero Kelvin and thus destabilize long range magnetic order. QSL are believed to hold great applications for future quantum computing and communication due to their rich physics, however experimental identification remains a challenge [1]. We have attempted to realise and characterise QSL materials using $\text{Ba}_3\text{BRu}_2\text{O}_9$ perovskites. High-pressure high-temperature treatment can be used to induce a transformation from an ambient pressure 6H structure to a trigonal $P\bar{3}m1$ ($\text{Ba}_3\text{SrTa}_2\text{O}_9$ – type) structure [2] (**Fig. 1**). This generates cation ordered layers of BO_6 and RuO_6 octahedra in a 1:2 ratio in the cubic [111] direction, generating a honeycomb lattice of magnetic Ru cations. This structure provides a 2D frustrated magnetic system, and the strong spin-orbit coupling of Ru will lower the effective j state of the system, making these materials promising potential QSL candidates.

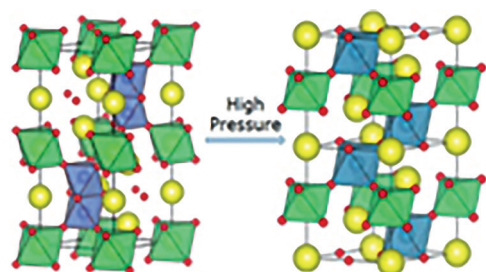


Figure 1:
(left) Hexagonal perovskite ($P6_3/mmc$)
(right) $3C_{1,2}$ cation ordered perovskite ($P\bar{3}m1$)

We have successfully synthesised polycrystalline $3C_{1,2}$ $\text{Ba}_3\text{BRu}_2\text{O}_9$ perovskites (B = Ca and Mg). The magnetic properties for both samples show very promising QSL behaviour, magnetisation shows no magnetic order transitions or hysteresis down to 2K, and an effective paramagnetic moments of around $1.0 \mu_B/\text{Ru}^{5+}$, much reduced from the spin only moment of $3.87 \mu_B$. Heat capacity down to 50 mK further supported the absence of any ordering, and integration of C_{mag}/T shows that the $S = 3/2\text{Ru}^{5+}$ spin entropy for $3C_{1,2}$ - $\text{Ba}_3\text{CaRu}_2\text{O}_9$ is released up to approximately 80 K, which is in keeping the Weiss temperature of -35 K. TOF PND confirmed that there was no long range ordering or structural transitions down to 1.5 K in both samples, making these materials promising quantum spin liquid candidates.

References

- [1] Rijssenbeek, J, T, Poepelmeier, R, K. (2005) *J. Am. Chem. Soc.*, 127, pg. 675–681.
- [2] Takagi, H. Takayama, T, Jackeli, G, Nagler, S. (2019) *Nature Reviews Physics*, 1(4), pg. 264–280.

Lithium transport mechanisms characterised by ssNMR and ToF-SIMS in hybrid electrolytes for solid-state batteries

T. Meyer¹, T. Gutel², M. Bardet³, H. Manzanarez², E. De Vito¹

¹ Univ. Grenoble Alpes, France, CEA, Liten, DTNM, 38000, Grenoble, France;

² Univ. Grenoble Alpes, CEA, Liten, DEHT, 38000 Grenoble, France;

³ Univ. Grenoble Alpes, CEA, IRIG, MEM, 38000, Grenoble, France

* The corresponding author e-mail: thomas.meyer@cea.fr

Keywords: composite solid electrolyte; lithium isotopes; modelling; ssNMR, ToF-SIMS

Battery manufacturers aim at designing safe cells with high energy density. To reach this goal, liquid electrolytes could be replaced by composite solid-state electrolytes.[1,2] It would allow to combine advantages of different materials: the straightforward implementation of a ionic conducting polymer that offers good interfaces with the electrodes and the high ionic conductivity of ceramics. Implemented characterisation methodologies based on ⁶Li-labelling accurately estimate lithium isotopic abundances. Time of Flight Secondary Ion Mass Spectrometry (ToF-SIMS) analyses consist in performing surface measurements of molecular fragments with a micrometric lateral resolution enabling a mapping of lithium isotopic abundance over a range of several millimetres. ⁶Li solid-state Nuclear Magnetic Resonance spectroscopy (ssNMR) analyses provide global information on lithium ion chemical environments and quantitative experiments can lead to the determination of absolute lithium isotopes concentrations. The selective introduction of ⁶Li-enriched components, such as a metal foil, allows to track lithium diffusion. By coupling these techniques, spontaneous lithium self-diffusion was measured through a polymer membrane at 60°C. Here, ⁶Li⁺ ions diffusion was characterised through different devices after galvanostatic cycling. The chosen materials were a garnet-type ceramic, Li_{6,4}La₃Zr_{1,4}Ta_{0,6}O₁₂ and a well-known polymer, poly(ethylene oxide) containing lithium bis(trifluoromethylsulfonyl)imide as a lithium salt. [3] ToF-SIMS analyses gave access to its evolution throughout the ceramic depth, whereas NMR analyses offered global lithium isotopic abundance of the different materials. By studying lithium diffusion paths, diffusion mechanisms were proposed. Numerical simulations helped to confirm the experimental results and led to diffusion coefficient values coherent with literature.

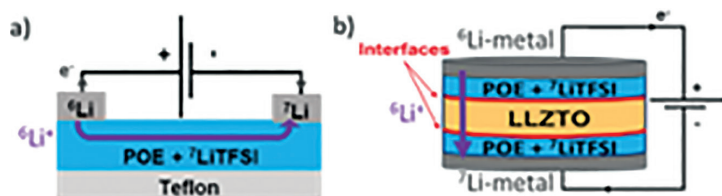


Figure:

- a) Polymer electrolyte
b) System composed of a ceramic pellet sandwiched within two polymer layers

[1] F. Zheng et al., *Journal of Power Sources*, 10, 4113–4120, (2018)

[2] S. Li et al., *Advanced Science*, 389, 198–213, (2020)

[3] A. Gupta and J. Sakamoto, *The Electrochemical Society Interface*, 11, 14463–14477, (2019)

Acknowledgments

Part of this work, carried out on the Platform for Nanocharacterisation (PFNC), was supported by the “Recherches Technologiques de Base” program of the French National Research Agency (ANR).

Packings of Sphere Packings – a New Path to Solid State Ionic Conductors?

M. Petrik^{1*}, W. Hornfeck²

¹ Formerly Philipps-Universität Marburg, Vogelsbergstraße 13, 35043 Marburg, Germany;

² FZU, Institute of Physics of the Czech Academy of Sciences,
Cukrovarnická 10/112, 162 00 Prague 6, Czech Republic

* The corresponding author e-mail: spherepacker@gmail.com

Keywords: solid state ionic conductors; sphere packings; packings of sphere packings; PSP; rechargeable batteries; structure-properties correlations; superionic conductors

When hard spheres of equal size are packed together in space – meaning that any two spheres in the packing are connected by an uninterrupted path of close contacts – then this is a classical sphere packing. When, by analogy, entire sphere packings are imagined to be packed together – so that they interpenetrate each other and, without distortion, establish contact with each other – then this is what we call a *packing* of sphere packings (PSP) [1]. Note that the requirement of contact between the interpenetrating sphere packings rules out commonly known interpenetrating nets like MgCu₂ or Cu₂O.

Since the discovery of the first PSP (in the course of theoretical work on the β -manganese structure) [2] dozens of further PSPs have emerged and we have set up an online compilation, issuing at the same time a call for public contributions of new PSPs [3]. In view of the growing number of known PSPs the purpose of the present contribution is to call attention to the possibility that PSPs might provide new structural motifs conducive to free movement of ions in the solid state. A novel approach in the current quest for solid state ionic conductors applicable in rechargeable batteries is thus proposed.

We disregard the chemistry involved and consider only the structural aspects. Obviously a structure which permits free movement of ions must possess a sufficient degree of “openness” in the form of channels through which ions may pass unobstructedly. Now, the very nature of PSPs demands that already the primary sphere packings themselves possess a major degree of “openness” in order to leave enough room for interpenetration. But – and this is the point to be stressed here – even after interpenetration of the primary sphere packings it turns out that enough interconnected free space may still remain in the resulting PSP.

Two classic examples of superionic conductors illustrate this fact. (i) The structure of α -AgI (an intermediate-temperature silver ion conductor) is a PSP of iodine atoms – designated as PSP-1^[3] and consisting of two identical primary packings of the diamond type – in which a three-dimensional framework of channels remains open for the silver atoms to pass along freely. (ii) The structure of RbAg₄I₅ (a room-temperature silver ion conductor) is a PSP again of iodine atoms – now constituting a complex structure isopointal with β -manganese designated as PSP-5^[3] and built of two different primary packings – where again silver ions move freely in a three-dimensional framework of open channels.

References

- [1] M. Petrik, W. Hornfeck, *Z. Anorg. Allg. Chem.*, **642**, 1023 (2016)
- [2] M. Petrik, W. Hornfeck, B. Harbrecht, *Z. Anorg. Allg. Chem.*, **640**, 2328 (2014)
- [3] <https://spherepacker.github.io/welcome.html>, under “Sphere Packings.”

Growth of metal oxide film electrodes for electrochemical capacitor by electrospray deposition

M. P. Chavhan^{1*}

¹ Faculty of Science, University of Ostrava, 30. dubna 22, Ostrava, 701 03, Czech Republic

* The corresponding author e-mail: Madhav.Chavhan@osu.cz

Keywords: supercapacitor; electrospray; calcination; electrochemical oxidation; mixed metal oxide

With growing emphasis on energy storage, and use of renewable energy, the electrochemical capacitors (ECs) gained significant attention over the past decades. For efficient charge transport in ECs, all the internal area of the electrode must be accessed by the ions from the electrolyte with minimum resistance. The electrodes of ECs are generally made by mixing the active material with binder and laying the slurry over current collectors. This work addresses an alternative binder-free method of electrode fabrication using electrospray deposition of metal precursors over current collectors, followed by thermal calcination [1]. The electrochemical performances of such metal oxide film electrodes are analyzed with respect to precursor concentrations used during the electrospray experiment, and the different calcination temperatures used for the growth of Ni, Co, and Mn oxides in a film. The synergy between these mixed oxides in a composite form of electrodes was investigated. Further, the electrochemical activation of such electrodes was studied using multiple cyclic voltammetry experiments. The electrodes were assembled in a hybrid/asymmetric cell using carbon film as counter electrodes, developed by the same method [2]. The maximum specific energy obtained from such ECs is found at the level of 60 Wh kg⁻¹ corresponding to a specific power of 5000 W kg⁻¹. The electrospray technique utilised in this work is inexpensive, simple, operate at room temperature, and thus, can be easily scale-up for developing electrodes for next-generation energy storage devices.

References

- [1] M. P. Chavhan, S. R. Sethi, S. Ganguly, *Ind. Eng. Chem. Res.*, **59**, 4428–4436 (2020)
- [2] M. P. Chavhan, S. Ganguly, *Ind. Eng. Chem. Res.*, **55**, 10073–10083 (2016)

New tungsten bronzes via electrochemical intercalation

L10

B. Rasche¹, **I. Neumann**¹, **Y. Chen**², **M. Yang**²

¹ University of Cologne, Department of Chemistry, Greinstr. 6, Cologne/D;

² University of Oxford, Oxford/UK;

* The corresponding author e-mail: bertold.rasche@uni-koeln.de

Keywords: tungsten bronzes; electrochemistry; intercalation; superconductivity; *in-situ* diffract

The class of alkali tungsten bronzes is well-known for its superconducting properties. [1] Nevertheless, some superconducting phase diagrams have been investigated only recently and hint toward composition depend properties. [2] Indeed, the broad phase width of the tungsten oxide host structure already indicates the flexibility concerning the electron count in these systems. [3]

In this contribution we demonstrate that electro-reduction of tungsten oxide WO_3 in aqueous alkali metal solutions leads to so far unknown phases. [4] Amongst others, in case of potassium, *in-situ* synchrotron powder X-ray diffraction unravels the concomitant structural changes (**Fig. 1**), and reveals two new bronzes K_xWO_3 with $x_{\text{phase1}} \approx 0.1$ (space group $P4/nmm$) and $x_{\text{phase2}} \approx 0.3$ (space group $\bar{I}43m$). Both structures are perovskite-derived, which so far only has been reported for the smaller cations' sodium or lithium. [5] Accessing this structure type seems only possible by the electrochemical reduction, demonstrating the versatility of the electrochemical approach.

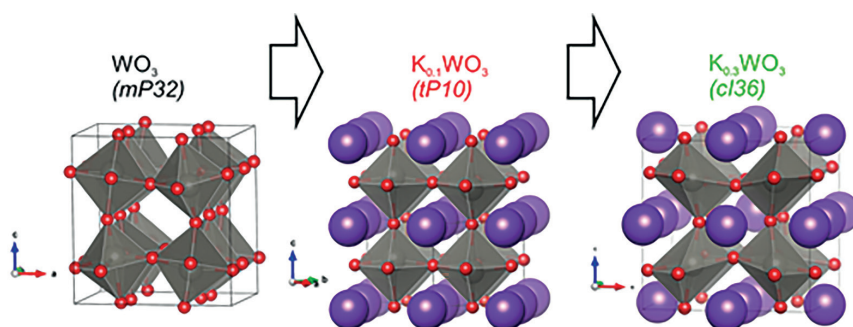


Figure 1: Structures (composition; Pearson symbol in brackets) as determined from *in-situ* X-ray diffraction during the electro-reduction of WO_3 in a KCl solution.

References

- [1] A. R. Sweedler, Ch. J. Raub, B. T. Matthias, *Physics Letters* **15**, 108–109 (1965).
- [2] N. Haldolaarachchige, Q. Gibson, J. Krizan, R. J. Cava, *Phys. Rev. B* **89**, 104520 (2014).
- [3] Landolt-Börnstein – *Group IV Physical Chemistry: Ni-Np – Pt-Zr*. vol. 5i (1998).
- [4] Y. Chen, et al. *ChemElectroChem* **7**, 3160–3167 (2020).
- [5] L. Bartha, A. B. Kiss, Szalay, *Int. J. Refract. Met. H.* **13**, 77–91 (1995).

Acknowledgments

We thank Dr Joshaniel Cooper and Dr. Claire Murray for their support at DIAMOND. This work was carried out with the support of the Diamond Light Source, instrument I11 (proposal CY24021-1). IN and BR acknowledge support by the “Fond der Chemischen Industrie” (FCI) via a Liebig-Group.

Composition-activity-stability relationship in Pt-Au alloys for oxygen reduction reaction

X. X. Xie¹, V. Briega-Martos², R. Farris³, M. Vorokhta¹, T. Skála¹, I. Matolínová¹, K. M. Neyman³, S. Cherevko², I. Khalakhan^{1*}

¹ Charles University, Faculty of Mathematics and Physics, Department of Surface and Plasma Science, V Holešovičkách 2, 18000 Prague 8, Czech Republic;

² Forschungszentrum Jülich GmbH, Helmholtz Institute Erlangen-Nürnberg for Renewable Energy (IEK-11), Cauerstr. 1, 91058 Erlangen, Germany;

³ Departament de Ciència de Materials i Química Física & Institut de Química Teòrica i Computacional (IQTCUB),

Universitat de Barcelona, c/Martí i Franquès 1, 08028 Barcelona, Spain

* The corresponding author e-mail: khalakhan@gmail.com

Keywords: fuel cells; oxygen reduction reaction; platinum dissolution; PtAu alloy; activity-stability relationship

Stabilizing cathode catalysts in hydrogen-fuelled proton-exchange membrane fuel cells (PEMFCs) is paramount to their widespread commercialization [1]. Incorporating specific elements into platinum catalysts has been recently proven favorable for their stability by inhibiting platinum dissolution. Among alloying elements, gold has been reported as one of the most promising choices so far [2]. However, a significant drawback exists. The gold is inactive for the oxygen reduction reaction (ORR) running at PEMFC cathode. Moreover, its alloying with Pt makes it unfavorable for ORR geometrical modifications. The effectiveness of Pt–Au for both activity and stability thus strongly depends on the alloy structure as well as the compositional profile and, therefore, should be balanced through precise catalyst engineering.

Targeting that aim, Pt–Au alloy catalysts with various compositions (Pt₉₅Au₀₅, Pt₉₀Au₁₀, and Pt₈₀Au₂₀) prepared by magnetron sputtering were investigated [3]. The promising stability improvement of PtAu catalyst, manifested in suppressed platinum dissolution with increasing Au content, was confirmed over an extended potential range up to 1.5 V_{RHE}. On the other hand, at elevated concentrations Au showed a detrimental effect on ORR activity. A systematic study involving a set of complementary characterization techniques, and electrochemistry enabled us to gain a comprehensive understanding of the composition-activity-stability relationship to find an optimum PtAu alloying for maintaining the activity of platinum and improving its resistance to dissolution.

References

- [1] X. X. Wang, M. T. Swihart, G. Wu, *Nat Catal*, **2**, 578–589 (2019)
- [2] P. P. Lopes, D. G. Li, H. F. Lv, *Nat. Mater*, **19**, 1207 (2020)
- [3] X. Xie, V. Briega-Martos, R. Farris, *ACS Appl. Mater. Interfaces*, **15**, 1192–1200 (2023)

Acknowledgments

This work was supported by Czech Science Foundation, project No. 22-03643S.

Metal-insulator transitions in hollandite vanadate and chromate

M. Isobe^{1*}, P. Puphal¹, H. Takagi¹

¹ Max Planck Institute for Solid State Research, Heisenbergstraße 1, 70569 Stuttgart, Germany

* The corresponding author e-mail: m.isobe@fkf.mpg.de

Keywords: hollandite; high-pressure synthesis; metal-insulator transition; charge ordering; ferromagnetic transition; topological phase transition

Hollandite is the name of a mineral. The structure of hollandite $A_2M_8O_{16}$ consists of a tubular M_8O_{16} -framework and A cations. The framework is closely related to the structure of rutile MO_2 , only that the single chains in the rutile phase are replaced here by double chains. Hollandite $A_2M_8O_{16}$ has a mixed valence state of the M cation and can be considered as the doped rutile MO_2 . Hollandite vanadates and chromates are not so easy to synthesize as they require high-pressure synthesis. Interestingly they exhibit metal-insulator transitions at low temperature.

The hollandite vanadate $K_2V_8O_{16}$, like the other mixed-valent vanadates, exhibits the metal-insulator transition due to charge ordering. Interestingly, the charge-ordering pattern is similar to that of doped VO_2 . Furthermore, it does not show any magnetic ordering at low temperature. We therefore suggest that it could be the one-dimensional magnet at low temperature [1].

In the hollandite chromate $K_2Cr_8O_{16}$, we have observed a ferromagnetic transition at 180 K and a metal-insulator transition at 95 K [2]. This compound exhibits paramagnetic metal, ferromagnetic metal and ferromagnetic insulator phases with decreasing temperature. We have studied this interesting compound using various measurements and theoretical calculations. Due to the mixed valence of Cr, we expected the metal-insulator transition to have a charge-ordering origin, but found it not to be the case using crystal structure analysis. In conclusion, it has been considered that the ferromagnetism arises from a double exchange mechanism and the metal-insulator transition arises from a Peierls transition [3]. Recently we have successfully synthesized the sister compound $Rb_2Cr_8O_{16}$. We will compare to the physical properties of the two compounds.

References

- [1] A. C. Komarek M. Isobe, *et al.*, *Phys. Rev. Lett.* **107**, 027201 (2011).
- [2] K. Hasegawa, M. Isobe, *et al.*, *Phys. Rev. Lett.* **103**, 146403(2009).
- [3] P. A. Bhobe, *et al.*, *Phys. Rev. X* **5**, (2015) 041004.

Fluoridoargentates(II) as potential analogues to superconducting cuprates

M. Dragomir^{1,2}, M. Belak Vivod^{1,2}, M. Lozinšek^{1,2}, Z. Jagličič^{3,4}, G. King⁵

¹ Jožef Stefan Institute, Jamova cesta 39, 1000 Ljubljana, Slovenia;

² Jožef Stefan International Postgraduate School, Jamova cesta 39, 1000 Ljubljana, Slovenia;

³ Institute of Mathematics, Physics and Mechanics, Jadranska 19, 1000 Ljubljana, Slovenia;

⁴ Faculty of Civil and Geodetic Engineering, University of Ljubljana, Jamova 2, 1000 Ljubljana, Slovenia;

⁵ Canadian Light Source, 44 Innovation Blvd, Saskatoon, SK S7N 2V3, Canada

* The corresponding author e-mail: mirela.dragomir@ijs.si

Keywords: mechanochemistry; fluorides, silver(II); fluoridoargentates(II); superconductors

In the last three decades, several attempts have been made to replicate the superconductivity observed in cuprates with transition metals other than Cu^{2+} [1-4]. One very promising element is Ni, the left neighbour of Cu in the periodic table. The first nickelate superconductor was synthesised in 2019 in the form of epitaxial thin films [1] although it was made 20 years after its theoretical prediction [5]. Moreover, nickelates now have the potential to open a new era in the field of superconductivity – the *nickelate age*.

With a $4d^9$ electronic configuration and $S = 1/2$, Ag^{2+} , has also been recognised as a promising Cu^{2+} analogue [3,4]. However, the chemistry of Ag^{2+} is slower to develop because this species is extremely reactive, photosensitive, and moisture sensitive. Moreover, the thermodynamic stability of Ag^{2+} mostly limits its chemistry to compounds in which this cation is present in a fluorine environment, making the synthesis, handling and the study of such systems very challenging. In addition, AgF_2 is insoluble even in anhydrous HF and decomposes at very low temperatures, limiting the synthetic routes for Ag^{2+} materials, fluoridoargentates(II).

This contribution includes our recent results on the synthesis of new Ag^{2+} -based materials. I will present our efforts to use mechanochemistry as an alternative synthetic route for fluoridoargentates(II) and discuss their structural and magnetic properties. Using ball mills we have synthesised a series of new Ag^{2+} -based compounds and characterised them with high-resolution powder X-ray diffraction, single-crystal diffraction, magnetic susceptibility, neutron diffraction, and Raman spectroscopy.

We hope that these results will help expand the chemistry of Ag^{2+} and bring us closer to a silver analogue of cuprate superconductors and other exotic magnetic materials.

References

- [1] D. Li, K. Lee, B. Y. Wang, M. Osada, S. Crossley, H. R. Lee, Y. Cui, Y. Hikita, H. Y. Hwang, *Nature*, **572**, 624–627 (2019).
- [2] F. Wang, T. Senthil. *Phys. Rev. Lett.*, **106**, 136402 (2011).
- [3] J. Gawraczyński, D. Kurzydłowski, R. A. Ewings, S. Bandaru, W. Gadomski, Z. Mazej, G. Ruani, I. Bergenti, T. Jaroń, A. Ozarowski, S. Hill, P. J. Leszczyński, K. Tokár, M. Derzsi, P. Barone, K. Wohlfeld, J. Lorenzana, W. Grochala, *Proc. Natl. Acad. Sci. U.S.A.*, **116**, 1495–1500 (2019).
- [4] W. Grochala, R. Hoffmann. *Angew. Chem. Int. Ed. Engl.*, **40**, 2742–2781 (2001).
- [5] V. I. Anisimov, D. Bukhvalov, T. M. Rice. *Phys. Rev. B*, **59**, 7901–7906 (1999).

Acknowledgments

This work was supported by the Slovenian Research Agency (J2-2496).3

FeMn₃Ge₂Sn₇O₁₆: a “Partial” spin-liquid candidate with a perfectly isotropic 2-D kagomé lattice

L14

C. D. Ling¹, M. C. Allison^{1,2}, S. Wurmehl², B. Büchner², J. L. Vella³, T. Söhnle³, S. A. Bräuninger⁴, H.-H. Klauss⁴

¹ The University of Sydney, Sydney, Australia;

² Leibniz IFW Dresden, Dresden, Germany;

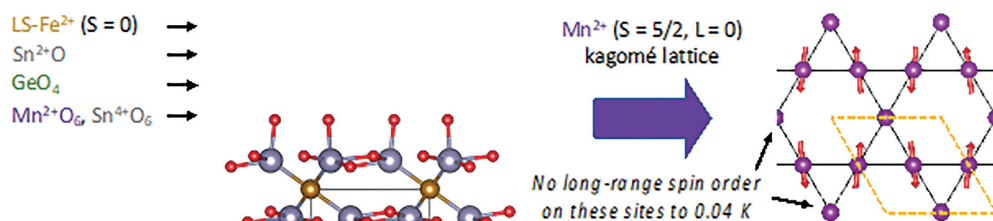
³ The University of Auckland, Auckland, New Zealand;

⁴ University of Dresden, Dresden, Germany

* The corresponding author e-mail: chris.ling@sydney.edu.au

Keywords: kagomé; spin-liquid; neutron scattering; layered composite; magnetism

FeMn₃Ge₂Sn₇O₁₆ [1] is a fully ordered stoichiometric phase with a complex composite layered structure that incorporates an undistorted hexagonal kagomé lattice of Mn²⁺ cations. Its discovery expands the chemistry of the hitherto singular FeFe₃Si₂Sn₇O₁₆ structure type [2] and improves on the perfection of its kagomé lattice by replacing anisotropic high-spin Fe²⁺ (d⁶, L = 2) with isotropic high-spin Mn²⁺ (d⁵, L = 0), achieved by the size-matched replacement of SiO₄⁴⁻ with GeO₄⁴⁻ polyanions in the bridging layer. Single-ion anisotropy of HS Fe²⁺ sites was suspected of playing a role in the unique “striped” magnetic structure of FeFe₃Si₂Sn₇O₁₆ below T_N = 3.5 K, [3] which breaks hexagonal symmetry and leaves 1/3 of the spins geometrically frustrated in an apparent “partial spin-liquid” state down to at least 40 mK. We can now rule that out by observing the same magnetic structure in FeMn₃Ge₂Sn₇O₁₆. We will discuss the potential for further chemical variation and physical modification, and present new neutron scattering data that shed light on the nature of the magnetic ground state.



References

- [1] M. C. Allison, S. Wurmehl, B. Büchner, J. L. Vella, T. Söhnle, S. A. Bräuninger, H.-H. Klauss, M. Avdeev, F. P. Marlton, S. A. Schmid, *Chem. Mater.* **34**, 1369–1375 (2022)
- [2] T. Söhnle, P. Böttcher, W. Reichelt, F. E. Wagner, *Z. Anorg. Allg. Chem.* **624**, 708–714 (1998)
- [3] C. D. Ling, M. C. Allison, S. A. Schmid, M. Avdeev, J. S. Gardner, C. W. Wang, D. H. Ryan, M. Zbiri, T. Söhnle, *Phys. Rev. B* **9**, 180410 (2017)

Acknowledgments

This work was supported by the Alexander von Humboldt Foundation (Friedrich Wilhelm Bessel Award), Deutsche Forschungsgemeinschaft, and the Australian Research Council.

Hidden orders in 2D van der Waals materials: the example of magnetic crossover in the mixed-anion compound CrSBr

S. A. López-Paz¹, Z. Guguchia², V. Y. Pomjakushin³, C. Witteveen¹, A. Cervellino⁴, H. Luetkens², N. Casati⁴, A. F. Morpurgo¹, F. O. von Rohr¹

¹ Department of Quantum Matter Physics, University of Geneva, CH-1211 Geneva, Switzerland;

² Laboratory for Muon Spin Spectroscopy, Paul Scherrer Institute, CH-5232 Villigen PSI, Switzerland;

³ Laboratory for Neutron Scattering and Imaging, Paul Scherrer Institute, CH-5232 Villigen PSI, Switzerland;

⁴ Laboratory for Synchrotron Radiation - Condensed Matter, Paul Scherrer Institute, CH-5232 Villigen, Switzerland

* The corresponding author e-mail: sara.lopezpaz@unige.ch

Keywords: 2D materials; van der Waals magnets; mixed-anion chemistry; quantum materials; spintronics

Two-dimensional (2D) materials that display intrinsic long-range magnetic order hold the promise to open up new avenues for the electrical manipulation of spins for use in next generation quantum technologies [1]. The mixed-anion van der Waals antiferromagnet CrSBr stands out as an interesting platform to enlarge the functionalities of 2D magnetic materials. This material combines a high magnetic critical temperature ($T_N \approx 140$ K), exotic magneto-transport properties, and complex mixed-anion chemistry [2-4]. Furthermore, an anomalous change on the sign of the magnetoresistance below $T^* = 40$ K hints at an exotic low-temperature hidden order in CrSBr.

Here, we present our results on the synthesis and the temperature-dependent structural, as well as magnetic properties of CrSBr by combining neutron powder diffraction (NPD), synchrotron X-ray diffraction (synchrotron XRD), muon spin relaxation spectroscopy (μ SR), and magnetization measurements. We evidence that CrSBr undergoes a transition to an A-type antiferromagnetic state below $T_N \approx 140$ K with a pronounced two-dimensional character, preceded by ferromagnetic correlations within the monolayers. Furthermore, we unravel the low-temperature hidden-order within the long-range magnetically ordered state. We find that it is associated to a slowing down of the magnetic fluctuations, accompanied by a continuous reorientation of the internal field. We argue this complex behavior to reflect a crossover driven by the in-plane uniaxial anisotropy, which is ultimately caused by the chemistry of this material, i.e. the mixed-anion character. Our findings reinforce CrSBr as an important candidate for devices in the emergent field of two-dimensional magnetic materials.

References

- [1] K. S. Burch, D. Mandrus, J. G. Park, *Nature*, **563**, 47–52 (2018)
- [2] E. J. Telford, A. H. Dismukes, K. Lee, M. Cheng, A. Wieteska, A. K. Bartholomew, Y. S. Chen, X. Xu, A. N. Pasupathy, X. Zhu, C. R. Dean, X. Roy, *Advanced Materials*, **32**, 2003240 (2020)
- [3] F. Wu, I. Gutiérrez-Lezama, S. A. López-Paz, M. Gibertini, K. Watanabe, T. Taniguchi, F. O. von Rohr, N. Ubrig, A. F. Morpurgo, *Advanced Materials* **34**, 2109759 (2022)
- [4] S. A. López-Paz, Z. Guguchia, V. Y. Pomjakushin, C. Witteveen, A. Cervellino, H. Luetkens, N. Casati, A. F. Morpurgo, F. O. von Rohr, *Nature Communications*, **13**, 4745 (2022)

Solid-state synthesis of carbon-coated lithium vanadate Li_3VO_4 - as anodes for High-Performance Li-ion Capacitors

S. Lonkar, C. Busa

Energy storage Group, Advanced Materials Research Centre, Technology Innovation Institute, P.O. Box 9639, Abu Dhabi, UAE

* The corresponding author e-mail: sunil.lonkar@tii.ae

Keywords: solid-state synthesis; energy storage; anodes; Li-ion capacitor; electrochemistry

The design and development of high-performance electrode materials are of paramount importance to achieve the goal of sustainable energy storage. Hence, the ability to control the composition and structure of the inorganic compound in conjunction with a simple, scalable synthesis method is also greatly sought.

Lithium-ion capacitors (LICs) are emerging as one of the most promising energy storage technologies. Owing to their high energy density and high power density, accompanied by more extended cycle stability, these devices showed enormous potential in energy storage. However, the quest to find an appropriate battery-type anode material with low Li-ion insertion potential and fast electrochemical kinetics is still on. On this front, Li_3VO_4 -based insertion-type anode materials have shown great promise in LICs, primarily due to their high theoretical capacity (595 mAh/g), low-Li insertion potential, natural abundance, and faster electrochemical kinetics. However, its inherent poor conductivity and absence of low-cost scalable synthesis, the potential for these materials are still deprived.

In this work, we report a facile, solid-state, and environment-friendly preparation process to produce nanocrystalline layered Li_3VO_4 on a large scale. Furthermore, its hybridization with carbonaceous materials such as carbon nanotubes and graphene was also demonstrated. The main objective of this paper is to explore solid-state synthesis encompassing the solventless mixing of metal salts (Vanadium and lithium) and carbon precursors under continuous solid-state dispersion followed by moderate thermo-annealing. The resulting nanohybrids were thoroughly investigated using several techniques. XRD, HRTEM, SEM, Raman, and BET have been applied to obtain information on the morphology and the structure of the nanohybrid and the vibrational and spectroscopic properties. Finally, the electrochemical performance of the resulting carbon-coated Li_3VO_4 hybrid material as an anode in fabricating the Li-ion capacitor was investigated. The electrochemical reaction kinetics of the C- Li_3VO_4 was studied by cyclic voltammetry (CV) at different scan rate. The charge-storage performance was deduced from galvanostatic charge-discharge (GCD). At the same time, the electrochemical impedance (EIS) studies highlight the internal resistances developed during the charge-discharge. Finally, long-term stability and device application were assessed by continuous cycling and glowing LED lights.

References

- [1] J. Ding, W. Hu, E. Paek, and D. Mitlin *Chem. Rev.* **118**, 6457–6498 (2018).
- [2] D. Karimi, H. Behi, J. Van Mierlo, M. Bercibar *M. Molecules.* **12**, 3119-3125 (2022).
- [3] A. Chojnacka, F. Beguin *Electrochemistry Communications* **139**, 107305-107311 (2022)

Elucidating catalytic performance of a family of low-valent metal nitrides for the hydrogen evolution reaction from water

A. Y. Ganin^{1*}, Y. Sun¹, O. Gusel'nikova², Y. Zhou³, N. López⁴

¹ School of Chemistry, University of Glasgow, Glasgow G12 8QQ UK;

² National Institute for Materials Science (NIMS), 1-1 Namiki, Tsukuba, Ibaraki 305-0044, Japan;

³ School of Materials Science & Engineering, Sun Yat-Sen University, Guangzhou 510006 Guangdong, P. R. China;

⁴ Institute of Chemical Research of Catalonia, The Barcelona Institute of Science and Technology, Tarragona, Spain;

* The corresponding author e-mail: alexey.ganin@glasgow.ac.uk

Keywords: green hydrogen; water electrolysis; catalysis; metal nitrides; crystal structure

Electrolysers are devices for splitting water into hydrogen and oxygen. The hydrogen is produced with a minimal environmental impact if the electrolyser is coupled with renewable energy source. However, for an optimised performance of the device an electrocatalyst is required. Pt is the best catalyst but production of just 1 g of Pt emits ~33 kg of CO₂ equivalents. [1] Pivotal change to inexpensive, catalytically active materials is necessary. Traditional metal alloys have been explored in the past, but they are chemically unstable in highly acidic conditions required of state-of-the-art electrolysers. [2] A recent report suggests that ternary nitrides are promising alternatives since they stay stable in acidic conditions and work as catalysts for the hydrogen evolution reaction (HER) from water at overpotentials similar to Pt. [3]

In this work we build upon our previous research and presents effective synthetic strategies for design and implementation of a family of chemically stable and active metal nitride catalysts for the HER. As exemplified in **Fig. 1** the most prominent member of the family, Co₃Mo₃N, is similar to Pt in acid conditions when immobilised on a high surface area substrate. Building on this nitride the effect of substitution of Co-sites with a range of transition metals is discussed, along with an intended impact of the substitutions on the catalytic performance of the nitrides. Along with the experimental findings the emphasis is given to DFT simulations as means of elucidating the nature of catalytic sites.

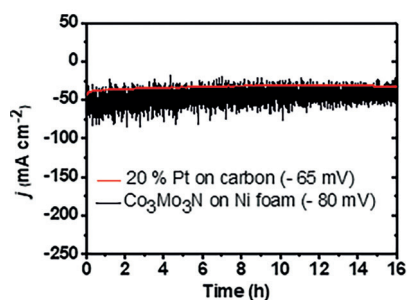


Figure 1: Current densities displayed by Pt and Co₃Mo₃N catalysts under constant potential

References

- [1] M. Mori, R. Stropnik, M. Sekavčnik, A. Lotrič, *Sustainability*, **13**, 3565 (2021).
- [2] Y. Sun, A.Y. Ganin *Hydrogen*, **1**, 11–21 (2022).
- [3] Y. Sun, L. Wang, O. Gusel'nikova, O. Semyonov, J. Fraser, Y. Zhou, N. López, A. Y. Ganin, *J. Mater. Chem. A*, **10**, 855–861 (2022).

Understanding the performance of high-power niobium oxide-based Li ion battery materials

A. Green^{1,2}, E. Driscoll^{1,2}, P. Slater^{1,2}

¹ School of Chemistry, University of Birmingham, Birmingham B15 2TT, UK,

² The Faraday Institution, Harwell Science and Innovation Campus, Didcot OX11 0RA, UK

* The corresponding author e-mail: p.r.slater@bham.ac.uk

Keywords: niobium oxide; anode; lithium ion; high power; Wadsley-Roth

A current growth area in the field of Li ion batteries is the development of improved high charge and discharge power Li-ion cells, driven from the commercial side by a range of market needs (e.g. HEV, grid stabilisation, premium power tools, motorsports). Current commercial technology is based on lithium titanate (LTO) or graphite/Si anodes, with both having significant limitations, in terms of charge safety and lifetime (graphite/Si), cost (LTO), and energy density (LTO). With a view to delivering new anode materials for these demanding applications, there has been increasing interest in niobium oxide-based materials, with additional examples based on compositions with other transition metals. These Nb-O based materials adopt Wadsley-Roth type structures, which contain open ReO_3 -like channels that enable high capacity and fast Li^+ diffusivity, combined with crystallographic shear planes that enable excellent stability and reversibility [1,2]. In this work, research on Wadsley-Roth systems containing tetrahedral linkages will be presented. Work will discuss the influence of the tetrahedral cation on the performance, as well as outline unusual structural changes observed on milling these systems.

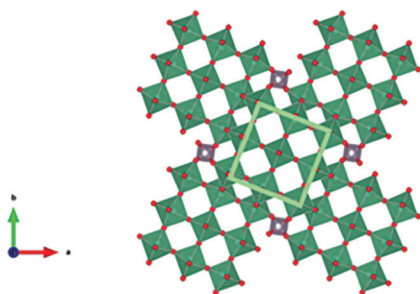


Figure 1:
Structure of $\text{Nb}_9\text{PO}_{25}$,
highlighting the 3 x 3 block size,
along with the tetrahedral linkages.

References

- [1] C. P. Koçer, K. J. Griffith, C. P. Grey, A. Morris *J. Am. Chem. Soc.* 141, 15121–15134 (2019).
- [2] Y. Lakhdar, H. Geary, M. Houck, D. Gastol, A. Groombridge, P. R. Slater, E. Kendrick, *ACS Applied Energy Materials*, 5, 11229–11240 (2022).

Acknowledgments

We would like to thank the Faraday Institution for funding.

Supraparticles as identifiers or temperature indicators with spectral magnetic readout

S. Müssig¹, J. Reichstein¹, S. Wintzheimer^{1,2}, K. Mandel^{1,2}

¹ Friedrich-Alexander-Universität Erlangen-Nürnberg (FAU), Erlangen, Germany;

² Fraunhofer Institute for Silicate Research ISC, Würzburg, Germany

* The corresponding author e-mail: karl.mandel@fau.de

Keywords: magnetic nanoparticles; supraparticles; smart additive; magnetic particle spectroscopy

Well-established marking technologies such as barcodes or radio-frequency identification (RFID) chips require miniaturization for many applications. Going beyond optical signal carriers for identification, magnetic signals can be transmitted through many materials that would not allow optical information to pass. Thus, their utilization in light absorbing or multicomponent materials becomes feasible. Thereby, objects in different application fields could be equipped with such a smart additive (**Fig. 1a**). [2]

In this work it is presented that nanostructured micron-sized particles (so called supraparticles [3]) can be *spectrally* encoded with more than 77 billion magnetic codes as resolved by magnetic particle spectroscopy (MPS). [2] Thereby, a magnetic identification tag, which does not rely on the spatial arrangement of magnetic particles, is established. Magnetically different superparamagnetic iron oxide nanoparticles (SPIONs) were combined within individual supraparticles in different ratios for code variation. The concept of the detected magnetic signature will be vividly explained in analogy to a musical ensemble. It was found that magnetic dipole-dipole interactions upon assembly strongly affects the SPIONs signal response. This concept was additionally exploited to synthesize a particle architecture, which morphologically changes upon temperature exposure. The morphology change alters the interactions of the SPIONs, making it possible to magnetically record bygone temperature exposure (**Fig. 1b**).

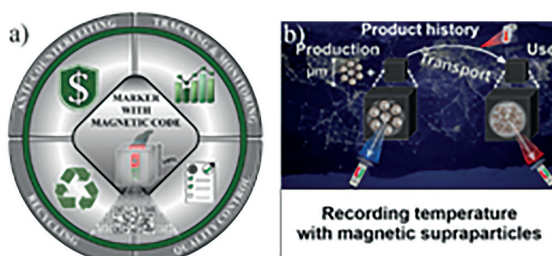


Figure 1: A magnetic particle with a spectrally resolved magnetic code equips arbitrary objects with information. The read out independent of optical constraints, enables a vast variety of unexploited marking and tracing applications. Reprinted from [2,4].

References

- [1] S. Shikha, T. Salafi, J. Cheng, Y. Zhang. *Chem. Soc. Rev.* 2017, **46**, 7054.
- [2] S. Müssig, J. Reichstein, J. Prieschl, S. Wintzheimer, K. Mandel. *Small*, 2021, **17**, 2101588
- [3] S. Wintzheimer, T. Granath, et. al. *ACS Nano* 2018, **12**, 6, 5093–5120.
- [4] J. Reichstein, S. Müssig et. al. *Adv. Mater.* 2022, 2202683.

Acknowledgments

This work was financially supported by the BMBF NanoMatFutur Grant 03XP0149 and S. M.'s doctoral scholarship funding of the German Federal Environmental Foundation.

Crystal and electronic structure of the lanthanide dibismuthides $REBi_2$ ($RE = La, Ce, Pr, Nd, Sm$)

A. Ovchinnikov^{1*}, M. Ruck¹

¹ Faculty of Chemistry and Food Chemistry, Technische Universität Dresden, 01062 Dresden, Germany

* The corresponding author e-mail: alexander.ovchinnikov@tu-dresden.de

Keywords: crystal structure; electronic structure; band inversion; intermetallic compounds; bismuthides

Intermetallic compounds containing bismuth are interesting systems for condensed matter research because their electronic properties are often determined by strong spin-orbit coupling (SOC). In particular, non-trivial electronic band topologies have been identified in such intermetallic systems as Na_3Bi [1], $CaMnBi_2$ [2], and $Bi_{14}Rh_3I_9$ [3].

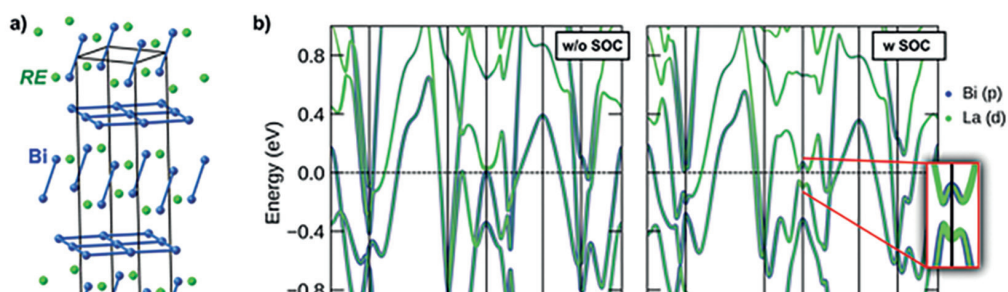


Figure: a) Crystal structure of $REBi_2$ ($RE = La, Ce, Pr, Nd, Sm$). The anionic Bi subunits are shown. b) Band structure of $LaBi_2$ without (left) and with (right) SOC included. The inset shows band inversion around the Y point.

Lanthanide dibismuthides $REBi_2$ ($RE = La, Ce, Pr, Nd, Sm$) have been known for more than a century. However, the crystal (and hence electronic) structure of these compounds has never been determined, likely due to their high malleability and associated poor crystallinity. Using an optimized synthetic procedure, single crystals of $REBi_2$ ($RE = La, Ce, Pr, Nd, Sm$) suitable for crystallographic investigations have been produced. These isostructural compounds crystallize in a new structure type, which can be described as a monoclinic distortion of the $ZrSi_2$ -type structure. Electronic structure calculations for $LaBi_2$ suggest metallic behavior with band inversion in the vicinity of a high-symmetry k -point in the momentum space.

References

- [1] Z. K. Liu, B. Zhou, Y. Zhang, et al., *Science*, **343**, 864–867 (2014)
- [2] A. Zhang, C. Liu, C. Yi, et al., *Nat. Commun.*, **7**, 13833 (2016)
- [3] B. Rasche, A. Isaeva, M. Ruck, et al., *Nature Mater.*, **12**, 422–425 (2013)

Acknowledgments

This work was supported by the Würzburg–Dresden Cluster of Excellence *ct.qmat*.

New nickel-based lithium rich layered/disordered rock salt cathode materials for lithium-ion batteries

B. Dong^{1,2*}, **J. Castells-Gil**^{1,2}, **P. Zhu**^{2,3}, **L. Driscoll**^{1,2}, **P. Allan**^{1,2}, **E. Kendrick**^{2,3}, **P. Slater**^{1,2*}

¹ School of Chemistry, University of Birmingham, Birmingham B15 2TT, U.K.

² The Faraday Institution, Harwell Science and Innovation Campus, Didcot, OX11 0RA, U.K.

³ School of Metallurgy and Materials, University of Birmingham, Birmingham, B15 2TT, U.K.

* The corresponding author e-mail: b.dong@bham.ac.uk; p.r.slater@bham.ac.uk

Keywords: Ni based cathode; disordered rock salt; lithium-ion batteries; oxyfluoride; polyanion doping

To meet the demand in the growing electrical energy storage, such as electric vehicles and grid storage applications, novel cathode materials with large storage capacity and high energy density are required [1,2]. Ni based lithium-rich oxides have attracted great interest and been extensively applied in the field. The high capacities achieved (250 mAh/g) associated with both cationic and anionic redox chemistry with these materials have therefore meant that lithium-rich oxides are attracting considerable interest as the next generation cathode materials for lithium-ion batteries [3]. Still these materials can suffer from several drawbacks, such as oxygen loss at high voltage, large hysteresis and poor rate capability.

In this work, we have studied the dual cation substitution ($\text{Mg}^{2+} + \text{Mo}^{6+} = 2\text{Ti}^{4+}$) in the disordered rocksalt (DRS) $\text{Li}_{1.2}\text{Ti}_{0.4}\text{Ni}_{0.4}\text{O}_2$ in order to try to improve the overall electrochemical performance of this DRS phase. Interestingly, rather than retaining the DRS structure, we show a change to a cation ordered layered material ($\text{Li}_{1.2}\text{Ni}_{0.4}\text{Mo}_{0.2}\text{Mg}_{0.2}\text{O}_2$) through this substitution strategy (**Fig. 1**), and here we report the structure of this new system and the electrochemical performance [4]. We also show the rate capability and electrochemical stability of these materials can be further improved by fluorine incorporation.

LiNiO_2 is also treated as the promising next generation cathode due to the high capacity of $\sim 270 \text{ mAhg}^{-1}$ and high average voltage of 3.8V vs Li/Li^{+4} . In this work, we examine the possible polyanion doping in LiNiO_2 and the corresponding effect on structural and electrochemical properties were investigated, illustrating enhanced electrochemical performance with more stable structure.

References

- [1] R. A. House, J.-J. Marie, M. A. Pérez-Osorio, G. J. Rees, E. Boivin, P. G. Bruce. *Nat. Energy*, **6**, 781–789 (2021).
- [2] G. Assat, J.-M. Tarascon, *Nat. Energy*, **3**, 373–386 (2018).
- [3] J. P. Huang, P. C. Zhong, Y. Ha, D.-H. Kwon, M. J. Crafton, Y. S. Tian, M. Balasubramanian, B. D. McCloskey, W. L. Yang, G. Ceder. *Nat. Energy*, **6**, 706–714 (2021).
- [4] M. Bianchini, M. Roca-Ayats, P. Hartmann, T. Brezesinski, J. Janek, *Angew. Chem. Int. Ed.* **58**, 10434–10458 (2019).

Acknowledgments

This work was supported by the Faraday Institution CATMAT (FIRG016) and NEXTRODE (FIRG015) projects.

Operando investigation of Ir-Ru-based catalyst for proton exchange membrane water electrolysis

T. Hrbek¹, P. Kůš¹, M. G. Rodriguez¹, H. Nedumkulam², M. Mirolo², J. Drnec², V. Matolín¹, I. Matolínová¹

¹ Charles University, Faculty of Mathematics and Physics, Department of Surface and Plasma Science, V Holešovičkách 2, 180 00 Prague 8, Czech Republic;

² European Synchrotron Radiation Facility, 71, avenue des Martyrs, CS 40220, 38043 Grenoble Cedex 9, France

* The corresponding author e-mail: tomas.hrbek@mff.cuni.cz

Keywords: hydrogen; PEM water electrolysis; thin-film catalyst; magnetron sputtering; operando study; Ir-Ru

Hydrogen is a crucial commodity in various fields, such as Chemistry, Metallurgy, and Medicine. However, in recent years, when society went toward reducing CO₂ emissions and when Europe hit an energetics Crisis, the energetics-related applications are most relevant and promising. Since those events effectively force us to leave conventional fossil fuels, there is a rising trend of utilization of renewables (i.e., wind and solar power plants). They allow the production of a significant amount of electrical energy; however, only at specific times as they operate solely under the right conditions – sunny or windy etc. Moreover, they cannot be built everywhere. Therefore, we need an energy vector, which would allow us to store and transport this energy. Hydrogen is an energy vector with the highest gravimetric density; therefore, its utilization is most practical for multiple applications. However, one of the crucial problems to be solved is efficient production. Proton Exchange Membrane Water Electrolyzers (PEM-WE) are the most mature yet efficient technology, which works very well, activity and stability-wise. Unfortunately, they require noble metals, mainly Ir on the anode and Pt on the cathode, for proper functioning. This talk will cover mainly the investigation of a novel, Ir-Ru-based catalyst prepared by magnetron sputtering. The primary motivation for the usage of Ru is its much lower price and scarcity compared to Ir; unfortunately, Ru is also electrochemically unstable compared to Ir. Therefore, we have to use the mixed Ir-Ru-based catalyst. Our recent results suggest that the best activity and stability are provided by Ir-Ru 25:75, which is a counter-intuitive phenomenon, as it contains mainly the unstable Ru. Here we will present a comprehensive operando study of this catalyst, in which we shed light on this phenomenon. The main focus will be on the PEM-WE working principle, the unique design of the utilized operando cells, and the chemical and structural composition of the catalyst as studied in the described operando cells by X-Ray Photoelectron Spectroscopy and X-Ray Diffraction.

References

- [1] T. Hrbek, P. Kůš, Y. Kosto, M. G. Rodriguez, I. Matolínová, *J. Power Sources*, **556**, 232375 (2023)
- [2] T. Hrbek, P. Kůš, T. Košutová, K. Veltruská, T. N. Dinhová, M. Dopita, V. Matolín, I. Matolínová, *Int. J. Hydrog. Energy*, **47** (49), 21033–21043 (2022)

Acknowledgments

This work was supported by the Grant Agency of Charles University in Prague (GAUK No. 336922) and the project Mobility 8J23FR025.

The influence of Al and Ga doping on the chemical and electrochemical cycling of T-LiFeO₂

S. Mahato^{1*}, X. M. De Irujo Labalde¹, S. Booth², M. Hayward¹

¹ Department of Chemistry, University of Oxford, Inorganic Chemistry Laboratory, OX1 3QR;

² Department of Chemical and Biological Engineering, The University of Sheffield

* The corresponding author e-mail: suraj.mahato@chem.ox.ac.uk

Keywords: energy storage; Li-ion cathode materials; topochemical structure manipulation; electrochemistry; crystal structure

Li-ion batteries have transformed our daily life by acting as energy dense, rechargeable power sources for a wide range of electronic devices. Exploration of alternative energy materials are required to satisfy the current and future demands of renewable energy in grid storage and transport industry. Due to limitations on the supply, cobalt and nickel derived cathodes would face problems being applied on a larger scale. To address this challenge, as part of the FutureCat project, we are studying Fe-based cathode materials which could be used for large scale application, and it would deliver high energy density owing to Fe³⁺/Fe⁴⁺ redox.

We decided to stabilise the T-LiFeO₂ structure by substituting Fe with Al and Ga keeping the atomic arrangements unaltered in the framework. Previously, it was reported that during cycling a structural transformation took place forming the spinel LiFe₅O₈ phase, irreversible oxygen loss and capacity fading was also observed [1]. LiFe_{1-x}M_xO₂ (M = Al, Ga) samples were prepared and subjected to chemical and electrochemical lithiation-delithiation, and the effect on the structure, bonding, and oxidation state at various lithium contents was monitored with XRD, SXRD, NPD, XANES, RIXS, titration, and SQUID measurements. The effect of Al and Ga pillaring the T-LiFeO₂ structure during the chemical lithium insertion will be discussed in details in the presentation.

References

- [1] A. R. Armstrong et al., *J. Am. Chem. Soc.* **130**, 3354–3559 (2008)
- [2] Y. Li et al., *Nano Energy* **47** 519–526 (2018)
- [3] E. McCalla et al., *J. Am. Chem. Soc.* **137**, 4804–4814 (2015)

Acknowledgments

This work was supported by the FutureCat project (The Faraday Institution) and the Clarendon fund scholarship.

Designing new lithium layered oxides from sodium layered oxides to stabilize oxygen redox

M. Guignard¹, V. Saïbi¹, L. Castro², I. Sugiyama³, C. Delmas¹

¹ Univ. Bordeaux, CNRS, Bordeaux INP, ICMCB, UMR 5026, F-33600 Pessac, France;

² Toyota Motor Europe, Belgium;

³ Toyota Motor Corporation, Japan

* The corresponding author e-mail: marie.guignard@icmcb.cnrs.fr

Keywords: lithium-rich layered oxide; lithium-ion batteries; operando X-ray powder diffraction; operando X-ray absorption spectroscopy

Lithium-ion technology is the most promising avenue for the electrification of vehicles. Although already currently in use for several decades, an optimization of the electrode materials is still possible. In this context, lithium-rich layered oxides $\text{Li}_{1+x}\text{M}_{1-x}\text{O}_2$ (where $0 < x < 1/3$, and M is usually a mix of manganese, nickel and cobalt) have been intensively studied as positive electrode materials in lithium-ion batteries due to their high capacity (more than 250 mAh/g). However, these materials also present some serious drawbacks. Batteries made with these materials at the positive electrode can show an important capacity loss after the first cycle due to the partial irreversibility of the oxygen redox process. They also exhibit a decrease in voltage during cycling which originates with the migration of manganese ions within the lithium layers and the formation of a spinel-like structure at the surface of the particles.

To overcome these problems, we decided to synthesize new lithium-rich layered oxides with the general formula $\text{Li}_{1+x}\text{Mn}_{1-x}\text{O}_2$ (with $0 < x < 0.25$) with a different oxygen stacking that would make the migration of manganese ions unfavourable thanks to a stronger coulombic repulsion between the layers (alternative of face- and edge-sharing LiO_6 and MO_6 octahedra). The O6-type lithium-rich layered oxide O6- $\text{LiNi}_{1/6}\text{Mn}_{4/6}\text{O}_2$ was obtained by ion exchange from the P2-type sodium layered oxide P2- $\text{Na}_{5/6}\text{Li}_{1/6}\text{Ni}_{1/6}\text{Mn}_{4/6}\text{O}_2$. In a first step, the ion exchange was monitored by variable temperature X-ray diffraction, and we observed that an intermediate compound was formed during the ion exchange reaction. X-ray diffraction suggested that this compound was a layered oxide, alternating layers of sodium ions located in prismatic sites and layers of lithium ions located in octahedral sites, these two layers being separated by a layer of MO_6 octahedra (where M is Li, Ni and Mn). At the end of the ion exchange reaction, a pure lithium layered oxide is obtained with no remaining sodium. Its structure was studied by coupling X-ray and neutron diffraction and high-resolution transmission electron microscopy. We concluded that the layered structure was not a pure O6-type structure and that some stacking faults existed (about 15 %). Finally, the O6- $\text{LiNi}_{1/6}\text{Mn}_{4/6}\text{O}_2$ compound was used as the positive electrode material in lithium batteries. The batteries were galvanostatically cycled between 2.6 and 4.6 V and they showed excellent capacities and capacities retention. The voltage plateau observed during the first charge at approximately 4.5 V seems to be related to oxygen oxidation. Operando X-ray powder diffraction experiment indicated that the O2-type structure was stable upon cycling and that no evidence of structure transition towards a spinel-like phase was found. Furthermore, operando X-ray absorption spectroscopy at the Ni and Mn K-edges showed indirectly that oxygen redox was mostly reversible.

As a conclusion, this new lithium-rich layered is a very promising material to achieve high capacity in lithium-ion batteries.

Sodium insertion into TiO₂ hollandite: structural and electrochemical study

F. García-Alvarado¹, A. Duarte¹, P. Díaz-Carrasco¹, A. Kuhn¹, A. Basa²

¹ Departamento de Química y Bioquímica, Facultad de Farmacia, Universidad San Pablo-CEU, CEU Universities, Urbanización Montepríncipe, 28668 Boadilla del Monte, Madrid, Spain;

² Faculty of Chemistry, University of Białystok, K. Ciolkowskiego 1K, 15-245 Białystok, Poland;

* The corresponding author e-mail: flaga@ceu.es

Keywords: TiO₂ hollandite; Na insertion; Na-ion anode material; structural characterization; electrochemical features

The electrochemical insertion of sodium into the hollandite TiO₂ polymorph, TiO₂(H), is characterized by a voltage profile that points to the formation of a solid solution TiO₂-Na_xTiO₂ (x: 0–0.4). Thus, the absence of constant voltage region seems to indicate a pseudocapacitive intercalation material. However, previous results showed that a phase transformation takes place upon sodium insertion. In this work we have deepened into the electrochemical features and revisited the structural effect of sodium insertion by means of HRTEM and operando XRD. It is concluded that TiO₂(H) is a battery-like material [2] in which a phase transition does occur; however, the biphasic dominion is very narrow. Two solids solution are detected, the initial tetragonal phase and very closely related monoclinic one. Thus, although the voltage profile has the appearance of a typical solid solution, is in fact two almost consecutive single phases, with the intermediate biphasic region being scarcely detected.

TiO₂(H) develops a stable capacity of 106 mAh g⁻¹ after 300 cycles at C/8 (42 mA g⁻¹) and maintains 100 mAh g⁻¹ after 600 cycles. Cycling produces nanosizing of the TiO₂ electrode (to 200–300 nm) by electrochemical milling, but cyclic voltammetry at different sweep rates indicates that diffusive controlled faradic contribution to the total capacity of TiO₂(H) due to Na insertion is significant even at high current. However, participation of pseudocapacitive charge storage is unveiled.

The diffusion coefficient of Na_xTiO₂ at dilute conditions determined by a combination of GITT and PEIS is low ($2.6 \cdot 10^{-13}$ cm² s⁻¹), although several orders of magnitude higher than those of other TiO₂ polymorph. Therefore, TiO₂(H) is a typical battery like materials but for which kinetics is not limited by a biphasic transformation. Instead, kinetics is limited mainly by slow diffusion in single phases with variable composition that are formed upon Na⁺ intercalation into the tunnels favoring the participation of pseudocapacitive charge storage.

References

- [1] J. C. Pérez-Flores, C. Baehtz, A. Kuhn, F. García-Alvarado¹, *Journal of Material Chemistry A*, **2**, 1825–1833 (2014)
- [2] Y. Gogotsi, R. M. Penner, *ACS Nano*, **12**, 2081–2083 (2018)

Acknowledgments

We thank MCIN/AEI/10.13039/501100011033 for funding the project “PID2019-106662RB-C41. Financial support from Universidad San Pablo is also acknowledged.

Structural evolution of layered $\text{H}_2\text{V}_3\text{O}_8$ high-capacity cathode material for lithium-ion batteries during lithium intercalation

A. Kuhn¹, J. C. Pérez-Flores², J. Prado-Gonjal³, E. Morán³, M. Hoelzel⁴, V. Díez-Gómez⁵, I. Sobrados⁵, J. Sanz⁵, F. García-Alvarado¹

¹ Department of Chemistry and Biochemistry, Facultad de Farmacia, Universidad San Pablo CEU, CEU Universities, Urbanización Montepríncipe, 28668 Boadilla del Monte, Madrid, Spain;

² Instituto de Investigación de Energías Renovables, Universidad de Castilla-La Mancha, Albacete, Spain;

³ Universidad Complutense de Madrid, Departamento de Química Inorgánica, Facultad de Ciencias Químicas, Ciudad Universitaria s/n, 28040 Madrid, Spain;

⁴ Forschungsneutronenquelle Heinz-Maier-Leibniz (FRM II), Technische Universität München, Lichtenbergstrasse 1, D-85747 Garching, Germany;

⁵ Instituto de Ciencia de Materiales Madrid (CSIC), 28049 Cantoblanco, Madrid, Spain

* The corresponding author e-mail: akuhn@ceu.es

Keywords: $\text{H}_2\text{V}_3\text{O}_8$; vanadate; li-ion battery (LIB); neutron diffraction; MAS NMR spectroscopy; DFT calculations

$\text{H}_2\text{V}_3\text{O}_8$ (HVO) is a promising high-capacity cathode material for lithium-ion batteries (LIBs). It allows reversible two-electron transfer during electrochemical lithium cycling processes, yielding a very attractive theoretical capacity of 378 mAh g^{-1} [1,2]. However, structural changes during the intercalation in $\text{H}_2\text{V}_3\text{O}_8$ were not scrutinized, and the crystallographic positions occupied by the guest species were not revealed. Aimed at providing insights into the lithium storage mechanism of HVO, in this work we employed a combination of high-resolution synchrotron X-ray and neutron diffraction to accurately describe the crystal structures of both pristine and lithiated $\text{H}_2\text{V}_3\text{O}_8$ [3]. The role of water in network stabilization was examined using density functional theory (DFT) calculations.

Easy hydrogen-bonding switch of structural water upon lithium intercalation not only allows better accommodation of intercalated lithium ions but also enhances Li-ion mobility in the crystal host, as evidenced by MAS-NMR spectroscopy. Facile conduction pathways for Li ions in the structure are deduced from bond valence sum difference mapping. It is concluded that the hydrogen bonds mitigate the volume expansion/contraction of vanadium layers during Li intercalation/deintercalation, resulting in improved long-term structural stability, explaining the excellent performance in rate capability and cycle life reported for HVO in LIBs. This study suggests that other hydrated materials can be good candidates for electrode materials not only in implemented Li technology but also emerging rechargeable post-lithium metal-ion batteries.

References

- [1] J. Prado-Gonjal, B. Molero-Sánchez, D. Ávila-Brandé, E. Morán, J.C. Pérez-Flores, A. Kuhn, F. García-Alvarado, *J. Power Sources*, **232**, 173–180 (2013)
- [2] S. Sarkar, A. Bhowmik, J. Pan, M. D. Bharadwaj, S. Mitra, *J. Power Sources*, **329**, 179–189 (2016)
- [3] Alois Kuhn, J. C. Pérez-Flores, J. Prado-Gonjal, E. Morán, M. Hoelzel, V. Díez-Gómez, I. Sobrados, J. Sanz, F. García-Alvarado, *Chem. Mater.*, **34**, 694–705 (2022)

Acknowledgments

We thank MCIN/AEI/10.13039/501100011033 for funding the project PID2019-106662RB-C41. Financial support from Universidad San Pablo is also acknowledged.

Evidence for a disorder-induced spin liquid in the tuneable spin ladder-chain system $\text{Ba}_2\text{CuTe}_{1-x}\text{W}_x\text{O}_6$ ($0 \leq x \leq 0.3$)

O. Mustonen^{1,2*}, C. Pughe², A. Gibbs^{3,4,5}, A. Yaresko⁵, P. Baker⁴, L. Mangin-Thro⁶, H. C. Walker⁴, E. J. Cussen^{2*}

¹ School of Chemistry, University of Birmingham, Birmingham B15 2TT, UK;

² Department of Material Science and Engineering, University of Sheffield, Sheffield S1 3JD, UK;

³ School of Chemistry, University of St Andrews, St Andrews KY16 9ST, UK;

⁴ ISIS Pulsed Neutron and Muon Source, STFC Rutherford Appleton Laboratory, Didcot OX11 0QX, UK;

⁵ Max Planck Institute for Solid State Research, 70569 Stuttgart, Germany;

⁶ Institute Laue Langevin, 71 Avenue des Martyrs, CS 20156, F-38042 Grenoble Cedex 9, France

* The corresponding author e-mail: o.mustonen@bham.ac.uk and e.j.cussen@sheffield.ac.uk

Keywords: quantum materials; magnetism; spin ladder; neutron diffraction; muon spectroscopy

Exotic quantum states can emerge in magnetic materials with $S = \frac{1}{2}$ quantum spins and low-dimensional interactions. An important class of such materials are spin liquids: materials that do not magnetically order or freeze even at absolute zero [1]. Spin liquid can be stabilised by competing magnetic interactions and structural disorder. We have developed a chemical doping method for tuning magnetic interactions using diamagnetic d^{10} and d^0 cations [2].

Here we use the d^{10}/d^0 effect to tune magnetic interactions in the hexagonal perovskite $\text{Ba}_2\text{CuTe}_{1-x}\text{W}_x\text{O}_6$, where Cu^{2+} ($S = \frac{1}{2}$) cations form a spin ladder. We show that W^{6+} (d^0) is almost exclusively doped into the ladder [3], which allows for the direct tuning of interactions from spin ladder to a spin chain for the first time. Muon spectroscopy reveals the suppression of magnetic order and a potential disorder-induced spin liquid state.

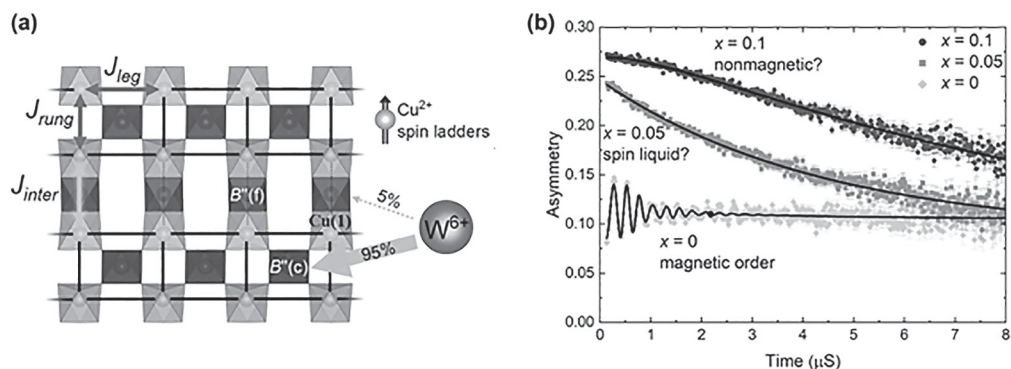


Figure: (a) The spin ladder in $\text{Ba}_2\text{CuTe}_{1-x}\text{W}_x\text{O}_6$ is formed by the Cu^{2+} ($S = 1/2$) cations. Of the two Te-sites, W is almost exclusively doped onto the corner-sharing $B''(c)$ site allowing the direct tuning of interactions in the spin ladder. (b) Muon spectroscopy reveals the parent phase $x = 0$ is magnetically ordered, while the $x = 0.05$ sample behaves like a spin liquid.

References

- [1] L. Balents, *Nature*, **464**, 199–208 (2010).
- [2] O. H. J. Mustonen *et al.*, *Chem. Mater.* **32**, 7070 (2020).
- [3] C. Pughe, O. H. J. Mustonen *et al.*, *Inorg. Chem.*, **61**, 4033–4045 (2022).

Structural variations of the magnetic topological insulators $\text{Mn}_{1+x}\text{Sb}_{2-2x/3}\text{Te}_4$

E. Kochetkova^{1,2}, O. Renier³, A. Isaeva^{1,3}, M. Sahoo¹, L. T. Corredor¹

¹ Institute of Solid State Research, Leibniz IFW Dresden, Germany;

² Technische Universität Dresden, Germany;

³ Institute of Physics, University of Amsterdam, The Netherlands

* The corresponding author e-mail: e.kochetkova@ifw-dresden.de

Keywords: magnetic topological insulators; manganese antimony tellurides

The recently discovered semiconductors with the general formula $\text{Mn}_{1+x}\text{Sb}_{2-2x/3}\text{Te}_4$ (MST), where x varies from -0.1 to 0.15 , are promising candidates for topological ferromagnetic insulators with a high T_C ranging from 27 to 45 K [1–3].

The MST system is very compositionally flexible because the ionic radii of Mn^{2+} (0.83 Å) and Sb^{3+} (0.90 Å) are quite similar, which helps to create strong intermixing up to several tens % between the manganese and antimony atoms in the crystal structures of the compounds. Thus, it is possible to vary both the content of manganese in the composition of the compound and in the crystallographic positions, which leads to a change in the physical properties.

In our experiments x varies in a broad range from -0.1 to 1.7 . Up to $x \approx 0.8$, the compounds crystallize in the GeAs_2Te_4 structure type (sp. gr. $Rm1$) with a layered structure, in which the septuple layers are stacked in a trigonal lattice and connected by weak van der Waals interactions. At x larger than 0.8 , the van der Waals gap is gradually filled, and the lattice subsequently transforms in a more close-packed structure with an F -centered cubic symmetry. As we can see from the single-crystal X-ray diffraction data, the crystals with the formula $\text{Mn}_{1.87(6)}\text{Sb}_{1.31(5)}\text{Te}_4$ (sp. gr. $Rm1$, $a = 4.1955(1)$ Å, $c = 41.5366(2)$ Å) have a partially occupied van der Waals gap by 17% of antimony atoms. The crystals with the maximum value of x have the formula $\text{Mn}_{2.72}\text{Sb}_{1.28}\text{Te}_4$ and an F -centered cubic lattice (sp. gr. Fdm , $a = 11.9147(6)$ Å) with all cationic sites occupied. The crystal structure of the cubic phase is derived from the cubic spinel structure type AB_2X_4 , where the B site (16d) is fully occupied by the Mn atoms, the X site (32e) is occupied by Te, and the position with intermixing by antimony and manganese atoms (16c) has a lower symmetry than the A site (8a) in the spinel structure type. The difference is that in the spinel crystal structure, the A cation is tetrahedrally coordinated, while in our structure a site with intermixing is octahedrally coordinated by the Te atoms.

In this series of MST compounds, we observe that increasing x leads to the changes in the magnetic properties of compounds from ferri- to ferromagnetic and T_C varies from 32 to 73 K.

References

- [1] Y. Liu et al. *Phys. Rev. X* **11**, 021033 (2021)
- [2] S. Wimmer et al. *Adv. Mater.*, **33**, 2102935 (2021)
- [3] L. Folkers et al. *Z. Krist.* DOI: <https://doi.org/10.1515/zkri-2021-2057> (2021)

2D-Metals with locked charge density wave, in the novel layered monophosphate tungsten bronzes $[\text{Ba}(\text{PO}_4)_2]_m \text{W}_m \text{O}_{3m-3}$

H. Nimoh^{1,2*}, R. Glaum², A. Cano³, A. M. Arévalo-López¹, O. Mentré¹

¹ UCCS (Unité de Catalyse et Chimie du Solide), Université de Lille, Centrale Lille/ENSCL, 59000, Lille, France;

² Institut für Anorganische Chemie, Rheinische Friedrich-Wilhelms Universität Bonn, Gerhard-Domagk-Str. 1 53121 Bonn, Germany;

³ Institut NEEL CNRS/UGA UPR2940, 25 rue des Martyrs, BP 166, 38042, Grenoble, France

* The corresponding author e-mail: hicham.nimoh.etu@univ-lille.fr

Keywords: phosphate-bronze; 2D metal, charge-density-wave; layered structure; hidden FS nesting

We have synthesized a whole novel structural branch of mixed-valent, layered barium tungsten monophosphate bronzes (so-called L-MPTB*) with the general formula $[\text{Ba}(\text{PO}_4)_2]_m [\text{W}_m \text{O}_{3m-3}]$ ($m = 3$ ($\text{W}^{5.33+}$), 4 ($\text{W}^{5.50+}$), and 5 ($\text{W}^{5.60+}$)). The structures are built from spacer-layers $[\text{Ba}(\text{PO}_4)_2]^{4-}$ and separating ReO_3 -like cationic layers of variable thickness (**Fig. 1**). The spacers guarantee a “genuine” 2D-behavior, and enforce an overall trigonal structure preserved down to 1.8 K for the whole series. The L-MPTB* display some analogies but also major differences in comparison to the long-known MPTBs. From a structural point of view, our L-MPTB* correspond to the scission of the well-known hexagonal tungsten phosphate bronzes (MPTB_h's) into the trigonal-oxide layers (**Fig. 1**). The L-MPTB* show steady 2D-metallic behavior and no anomaly in their heat capacity/thermopower down to 1.8 K. This is in contrast with the other tungsten bronzes of the literature [1] which systematically develop Charge Density Wave (CDW) instabilities with significant W-shifts or low-T superconductivity (**Fig. 1**). However, they hold the whole set of ingredients to develop CDW in terms of their tungsten valence and 2D-Fermi surfaces (**Fig. 1**) thus prompting for hidden nesting. This novel structural family with “locked CDW” opens wide perspectives in the field of correlated metals.

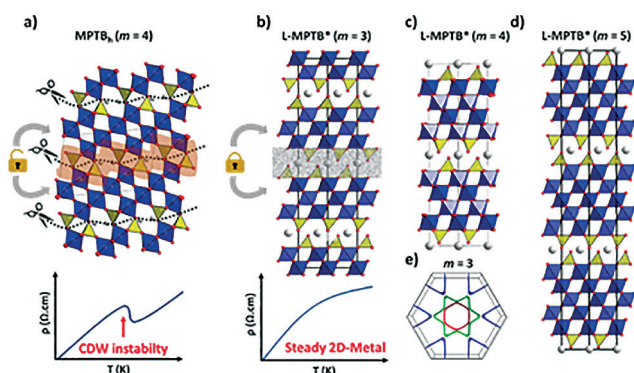


Figure 1: Structural analogy between a) $\text{K}_{1/3}\text{P}_4\text{W}_8\text{O}_{32}$ [2] and b) L-MPTB* ($m = 3$) with ideal resistivities. c) $m = 4$ d) $m = 5$ e) $m = 3$ Fermi surface

References

- [1] M. Greenblatt, *Acc. Chem. Res.* **29**, 219–228 (1996).
- [2] M. Dusek, J. Luedecke, S. van Smaalen, *J. Mater. Chem.* **12**, 1408–1414 (2002).

Experimental investigation of magnetic dilution effect on the frustrated quantum antiferromagnet SrCu₂(BO₃)₂

L. Šibav^{1,2}, G. King³, Z. Jagličič^{4,5}, M. Kobljar^{1,2}, M. Otoničar^{1,2}, D. Arčon^{1,6}, M. Dragomir^{1,2}

¹ Jožef Stefan Institute, Jamova 39, 1000 Ljubljana, Slovenia;

² Jožef Stefan International Postgraduate School, Jamova 39, 1000 Ljubljana, Slovenia;

³ Canadian Light Source, 44 Innovation Blvd, Saskatoon, SK S7N 2V3, Canada;

⁴ Institute of Mathematics, Physics and Mechanics, Jadranska 19, 1000 Ljubljana, Slovenia;

⁵ Faculty of Civil and Geodetic Engineering, University of Ljubljana, Jamova 2, 1000 Ljubljana, Slovenia;

⁶ Faculty of Mathematics and Physics, University of Ljubljana, Jadranska 19, 1000 Ljubljana, Slovenia

* The corresponding author e-mail: lia.sibav@ijs.si

Keywords: quantum materials; magnetic frustration; exotic states; chemical doping; spin gap

Strontium copper borate, SrCu₂(BO₃)₂, is a two-dimensional magnetic material with a layered structure of sheets composed of triangular BO₃ and CuO₄ square planar groups separated by Sr²⁺ ions [1]. This compound has been the subject of research due to its enhanced quantum properties such as the presence of a spin gap and frustrated magnetism. The first is of purely quantum origin, while the latter is a consequence of antiferromagnetic Cu²⁺ ($S = 1/2$) spin dimers arranged orthogonally on a square lattice [2]. Theoretical predictions have predicted a quantum spin liquid state for B-site isovalent doping with nonmagnetic ions, i.e., magnetic dilution. Substitution with Mg²⁺ would break the spin dimers, and consequently long-range correlations could form between the dimer-free Cu²⁺ magnetic centres, possibly leading to quantum entanglement. The experimental realisation of B-site doping of this compound has been little explored and there is limited data available [3].

With the aim of experimentally verifying the predicted exotic quantum states, the effects of Mg-doping on the magnetism of SrCu₂(BO₃)₂ were re-examined in this study. Here, a series of Mg-concentrations (3, 5, 10 mol%) was investigated, which includes a higher concentration of Mg-doping than previously reported (3 and 5 mol%^[3]). Polycrystalline Mg-doped SrCu₂(BO₃)₂ was obtained by an optimised solid-state synthesis [4]. This resulted in partial substitution of Cu²⁺ by Mg²⁺ as determined from high-resolution powder X-ray diffraction and energy-dispersive spectroscopy analysis. Both magnetic susceptibility and electron paramagnetic resonance spectroscopy measurements performed on these samples showed systematic changes, i.e., a decrease in spin gap and Weiss constant with an increasing Mg concentration. This indicates a successful partial breaking of Cu²⁺ spin dimers of SrCu₂(BO₃)₂.

Currently, growth of Mg-doped SrCu₂(BO₃)₂ single crystals is underway. The crystals will be used for high-field magnetic susceptibility and high-field EPR spectroscopy measurements.

References

- [1] R. W. Smith and D. A. Keszler, *J. Solid State Chem.*, **93**, 430–435 (1991)
- [2] B. S. Shastry, B. Sutherland, *Phys. B+C*, **108**, 1069–1070 (1981)
- [3] Z. Shi, W. Steinhardt, D. Graf *et al.*, *Nat. Commun.*, **10**, 1–9 (2019)
- [4] L. Šibav, M. Dragomir. *Manuscript in preparation.* (2022)

Acknowledgments

This work was supported by the Slovenian Research agency, Marie Curie Individual Fellowship (Grant No. 101031415) and Director's Fund Project, JSI, 2019.

Magnetic structures of Dirac nodal-line semimetals LnSbTe

I. Plokhikh¹

¹ Laboratory for Multiscale Materials Experiments, Paul Scherrer Institut, PSI, Villigen, CH-5232, Switzerland

* The corresponding author e-mail: igor.plokhikh@psi.ch

Keywords: dirac semimetals; neutron diffraction; skyrmions; topology; multi-k structures

Topological materials are in the focus of solid-state research within the last few decades owing to offering multiple practically important properties like large magnetoresistance, ultra-high charge carrier mobility of Dirac and Weyl fermions as well as the possibility to use long-period non-collinear spin textures (skyrmions) in next-generation memory storage devices. The ZrSiS-type ($P4/nmm$) group of materials $LnSb_xTe_{2-x-\delta}$ (Ln – lanthanide) is of particular interest due to a unique combination of non-trivial band topology in reciprocal space and signatures of topological magnetic states (antiferromagnetic skyrmions) in direct space [1]. Whereas topological features of electronic structure in this family were studied in detail, little was known about microscopic magnetism. We present a systematic neutron diffraction study of stoichiometric $LnSbTe$ (1:1:1) materials and the $TbSb_xTe_{2-x-\delta}$ solid solution series.

A set of commensurate propagation vectors ($k_1 = (\frac{1}{2} 0 0)$, $k_2 = (\frac{1}{2} 0 \frac{1}{4})$, $k_3 = (\frac{1}{2} 0 \frac{1}{2})$ and $k_4 = (0 0 \frac{1}{2})$) or their incommensurate counterparts can describe magnetic scattering in the studied material. This might indicate similarities in Fermi surface nesting instabilities across this series. The coexistence of several magnetically ordered phases corresponding to different propagation vectors was observed in $TbSbTe$ (k_1 and k_2), $HoSbTe$ (k_1 and k_2), and $DySbTe$ (k_2 and k_4). In the case of $TbSbTe$, magnetic symmetry arguments hint at multi- k magnetic structures based on k_1 and k_2 already in zero-field [2], which is a necessary prerequisite for forming long-period spin textures like skyrmions. Te-doped $TbSbTe$, *i.e.*, $TbSb_xTe_{2-x-\delta}$ solid solutions adopt a distorted orthorhombic variant of the initially tetragonal structure with charge density wave (CDW) superstructure. This CDW templates magnetically ordered state with $|k_{CDW}| = 2 \cdot |k_{magn}|$.

The results of microscopic studies of magnetic structures, together with their relation to the topological electronic structure will be discussed and presented in the contribution.

References

- [1] S. Lei, A. Saltzman, L. M. Schoop, *Phys. Rev. B* **103**, 134418 (2021)
- [2] I. Plokhikh, V. Pomjakushin, D. Gawryluk, O. Zaharko, E. Pomjakushina, *Inorg. Chem.* **61**, 11399–11409 (2022)

Acknowledgments

The neutron powder diffraction experiments were performed at the Swiss spallation neutron source SINQ, Paul Scherrer Institute (Villigen, Switzerland). We thank the Swiss National Science foundation grants No. 200020-182536/1, 200021_188706 and R'equip Grant No. 461 206021_139082 and SNI Swiss Nanoscience Institute for financial support.

Light-induced surface microstructures on Ge-As-S glasses

L32

E. Samsonova¹, P. Kutálek², E. Černošková², P. Knotek¹, J. Schwarz¹

¹ Department of General and Inorganic Chemistry, Faculty of Chemical Technology, University of Pardubice, Studentská 573, 532 10 Pardubice, Czech Republic;

² Joint Laboratory of Solid State Chemistry, Faculty of Chemical Technology, University of Pardubice, Studentská 84, 532 10 Pardubice, Czech Republic

* The corresponding author e-mail: ekaterina.samsonova@student.upce.cz

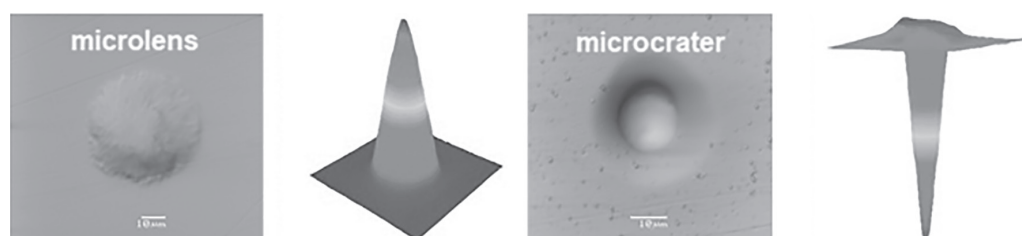
Keywords: laser direct writing; microlens; microcrater; chalcogenide glasses; CW laser

Micro-optical elements are increasingly considered in free space optical systems providing an optical interconnection between very large scale integrated electronic chips, between modules containing chips and in “stacked planar optics” [1].

The present work is focused on the microstructure formation (microlenses, microcraters) on the surface of stoichiometric and non-stoichiometric Ge-As-S bulk glasses. The extremely high-resolution capability and high transmission in VIS and IR regions of the spectrum enable the chalcogenide glasses to be applied for the production of diffractive optical elements as gratings, lenses, filters, beam couplers and/or beam combiners, operating in the broad spectral region [2].

The glassy bulks were prepared by direct synthesis from elements (5N purity). The prepared samples were polished to the optical quality (RMS < 5nm) and were illuminated in the air using focused continuous-wave lasers operating at the different wavelengths. From the dependence of formed microstructure height on the logarithm of radiation intensity which hit the surface, the threshold value of microstructure elements formation was determined. For the comparison, in-situ microstructure formation was studied by the modified thermomechanical analyzer which allows the action of force and illumination in the same direction on the same place of the sample.

The role of several parameters (chemical composition, exposition conditions) on the microstructure formation was investigated. The created microstructures and non-illuminated areas were characterized by several techniques (Raman and Force spectroscopies, EDS, DHM) in order to find the potential differences in properties between them.



References

- [1] B. Bureau, S. Mauriceon, F. Charpentier, etc, *Fiber Integr. Opt.*, **28**, 65-80, (2009).
- [2] K. Shimakawa, A. Kolobov, S. R. Elliott, *Adv. Phys.*, **44**, 475 (1995).

Acknowledgments

The work was supported by University of Pardubice, the Czech Republic (SGS2023_009).

Locking any magnetization by freezing of magnetic domains in a transient soft to super-hard magnet

O. Mentré^{1*}, B. Leclercq¹, A. Pautrat², A. M. Arevalo-Lopez¹, S. Petit³, V. Stolyarov⁴

¹ UCCS, University of Lille, CNRS, Villeneuve d'Ascq, France;

² CRISMAT, Normandie University, CNRS, Caen, France;

³ LLB, CEA-CNRS, Saclay, France; ⁴ Adv. Mesoscience and Nanotechnology Centre Moscow, Dolgoprudny, Russia

* The corresponding author e-mail: olivier.mentre@univ-lille.fr

Keywords: layered oxide; 2D-Ising FM; magn. domains; soft-to-hard; magnetic memory

We observed a rare “freezing of magnetic domains” phenomenon in the $\text{BaFe}_2(\text{PO}_4)_2$ compound. This $S = 2$ Honeycomb lattice ($J = 15\text{K}$), was early described by our group as “genuine” 2D-Ising FM materials below $T_c \sim 70\text{K}$, after extraction of the pertinent critical exponents [1,2]. This statement involves soft-magnetism with the only possible \downarrow, \uparrow spin-degeneracy and FM-ordering hold by individual layers, i.e. independent on the BFPO thickness. We observed the opening of large hysteresis below $T_F \sim 15\text{K}$ with $H_c > 14\text{T}$ @ 2K , much larger than in the LuFe_2O_4 case with similar phenomenology [3]. Narrow domain walls $\sim 13\text{\AA}$ thick (i.e. 5-6 Fe-Fe contacts) were deduced from the huge anisotropy ($K/K_b = 2.84 \text{ K}/\text{\AA}^3$) calculated from INS spectra and $M(H)$ curves. After modification of our crystal growth conditions leading to thin plate-like crystals, MFM images evidenced a labyrinthine domain structure. It is fully-preserved until very high magnetic field below T_F , see Fig. 1a,b. The energy scales of the exchanges, domain walls, and pinning centers, create a complex context, to be discussed on the basis of the χ -dynamic, INS and $M(H)$ measurements. The offered potentialities are wide, due to the occurrence of large magneto-electric effects at T_F . For the first time, the demonstrated ability to imprint any magnetization between $-M_s$ and $+M_s$ around T_F , not returnable up to 9T at 2K (see Fig. 1c,d), also gives a unique oddity of prime importance for multiple-states magnetic memory technologies.

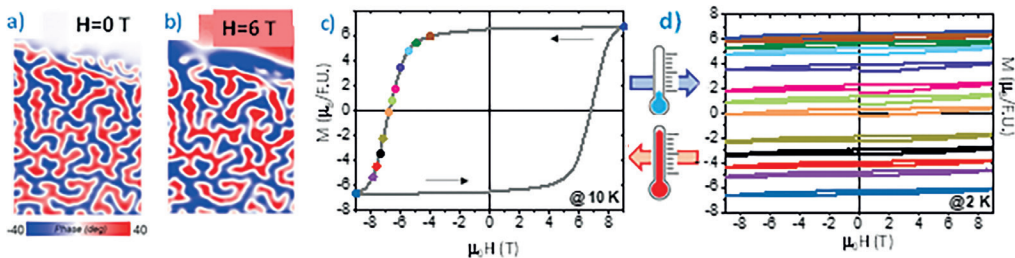


Figure 1: a-b) Freezing of magn. domain on BFPO single crystal at $H=0$ and 6T . c) Imprinting any magnetization M (coloured points) @ 10K (open $M(H)$ loop) and d) Locking of M (-9 to 9T) @ 2K .

References

- [1] H. Kabbour *et al.* *Angew. Chem. Int. Ed.* **51**, 11745–11749 (2012).
- [2] R. David *et al.* *J. Am. Chem. Soc.* **135**, 13023–13029 (2013).
- [3] W. Wu *et al.*, *Phys Rev. Letters*, **101**, 137203(1–4) (2008).

Er³⁺-doped TeO₂-ZnO-La₂O₃ Optical Glasses

J. Suský^{1*}, S. Šlang², L. Beneš³, B. Frumarová², R. Svoboda⁴, T. Wágner^{1,2}, L. Stržířík¹

¹ Department of General and Inorganic Chemistry, Faculty of Chemical Technology, University of Pardubice, Studentská 573, Pardubice 532 10, Czech Republic;

² Center of Materials and Nanotechnologies, Faculty of Chemical Technology, University of Pardubice, nám. Čs. legií 565, Pardubice 530 02, Czech Republic;

³ Joint Laboratory of Solid State Chemistry, Faculty of Chemical Technology, University of Pardubice, Studentská 84, Pardubice 532 10, Czech Republic;

⁴ Department of physical chemistry, Faculty of Chemical Technology, University of Pardubice, Studentská 573, Pardubice 532 10, Czech Republic

* The corresponding author e-mail: jakub.susky1@student.upce.cz

Keywords: tellurite glasses; TeO₂-ZnO-La₂O₃; Er³⁺-doped glass; photoluminescence; optical properties

Tellurite glasses exhibiting high refractive index values, low phonon energy and their easy fabrication are attractive materials in fibre optics and photonics [1]. In the present work, we have synthesized selected Er³⁺-doped glasses of the TeO₂ZnOLa₂O₃ (TZL) family and studied their basic physico-chemical properties with emphasis on their Stokes and antiStokes (upconversion) photoluminescence (PL) dynamics. The glasses were synthesized by the melt-quenching method at 900 °C and were basically characterized in terms of their chemical composition (EDX microanalysis), volumetric density (Archimedes method, $\rho \approx 5.40\text{--}5.61 \text{ g cm}^{-3}$), glass transition temperature T_g (DSC calorimetry, $T_g \approx 360\text{--}420 \text{ °C}$), structure (Raman scattering, XRD analysis), refractive index n (spectroscopic ellipsometry $n \approx 1.96\text{--}1.99$ at $\lambda \approx 1550 \text{ nm}$) and intra $4f$ electronic transitions via UVVisNIR spectroscopy. Furthermore, steadystate and timeresolved PL emission spectroscopy at pumping wavelength of $\approx 977 \text{ nm}$ have been used to study overall PL dynamics.

It has been found that the substitution of La₂O₃ (<10 mol.%) for ZnO in TZL glasses results in increase of glass density, molar volume and glass transition temperature as well as increase in the concentration of [TeO₃] and [TeO₃₊₁] units at the expense of [TeO₄] units. All studied glasses exhibit intense Stokes Er³⁺: $^4I_{13/2} \rightarrow ^4I_{15/2}$ ($\lambda \approx 1.56 \mu\text{m}$) as well as upconversion Er³⁺: $^2H_{11/2}/^4S_{3/2} \rightarrow ^4I_{15/2}$ ($\lambda \approx 520\text{--}550 \text{ nm}$), $^4F_{9/2} \rightarrow ^4I_{15/2}$ ($\lambda \approx 670 \text{ nm}$) and $^4I_{9/2} \rightarrow ^4I_{15/2}$ ($\lambda \approx 800 \text{ nm}$) photoluminescence emission. In contrast to TeO₂ZnO glasses, the addition of La₂O₃ resulting in TZL glasses suppresses the PL concentration quenching which is addressed to the increase in the interionic distance between Er³⁺ ions in TZL matrix.

The studied TZL glasses seem to be promising host materials for rareearth ions with potential in optical applications.

Acknowledgments

This work was supported by the Ministry of Education, Youth and Sports CR (LM2018103). I also thank projects SG2023 and VA390011.

References

- [1] J. Hrabovsky, F. Desevedavy, L. Strizik, G. Gadret, P. Kalenda, B. Frumarova, L. Benes, S. Slang, M. Veis, T. Wagner, F. Smektala, *J. NonCryst. Solids*, **582**, 121445 (2022).

Structural analyses and properties of complex sulphides in the Cr-Sn-S system

F. Guiot^{1*}, V. Dorcet¹, E. Guilmeau², B. Malaman³, T. Schweitzer³, P. Lemoine³, C. Prestipino¹

¹ Univ. Rennes, CNRS, ISCR-UMR 6226, F-35000 Rennes, France;

² Laboratoire CRISMAT, UMR 6508, CNRS, ENSICAEN, 14050 Caen, France;

³ Institut Jean Lamour, UMR-CNRS 7198, Université de Lorraine, 54011 Nancy, France

* The corresponding author e-mail: florentine.guiot@univ-rennes.fr

Keywords: structure; properties; thermoelectric

The design and optimization of thermoelectric (TE) materials rely on the intricate balance between thermopower (S), electrical resistivity (ρ) and thermal conductivity (κ). Perfecting such a balance is the key to reach high TE performances - determined by the dimensionless figure of merit $ZT = S^2T/\rho\kappa$ - necessary to improve energy recovery systems and thermoelectric cooling devices. [1] Among the most promising TE materials at medium temperature, complex copper-based sulphides are of double interests as they are usually made of eco-friendly and low cost elements [2] and exhibit intrinsically low thermal conductivity. [3] However, the use of copper-based sulphides in TE devices is limited by the lower TE performances of the n-type materials compared to those of the p-type. [4]. Hence, it appears necessary to develop more performant n-type sulphide materials.

In this context, we have synthesized and studied the structural and physical properties of two phases in the Cr-Sn-S ternary system: $\text{Cr}_2\text{Sn}_3\text{S}_7$ and Cr_2SnS_4 . The former is characterised by a semi-ordered crystal structure and a n-type semiconductor behaviour, and the latter is characterised by a complex crystal structure (Fig. 1) and a p-type semiconductor behaviour. The intrinsic structural complexity of these materials leads to very low thermal conductivities, which are promising features to develop new performant thermoelectric materials.

In this presentation, I will (i) present results obtained from X-ray diffraction, scanning and transmission electron microscopies, magnetic measurements, spectroscopy techniques and transport measurements and (ii) discuss on the relationships between chemical compositions, crystal structures and properties (TE and magnetic) of $\text{Cr}_2\text{Sn}_3\text{S}_7$ and Cr_2SnS_4 .

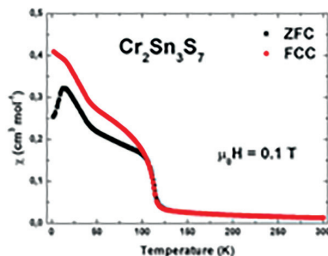


Figure 1: Electron diffraction pattern (incidence beam parallel to [101]) of Cr_2SnS_4 revealing its complex crystal structure highlighted by diffuse scattering. Analysis based on the fundamental hexagonal cell ($a = 21.332 \text{ \AA}$, $c = 3.466 \text{ \AA}$). **Figure 2:** Magnetic measurement of the $\text{Cr}_2\text{Sn}_3\text{S}_7$, highlighting its antiferromagnetic behavior and the presence of the ferrimagnetic impurities Cr_2SnS_4 . [4]

References

- [1] S. Hébert, D. Berthebaud, R. Daou, Y. Bréard, D. Pelloquin, E. Guilmeau, F. Gascoin, O. Lebedev, A. Maignan, *J. Phys.: Condens. Matter*, **28** (2016) 013001.
- [2] O. Caballero-Calero, J. R. Ares, M. Martín-González, *Adv. Sustainable Syst.* (2021) 2100095.
- [3] A. V. Powell, *Journal of Applied Physics*, **126** (2019) 100901.
- [4] G. Guérou, P. Lemoine, B. Raveau, E. Guilmeau, *J. Mater. Chem. C*, **9** (2021) 773–795.
- [5] P. Lemoine, G. Guérou, B. Raveau, E. Guilmeau, *Angew. Chem. Int. Ed.* (2021) anie.202108686.

Holmium-doped TeO₂-ZnO-La₂O₃ tellurite glasses for photonics applications and fibre optics

J. Hrabovsky^{1,*}, F. Desevedavy², L. Strizik³, J. Oswald⁴, L. Nowak¹, T. Wagner^{3,5}, F. Smektala², M. Veis¹

¹ Institute of Physics of Charles University, Faculty of Mathematics and Physics, Charles University, Ke Karlovu 5, 121 16 Prague, Czech Republic;

² ICB Laboratoire Interdisciplinaire Carnot Bourgogne, UMR 6303 CNRS-Université Bourgogne Franche Comte, 9 Av. Alain Savary, Dijon, 21078, France;

³ Department of General and Inorganic Chemistry, Faculty of Chemical Technology, University of Pardubice, Studentska 573, 532 10 Pardubice, CR;

⁴ Institute of Physics of the Czech Academy of Sciences, Cukrovarnicka 10, 162 00 Prague 6, CR;

⁵ Center of Materials and Nanotechnologies, University of Pardubice, nam. Cs. legii 565, 530 02 Pardubice, CR.

* The corresponding author e-mail: hrabovj@karlov.mff.cuni.cz

Keywords: photoluminescence; tellurite glasses; Ho³⁺-doped glass; optical fibres, rare-earth

Optical materials doped with rare earth (RE) ions still represent great potential for photonics applications, especially in the design of light-emitting materials and optical amplifiers. Despite the continuous increase in transfer capacities in the current telecommunications bands, it is clear that new bands are to be involved. The first alternative to the most widely used C-band (1.53–1.565 μm) was initially the extension to the L-band (1.565–1.62 μm). However, even this extension does not represent a long-term sustainable solution. One of the suggested options is to use an additional optical band located at the 2 μm, which could use materials doped with Ho³⁺ or Tm³⁺ ions for the design of optical amplifiers to compensate optical losses. While erbium-doped fibre amplifiers can thus operate effectively in the C and L transmission bands, no similarly capable alternative is currently available for the intended optical band at 2 μm. Although the tested holmium-doped fibre amplifiers exhibit high conversion efficiency and low optical losses compared to, for example, Tm-doped materials, a suitable pumping scheme using commercially available pumping lasers is still not available.

This work presents a thorough investigation of the effect of simultaneous doping of host TeO₂-ZnO-La₂O₃: 0.5 mol.% Ho₂O₃ glasses by various RE³⁺ ions, such as Yb³⁺, Er³⁺, Nd³⁺, Tm³⁺, Sm³⁺, Dy³⁺ and their combinations on photoluminescent properties under 800 nm and 980 nm excitation. The experimental results thus allow a comprehensive study of the excitation mechanism for Ho³⁺ ions in tellurite glasses with respect to observed photoluminescence and photon upconversion from the visible to the mid-infrared region of the spectrum. Targeted 2.0 μm photoluminescence emission (λ_{exc} = 980 nm) was observed for all Ho³⁺/RE and Ho³⁺/RE₁/RE₂ doped glasses, except for Ho³⁺/Sm³⁺ glasses. The highest intensity under 980 nm excitation was observed for samples containing Yb³⁺ ions.

References

- [1] R. A. H. El-Mallawany, *Tellurite Glass Smart materials: Applications in Optics and Beyond* (2018) 13: 978-3-319-76567-9.

Acknowledgments

The work was supported by the Charles University Grant Agency (GAUK662220) and by grant SVV-2020-260590. Authors thank the University of Pardubice (VA390011), the Ministry of Education, Youth and Sports (LM2018103) and CzechNanoLab (LM2023051).

Gold(I)-thiolate coordination polymers as transparent glasses and cyclic phase-changing materials

S. Vaidya*^{1,2}, O. Veselska^{1,2}, Z. Fan³, A. Zhadan², A. Fateeva⁴, P. Bordet⁵, S. Horike⁶, A. Demessence²

¹ Institute of Experimental and Applied Physics, CTU in Prague, Prague, Czech Republic;

² Univ Lyon, Université Claude Bernard Lyon 1, CNRS, IRCELYON, Villeurbanne, France;

³ Department of Synthetic Chemistry and Biological Chemistry, Graduate School of Engineering, Kyoto University, Kyoto, Japan;

⁴ Univ Lyon, Université Claude Bernard Lyon 1, CNRS, LMI, Villeurbanne, France;

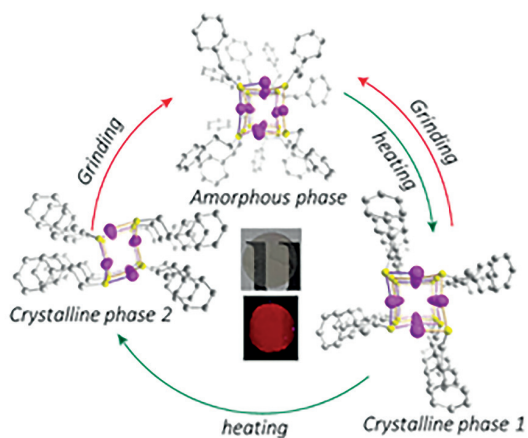
⁵ Université Grenoble Alpes, CNRS, Institut Néel, Grenoble, France;

⁶ iCeMS, Institute for Advanced Study, Kyoto University, Kyoto, Japan.

* The corresponding author e-mail: shefali.vaidya@cvut.cz

Keywords: coordination polymers; glass; ceramics; transparency; luminescence

Crystalline and amorphous coordination polymers (CPs) have applications in gas adsorption and separation, catalysis and drug delivery to name some. The direct synthesis of amorphous CPs is often encountered with difficulty. Amorphous CPs in general can be used to construct glasses. Additionally, the CPs with multiple phases capable of undergoing cyclic phase change can be potentially used in phase-change random access memory (PCRAM). Au(I)-thiolate CPs can be obtained easily both as amorphous and crystalline materials. Here we show the resourcefulness of Au(I)-thiolate CPs in the formation of glasses and as phase-changing materials. The examples presented here show the diverse applications of these CPs. A series of Au(I)-thiolate CPs $[\text{Au}(\text{S}(\text{CH}_2)_x\text{Ph})_n]$ ($X = 0, 1$ or 2) are shown to form glasses by mechanical pressing at room temperature of the as-synthesised amorphous phases as opposed to other energy-consuming processes. The glasses exhibit varying degrees of transparency as a function of the alkyl chain. [1] Also, the effect of heating on the transparency of the glasses is studied. In one of the CPs in the series i.e $[\text{Au}(\text{SEtPh})_n]$, the ethyl group between the phenyl ring and the thiol group gives flexibility for the formation of multiple phases. Here we present the cyclic phase change of $[\text{Au}(\text{SEtPh})_n]$ from the amorphous phase to crystalline phase 1 to crystalline phase 2 by mere heating and grinding. [2]



References

[1] S. Vaidya *et al.*, *Chem. Sci.*, **11**, 6815 (2020).

[2] O. Veselska *et al.*, *Angew. Chem. Int. Ed.*, **61**, e202117261 (2022)

Acknowledgments

Funded by the financial support of ANR and CNRS (France) and Institutional support of IEAP, CTU in Prague (DKRVO), Czech Republic.

Tuning the metallic glasses properties via ultrafast heating/cooling

L38

J. Orava^{1*}, Y. H. Sun², I. Kaban³

¹ Faculty of Environment, J. E. Purkyne University in Usti nad Labem, Pasteurova 3632/15, Usti nad Labem, Czech Republic;

² Institute of Physics, Chinese Academy of Sciences, 100190, Beijing, China;

³ IFW Dresden, Institute for Complex Materials, Helmholtzstr. 20, 01069 Dresden, Germany

* The corresponding author e-mail: jiri.orava@ujep.cz

Keywords: metallic glasses; supercooled liquid; ultrafast kinetics; phase transformations; mechanical properties; glass stability

Properties of metallic glasses (MGs), as of any other glass-forming liquids, are affected and controlled by the liquid thermal history. For MGs, the conventional heating/cooling rates $<10^1$ K s⁻¹ give access to a narrow range of energy states, thus limiting MGs properties. We will demonstrate and discuss the underlying mechanism of how the properties of the same glass can be tuned by extending the heating/cooling rates (**Figure**). For example, faster cooling combined with higher quenching temperatures can give so-called chemically-homogeneous glasses [1] with greatly enhanced resistance to crystallization contrary to conventionally-made glasses. For such glasses, e.g., the crystallization kinetics on heating does not anymore depend on the liquid thermal history. Alternatively, upon ultrafast heating, metastable phases, otherwise unstable at room temperature, beneficial to the glass plasticity can be formed. The enhanced thermal stability of the supercooled liquid promises practical engineering applications of MGs such as in thermoplastic forming, additive manufacturing or welding.

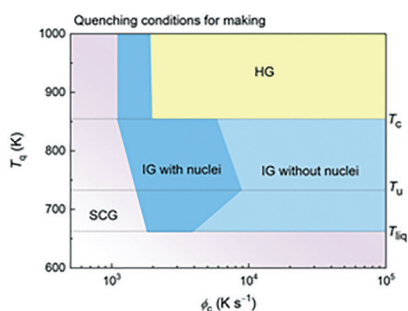


Figure: Quenching map highlighting different processing conditions under which various glasses can be made. Different quenching and equilibrating regions are defined. The region of T_q (quenching temperature) $> T_c$ (critical temperature) corresponds to the homogenization of the metallic melt. The preparation of a homogeneous glass (HG) is thus enabled by using a high cooling rate $\phi_c > 2000$ K s⁻¹. Inhomogeneous glass (IG) prepared at high $\phi_c > 4000$ K s⁻¹ maintains its inhomogeneous structure devoid of nuclei (IG without nuclei), while a glass quenched at low ϕ_c contains nuclei (IG with nuclei). For low $\phi_c < 1100$ K s⁻¹ or at $T_q < T_{liq}$, a semi-crystalline glass (SCG) forms [2].

References

- [1] J. E. K. Schawe, J. Löffler, *Nat. Commun.* **10**, 1337 (2019).
 [2] Q. Cheng, Y. H. Sun, J. Orava, W. H. Wang, *Mater. Today Phys.* **31**, 101004 (2023).

Acknowledgments

J. O. acknowledges the assistance at J. E. Purkyne University in Usti nad Labem provided by the research infrastructure NanoEnviCz, which is supported by the Ministry of Education, Youth and Sports of the Czech Republic (LM2018124).

Cation ordered doping of ferrite perovskites: influence on redox behaviour, magnetism, and mixed ionic electronic conductivity

A. J. Brown¹, O. Wagstaff², A. Manjón-Sanz³, H. Brand⁴, M. Avdeev^{1,4}, I. Evans², C. D. Ling^{*1}

¹ School of Chemistry, The University of Sydney, NSW 2006, Australia;

² Neutron Scattering Division, ORNL, Oak Ridge, Tennessee, United States;

³ Australian Synchrotron, 800 Blackburn Rd Clayton, VIC Australia;

⁴ Australian Centre for Neutron Scattering, ANSTO Lucas Heights, NSW Australia;

⁵ Department of Chemistry, Durham University, Science Site, South Road, Durham, U.K.

* The corresponding author e-mail: chris.ling@sydney.edu.au

Keywords: oxide conduction; phase transitions; redox; magnetism; cation-ordered

The $\text{Ba}_3\text{LnFe}_2\text{O}_{7.5}$ family of compounds are oxygen-deficient perovskites the structures of which can be described as ordered arrays of corner-linked LnO_6 octahedra and FeO_4 tetrahedra on the perovskite B-sites. [1,2] Reports of magnetic properties of these compounds have been mixed. The initial study of $\text{Ba}_3\text{YFe}_2\text{O}_{7.5}$ found no evidence for long-range magnetic order down to 5 K; however, subsequent studies found they do show low-temperature magnetic order. [1,2] The $\text{Ba}_3\text{LnFe}_2\text{O}_{7.5}$ family therefore present a good opportunity to study complex magnetic interactions between magnetic Ln^{3+} 4f and Fe^{3+} 3d cations. We made the Y and Dy compositions with this structure and observed long-range antiferromagnetic order at $T_N = 6$ and 14 K respectively. The Dy composition also shows evidence for metamagnetism with field-dependant hysteresis below T_N . *Ab initio* density functional theory (DFT) calculations comparing the energies of different magnetic structures support our experimental data.

Additionally, at high temperatures (above 500 K) we found that these materials undergo multiple redox-associated phase transitions and show high mixed ionic-electronic conductivity. We used variable temperature *in situ* synchrotron X-ray diffraction to investigate the phase transitions. At approximately 500-600 K (depending on the Ln^{3+} cation), $\text{Ba}_3\text{LnFe}_2\text{O}_{7.5}$ compounds undergo first-order phase transitions to an orthorhombic phase. The phase transition is correlated with an uptake of oxide ions into lattice vacancies accompanied by the partial redox of Fe^{3+} to Fe^{4+} . Impedance spectroscopy measurements show that these phases also have high total conductivities ($>10^{-2} \text{ S}\cdot\text{cm}^{-1}$ at 773 K), making them very promising as mixed oxide-ionic and electronic conductors.

References

- [1] K. Luo and M. A. Hayward, *Inorganic chemistry* 51 (22), 12281–12287 (2012).
- [2] A. K. Kundu, *et al.*, *Journal of Materials Chemistry C* 5 (29), 7236–7242 (2017).

Acknowledgments

This work was supported by an Australian Government Research Training Stipend. We thank the Australian Nuclear Science and Technology Organisation for providing access to the Australian Synchrotron (PD) and Australian Centre for Neutron Scattering (Echidna) beamlines. We also thank Oak Ridge National Laboratory for beamtime on POWGEN.

Understanding the texture degree on Zinc Aluminate Nd, Ce sub-micrometer films by screen printing for NIR Emitting applications

R. E. Rojas-Hernandez^{1*}, F. Rubio-Marcos², J. F. Fernandez², I. Hussainova¹

¹ Department of Mechanical and Industrial Engineering, Tallinn University of Technology, Ehitajate 5, 19180 Tallinn, Estonia; ² Electroceramic Department, Instituto de Cerámica y Vidrio, CSIC, Kelsen 5, 28049, Madrid, Spain;

* The corresponding author e-mail: rocio.rojas@taltech.ee

Keywords: screen-printing; luminescence; molten salts; film; rare-earths

A simple and cost-effective screen-printing route assisted by molten salts has been developed to produce luminescent ZnAl₂O₄: Nd, Ce sub- micron films over poly and monocrystalline alumina substrates. The films are uniform and dense, and the use of sapphire substrate opens up new possibilities in optoelectronic and photonic devices due to their optical transparency in a wide wavelength range.

An adequate compositional engineering strategy as well as the Ce content play fundamental role in the fabrication of homogeneous ZnAl₂O₄-based films with the high optical performance. It has been demonstrated that the incorporation of Cerium together with Neodymium promotes NIR emission of the material^[1]. In-depth analysis were done by XPS and XANES spectroscopy

to quantify the Ce³⁺/Ce⁴⁺. The NIR luminescence under 357 nm is achieved by the incorporation of Cerium and its stabilization as Ce⁴⁺.

The controlling of the crystallinity of the phase structure of the films is a mandatory requirement for a high- efficiency films. Certain texture was achieved over polycrystalline substrates, however predominant (hk0)-textured films were obtained over sapphire substrates. The preferential orientations degree has a role in the final luminescence response.

We believe that the proposed methodology to design ZnAl₂O₄-based films makes a crucial contribution to develop the efficient NIR emitters and may be applied to other aluminate-based systems.



References

- [1] M. Yamaga, Y. Oda, H. Uno, K. Hasegawa, H. Ito, S. Mizuno, Phys. Status Solidi C 9(12), 2300–2303 (2012)

Acknowledgments

The financial support from the Estonian Research Council (grants PSG-466, PRG-643) is gratefully acknowledged.

Many body localisation in $\text{CeMnAsO}_{1-x}\text{F}_x$?

A. C. McLaughlin¹, G. Lawrence¹, S. Simpson¹ and E. J. Wildman¹

¹ Department of Chemistry, University of Aberdeen, Aberdeen AB24 3UE, United Kingdom

* The corresponding author email: a.c.mclaughlin@abdn.ac.uk

Keywords: insulator-insulator transition; antiferromagnet; Mott insulator; many body localisation; quantum materials

Transition metal oxypnictides are known to exhibit a range of exotic phenomena. For example, high temperature superconductivity in $\text{LnFeAsO}_{1-x}\text{F}_x$ [1] and colossal magnetoresistance in $\text{LnMnAsO}_{1-x}\text{F}_x$ [2] ($\text{Ln} = \text{Nd}, \text{Pr}$) where the resistivity reduces by 95% at 4 K in a 7 T field. We have been investigating $\text{CeMnAsO}_{1-x}\text{F}_x$ ($x = 0 - 0.075$) and here we show how the electronic properties change with F^- doping. CeMnAsO is a Mott insulator. Upon electron doping via substitution of O^{2-} with F^- an unusual insulator – insulator transition is observed for $x \geq 0.035$. The resistivity increases by more than two orders of magnitude over a 2 K temperature range and the transition temperature can be tuned by increasing x . Variable temperature synchrotron and neutron diffraction studies confirm that there is no change in the crystal or magnetic structure at the insulator-insulator transition. Results from AC transport and Hall measurements suggest this transition could be the first observation of many body localisation (MBL) in the solid state. The most significant characteristic of MBL systems is that below a transition temperature (T_{MBL}) they become perfect insulators, exhibiting zero electronic conductivity [3]. The MBL phase also acts as a quantum memory and can be used to protect quantum memory allowing the tantalising possibility of performing topological quantum computation at finite temperatures.

References

- [1] Y. Kamihara, T. Watanabe, M. Hirano and H. Hosono, *J. Amer. Chem. Soc.*, **130**, 3296–3297 (2008).
- [2] E. J. Wildman, J. M. S. Skakle, N. Emery and A. C. McLaughlin, *J. Amer. Chem. Soc.*, **134**, 8766–8769 (2012).
- [3] D. A. Abanin, E. Altman, I. Bloch and M. Serbyn, *Rev. Mod. Phys.*, **91**, 021001 (2019); M. J. Gullans and D. A. Huse, *Phys. Rev. Lett.*, **123**, 110601 (2019).

V-V dimerization in MnVO₃ ilmenite low-pressure polymorph: Crystal and magnetic structures and properties

A. M. Arévalo-López^{1*}, D. Khalyavin,² O. Mentré¹

¹ Univ. Lille, CNRS, Centrale Lille, Univ. Artois, UMR 8181 – UCCS F-59000 Lille, France;

² ISIS facility, Rutherford Appleton Laboratory, Harwell Oxford, Didcot OX11 0QX, UK.

* The corresponding author e-mail: angel.arevalo-lopez@univ-lille.fr

Keywords: strongly-correlated electrons; high-pressure; diffraction; magnetism

Systems with partially filled valence electrons may suffer electronic and structural changes due to instabilities, for instance the Peierls transition (cation dimerization) in VO₂ accompanied by a metal-insulator transition (MIT). In here, MnVO₃-I in its ilmenite polyform will be presented with such instabilities.

MnVO₃-I was reported long time ago by Syono *et al.* [1] However, the triclinic symmetry (*P*-1) precluded the authors for a proper structural determination. We have prepared MnVO₃-I via high-pressure high-temperature synthesis at 4 GPa and 1100 °C with a Walker-type multi anvil apparatus. The crystal structure was solved from an isolated small single crystal. At 300 K, MnVO₃-I possess *P*-1 symmetry with $a = 5.01770(2)$ Å, $b = 5.05130(1)$ Å, $c = 5.52100(2)$ Å, $\alpha = 116.6793(3)^\circ$, $\beta = 90.0439(2)^\circ$ and $\gamma = 118.9243(3)^\circ$ unit cell parameters. The polymorph represents a distorted version of the ilmenite-type structure with alternating Mn-V honeycomb-layers, Fig. 1a, similar to the recently reported MgVO₃ and CoVO₃. [2,3]

The triclinic distortion in MnVO₃-I arises from V-V dimerization with a short bond of 2.85 Å as shown in Figure 1a. It also shows an AFM transition at $T_N = 58$ K with a Curie-Weiss behaviour above 70 K and presents a $|\theta_W| = 236(1)$ K and a $\mu_{\text{eff}} = 5.8(1)$ μ_B . The latter is close to the theoretical value of 6.16 μ_B for V⁴⁺ and Mn²⁺, assuming the spin contribution only. This suggests that although the vanadium atoms are involved in a cation dimerization they also contribute to the magnetic behaviour, contrary to what observed in CoVO₃.

I will also present our results on the structural evolution at high-temperature along with the MIT transition and the low-temperature magnetic structure with respective refined moments of 3.7(1) μ_B and 0.45(1) μ_B for Mn and V at 1.5 K.

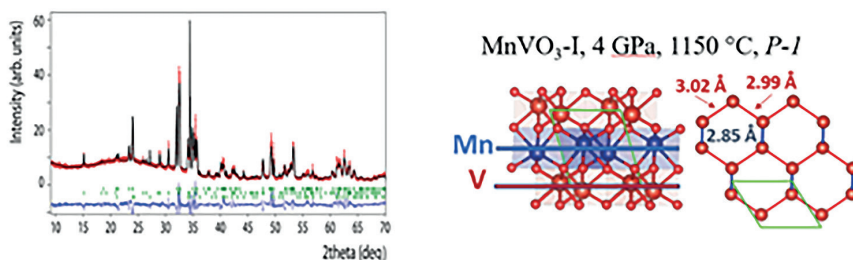


Figure: Lab X-ray CuK α diffraction and distorted MnVO₃-I structure, *P*-1, the dimerization in the Vanadium honeycomb layer is shown.

References

- [1] Y. Syono, S. Akimoto, Y. Endoh, *J. Phys. Chem. Solids*, **32**, 243 (1971)
- [2] H. Yamamoto, S. Kamiyama, I. Yamada, H. Kimura, *J. Am. Chem. Soc.*, **144**, 1082 (2021)
- [3] S. Kamiyama, I. Yamada, M. Fukuda, Y. Okazaki, T. Nakamura, T. Nishikubo, M. Azuma, H. Kimura, H. Yamamoto. *Inorg. Chem.*, **61**, 7841 (2022)

Multifunctional coordination polymers for fluorescent sensing of VOCs and hazardous ions from contaminated water

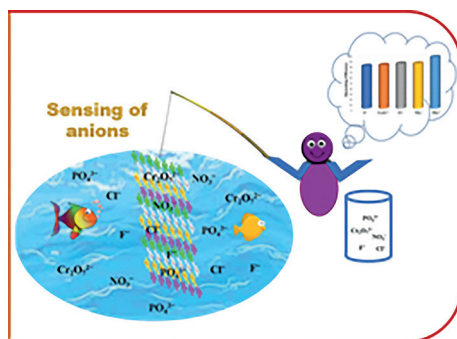
K. A. Siddiqui

Department of Chemistry National Institute of Technology Raipur
G. E. Road Raipur-492010, Chhattisgarh, India

* The corresponding author e-mail: kasiddiqui.chy@nitrr.ac.in

Keywords: functional coordination polymers; hazardous ions; fluorescent sensing

CP-based fluorescence sensors in particular have advanced dramatically owing to their potential significance in environmental and biological systems. Currently, the vast majority of CPs employed for the detection of hazardous anions and small organic solvents induce fluorescence quenching and are effective for volatile organic compounds. Volatile organic compounds are a diverse class of substances that are found in both commercial and residential settings. Effective identification of these chemical species in the vapor phase is crucial due to their prevalence and potential health hazards. Volatile organic compounds exposure can be caused by a range of substances, including solvents, lubricants, fuels, plasticizers, and others. Because of its quick response, high sensitivity, high accuracy, and reusability, as well as the impressive tunability built into CPs. Additionally, they also require less complicated instrumentation and sample preparation. In this work we present the application of functional coordination polymers towards luminescent sensing of hazardous ions like cations, anions and volatile organic molecules that have huge impact on environment.



References

- [1] Somnath, M., Ahmad, K. A. Siddiqui, *New J. Chem.*, (2022), <https://doi.org/10.1039/D2NJ04957K>
- [2] P. Singh, M., Ahmad, K. A. Siddiqui, *Crystengcomm*, (2022), <https://doi.org/10.1039/D2CE01387H>

Acknowledgments

This work was supported by the NIT Raipur under CPDA grant.

Structural investigation of new Li ion containing oxides using combined diffraction and NMR and EXAFS spectroscopy

F. N. Sayed^{1,2*}, Q. Jacquet^{1,3}, P. Groszewicz^{1,4}, S. P. Emge¹, P. C. M. M. Magusin¹, C. O'Keefe¹, S. Dey¹, C. Kocer⁵, A. Morris⁵, C. P. Grey^{1,2*}

¹ Yusuf Hamied Department of Chemistry, Lensfield Road, CB2 1EW, Cambridge, UK;

² The Faraday Institution, Harwell Science and Innovation Campus, Didcot OX11 0RA, UK;

³ Univ. Grenoble Alpes, CEA, CNRS, Grenoble INP, IRIG-SyMMES, 38000 Grenoble, France;

⁴ Delft University of Technology, Mekelweg 5, 2628 CD Delft, Netherlands;

⁵ Cavendish Laboratory, 19 JJ Thomson Avenue, Cambridge, CB3 0HE UK;

* The corresponding author e-mail: fs491@cam.ac.uk; cpg27@cam.ac.uk

Keywords: Li based oxides; X-ray diffraction; neutron diffraction; solid-state nuclear magnetic resonance spectroscopy; X-ray absorption spectroscopy

The role of lithium (ion and metal) based batteries in energy storage is unprecedented thanks to electrode structure-property understanding. This has not only helped in achieving the desired performance (capacity, power, electro-chemical stability) but has also been useful in controlling the long-term degradation issues. Beyond anode and cathodes, new Li-ion conductors need to be designed for artificial interface or solid electrolytes. Due to sparse reports of electronically insulating Li rich materials containing Group V d⁰ metal oxides, we have decided to explore the Li-M-O phase diagrams (M being Ta and Nb).

By drastically increasing the Li content in precursor stoichiometry, we have successfully synthesised new phases by a solid-state route. In order to identify the structures of these new phases and owing to the low X-ray scattering cross section of Li compared to Ta/Nb, we combined synchrotron X-ray diffraction (SXR) and neutron diffraction (ND) revealing a layered structure with a complex superstructure. To get a full structural pictures, local M-O distances and symmetries were assessed by Ta and Nb K edge extended X-ray absorption fine structure (EXAFS) analysis combined to solid state nuclear magnetic resonance (ssNMR) spectroscopy. Symmetric MO₆ featuring M-O distances in the range of reported values were found and these results were used as feedback into the combined SXR and ND analysis, validating the identified crystal structure. In the presentation we will talk in detail about the synthesis and structural characterisation of newly identified Li rich phases.

References

- [1] Zhang, Zhizhen, Yuanjun Shao, Bettina Lotsch, Yong-Sheng Hu, Hong Li, Jürgen Janek, Linda F. Nazar, et al. 'New Horizons for Inorganic Solid State Ion Conductors'. *Energy Environ. Sci.* 11, no. 8 (2018): 1945–76.
- [2] Segura, Marco Amores. 'Design and Advanced Characterisation of Lithium-Rich Complex Oxides for All-Solid-State Lithium Batteries', Ph.D Thesis.

Acknowledgment

This work was supported by the Faraday Institution CATMAT (grant number FIRG016) project.

Theoretical insights into the monolayer adsorption and characterization of HB238 merocyanine on Ag(100) surface

R. Tomar¹, A. Kny², M. Sokolowski², T. Bredow¹

¹ Mulliken Centre for Theoretical Chemistry, Clausius Institute for Physical and Theoretical Chemistry, University Of Bonn - Beringstrasse 4, D-53115 Bonn (Germany);

² Institute of Physical Chemistry, Clausius Institute for Physical and Theoretical Chemistry, University Of Bonn - Wegelerstrasse 12, D-53115 Bonn(Germany)

* *The corresponding author e-mail: tomar@uni-bonn.de*

Keywords: mmerocyanine; Density Functional Theory (DFT); SPA-LEED; STM; Ag(100); adsorption; electronic structure; Extended Tight Binding (xTB)

Merocyanines are promising prototypical molecules for applications in optoelectronic devices, including organic solar cells, OLEDs, and OFETs. We performed a combined experimental and theoretical study to investigate the adsorption of HB238 merocyanine on the surface of Ag (100). STM and SPA-LEED experiments suggested that HB238 self-organizes as chiral tetramers upon adsorption. It is critical to control the structure and morphology of merocyanine films in order to enhance their light absorption and optimize their optoelectronic properties. Therefore, quantum chemical calculations were performed to corroborate these experimental findings.

Initially, we screened the conformations of HB238 and used the most stable structure to determine the optimal adsorption orientation of HB238 on the Ag surface using the semi-empirical method GFN1-XTB implemented in DFTB+. Next, we optimized the single-molecule and monolayer adsorption on the surface of Ag(100) at the PBE/D3 level to analyze the assembly of chiral tetramers while maintaining the supercell lattice constant values, as in the experiment. HB238 preferentially adheres face-on to the Ag surface with S atoms on top of Ag and over bridge positions. It was confirmed that a monolayer corresponding to the experimentally observed α phase is stabilized with respect to the single molecule. Furthermore, we calculated the electronic structure at the PBE/D3+U level and compared our results to experimental UPS and STM images. The theoretical results support the experimental findings. Further modeling of merocyanines as efficient absorbers for organic solar cells is in progress.

Acknowledgments

This work was supported by the Deutsche Forschungsgemeinschaft(DFG) with the grant (FA 1502/1-1) and the High-Performance Computing(HPC) of the University of Bonn with computing time and resources on the HPC cluster Bonna.

Understanding the synthetic reliability of Na_xMnO_2 and similar layered phases

L46

J. Beecham-Lonsdale¹, D. C. Arnold¹, S. Ramos-Perez²

¹ School of Chemistry and Forensic Science & ² School of Physics and Astronomy, Division of Natural Science University of Kent, Canterbury, Kent, CT2 7NH, UK,

* The corresponding author e-mail: jhb24@kent.ac.uk

Keywords: Na_xMnO_2 ; layered phases; hydration; cathode materials; antiferromagnetism

Sodium manganese oxides have garnered extensive interest as both battery cathodes and frustrated magnetic materials. [1] The former relates to their ability to intercalate/deintercalate interlayer Na and/or Li-cations, the latter focuses on the $[\text{MnO}_6]^{2-}$ octahedral layers possessing frustrated antiferromagnetic triangular connectivity of the magnetic cations.

Despite their interesting properties, little work has been done to understand structural differences between Na-deficient phases (Na_xMnO_2). XRPD phase identification is non-trivial owed to synthetic Na-volatility resulting in site defects alongside Na-cation disorder, stacking faults and phase intergrowths. For example, resultant peak broadening yields ambiguity between comparative phases $\text{Na}_{0.478}\text{MnO}_2$, $\text{Na}_{0.7}\text{MnO}_2$ and related $\text{Na}_2\text{Mn}_3\text{O}_7$ which can be comparatively written as $(\text{Na}_{0.67}\text{MnO}_{2.33})$ (**Fig. 1**). Further complexity arises from phase hydration in air, yielding Birnessite-like phases.

$\text{Na}_{0.7}$ exist as *Cmcm* with octahedral Na-sites, stacked between $[\text{MnO}_6]$ octahedral layers with AAAA stacking, whilst $\text{Na}_{0.478}$ has *P6₃/mmc* symmetry, trigonal prismatic Na-cations possessing ABAB stacking, where $[\text{MnO}_6]$ interlayer octahedra form the delafossite magnetic structure. $\text{Na}_2\text{Mn}_3\text{O}_7$ however has a maple-leaf magnetic structure built from interlayer octahedral $[\text{MnO}_6]$ units. Between $[\text{MnO}_6]$ layers exist Na-layers with both trigonal prismatic and distorted octahedral Na-sites producing an ABAB stacking, existing as P. Due to the importance of these sodium deficient phases as cathode materials, clarity surrounding synthetically realised targets is required. This work seeks to elucidate the structural and magnetic significance of varying Na-content and determine the role of hydration in these materials.

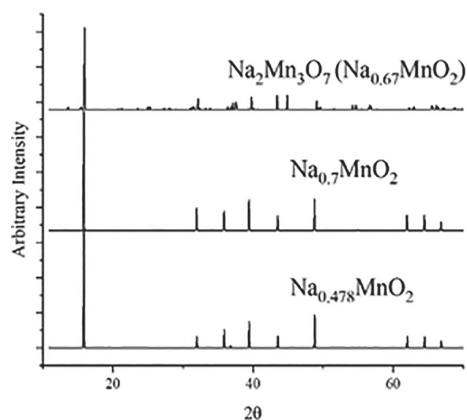


Fig. 1: Comparative calculated XRPD patterns of $\text{Na}_2\text{Mn}_3\text{O}_7$, $\text{Na}_{0.7}\text{MnO}_2$ and $\text{Na}_{0.478}\text{MnO}_2$, highlighting similarity in calculated patterns.

References

- [1] C. Hakim *et al.* *Energy Fuels* 2022, 36, 7, 4015–4025 [2] Venkatesh *et al.* *Phys. Rev. B* 101, 184429

Acknowledgments

Thanks to the Leverhulme Trust, ISIS Neutron and Muon Source, and Diamond Light Source.

X-ray Photoelectron Spectroscopy: a key tool for assessment of 2D Molybdenum Dichalcogenides synthesized by ALD

J. Rodriguez-Pereira^{1,2}, R. Zazpe^{1,2}, J. Charvot³, F. Bures³, J.M. Macak^{1,2}

¹ Center of Materials and Nanotechnologies, Faculty of Chemical Technology, University of Pardubice, Nam. Cs. Legii 565, 530 02 Pardubice, Czech Republic;

² Central European Institute of Technology, Brno University of Technology, Purkynova 123, 61200 Pardubice, Czech Republic;

³ Institute of Organic Chemistry and Technology, Faculty of Chemical Technology, University of Pardubice, Studentska 573, 53210 Pardubice, Czech Republic

* *The corresponding author e-mail:* jhonatan.rodriquezpereira@upce.cz

Keywords: XPS; atomic layer deposition; 2D materials; transition metal dichalcogenides; surface science

The success of graphene opened a door for a new class of semiconducting 2D transition metal dichalcogenide materials (TMDs) displaying unique properties [1]. ALD MoS₂, as TMDs benchmark, has been widely studied for several applications. In parallel, 2D selenide and telluride analogues, i.e. MoSe₂ and MoTe₂, have also attracted important interest due to intriguing properties, such as a higher electrical conductivity than MoS₂ among others [2,3].

Recently, we have demonstrated the ALD synthesis of both 2D MoSe₂ [4-7] and 2D MoTe₂ [8] (using an in-house synthesized precursors), as well as their outstanding performances in different applications. XPS turned a key tool to provide detailed chemical composition analysis of as-deposited 2D Mo TMDs family on different nature substrates. Besides, the post-performance XPS characterization was appealing since the applications of the aforementioned 2D materials involved chemical and/or electronic processes on the surface and allowed to identify potential chemical composition changes and physicochemical photo-electro stability of the 2D TMDs.

This presentation will thus focus on the XPS as key tool for assessment of chemical composition of both as-deposited and post-performance 2D Mo TMDs family, recent experimental results as well as the description of some inherent drawbacks that XPS must face during the analysis of the 2D materials.

References

- [1] A.V. Kolobov, J. Tominaga, Two-Dimensional Transition-Metal, Dichalcogenides. Springer Series in Materials Science, Springer International Publishing AG, Switzerland 2016
- [2] D. Kong et. al., Nano Letters, **13**, 1341 (2013)
- [3] A. Eftekhari, Applied Materials Today, **8**, 1-17 (2017)
- [4] R. Zazpe et. al., FlatChem, **21**, 100166 (2020)
- [5] J. Charvot et. al., ChemPlusChem, **85**, 576 (2020)
- [6] J. Rodriguez-Pereira et. al., Surface Science Spectra, **27**, 024006 (2020)
- [7] R. Zazpe et. al., ACS Applied Nano Materials, **3**, 12034 (2021)
- [8] R. Zazpe et. al., Applied Materials Today, **23**, 101017 (2021)

Charge density refinement on inorganic crystals using electron diffraction

L48

E. Yörük¹, A. Suresh¹, P. Brázda¹, M. K. Cabaj¹, L. Palatinus¹

¹ Institute of Physics of the CAS, Na Slovance 2, Prague 8, Czechia

* The corresponding author e-mail: yoruk@fzu.cz

Keywords: charge density; kappa refinement; electron diffraction; TEM, crystallography

We investigate whether the charge density can be refined for compounds with heavy atoms using 3D electron diffraction (3D ED), which is an increasingly popular technique for structural analysis of nanocrystals [1]. Charge transfer due to bonding can lead to non-modelled residues in electron density maps [2]. Knowledge of the charge transfer may also be important for understanding the investigated material. For compounds with heavy atoms, the small ratio of valence/core electrons contributing to the electron density necessitates an extreme precision in diffraction data to refine the valence electron contributions to the density. Since electron scattering is more sensitive to fine details in the electron density distribution compared to X-ray scattering [3], we seek to explore whether 3D ED data can be used for charge density analysis of heavy atoms. We use a spherical atom kappa formalism [4] where atomic contributions to the charge density remain spherical, but the population of the valence shell is refined while allowing it to expand or contract as a result of changes in electron-electron repulsion.

We present results from a number of inorganic compounds, including CsPbBr₃, Lu₃Al₅O₁₂, SiO₂, Na₂Al₂Si₃O₁₀·2H₂O and B₁₈H₂₂. All refinements were performed in Jana2020 [5]. There is reduced noise in potential difference maps and refined valence shell populations are visible on static deformation maps (Fig. 1). The experimentally refined charge flows agree with chemical predictions based on electronegativity, and there are improvements in the displacement parameters and R-factors. The results were compared with DFT calculations.

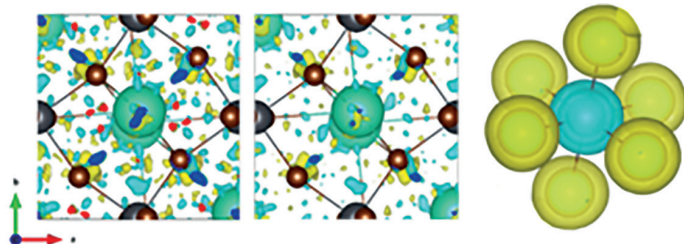


Figure 1: Electrostatic potential difference Fourier maps at the same isosurface level before (left) and after (middle) kappa refinement on CsPbBr₃. On the right, static deformation map after kappa refinement on the PbBr₆ octahedra. Accumulation of charge on the Br atoms (yellow) and the depletion of charge on Pb (blue) is seen.

References

- [1] Gemmi M. et al. (2019) *ACS Cent. Sci.* **5**, p. 1315.
- [2] Grabowsky S. (2021) De Gruyter, *Complementary Bonding Analysis*.
- [3] Zheng J. et al. (2004) *J. of Applied Cryst.*, **38** (4) p. 648.
- [4] Coppens P. (1997) Oxford Univ. Press, *X-Ray Charge Densities and Chemical Bonding*.
- [5] Petříček V. et al. (2014) *Zeitschrift für Kristallographie*, **229** (5), p. 345.

Acknowledgments

This work was funded by the Czech Science Foundation, Grant No. 21-05926X, and H2020 ITN project NanED, grant agreement No. 956099

Chemistry at the nanoscale – AFM meets IR Spectroscopy

J. Horák^{1*}

¹ Měřicí technika Morava s. r. o., Babická 619, 664 84 Zastávka, Czech Republic

* *The corresponding author e-mail: jakub.horak@mt-m.eu*

Keywords: AFM; IR spectroscopy; photothermal; AFM-IR; correlative microscopy

Nanoscale Infrared spectroscopy [1] has been successfully demonstrated in an expanding range of applications in recent years due to significant increases in capability. One method of nanoscale infrared spectroscopy, atomic force microscope based infrared spectroscopy (AFM-IR) uses the tip of an AFM as a nanoscale detector of the expansion caused by absorption of IR radiation.

AFM-IR can be used to obtain IR absorption spectra and chemical imaging with resolution as fine as the AFM tip radius, >100X smaller than spatial resolution limits of conventional infrared spectroscopy. The photothermal AFM-IR technique has demonstrated improvements in sensitivity, down to the scale of single monolayers, and speed with spectral acquisition times dropping by an order of magnitude.

This presentation will describe the underlying technology and complementary techniques for nano-mechanical/nano-electrical and nano-thermal analysis. Additionally, we will also highlight numerous applications of nanoscale spectroscopy and chemical imaging in physics, materials and life sciences. Applications include nanoscale chemical analysis of polymers, composites, semiconductors, biological cells, proteins, tissue, and other areas.

References

- [1] J. Mathurin, A. Deniset-Besseau, D. Bazin, E. Dartois, M. Wagner, A. Dazzi, *J. Appl. Phys.* **131**, 010901 (2022)

CeScSi-type intermetallics: Modulation of magnetic properties through light elements insertion and catalysis of ammonia

E. Gaudin¹, K. Alabd¹, C. Croisé², F. Can², X. Courtois², N. Bion², A. Villesuzanne¹, S. Tencé¹

¹ CNRS, Univ. Bordeaux, ICMCB, UMR 5026, F33600 Pessac, France;

² IC2MP, UMR 7285, Université de Poitiers, CNRS, F-86073 Poitiers, France

* The corresponding author e-mail: etienne.gaudin@u-bordeaux.fr

Keywords: intermetallic; insertion; magnetism; catalysis; electride

The CeScSi-type structure observed for the intermetallics RETX (RE = rare-earth, T = Sc or Ti, X = Si or Ge) is an ordered variant of the La₂Sb-type that exhibits [RE₄] tetrahedral and [T₄RE₂] octahedral interstitial sites. These sites can be filled by light elements such as hydrogen, carbon or oxygen leading to modification of the physical properties.

In the first part of this presentation, we will show the effect on magnetic properties of the filling of these interstitial sites by hydrogen, carbon and oxygen. The first example concerns the insertion of C and/or H into the antiferromagnetic CeScSi parent phase [1]. The different magnetic structures were determined by neutron diffraction. Very recently, we also succeeded to insert oxygen into these intermetallic phases without decomposing them into binary or ternary oxides. The preliminary results on the structural and magnetic properties of the new phases REScSiO_x will be presented.

The second part of this communication will be devoted to the use of the CeScSi-type RETX intermetallics as Ru-supported catalysts for ammonia synthesis in the Haber-Bosch process ($N_2 + 3H_2 \rightarrow 2NH_3$). Their electride character, firstly evidenced by Hosono group in 2017 plays an important role for the dissociation of N₂ [2]. We have investigated the influence of the rare-earth (RE) element in Ru/REScSi catalysts under mild conditions (300–450 °C; 1–5 bar) [3]. Ru/CeScSi shows remarkable catalytic activity under moderate condition associated with its reversible hydrogen storage–release properties. The hydrogen desorption temperature seems to play a role as well in the catalytic activities at low temperature (300 °C). It suggests that the electride character and thus the electron donor effect can be tuned through partial hydrogenation of the REScSi materials. DFT calculations, thermodynamic and kinetic studies of hydrogen sorption are under way to answer these questions.

References

- [1] T. Mahon, E. Gaudin, V. Nassif, S. Tencé, *to be submitted*
- [2] J. Wu, Y. Gong, T. Inoshita, D. C. Fredrickson, J. Wang, Y. Lu, M. Kitano, H. Hosono, *Adv. Mater.*, **29**(36), 1–7 (2017)
- [3] C. Croisé, K. Alabd, S. Tencé, E. Gaudin, A. Villesuzanne, X. Courtois, N. Bion, F. Can, *ChemCatChem*, *in press* (2023)

Acknowledgments

The authors acknowledge the support of the French Agence Nationale de la Recherche (ANR), under grant ANR-19-CE07-0023 (project INTERMETALYST).

Analysis of ground particle behaviour in wet ball milling by DEM-CFD simulation

K. Kushimoto¹, J. Kano¹

¹ Institute of Multidisciplinary Research for Advanced Materials, Tohoku University, Katahira 2-1-1, Aoba-ku, Sendai 980-8577, Japan

* The corresponding author e-mail: kano@tohoku.ac.jp

Keywords: wet ball milling; DEM-CFD; nanoparticles; aggregation; grinding limit

The particle diameter required for particles produced by milling has been decreasing year by year, and recently there has been a growing demand to realize the production of nanoparticles. In this situation, the wet ball mill, which has the smallest achievable particle diameter among the many milling methods, is expected to be used to produce nanoparticles. However, the production of nanoparticles is currently difficult even with wet ball milling. This is because of the “grinding limit,” where particle diameter reduction stops at about 1.0 μm , and “re-aggregation,” where the particle diameter increases even if the grinding time is extended. The mechanisms of these two phenomena have not yet been clarified. This is due to the fact that experimental analysis of the behaviour of ground particles in a wet ball mill is difficult. On the other hand, numerical simulation is an effective method for analysing phenomena that are difficult to analyse experimentally.

In this study, the behaviour of ground particles in a wet ball mill is represented by numerical simulation, and the mechanism of the grinding limit and re-aggregation observed during wet ball milling are analysed.

The ground particles during wet ball milling are mainly captured between the media balls. Therefore, in this simulation, the behaviour of ground particles in a slurry of suspended ground particles is represented by the approach and collision of two media balls. The Discrete Element Method (DEM) and the Finite Difference Method (FDM) are used for the particle motion and fluid motion, respectively, while the DEM-CFD coupling model [1] is used for the particle-fluid interaction and the ball-fluid interaction is described by the volume force type embedded boundary method [2] for the ball-fluid interaction and the volume force type immersed boundary method [3], respectively. The media ball is treated as a wall boundary moving along a fixed trajectory.

When the media balls collide with the slurry in a completely dispersed state, the ground particles form aggregates. The aggregates grow even more when the media balls repeatedly collide with each other, even under conditions of relatively strong electrostatic repulsion. This aggregation behaviour is attributed to the fact that the van der Waals force becomes dominant due to the reduction of the distance between the compressed particles caused by the collision of the media balls. In other words, the grinding limit is reached when the collision of the media balls begins to contribute to the progression of aggregation, and then re-aggregation occurs when the collision acts on the growth of the aggregates.

References

- [1] Y. Tsuji, T. Tanaka, T. Ishida, *Powder Technol.*, **71** (1992) 239-250.
- [2] S. Takiguchi, T. Kajishima, Y. Miyake, *Transactions of the Japan Society of Mechanical Engineers, Series B*, **633** (1998) 2804-2810.
- [3] K. Kushimoto, S. Ishihara, J. Kano, *Adv. Powder Technol.*, **30** (2019) 1131-1140.

Acknowledgments

This research was supported in part by “JSPS KAKENHI Grant Number JP20K22457.

Lumino- and optomagnetic composites for the design of multifunctional materials

K. Müller-Buschbaum¹, M. Seuffert¹, T. Wehner¹

¹ Institute of Inorganic and Analytical Chemistry, Justus-Liebig-University Giessen, Heinrich-Buff-Ring 17, 35392 Gießen, Germany

* The corresponding author e-mail: kmbac@uni-giessen.de

Keywords: composites; luminescence; magnetism; sensing

Solid-state composites allow for a property driven combination of components that can add their properties to a multifunctional material. Thereby, an arrangement of several chemical components can be utilized to combine very different chemical and physical properties into one material that cannot easily be found for homogenous matter. An interdependence of the constituents and thus of their properties can be achieved, resulting in beneficial synergistic arrangements.

Novel lumino magnetic materials are achieved as multifunctional supraparticular systems by combinations of hard and soft magnetic materials, such as α -Fe and Fe_3O_4 together with, e.g. luminescent MOFs [1,2]. Different from these composites, a combination of luminescence and strong magnetism is typically not observed for a single homogenous phase with one electronic system. The interaction of the electronic systems of the components of a composite proves vital for the property combination, and its control allows for combination of both, luminescence and magnetism [3]. By combination of optical components with high light reflection, refraction as well as white light emission with strong magnetic materials, a microscopically white magnet was achieved that is white by all optical means [4], showing how far this concept can be driven. The novel composites are highly useful for chemical and physical sensing by applying external chemical or physical stimuli [5]. The read-out is based on the stimuli dependent change of the optical properties. Combination with strong magnetism allows for harvesting options and thus retrieving the sensor particles. This also beneficially influences the overall impact of the new sensors resulting in a strong sensitivity increase even for low sensor amounts. An expansion to novel shear stress sensors allows for the detection of shear stress via such an optical property change by a stress/time dependent optical signal [6].

References

- [1] T. Wehner, K. Mandel, M. Schneider, G. Sextl, K. Müller-Buschbaum, *ACS applied materials & interfaces*, **8**, 5445–5452 (2016)
- [2] K. Mandel, T. Granath, T. Wehner, M. Rey, W. Stracke, N. Vogel, G. Sextl, K. Müller-Buschbaum, *ACS nano*, **11**, 779–787 (2017)
- [3] M. T. Seuffert, T. Granath, T. Kasper, R. Maile, R. Pujales-Paradela, J. Prieschl, S. Wintzheimer, K. Mandel, K. Müller-Buschbaum, *ChemPlusChem*, e202200395 (2022)
- [4] M. T. Seuffert, S. Wintzheimer, M. Oppmann, T. Granath, J. Prieschl, A. Alrefai, H.-J. Holdt, K. Mandel, K. Müller-Buschbaum, *J. Mater. Chem. C*, **8**, 16010–16017 (2020)
- [5] T. Wehner, M. T. Seuffert, J. R. Sorg, M. Schneider, K. Mandel, G. Sextl, K. Müller-Buschbaum, *J. Mater. Chem. C*, **5**, 10133–10142 (2017)
- [6] S. Wintzheimer, J. Reichstein, S. Wenderoth, S. Hasselmann, M. Oppmann, M. T. Seuffert, K. Müller-Buschbaum, K. Mandel, *Adv. Funct. Mater.*, **29**, 1901193 (2019)

Exploring structure-property correlations in the frustrated layered material, $\text{Mn}_2\text{Mo}_3\text{O}_8$

D. C. Arnold¹, H. L. McPhillips^{1,2}, S. Ramos^{1,2}

¹ School of Chemistry and Forensic Science; Division of Natural Sciences, University of Kent, Canterbury, Kent, CT2 7NH, UK;

² School of Physics and Astronomy; Division of Natural Sciences, University of Kent, Canterbury, Kent, CT2 7NH, UK

* The corresponding author e-mail: d.c.arnold@kent.ac.uk

Keywords: frustrated magnetism; materials science; inorganic chemistry; crystallography; oxides

Multiferroic materials continue to attract extensive attention within the literature due to potential application in lower energy consuming devices. These materials exhibit both ferroelectric and magnetic ordering in a single phase. In type 1 materials these two components are independent. In contrast, in type 2 materials ferroelectricity arises as a result of complex magnetic ordering related to geometric frustration. This has the benefit of strong magnetoelectric coupling, essential for efficient device design, but with the disadvantage that ordering occurs at very low temperatures which is not desirable.

We have been investigating structure-property correlations in complex layered materials with the aim of elucidating the role of magnetic topography in controlling magnetic order and transition temperature. Of interest is the polar hexagonal ($S = 5/2$) layered oxide $\text{Mn}_2\text{Mo}_3\text{O}_8$ which crystallises in the $P6_3mc$ space group and exhibits strong linear magnetoelectric coupling. Along the lattice c -direction, $\text{Mn}_2\text{Mo}_3\text{O}_8$ ($a = b = 5.80 \text{ \AA}$, $c = 10.24 \text{ \AA}$) is composed of stacked honeycomb-like Mn-O layers separated by trimerized Mo_3O_{13} sheets. In the ab -plane, the honeycomb layer contains a 1:1 ratio of alternating corner-sharing MnO_4 tetrahedra (Mn1) and MnO_6 octahedra (Mn_2), giving rise to honeycomb connectivity. This gives rise to an easy-axis-type ferromagnetic ground state below $T_c = 41 \text{ K}$ [1]. However, a full understanding of the structural and magnetic behaviour of $\text{Mn}_2\text{Mo}_3\text{O}_8$, including when the honeycomb lattice is doped with other $3d$ transition metals, remains limited [2,3].

In this paper we will report the structure (including neutron diffraction) and properties of $\text{Mn}_2\text{Mo}_3\text{O}_8$ and MnAMo_3O_8 materials (where $A^{2+} = \text{Fe}^{2+}$, Co^{2+} and Zn^{2+}). We will discuss the role of site preference of cations (octahedral vs tetrahedral) and provide new insight into the magnetic behaviour of these materials.

References

- [1] D. Szaller, K. Szász, S. Bordács, J. Viirok, T. Rődöm, U. Nagel, A. Shuvaev, L. Weymann, A. Pimenov, A. A. Tsirlin, A. Jesche, L. Prodan, V. Tsurkan, I. Kézsmárki, *Phys Rev B*, **102**, 144410 (2020)
- [2] T. Kurumaji, S. Ishiwata, Y. Tokura, *Phys Rev B*, **95**, 045142 (2017).
- [3] S. Nakayama, R. Nakamura, M. Akaki, D. Akahoshi, H. Kuwahara, *J. Phys. Soc. Japan*, **80**, 104706 (2011)

Acknowledgments

Leverhulme Trust for funding. ISIS Neutron and Muon User Facility and Diamond Light Source for facilities access and materials characterisation lab (ISIS) for instrument access.

Developments in high-pressure growth of rare earth nickelates single crystals

D. J. Gawryluk¹

¹ Laboratory for Multiscale Materials Experiments, Paul Scherrer Institut, 5232 Villigen PSI, Switzerland

* The corresponding author e-mail: dariusz.gawryluk@psi.ch

Keywords: rare earth nickelates; single crystal growth; high oxygen pressure synthesis; solvothermal method; strongly correlated material; perovskites; ruddlesden-popper

Metastable rare earth nickel oxides, crystallizing in perovskite-related structures are an outstanding example of strongly correlated, functional materials with proximity to instabilities ranging from metal-to-insulator through multiferroicity to superconductivity. Thanks to that, rare earth nickelates provide a remarkable opportunity to study the interplay between dimensionality, structure, charge, spin and orbital momentum degrees of freedom. For instance, *3D* perovskite-like nickelates ($RENiO_3$) intrinsically exhibit thermally-driven Metal-to-Insulator Transition (MIT) [1]. Additionally, in insulating state $RENiO_3$ order magnetically below Néel temperature, what is likely the driven force of an inversion symmetry breaking in the compound [2]. Whereas, superconductivity may be induced by the dimensionality tuning of the system [3]. Nevertheless, lack of single crystals linked with necessity of high-pressure (up to 60 kbar) application during synthesis procedure has prevented better understanding of emerging physical phenomena in the nickelates perovskite super-family members.

Here, I will demonstrate novel crystallization route for growing the first ever high-quality bulk $RENiO_3$ ($RE = Nd - Lu$) single crystals [4] under moderated oxygen pressure of 2 kbar. Furthermore, I will show results of 150 bar oxygen pressure application during Traveling Solvent Floating Zone (TSFZ) growth in context of selected Ruddlesden-Popper *2D* nickelates phases [5]. Finally, I will present outcome of *quasi-1D* nickelates obtained by topochemical oxygen uptake from both, *3D* and *2D* structures [6,7].

References

- [1] D. J. Gawryluk, et al., Phys. Rev. B, 100, 205137 (2019)
- [2] I. Ardizzone, J. Teyssier, I. Crassee, A. B. Kuzmenko, D. G. Mazzone, D. J. Gawryluk, M. Medarde, and D. van der Marel, Phys. Rev. Research, 3, 033007 (2021)
- [3] D. Li, et al., Nature, 572, 624-627 (2019)
- [4] Y. M. Klein, et al., and D. J. Gawryluk, Cryst. Growth Des., 21, 4230-4241 (2021)
- [5] S. Huangfu, D. J. Gawryluk, et al., Phys. Rev. B, 101, 104104 (2020)
- [6] S. Huangfu, Z. Guguchia, D. Cheptiakov, X. Zhang, H.s Luetkens, D. J. Gawryluk, T. Shang, F. O. von Rohr, A. Schilling, Phys. Rev. B, 102, 054423 (2020)
- [7] H. Lin, D. J. Gawryluk, et al., New J. Phys., 24, 013022 (2022)

Acknowledgments

This work was partially supported by the Swiss National Science Foundation through the NCCR MARVEL (Grant No. 51NF40-182892), and the R'equip Grants No. 206021_139082 and 206021_163997.

Tuning physicochemical properties in $\text{TbMgNi}_{4-x}\text{Co}_x\text{-(H,D)}_2$ system

V. Shtender

Department of Chemistry Ångström Laboratory, Uppsala University, Box 538, 751 21 Uppsala, Sweden

* The corresponding author e-mail: vitalii.shtender@kemi.uu.se

Keywords: intermetallic compounds; metal hydrides; crystal structure; magnetic properties; XRD

Many of the alloys and intermetallic compounds (IMCs) being studied today or already studied are considered for their properties in various applications related to energy, such as hydrogen storage and magnetic properties. This is dictated by the need for a sustainable future. And since intermetallic compounds are often termed functional materials owing to their superior properties in different fields, it makes such materials of great importance for investigation. [1]

Hydrogen storage properties of $\text{TbMgNi}_{4-x}\text{Co}_x$ ($x = 0 - 4$) IMCs have been studied in the first instance. [2] Their crystal structure is characterized by a cubic system and subscribed to a SnMg-Cu_4 -type structure. They also can be described as extended solid solutions based on TbT_2 ($T = \text{Ni and Co}$) compounds, leading to a disordered variant of the MgCu_2 -type structure. It was shown that Co for Ni substitution allows: i) a substantial increase of hydrogen capacity by at least 40% (TbMgNi_4 vs. TbMgCo_4); ii) a lowering of the equilibrium plateau of hydrogen pressure (from 1.09 down to 0.1 MPa H_2 , respectively); iii) an improvement of the kinetic of the formation of hydrides (reaction rate constant changes from $\ln(k) = -9.38$ up to -6.12).

Magnetic properties of $\text{TbMgNi}_{4-x}\text{Co}_x$ ($x = 0 - 4$) IMCs depend on the Co concentration as well and range from Pauli-like paramagnets to ferromagnetic materials. Curie Temperature increasing with a higher concentration of Co. Hidden structural changes were found as well at low temperatures.

References

- [1] M. Nakamura, *Mrs Bull*, **20(8)**, 33–39 (1995).
- [2] V. V. Shtender, V. Paul-Boncour, R. V. Denys, J. C. Crivello, I. Y. Zavaliy, *J Phys Chem C*, **124(1)**, 196–204 (2020).

Acknowledgments

This work was done in a close collaboration with V. Paul-Boncour and R.V. Denys.

Magnetic properties controlled by short-range structural and spin order in layered materials

J. D. Bocarsly¹, S. E. Dutton², C. P. Grey³

¹ Department of Chemistry, University of Cambridge, Lensfield Rd., Cambridge, CB2 1EW, UK;

² Cavendish Laboratory, University of Cambridge, J. J. Thomson Ave., Cambridge, CB3 0HE, UK

* The corresponding author e-mail: jb2382@cam.ac.uk

Keywords: magnetism, coercivity, 2D materials, disorder, short-range order, neutron scattering

Layered magnetic materials have received great interest due to the prospect of using 2D magnetic sheets in spintronic devices for energy-efficient, high-performance nanoelectronics. However, magnetic order is rare in 2D, and only a few families of promising layered magnetic materials have been reported. Here, we present a family of layered sulfides that show surprising magnetic properties including extraordinarily large magnetic hysteresis, strong spin-orbit coupling, and tunable metamagnetism. Despite the dramatic magnetic behavior, we find no evidence of long-range magnetic order down to 1.6 K using neutron powder diffraction. Instead, the macroscopic magnetic properties are found to be driven by short-range ordering of both the structure and the magnetic spins. We use neutron pair distribution function (PDF), solid-state nuclear magnetic resonance (NMR), diffuse magnetic neutron scattering, and Monte Carlo modelling methods to characterise the short-range structures of the atoms and spins. The large amount of atomic disorder and the presence of short-range ordering are found to modify the magnetic structure so that unusual 2D magnetic states can be realized. This work suggests that disorder and short-range order may be used to expand the types of magnetic behaviour that may be achieved in 2D for next-generation applications.

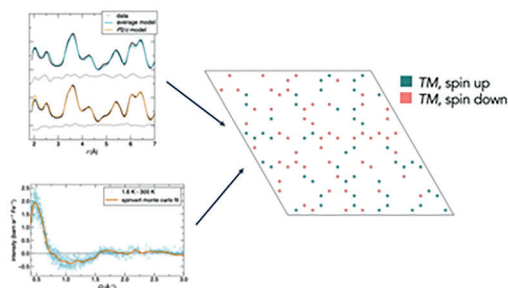


Fig. 1: Use of neutron PDF and magnetic neutron scattering to simultaneously determine local atomic and magnetic structure.

References

- [1] X. Lin, W. Yang, K. L. Wang, W. Zhao, *Nature Electronics*, **2**, 274–283 (2019)

Acknowledgments

This work was supported by the Faraday Institution CATMAT project.

Crystal growth of new uranium and transuranic phases via high temperature solution and mild hydrothermal methods: Exploration of new materials as potential nuclear waste forms

H.-C. zur Loye^{1,2,3*}, T. K. Deason^{1,2,3}, A. T. Hines^{1,2}, H. Tisdale^{1,2}, T. M. Besmann^{1,2}, J. Amoroso^{1,3}, D. P. DiPrete^{1,3}

¹ Center for Hierarchical Waste Form Materials, Columbia, South Carolina 29208, United States;

² University of South Carolina, Columbia SC, 29208, United States;

³ Savannah River National Laboratory, Aiken, South Carolina 29808, United States

* The corresponding author email: zurloye@mailbox.sc.edu

Keywords: crystal growth; actinides; transuranic; phosphates; borates; silicates

The crystal growth of uranium and transuranium containing phases has been accomplished via two different crystal growth routes, mild hydrothermal and high temperature solution flux growth. In both cases we are targeting the preparation of new compositions to evaluate their potential use as nuclear waste forms. The mild hydrothermal route works extremely well for crystallizing complex fluoride phases, such as $\text{Na}_3\text{GaU}^{\text{IV}}\text{F}_{30}$, $\text{Na}_3\text{AlNp}^{\text{IV}}\text{F}_{30}$, $\text{Na}_3\text{FePu}^{\text{IV}}\text{F}_{30}$, and $\text{Cs}_2\text{NiNp}^{\text{IV}}\text{F}_{16}$, [1,2] while the high temperature flux route works well for crystallizing oxide phases, such as $\text{Cs}_2\text{Pu}^{\text{IV}}\text{Si}_6\text{O}_{15}$, $\text{K}_3\text{Am}(\text{PO}_4)_2$, and $\text{Na}_2\text{Pu}^{\text{V}}\text{O}_2(\text{BO}_3)$. [3,4] The synthesis and structures of these phases will be discussed, along with our approach of identifying potential compositions that we can pursue synthetically. [5] Surrogate containing analogs are further investigated for their resilience to radiation damage to help identify new nuclear waste forms. [6]

References

- [1] K. A. Pace, V. V. Klepov, T. K. Deason, M. D. Smith, D. P. DiPrete, J. Amoroso, H.-C. zur Loye, *Chem. Eur. J.*, **26**, 12941–12944 (2020)
- [2] T. K. Deason, G. Morrison, A. Mofrad, H. Tisdale, J. Amoroso, D. P. DiPrete, G. Was, K. Sun, T. M. Besmann, H.-C. zur Loye, *J. Am. Chem. Soc.*, **145**, 465–475 (2023)
- [3] K. A. Pace, V. V. Klepov, M. S. Christian, G. Morrison, T. K. Deason, T. M. Besmann, D. P. DiPrete, J. Amoroso, H.-C. zur Loye, *Chem. Commun.*, **56**, 9501–9504 (2020)
- [4] L. S. Breton, V. V. Klepov, H.-C. zur Loye, *J. Am. Chem. Soc.*, **142**, 14365–14373 (2020)
- [5] M. Christian, K. A. Pace, V. V. Klepov, G. Morrison, H.-C. zur Loye, H.-C., T. M. Besmann *Cryst. Growth Design*, **21**, 5100–5107 (2021)
- [6] H. Tisdale, M. S. Christian, G. Morrison, T. M. Besmann, K. Sun, G. Was, H.-C. zur Loye, *Chem. Mater.*, **34**, 3819–3830 (2022)

Acknowledgments

This work was supported as part of the Center for Hierarchical Waste Form Materials, an Energy Frontier Research Center funded by the U.S. Department of Energy under Award No. DE-SC0016574 and by the US Department of Energy, Office of Basic Energy Sciences under award DE-SC0018739. Work conducted at Savannah River National Laboratory was supported by the U.S. Department of Energy under contract DE-AC09-08SR22470.

In-situ XRD and PDF investigation of battery fluoride materials $\text{MF}_3 \cdot 3\text{H}_2\text{O}$ ($\text{M} = \text{Fe}, \text{Cr}$) in controlled atmosphere: accessing new phases with controlled chemistry

G. Nénert¹, L. Ding¹, K. Forsberg², C. V. Colin³

¹ Malvern Panalytical B. V., Lelyweg 1, 7602 EA, Almelo, address;

² School of Chemical Science and Engineering, Royal Institute of Technology, Teknikringen 42, Stockholm, Sweden;

³ Université Grenoble Alpes, Institut Néel, F-38042 Grenoble, France

* The corresponding author e-mail: gwilherm.nenert@malvernpanalytical.com

Keywords: fluorides; *in-situ*; PDF; XRD; battery

Iron fluoride ($\text{FeF}_3 \cdot n\text{H}_2\text{O}$) shows high capacity as cathode material for lithium-ion batteries combined to low toxicity and low cost. The water content of iron fluoride has been shown to be of prime importance in the performances of the cathode. So far, the various synthesis route doesn't allow for a precise water content control, especially on the low amount regime which is the most interesting range of composition [1]. In addition, CrF_3 has been shown to significantly increase the conductivity of LiF film [2]. Consequently, it is of interest to look for the *in-situ* formation of the various $\text{MF}_{3-x}(\text{OH})_x \cdot n\text{H}_2\text{O}$ phases ($\text{M} = \text{Cr}, \text{Fe}$) (any version).

In this contribution, we report on the *in-situ* formation of $\text{MF}_{3-x}(\text{OH})_x \cdot n\text{H}_2\text{O}$ ($\text{M} = \text{Fe}, \text{Cr}$) phases using self-generated atmosphere. Traditionally, the heating $\text{MF}_3 \cdot 3\text{H}_2\text{O}$ in open air results in the full oxidation and decomposition of the fluorides giving rise to nano based oxides. Here, we make use of self-generated atmosphere to control the precise crystal chemistry of those phases upon heating preventing full oxidation at mild temperatures while stabilizing new phases relevant for battery applications. This work demonstrates the added value of *in-situ* experiment using self-generated atmosphere for synthesizing new fluoride phases.

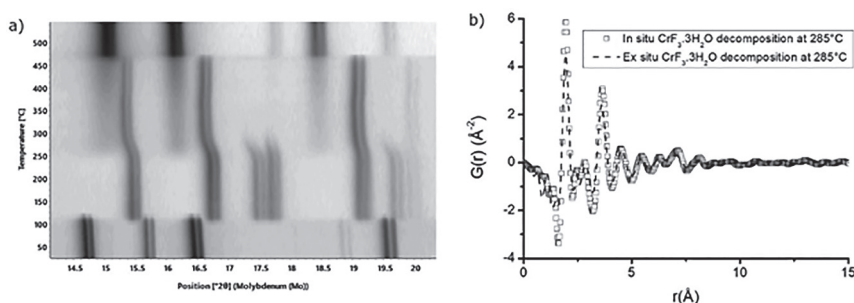


Figure 1: a) *In-situ* temperature evolution of $\text{FeF}_3 \cdot 3\text{H}_2\text{O}$ and b) PDF analysis of $\text{CrF}_3 \cdot 3\text{H}_2\text{O}$ as function of the atmosphere synthesis.

References

- [1] S. W. Kim, D. H. Seo, H. Gwon, J. Kim, K. Kang, *Adv. Mater.* 22, 5260–5264 (2010)
- [2] T. Oi, *Materials Research Bulletin*, 19, 451–457 (1984)

A facile preparation of Y_2O_2S nanoparticles through sulfidation under a CS_2 atmosphere

Y. Kanazawa¹, M. Matsubara¹, R. Ohsuga¹, A. Muramatsu^{1,2}, K. Domen^{3,4}, K. Kanie^{1,2*}

¹ Institute of Multidisciplinary Research for Advanced Material, Tohoku University, Sendai, Miyagi 980-8577, Japan;

² International Center for Synchrotron Radiation Innovation Smart, Tohoku University, Sendai, Miyagi 980-8577, Japan;

³ Research Initiative for Supra-Materials, Shinshu University, Nagano-shi, Nagano 380-8553, Japan;

⁴ Office of University Professors, The University of Tokyo, 2-11-16 Yaoi, Bunkyo-ku, Tokyo 113-8656, Japan.

* The corresponding author e-mail: kanie@tohoku.ac.jp

Keywords: nanoparticle; photocatalyst; solvothermal synthesis; thermal sulfidation; oxysulfide

Introduction Introduction of sulfur into metal oxide nanoparticles (NPs) has been attracted a great deal of attention, especially in a field of photocatalyst because it provides a narrower energy band gap into the base NPs to induce visible light responsivity. The sulfur atoms can be introduced by using H_2S gas as the source. However, high toxicity of H_2S is a potential problem for the practical applications. On the other hand, Sato, Muramatsu *et al.* reported that partial sulfidation of TiO_2 under a CS_2 atmosphere can be induced visible light responsivity into the resulting $TiO_{(2-x)}S_x$ as a photocatalyst. [1] The thermal sulfidation using CS_2 gas is advantageous not only from a viewpoint of the toxicity of H_2S but also low temperature processibility. In the present study, we focused on a facile preparation of yttrium-based oxysulfide NPs under the CS_2 atmosphere.

Methods $Y(OH)_3$ NPs, used as the precursor for thermal sulfidation, were prepared by a solvothermal method [2] as follows: Ethylene glycol solutions of $YC_{13} \cdot 6H_2O$ (0.50 mol L^{-1}) and tetramethyl ammonium hydroxide (2.0 mol L^{-1}) were mixed in a 1:1 volume ratio and stirred for 10 minutes. Then, the mixture was transferred into an autoclave and aged at $210 \text{ }^\circ\text{C}$ for 4 days. As-obtained products were washed with ethanol and H_2O followed by freeze-drying. A portion of the powder was annealed under a CS_2 flow at $500 \text{ }^\circ\text{C}$ for 1 h. The heating rate was $10 \text{ }^\circ\text{C}/\text{min}$, and during temperature rising, only an Ar gas was passed through. Resulting particles were characterized by X-ray powder diffraction and transmission electron microscopy.

Results and Discussion The solvothermally synthesized precursor NPs were an amorphous-like spherical shape (Fig. 1a). The shape of the NPs was maintained after thermal sulfidation (Fig. 1b). The XRD pattern of product in Fig. 2 indicated a Y_2O_2S phase was obtained at a relatively low temperature at $500 \text{ }^\circ\text{C}$ and in only an hour. The present process to obtain oxysulfide compounds under mild reaction conditions might be applicable to develop high-efficiency photocatalytic materials with visible light responsivity.

References

- [1] T. Nakamura, M. Arata, H. Takahashi, K. Yamamoto, N. Sato, A. Muramatsu, E. Matsubara, *Mater. Trans.* **44**, 685–687 (2003).
- [2] Y. Nishi, Y. Kasai, R. Suzuki, M. Matsubara, A. Muramatsu, K. Kanie, *ACS Appl. Nano Mater.*, **3**, 9622–9632 (2020).

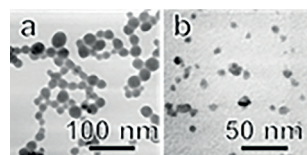


Figure 1: A XRD pattern of product after thermal sulfidation

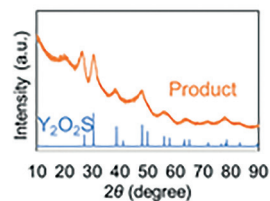


Figure 2: TEM images of a) $Y(OH)_3$, and b) Y_2O_2S particles.

Mechanochemical process to prepare amorphous oxides precursor with isomorphous substitution of Si(IV) by heteroatoms and successive hydrothermal synthesis to crystalize zeolites

A. Muramatsu^{1,2}, H. Kobayashi², G. Tanaka², M. Yabushita³, R. Osuga², K. Ninomiya^{1,2}, M. Matsubara², S. Maki^{1,2}, M. Nishibori^{1,2}, K. Kanie^{1,2}

¹ International Center for Synchrotron Radiation Innovation Smart, Tohoku Univ., Katahira 2-1-1, Aoba-ku, Sendai 980-8577, Japan;

² Institute of Multidisciplinary Research for Advanced Materials, Tohoku Univ., Katahira 2-1-1, Aoba-ku, Sendai 980-8577, Japan;

³ Department of Applied Chemistry, School of Engineering, Tohoku University, 6-6-07 Aoba, Aramaki, Aoba-ku, Sendai, 980-8579, Japan

* The corresponding author e-mail: mura@tohoku.ac.jp

Keywords: mechanochemical process; zeolites; hydrothermal synthesis; dissolution-reprecipitation; isomorphous substitution

Mechanochemical process is a novel procedure to synthesize amorphous oxides solid intermediates for production of crystalline metasilicates, zeolites [1]. These oxides precursor plays a promising role on the incorporation of heteroatoms into zeolite frameworks. Possibly, a direct-precursory complex of Si⁴⁺ and heteroatom is once dissolved from amorphous oxides and then recrystallized as a form of zeolite. Crystalline system of as-formed zeolite is freely controlled with the presence of SDA, structure directing agent, even if the same amorphous oxides are used. This mechanochemically assisted procedure yields a more homogeneous distribution of substituting heteroatoms in the zeolite framework, compared to the conventional hydrothermal synthesis.

Among various applications of zeolites, the catalytic application in the petrochemical field is one of the important roles. Brønsted acidity is the main catalysis of the zeolites, which originates from the bridging OH groups between the framework Si⁴⁺ and isomorphously substituted trivalent heteroatoms such as B³⁺, Al³⁺, Fe³⁺ and Ga³⁺. In addition, the acid strength strongly depends on the kind of heteroatoms. Therefore, the isomorphous substitution of the framework Si⁴⁺ atoms with other trivalent cations is an effective approach to controlling the acid property of zeolite catalysts [2].

We synthesized the Fe-containing zeolites with various zeolite topologies such as MFI-, MWW- and CHA-type frameworks [3,4]. In this study, the textural properties of the thus-prepared Fe-containing zeolites and their catalytic performance were examined and compared with those zeolites prepared via conventional hydrothermal synthesis in order to clarify the effects of the preparation method. Moreover, we applied the mechanochemical method for the synthesis of Al and Fe-containing MFI-type zeolites, where an excellent catalytic performance was observed in the dimethyl ether to olefins reaction.

References

- [1] K. Yamamoto, S. E. Borjas, F. Saito, A. Muramatsu, *Chem. Lett.*, **35**, 570–571 (2006)
- [2] M. Yabushita, R. Osuga, A. Muramatsu, *CrystEngComm*, **23**, 6226–6233 (2021)
- [3] M. Yabushita, H. Kobayashi, R. Osuga, M. Nakaya, M. Matsubara, S. Maki, K. Kanie, A. Muramatsu, *Ind. Eng. Chem. Res.*, **60**, 2079–2088 (2021)
- [4] R. Osuga, G. Tanaka, M. Yabushita, K. Ninomiya, S. Maki, M. Nishibori, K. Kanie, A. Muramatsu, *J. Jpn. Petrol. Inst.*, **65**, 67–77 (2022)

Alkali shuffling in honeycomb layered oxides

E. Mumba-Mpanga¹, R. Berthelot^{1*}

¹ Institut Charles Gerhardt Montpellier, CNRS, ENSCM, Université de Montpellier, France

* The corresponding author e-mail: romain.berthelot@umontpellier.fr

Keywords: honeycomb layered oxides; alkali ordering; in situ diffraction; HRTEM, NMR

Alkali transition metals layered oxides have aroused great interest in the field of solid-state chemistry for decades. The chemical richness due to possible cationic substitutions in the transition metal layer enables the discovery of materials especially with applications as lithium-ion batteries cathodes. In contrast, mixing alkali elements in such layered systems has not been extensively investigated. In this presentation, we want to share our solid-state journey inside the ternary system $\text{Li}_2\text{Ni}_2\text{TeO}_6 - \text{Na}_2\text{Ni}_2\text{TeO}_6 - \text{K}_2\text{Ni}_2\text{TeO}_6$. These three phases possess a layered structure with moreover an in-plane honeycomb ordering between nickel and tellurium cations.[1-3] In parallel to the already-reported composition $\text{NaKNi}_2\text{TeO}_6$ which exhibits the unique example of alternation of sodium and potassium layers, [4,5] we successfully obtained by direct or multistep solid-state reactions new examples of alternated stacking gathering two or even three alkali cations.

The challenging structural investigation of these new compounds especially lies on localizing the alkali cations and on the possible presence of stacking defects, and consequently forced us to combine multiple characterization techniques. Whereas diffraction techniques (lab and synchrotron XRD, ND) show long-range alternation of alkali layers, local analyses like high-resolution TEM and solid-state NMR reveal a more complex picture at the atomic scale. In the search for rationalizing the existence of such alkali-ordered layered compounds, we also investigated their formation mechanism. To do so, the solid-state reactions were probed by in situ diffraction. Interestingly, the synthesis is triggered at very moderate temperatures, certainly driven by the high mobility of alkali cations inside these layered structures. However, a topotactic ionic exchange seems to be discarded for the benefit of a classical nucleation/growth process.

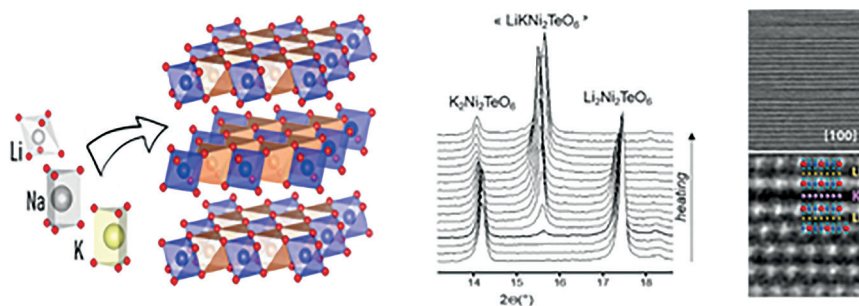


Figure: General structure of $\text{A}_2\text{Ni}_2\text{TeO}_6$ compounds, XRD follow-up of the formation of $\text{LiKNi}_2\text{TeO}_6$ and corresponding high-resolution TEM image showing the alkali layer alternation.

References

- [1] M. Evstigneeva, V. Nalbandyan, A. Petrenko, *Chem. Mater.*, **23**, 1174–1181 (2011)
- [2] T. Masese, K. Yoshii, Y. Yamaguchi, *Nature Commun.*, **9**, 3823 (2018)
- [3] N. Grundish, I. Seymour, G. Henkelman, *Chem. Mater.*, **32**, 9379–9388 (2019)
- [4] T. Masese, Y. Miyazaki, G. Kanyolo, *Nature Commun.*, **12**, 4660 (2021)
- [5] R. Berthelot, J. Serrano-Sevillano, B. Fraisse, *Inorg. Chem.*, **60**, 14310–14317 (2021),

Inorganic materials synthesis in ultra-alkaline hydroflux

L62

H. He¹, Y. Li¹, R. Albrecht¹, M. Ruck^{1*}

¹ TU Dresden, Faculty of Chemistry and Food Chemistry, 01062 Dresden, Germany

* The corresponding author e-mail: michael.ruck@tu-dresden.de

Keywords: hydroflux; synthesis; crystal structure; electronic structure; physical properties

Hydroflux is a new approach to the synthesis of inorganic materials that operates at conditions between salt flux and hydrothermal reactions [1,2]. For a hydroflux, the hydroxide of an alkali metal or alkaline earth metal is combined with water in molar ratios between 1:1 and 1:2, corresponding to 50 or 25 molar solutions. The melting point depends on the water content, but lies typically below 100 °C. The hydroflux differs from hydrothermal conditions by the very low activity of water, so that syntheses are almost pressureless at about 200 °C. The ultra-alkaline medium is very aggressive and dissolves many oxides and other materials. Hydroflux syntheses proceed within a few hours and require only a PTFE-lined autoclave that is inert to the medium and ensures that no water is lost during the reaction.

Using this approach, we were able to synthesize crystalline products of numerous oxo- and hydroxometalates in high yield and purity. Among them are cation conductors, while others can be used as carbon-free precursors to functional oxides. However, the method is by no means limited to these compound classes. An outlook on the possible applications of the hydroflux is given by the successful syntheses of the oxide iodide Tl_3OI , the periodato complex $K_8[Rh(IO_6)_2]OH \cdot 3H_2O$, the orthoselenate(IV) K_2SeO_3 , or the tetraselenodiarsenate(II) $K_4(As_2Se_4) \cdot 2H_2O$.

The acid-base chemistry in hydroflux can be rather unusual. For example, boric acid acts as a proton donor (Brønsted acid) rather than a hydroxide acceptor (Lewis acid) as evidenced by the crystallization of the non-linear optics material $Ba(BO_2OH)$ [3].

The redox chemistry proceeds far from tabulated standard potentials and yields surprising results. For example, very large crystals of the highly water-sensitive tritelluride K_2Te_3 are obtained by reduction of TeO_2 with As_2O_3 [4].

The crystallization of hygroscopic products from an aqueous medium demonstrates another important aspect of the low chemical activity of water in the hydroflux.

One of the latest products from hydroflux is $K_2(Sb_2O_3)_2Te$, an air-stable optoelectronic material exhibiting energy up-conversion as well as intrinsic transistor/varistor behavior that can be controlled by the wavelength of light incident on it.

References

- [1] D. E. Bugaris, M. D. Smith, H.-C. zur Loye, *Inorg. Chem.* **52**, 3836–3844 (2013).
- [2] R. Albrecht, J. Hunger, T. Doert, M. Ruck, *Eur. J. Inorg. Chem.* **2019**, 1398–1405 (2019).
- [3] Y. Li, P. A. Hegarty, M. Rüsing, L. M. Eng, M. Ruck, *Z. Anorg. Allg. Chem.* **648**, e202200193 (2022).
- [4] R. Albrecht, M. Ruck, *Angew. Chem. Int. Ed.* **60**, 22570–22577 (2021).

Acknowledgments

This work was supported by the German Science Foundation (438795198).

Anion redox as a means to derive layered manganese oxychalcogenides with exotic intergrowth structures

S. Giri¹, S. Sasaki¹, S. Cassidy¹, S. Dey², G. Cibin³, C. Grey², S. Clarke^{1*}

¹ Department of Chemistry, University of Oxford, Inorganic Chemistry Laboratory, South Parks Road, Oxford OX1 3QR, UK;

² Department of Chemistry, University of Cambridge, Cambridge CB2 1EW, UK;

³ Diamond Light Source, Harwell Science and Innovation Campus, Didcot, OX11 0DE, UK.

* The corresponding author email: simon.clarke@chem.ox.ac.uk

Keywords: mixed anion compounds; transition metal oxychalcogenide; topochemical reactions; anion redox; novel intergrowth structure

Topochemistry enables step-by-step conversions of solid-state materials often leading to metastable compounds that retain initial structural motifs. Recent advances in this field revealed many examples where anionic constituents were actively involved in redox reactions during (de) intercalation processes. Such oxidations are often accompanied by anion-anion bond formation, which heralds possibilities to design novel structure types disparate from known precursors, in a controlled manner. Here multistep conversion, via reactive intermediates, is presented of the layered oxyselenide $\text{Sr}_2\text{MnO}_2\text{Cu}_{1.5}\text{Se}_2$ into a Cu-deintercalated phase where antifluorite type $(\text{Cu}_{1.5}\text{Se}_2)^{2.5-}$ slabs collapsed into 2D arrays of chalcogen dimers. The collapse of the selenide layers on deintercalation led to various stacking types of $\text{Sr}_2\text{MnO}_2\text{Se}_2$ slabs, which formed unprecedented polychalcogenide structures unattainable by conventional high-temperature syntheses. We understand the structure using X-ray diffraction and spectroscopy along with various other techniques. Anion-redox topochemistry is demonstrated to be of interest not only for electrochemical applications but also to design of complex novel layered architectures.

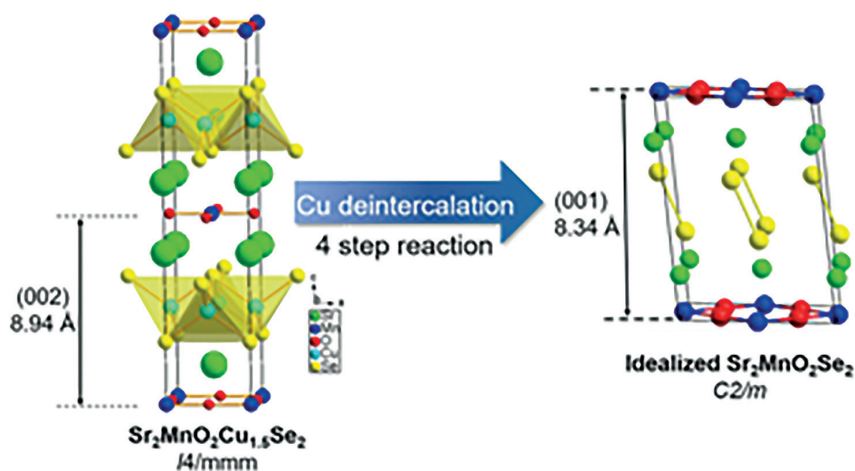


Figure: Multistep oxidative Cu deintercalation leads to collapse of CuCh layer forming 2D array of anion dimers

Quadrature frequency resolved spectroscopy on green upconversion photoluminescence in GeGa(As)S:Er³⁺ chalcogenide glasses

L. Strizik^{1*}, T. Aoki², V. Prokop¹, J. Hrabovsky^{1,3}, T. Wagner^{1,4}

¹ Department of General and Inorganic Chemistry, Faculty of Chemical Technology, University of Pardubice, Studentska 573, 532 10 Pardubice, Czech Republic;

² Joint Research Center of Hightechnology, Tokyo Polytechnic University, Iyama, Atsugi 2430297, Japan;

³ Institute of Physics of Charles University, Faculty of Mathematics and Physics, Charles University in Prague, Ke Karlovu 5, 121 16 Prague, Czech Republic;

⁴ Center of Materials and Nanotechnologies, University of Pardubice, nam. Cs. legii 565, 530 02 Pardubice, Czech Republic.

* The corresponding author e-mail: lukas.strizik@upce.cz

Keywords: upconversion; photoluminescence; energy transfer; chalcogenides; Er³⁺-doped glass

Upconversion photoluminescence (UCPL) observed in rare-earth(RE)-doped materials attracts attention due to its applications in lasers, bioimaging, sensors and detectors, etc. UCPL comprises of three basic mechanisms:

1. Ground State Absorption (GSA) followed by Excited State Absorption (ESA);
2. GSA followed by Energy Transfer Upconversion (ETU);
3. Photon Avalanche (PA) UCPL via cross-relaxation processes.

GSA/ESA and GSA/ETU are the most common and the most studied UCPL processes. The UCPL mechanisms are frequently studied via absorption-excitation spectroscopy and/or time-resolved spectroscopy (TRS). Since UCPL is governed by nonlinear dynamics, its time evolution in TRS experiments cannot be always analysed in a closed form. Unlike TRS, Quadrature Frequency Resolved Spectroscopy (QFRS) utilizes a phase-sensitive lock-in detection and a sinusoidal modulation (perturbation) on continuouswave (cw) bias light which can be advantageously applied for UCPL study. Perturbation on cw bias light induces the perturbation in the population densities at RE³⁺ levels, which can linearize otherwise nonlinear UCPL dynamics and thereby provides physical parameters [1].

We have applied QFRS on green ($\lambda \approx 550$ nm) UCPL in Er³⁺-doped GeGa(As)S chalcogenide glasses using a 975 nm modulating laser and various excitation photonflux densities Φ . The observed double-peaked QFRS spectra compose of two lifetime components; a long-lifetime component $\tau_1 \sim 0.1\text{--}1$ ms reflecting the relaxation at Er³⁺: $^4I_{11/2}$ level; and a short lifetime component $\tau_2 \sim 10$ μ s reflecting the relaxation at Er³⁺: $^4F_{7/2}^2/{}^2H_{11/2}/{}^4S_{3/2}$ coupled manifolds. The GSA/ESA and GSA/(ESA+ETU) UCPL processes can be differentiated based on the Φ -evolved QFRS spectra with respect to the Er³⁺ concentration under three-level model approximation. The ETU parameter is determined by analysis the model in terms of a transfer function for a variety of the Er³⁺-doped chalcogenide glasses [1].

References

- [1] T. Aoki, *Photoluminescence*, in *Optical Properties of Materials and Their Applications*, J. Singh ed., 2nd ed., Chapter 6, Wiley, 2020, p.157, ISBN: 9781119506317.

Acknowledgments

Authors thank the University of Pardubice (Grant VA390011) and the Ministry of Education, Youth and Sports (LM2018103).

TESCAN's Analytical Solutions for Lithium-Ion Battery Research

J. Honč¹, T. Šamořil¹, J. Dluhoř¹, T. Sui², X. Yao³

¹ TESCAN ORSAY HOLDING, Libušina tř. 21, 623 00 Brno, Czech Republic;

² Department of Mechanical Engineering Sciences, University of Surrey, Guildford Surrey GU2 7XH, UK;

³ Advanced Technology Institute, University of Surrey, Guildford Surrey GU2 7XH, UK

* The corresponding author e-mail: geetu.kumari@ul.ie

Keywords: lithium-ion battery; ToF-SIMS; FIB-SEM; analytical workflow; surface and subsurface analysis; micro- and nanocharacterization

Electrochemical materials in battery designs and research on them are critical in achieving a sustainable energy future as well as energy independence from fossil fuels. In practice, energy density, cell lifespan, and charge rate are bonded to chemical composition and specific structural features within the batteries. In general, optimization of all these parameters is a multiscale, multimodal challenge that consists of the analysis of the anode, cathode, electrolyte, and their interphases.

In this presentation, we focus on characterization techniques and their usage that offer critical insight to optimize Li-ion battery (LIB) performance and lifetime. Especially, we focus on micro- and nanocharacterization of battery active materials by Time-of-Flight Secondary Ion Mass Spectrometry (ToF-SIMS) combined with Focused Ion Beam Scanning Electron Microscope (FIB-SEM) [1,2]. This analytical tool helps to identify the LIB capacity fade mechanism based on the loss of lithium inventory caused by parasitical chemical reactions [3] or lithium trapping within electrode particles [4]. High-sensitive ToF-SIMS technique also allows the chemical identification of contaminants within the battery material, the study of the degradation process of electrode particles [5], and the properties of solid electrolyte interface (SEI) within the anode material. The ability to correlate SEM observation with ToF-SIMS and other analytical techniques such as Energy Dispersive X-Ray Spectroscopy (EDS) and Raman spectroscopy [6] on the same FIB-SEM system allows extended analytical capabilities and so comprehensive understanding of LIBs material behaviour from the mechanical, chemical, and electrochemical point of view.

References

- [1] J. A. Whitby, et. al., *Advances in Mat. Sci. and Eng.*, **2012**, 1–13, (2012)
- [2] D. Alberts, et. al., *Instr. Sci. & Technol.*, **42**, 432–445, (2014)
- [3] X. Yao, et. al., *Energy Environ. Mater.*, **5**, 662–669, (2021)
- [4] T. Sui, et. al., *Nano Energy*, **17**, 254–260, (2015)
- [5] S. Bessette, et al., *Scientific Reports*, **8**, 1–9, (2018)
- [6] D. J. Miller, et. al., *Microsc. Microanal.*, **25**, 862–863, (2019)

Local structure and high performance catalysts

L66

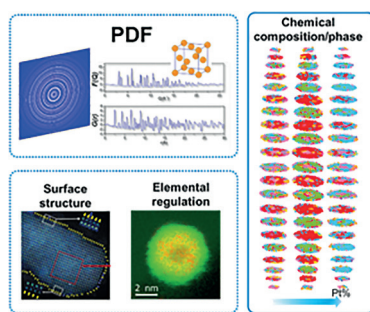
X. Xing^{1*}, Q. Li¹

¹ Institute of Solid State Chemistry, University of Science and Technology Beijing, Beijing 100083, China

* The corresponding author e-mail: xing@ustb.edu.cn

Keywords: local structure; pair distribution function; reverse monte carlo; catalysts; bimetallic alloy

Local structure in solid state catalysts, indicating the atomic arrangements from several angstroms to several nanometers, determines the phase distribution, ab/desorption process, and surficial electron transfer. However, the revelation of atomic 3D structure for nanocatalysts challenges the limitations of conventional methods. Notably, the identification of the cooperative relationship between the active sites and nearby coordination environment during catalytic reactions depends on the stereo distribution of local phases and chemical composition within a short range. Here, supported by the comprehensive method combining with Pair Distribution Functions (PDF) with Reverse Monte Carlo (RMC), we have performed a local structural insight into the elemental distribution, phase segregation and anomalous structural transition in the nanosized catalysts. A segregation of local phase segments as disordered Pt-rich A1 and Pt₃Fe L1₂ phases were revealed to attribute to the marked improvement of HER activity and stability in Pt₅₆Fe₄₄. The high dispersity of active sites in the Pd₃₄Cu₆₆ alloy provided the excellent catalytic performance with 98% ethylene selectivity at complete acetylene conversion, which was surpassing than the most advanced catalysts available. Our study will provide an intuitionistic method to resolve the spatial structure of active sites and be essential to design nanocatalysts.



References

- [1] Qiang Li, He Zhu, and Xianran Xing* et al, *J. Am. Chem. Soc.*, **144**, 20298–20305 (2022).
 [2] He Zhu, Qiang Li and Xianran Xing* et al, *Nat. Commun.*, **9**, 5063 (2018).

Acknowledgments

This work was supported by the National Natural Science Foundation of China (22090042, 21731001 and 22175018).

Defect engineering: Eu^{3+} emission enhancement via induced local distortion

S. C. S. Lemos^{1*}, M. Assis¹, L. Gracia^{1,2}, L. K. Ribeiro^{1,3}, A. F. Gouveia¹, Y. G. Galvão⁴, E. Cordoncillo⁵, R. C. Lima⁶, Elson Longo³, J. Andrés¹

¹ Department of Physical and Analytical Chemistry, Universitat Jaume I, 12071- Castellon, Spain;

² Departament de Physical Chemistry, Universitat de València (UV), 46010 - Valencia, Spain;

³ CDMF, Universidade Federal de São Carlos (UFSCar), São Carlos – SP, 13565-905, Brazil;

⁴ Department of Physics, Universidade Federal de São Carlos (UFSCar), São Carlos – SP, 13565-905,

⁵ Department of Inorganic and Organic Chemistry, Universitat Jaume I, 12071, Castelló de la Plana (Spain);

⁶ Chemistry Institute, Universidade Federal de Uberlândia, 38400-902 - Uberlândia, MG, Brazil

* The corresponding author e-mail: custodio@uji.es

Keywords: indium oxide; photoluminescence; DFT; europium; lithium

Advances in light emitting technology requires the development of materials with a broad applicability to constitute devices in diverse field ranging from physics to biological imaging [1-3]. The study of synthetic methodologies of inorganic materials and approaches to design its physicochemical properties is required to fulfill the demand for stable and efficient luminescent materials, achieving the optimum association of host lattice and activator element.

In this work, we report on the effect of inserting by $\text{Li}^+/\text{Eu}^{3+}$ on the structure, electronic and luminescent properties of $\text{bcc-In}_2\text{O}_3$ oxide matrix by combining experimental characterization and theoretical simulation. The synthesized samples were characterized by XRD, Raman, TEM and FE-SEM, and PL spectroscopy. DFT calculations were performed, providing a deep structural and electronic description of the local arrangement of the $[\text{EuO}_6]$ clusters in the In_2O_3 lattice. The results demonstrated that lattice distortion induced in the In_2O_3 by Li^+ co-doping effectively alter the local environment of the Eu^{3+} ions in the host lattice, favoring an asymmetrical crystal field, which in turn lead to a strong enhancement of the electric dipole transition $^5\text{D}_0 \rightarrow ^7\text{F}_2$ (characteristic Eu^{3+} sharp red emission) intensity.

This approach provides a strategy to improve the performance of rare earth activators in inorganic solid-state materials, with potential to be applied in the development of high efficiency light emitting devices.

References

- [1] Z. Wei, Y. Liu, B. Li, et al. *Light Sci Appl* **11**, 175 (2022)
- [2] N. Zhang, J. Li, J. Wang. *RSC Advances* **9**, 30045, (2019).
- [3] T. Chihara, M. Umezawa, K. Miyata et al. *Sci Rep* **9**, 12806 (2019)

Acknowledgments

S. C. S. Lemos acknowledges the postdoctoral programme POSDOC-2021-Universitat Jaume I (POS-DOC/2021/18).

Urinary oxidative stress sensor based on zinc oxide nanorods

L68

A. Ejaz¹, D. Gibson^{1,2}, C. Garcia Nuñez^{1*}

¹ Institute of Thin Films, Sensors, and Imaging, University of the West of Scotland, PA1 2BE Paisley, UK;

² AlbaSense Ltd, PA1 2BE Paisley, UK

* The corresponding author's e-mail: carlos.garcianunez@uws.ac.uk

Keywords: stress sensor; urine biomarker; graphene oxide; nitrogen configurations; ZnO nanorods aspect ratio

This paper reports a substantial improvement over state-of-the-art stress sensors' performance by detecting a pivotal urinary biomarker, (i.e., H₂O₂) to manifest its clinical application into a miniaturized system. The sensitivity of the stress sensor was improved by increasing the aspect ratio of the ZnO nanorods [1]. The paper discusses the varied population of ZnO nanoparticles achieved in ethanol and water solvents towards the growth kinetics and achieving a desired aspect ratio of the ZnO nanorods. The experimental and statistical analysis shown in Figures A and B, respectively, reveal a remarkable quantitative reduction of H₂O₂ into H₂O with a limit of detection (0.3 μM), high sensitivity (0.3984 mAmm⁻¹cm⁻²), and a wide linear range of 1.0 μM – 15.0 mM. A wide comparison with the literature advocates an improved sensitivity of the NGO-ZnO/E as a stress sensor for clinical applications in the future.

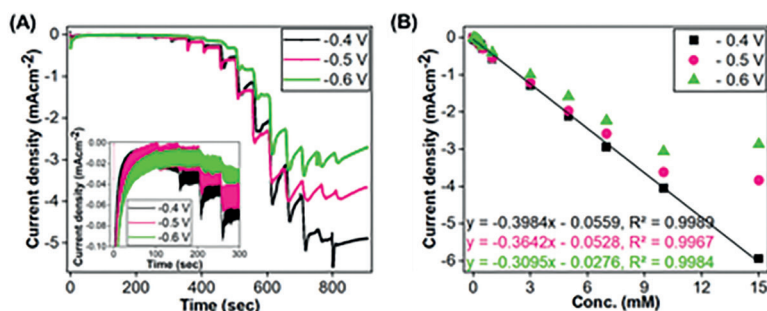


Figure: (A) Amperograms of the NGO/ZnO/E in Ar-saturated 0.1 M Phosphate Buffer Saline (PBS) (pH 7.4) at different applied potentials, containing various concentrations of H₂O₂ (1.0 × 10⁻⁶, 1.5 × 10⁻² M), inset: data corresponding to low H₂O₂ concentration, and (B) linear ranges obtained from the plot of cathodic current density at each applied potential vs. H₂O₂ concentration.

References

[1] A. Ejaz, J. H. Han, R. Dahiya, *Journal of Colloid and Interface Science*, **570**, 322–331 (2020)

Acknowledgments

This work was funded by the British Council & Higher Education Commission (20-ICRG-165/RGM/HEC/2020).

Tecto-borosulfates–syntheses, structures and properties

E. Turgunbajev¹, P. Netzsch¹, M. Hämmer¹, G. Buchner¹, H. A. Höppe^{1*}

¹ Festkörperchemie und Materialwissenschaften, Universität Augsburg, Universitätsstr. 1, 86159 Augsburg

* The corresponding author e-mail: henning@ak-hoeppe.de

Keywords: borate; sulfate; silicate-analogous; luminescence; crystal structures

Silicate-analogous solid state compounds feature tetrahedral basic building units such as borate and sulfate tetrahedra in borosulfates, an emerging class of compounds [1-3]. Analogous to silicates such basic building units may condense to form anionic frameworks to host cations.

In case of the borosulfates normally $B(SO_4)_4$ moieties (**Fig. 1**) form like in the tectosilicate-analogous series of $RX[B(SO_4)_2]_4$ ($X = M^I, H_3O^+ \dots$, $R = La \dots Lu, Y, Bi$) [1], the nesosilicate-analogous $K_3[B(SO_4)_4]$ [2] or the ringsilicate- and inosilicate-analogous borosulfates $R_2[B_2(-SO_4)_6]$ ($R = La \dots Lu, Y$) [4,5], $Sr[B_2(SO_4)_4]$ and $(NH_4)_3[B(SO_4)_3]$ [6], the latter being of interest as proton conductor [7]. This contribution focusses on progress regarding tectosilicate-analogous borosulfates and will elucidate synthesis principles, the structural chemistry and selected further optical and thermal properties.

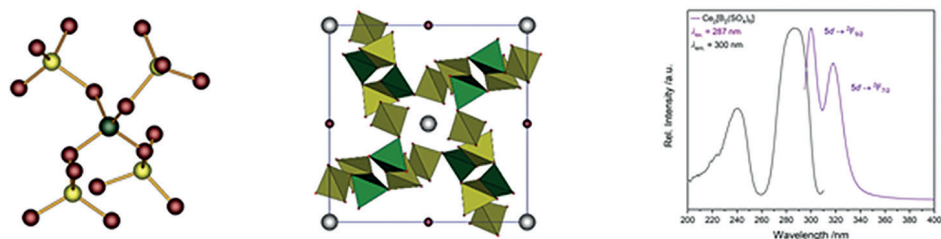


Figure 1: $B(SO_4)_4$ moiety in $K_3[B(SO_4)_4]$, unit cell of $RX[B(SO_4)_2]_4$, luminescence spectra of $Ce_2[B_2(SO_4)_6]$

References

- [1] M. Hämmer, L. Bayarjargal, H. A. Höppe, *Angew. Chem. Int. Ed. Engl.*, **60**, 1503–1506 (2021) (doi: 10.1002/anie.202011786).
- [2] H. A. Höppe, K. Kazmierczak, M. Daub, K. Förg, F. Fuchs, H. Hillebrecht, *Angew. Chem. Int. Ed.*, **51**, 6255–6257 (2012) (doi: 10.1002/anie.201109237).
- [3] J. Bruns, M. Daub, H. Hillebrecht, H. A. Höppe, H. Huppertz, *Chem. Eur. J.*, **26**, 7966–7980 (2020) (doi: 10.1002/chem.201905449).
- [4] P. Gross, A. Kirzhain, H. A. Höppe, *Angew. Chem. Int. Ed.*, **55**, 4353–4355 (2016) (doi: 10.1002/anie.201510612).
- [5] P. Netzsch, M. Hämmer, P. Gross, H. Bariss, T. Block, L. Heletta, R. Pöttgen, J. Bruns, H. Huppertz, H. A. Höppe, *Dalton Trans.*, **48**, 4387–4397 (2019) (doi: 10.1039/C9DT00445A).
- [6] P. Netzsch, H. A. Höppe, *Z. Anorg. Allg. Chem.*, **646**, 1563–1569 (2020) (doi: 10.1002/zaac.202000105).
- [7] M. D. Ward, B. L. Chaloux, M. D. Johannes, A. Epshteyn, *Adv. Mater.*, **2020**, e2003667.

Acknowledgments

This work was supported by the Deutsche Forschungsgemeinschaft (HO 4503/5-1).

Crystal structures of new phosphidosilicates and its homologous

L70

D. Johrendt^{1*}, A. Haffner¹, V. Weippert¹, J. Aicher¹, K. Witthaut¹

¹ Department Chemie, Ludwig-Maximilians-Universität München, 81377 München, Germany

* The corresponding author e-mail: dirk.johrendt@cup.uni-muenchen.de

Keywords: silicon; phosphorous; crystal structures; ion conduction; thermoelectric

Phosphidosilicates and related compounds attract considerable interest due to their versatile structural chemistry and potential ion-conducting and thermoelectric properties. SiP₄ tetrahedra as basic building units show an enormous variety of linkage patterns, which even exceeds that of oxidosilicates, also because additional homonuclear bonds can occur between the anions. Such phosphidosilicates can be classified as Zintl-compounds.

Compounds with the simple composition ASi₂P₃ (A = Li, Na, K) form complex structures with large interpenetrating networks of supertetrahedra (up to T5), which are hierarchical variants of diamond. Alkaline ions move between the supertetrahedra with conductivities up to 2×10^{-4} S cm⁻¹ (300 °C), 4×10^{-4} S cm⁻¹ (25 °C) and 2.6×10^{-4} S cm⁻¹ (25 °C) for Li⁺, Na⁺, and K⁺, respectively.[1-3] In the case of sodium, we find that the ion conductivity increases with the size of the supertetrahedral entities.

Ba₂SiP₄ is dimorphic with SiP₄-tetrahedra connected via P-P bonds. The tetragonal form is analogous to β-Christobalite, where oxygen is replaced by P₂-dimers. The orthorhombic polymorph has chains of SiP₄-tetrahedra, reminiscent to the elusive fibrous SiO₂. [4-5]

Mixing of alkaline earth ions produces even more structural motifs. One example is hexagonal MgSr₃Si₃P₇, where a MgP₆/SiP₄-network forms large hexagonal channels filled with chains of face-sharing Sr_{6/2}-octahedra, which in turn contain chains of P₂-dimers. MgSr₃Si₃P₇ underlines the structural versatility of phosphidosilicates by combining motifs of silicates with those of Zintl-compounds.

The arsenidogermanate BaGe₈As₁₄ is a rare example of a semiconducting sodalite-type compound. [6] Barium is too small to fit the large β-cage and, according to DFT calculations, the resulting rattling leads to a small lattice thermal conductivity. The electrical conductivity is good thanks to the small gap, thus our calculations predict a record thermoelectric figure of merit up to $zT = 2.7$, which has still to be proved by experiments. [7]

References

- [1] A. Haffner, T. Bräuniger, D. Johrendt, *Angew. Chem. Int. Ed.*, **2016**, *55*, 13585–13588.
- [2] A. Haffner, A.-K. Hatz, I. Moudrakovski, B. V. Lotsch, D. Johrendt, *Angew. Chem. Int. Ed.* **2018**, *57*, 6155–6160.
- [3] A. Haffner, A.-K. Hatz, O. E. O. Zeman, C. Hoch, B. V. Lotsch, D. Johrendt, *Angew. Chem. Int. Ed.*, **2021**, *60*, 13641–13646.
- [4] A. Haffner, D. Johrendt, *Z. Anorg. Allg. Chem.*, **2017**, *643*, 1717–1720.
- [5] A. Haffner, V. Weippert, D. Johrendt, *Z. Anorg. Allg. Chem.*, **2020**, *646*, 120–124.
- [6] V. Weippert, T. Chau, K. Witthaut, L. Eisenburger, D. Johrendt, *Chem. Commun.*, **2021**, *57*, 1332–1335.
- [7] V. Weippert, K. Witthaut, M. Pointner, M. Sachs, L. Eisenburger, F. Kraus, D. Johrendt, *Chem. Mater.*, **2021**, *33*, 8248–8258.

Exploring trirutile materials as a platform for energy storage

E. Djafri¹, D. Arnold², O. Mentré³

¹ University of Kent, Canterbury CT2 7NZ;

² University of Kent, Canterbury CT2 7NZ;

³ Université de Lille, Villeneuve-d'Ascq 59650

* The corresponding author e-mail: ed424@kent.ac.uk

Keywords: functional material; energy; relaxor ferroelectrics; disordered structures; dielectric

In the past decades, one of the major challenges is to find ways to reduce our influence in the climate change, by reducing the quantity of trash, recycling it, and reduce the greenhouse gas emission. In the energy field, using low carbon emission sources, like nuclear energy or renewable sources. For the last ones, the intermittent nature makes it mandatory to store the surplus and allowed the renewable sources to be more of a controllable energy.

In term of storage, two main categories can be distinguished: batteries and capacitors. The first one, by being able to convert electrical energy into chemical energy, is able to store a large amount of energy, i.e high energy density. The electrical output is limited, due to the slow movement of the charge carriers. On the other hand, capacitors can store and discharge energy in a very small amount of time. But the energy density is limited by the surface of the device. In recent years, a new category starts to draw attention, the (anti)ferroelectric materials.

Ferroelectric materials are known to have spontaneous electric polarization below a given temperature, the Curie temperature (T_c). This polarization can be reverse by applying an external electric field. Relaxor ferroelectric behave relatively close to a ferroelectric material. The main differences are the presence of a wide peak in the temperature dependence of the dielectric permittivity. The frequency dependence of this peak is the other main difference. This shift in frequency is mainly due to the disordered nature of the structure. Antiferroelectric materials, like FE materials, possess a spontaneous polarization, but an antiparallel one, making it zero at the macroscopic level. Under an electric field, the AFE material undergoes a reversible first order phase transition to a ferroelectric (FE) phase, behaving like a FE material at high electric field.

TiFeNbO₆ is known as a disordered rutile, with a relaxor behavior [1,2]. It has drawn attention, due to its high dielectric constant. Previous papers attempted to replace the Nb cation by Ta, or Fe by Al. On the other hand, Ti has never been replaced. It could be interesting to replace this one by another one but bigger, like Zr and Hf. With those cations, it may force the structure to order, in a layered form. This type of structure could possibly lead to an antiferroelectric behavior, where the layer of one cation could polarize to one side, where the layer above/below polarize to the other side.

References

- [1] Wang, S. et al. *Materials Research Bulletin* **48**, 3098–3102 (2013)
- [2] Ananta, S., Brydson, R. & Thomas, N. W. *Journal of the European Ceramic Society* **19**, (1999)

Acknowledgments

Many thanks to the DSTL UK France studentship scheme for funding.

Understanding the formation mechanism of intermetallic nanoparticles in polyol processes

M. Smuda¹, J. Ströh², N. Pienack², A. Khadiev³, H. Terraschke², M. Ruck^{1,4}, T. Doert^{1*}

¹ Technische Universität Dresden, Helmholtzstr. 10, 01069 Dresden, Germany,

² Christian-Albrechts-Universität Kiel, May-Eyth-Str. 2, 24118 Kiel, Germany,

³ Deutsches Elektronen-Synchrotron DESY, Notkestr. 85, 22607 Hamburg, Germany,

⁴ Max Planck Institute for Chemical Physics of Solids, Nöthnitzer Str. 40, 01187 Dresden; Germany

* The corresponding author e-mail: thomas.doert@tu-dresden.de

Keywords: intermetallics; polyol process; reaction mechanism; *in situ* studies

Intermetallic nanoparticles have achieved great scientific and technological interest with their superior properties in catalysis and electronics. The polyol process, the reduction of metal salts in polyalcohols, is an excellent method to synthesize such nanoparticles in high yields with controlled size and morphology, using low reaction temperatures and short reaction times. However, a detailed knowledge about the formation mechanism of intermetallic nanoparticles under these conditions is lacking, even though a deeper understanding is crucial for targeted synthesis and material design for specific applications. Therefore, systematic investigations were carried out to identify the influence of key parameters, such as temperature, pH value and anions, using (*in-situ*) PXRD, SEM, and TEM, e.g.

The formation of crystalline BiNi powders starts with the successive reduction of Bi³⁺ and Ni²⁺, leading to core-shell nanoparticles “Bi@Ni”. Successive diffusion of nickel into the bismuth core leads to the formation of the bismuth-rich compound Bi₃Ni, which subsequently reacts to BiNi. High pH values and reaction temperatures promote the formation, whereas halide ions reduce the reactivity. [1] In contrast, investigations of the formation of Bi₂Ir particles revealed a partial co-reduction of Bi³⁺ and Ir³⁺, which results in the newly discovered intermetallic suboxide Bi₄Ir₂O. At higher reaction temperatures, this suboxide is then fully reduced to the target phase Bi₂Ir. [2] Another example is the formation of Bi₂Rh particles, which follows a co-reduction of Bi³⁺ and Rh³⁺, yielding BiRh in a first step. The obtained BiRh particles act as reduction sites for the residual bismuth cations, leading to a gradual transition from BiRh to Bi₂Rh. The rhodium precursor plays a crucial role in the formation of undesirable intermediates and feasibility of the reaction, whereas a high pH value has a positive effect. [3]

References

- [1] M. Smuda, C. Damm, M. Ruck, T. Doert, *ChemistryOpen* **9**, 1085–1094 (2020).
- [2] M. Smuda, K. Finzel, M. Hantusch, J. Ströh, N. Pienack, A. Khadiev, H. Terraschke, M. Ruck, T. Doert, *Dalton Trans.* **50**, 17665–17674 (2021).
- [3] M. Smuda, J. Ströh, N. Pienack, A. Khadiev, H. Terraschke, M. Ruck, T. Doert, *Dalton Trans.* **51**, 17405–17415 (2022).

Acknowledgments

This work was financially supported by the Deutsche Forschungsgemeinschaft (project-id 413437826).

Structural trends and ion diffusion mechanisms in the postspinel-type $\text{NaFe}_{1+x}\text{Ru}_{1-x}\text{O}_4$ system

L. Benincasa¹, M. Duttine¹, M. Suchomel¹, M. Guignard¹

¹ Univ. Bordeaux, CNRS, Bordeaux INP, ICMCB, UMR 5026, F-33600 Pessac, France

* The corresponding author e-mail: louise.benincasa@icmcb.cnrs.fr

Keywords: solid state; sodium-ion batteries; high pressure synthesis; structure; ion diffusion

NaM_2O_4 compounds ($M = 3d$ or $4d$ transition metals) with a postspinel CaFe_2O_4 structure-type offer many advantages as positive electrodes for sodium-ion batteries, such as a theoretical fast charging and excellent stability during cycling.^[1,2] In this context, our current project focuses on novel NaFe_2O_4 based compositions, selected for the sustainable chemistry of Na and Fe cations, and the enhanced possible energy density associated with the high redox potential of the $\text{Fe}^{3+/4+}$ couple. Beyond their electrochemical performance, these materials present an intriguing solid-state framework (cation ordering, Jahn-Teller distortions, etc) which has been so far under-explored.

The current presentation will focus in particular on recent results concerning the synthesis and extensive property characterizations of the $\text{NaFe}_{1+x}\text{Ru}_{1-x}\text{O}_4$ system. Select compositions have been synthesized by various solid-state routes, performed with careful consideration of maintaining a +3.5 average oxidation state of transition metals when increasing iron content. Our presentation will describe and contrast the efficacy of these different approaches, including ambient pressure calcination type synthesis, and the use of both high oxygen gas pressures and high (> 1 GPa) mechanical pressure conditions explored to stabilize the targeted compositions.

Although the final NaFe_2O_4 parent composition has not been realized in this current study, a discussion of the structural and property characterizations performed on samples over the range $0 \leq x \leq 0.5$ will be used to illustrate the opportunities and limits of this approach. Specifically, the presented results validate the overall strategy even if iron substitution in the postspinel-type structure is limited over the explored pressure ranges. It will be shown how this conclusion is supported by multiple probes. Mössbauer and X-ray spectroscopy have been used to confirm the elemental compositions and to examine the interplay of Fe and Ru oxidation states in the materials. Electrochemical curves obtained by galvanostatic cycling (at C/50) of NaFeRuO_4 show that Na intercalation/deintercalation is possible but limited. Preliminary transport measurements and calculations performed to better understand diffusion constraints will be presented, followed by a discussion on the implications of these structural and transport findings for a broader family of postspinel-type NaM_2O_4 compounds.

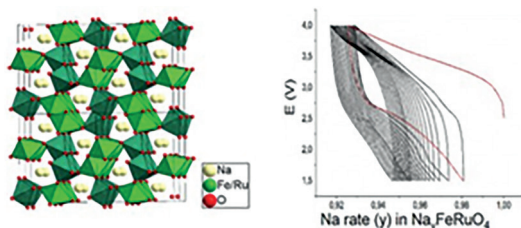


Figure: Postspinel-type structure (left), and NaFeRuO_4 electrochemical curve by galvanostatic cycling (right)

References

- [1] C. Ling, F. Mizuno, *Chem. Mater.*, **25** (15), 3062–3071 (2013)
- [2] Q. Li, S. Guo, K. Zhu, K. Jiang, X. Zhang, P. He, H. Zhou, *Adv Energy Mater.*, **7** (21), 1700361 (2017)

Base-metal nanoparticles as reactants at room temperature

C. Feldmann^{1*}

¹ Institute for Inorganic Chemistry, Karlsruhe Institute of Technology, Engesserstraße 15, 76131 Karlsruhe, Germany

* The corresponding author e-mail: claus.feldmann@kit.edu

Keywords: base-metal nanoparticles; reactivity; follow-up; room-temperature synthesis

The knowledge on metal nanoparticles is the lower the more negative the electrochemical potential and the smaller the particle size. As a result, little is known on nanoparticles of the most basic and most reactive metals. During the last five years, we have addressed the synthesis of base metal nanoparticles (with $E_0(\text{bulk})$ below -1.5 V). For the first time, we now have high-quality metal nanoparticles (1–3 nm in diameter) of all red-marked metals in **Figure 1** available (as THF suspensions or powder samples) [1–5]. The as-prepared base-metal nanoparticles are highly reactive (e.g. reaction with H_2O or O_2 comparable to alkali metals).

The high reactivity of base-metal nanoparticles, however, can be used for synthesis in the liquid phase near room temperature (20–60 °C). Thus, novel coordination compounds, clusters and oxoclusters, metalorganic compounds as well as novel materials for catalysis, H_2 sorption, etc. can be realized [1–5].

Having almost all base-metal nanoparticles available for the first time since recently (**Fig. 1**), we present the base metal nanoparticles and their use as reactants at room temperature.

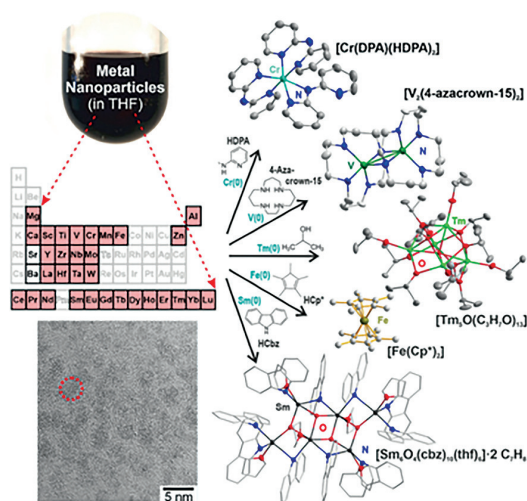


Figure 1: Base metal nanoparticles (all red marked available with 1–3 nm in size) and selected follow-up reactions.

References

- [1] S. Riegsinger, R. Popescu, D. Gerthsen, C. Feldmann, *Chem. Commun.* **2022**, *58*, 7499.
- [2] D. Bartenbach, R. Popescu, D. Gerthsen, C. Feldmann, *Inorg. Chem.* **2022**, *61*, 3072.
- [3] A. Reiß, C. Donsbach, C. Feldmann, *Dalton Trans.* **2021**, *50*, 16343.
- [4] D. Bartenbach, O. Wenzel, R. Popescu, L.-P. Faden, A. Reiß, M. Kaiser, A. Zimina, J.-D. Grunwaldt, D. Gerthsen, C. Feldmann, *Angew. Chem. Int. Ed.* **2021**, *60*, 17373.
- [5] A. Egeberg, L.-P. Faden, A. Zimina, J.-D. Grunwaldt, D. Gerthsen, C. Feldmann, *Chem. Commun.* **2021**, *57*, 3648.

Functionalization of chalcogenide IR photonic sensor by polymer membrane for the purpose of detecting aromatic hydrocarbon pollutants in water

M. Vrazel¹, R. K. Ismail², M. Baillieul¹, P. Nemeč¹, P. Loulergue², A. Szymczyk², K. Boukerma³, R. Courson³, A. Hammouti⁴, L. Bodiou⁴, J. Charrier⁴, T. Halenkovic¹, M. Bouska¹, V. Nazabal^{2,1}

¹ Department of Graphic Arts and Photophysics, Faculty of Chemical Technology, University of Pardubice, Studentska 573, 53210 Pardubice, Czech Republic;

² Univ Rennes 1, CNRS, ISCR - UMR6226, F-35000 Rennes, France;

³ IFREMER, Laboratoire Détection, Capteurs et Mesures, 29280 Plouzané, France;

⁴ Univ Rennes 1, CNRS, Institut Foton - UMR 6082, F-22305 Lannion, France

* *The corresponding author e-mail:* martin.vrazel@student.upce.cz

Keywords: BTX; polymer; mid-infrared sensor; attenuated total reflectance; mid-infrared spectroscopy; water pollution

Due to increasing levels of pollution in water, the need for rapid and accurate detection of life-threatening substances is becoming increasingly urgent. This work focused on the detection of aromatic hydrocarbons due to their highly carcinogenic and genotoxic properties. While several chemical sensors are commercially available for field measurements, they still have shortcomings due to cost, multiple detection failures, actual portability, and/or reliability. Creating a sensor that would improve these characteristics is the main objective of this paper.

Various water solutions containing pollutants were prepared, with concentrations ranging from 50 ppb to 100 ppm. The individual water samples were measured using a Fourier-transform infrared spectroscopy with an attenuated total reflectance accessory. Various polymers, including polyisobutylene (PIB) and polyhydroxybutyrate-co-hydroxyvalerate from a family of polyhydroxyalkanoates (PHAs), were tested as membranes, responsible for extracting molecules from water. Thin films (in a range of 5–15 μm) from the polymers were prepared on ZnSe prisms and then tested for fabrication reproducibility, analysis time, limit of detection, long-term cycle repeatability and regeneration.

For PIB, the thickness of 5 μm was chosen as a compromise between the ability to extract water and the time required to reach saturation of the membrane. The polymer showed ability to measure samples consistently and repeatedly. The detection limit of hydrocarbons was also reduced from 250 ppb to 150 ppb, promising good results in this detection range. The next step will be the transposition of pollutants detection on chalcogenide waveguide with an integrated microfluidic system.

For PHAs films, which are considered a biodegradable polymers, the goal was to improve the contact between ZnSe prism and the polymer which had in previous experiments negative effect on the hydrocarbon extraction capacity from the water.

Acknowledgments

The authors would like to acknowledge ANR AQUAE (ANR-21-CE04-0011-04) project of French National Research Agency (ANR), IBAIA (101092723) Horizon Europe project and POSEIDON (22-05179S) project of Czech Science Foundation (GA ČR) for financial support.

Soft chemistry of layered titanium and vanadium oxytellurides

L76

N. D. Kelly^{1*}, S. J. Clarke^{1*}

¹ Inorganic Chemistry Laboratory, University of Oxford, South Parks Rd, Oxford, OX1 3QR, UK

* The corresponding author e-mail: nicola.kelly@chem.ox.ac.uk

Keywords: mixed-anion; topochemical; synthesis; intercalation; layered

Solid-state compounds containing multiple anions can display complex crystal structures, unusual magnetic ordering, and/or useful physical properties for applications ranging from batteries to photocatalysis [1]. Of particular recent interest in this field are compounds containing square planar metal-oxygen layers formed from edge-sharing *trans*- MO_2X_4 octahedra, where M is a $3d$ transition metal cation and X is a chalcogenide (S, Se, Te) or pnictide (As, Sb, Bi) anion. Such layers have been reported with transition metals Ti, V, Cr, Mn, Fe, Co and Ni, and the layers can act as 2D “building blocks” within more complex crystal structures [2]. In 2018, Ablimit *et al.* reported the solid-state synthesis of RbV_2Te_2O and subsequent topochemical deintercalation of the alkali metal ions to give a layered van der Waals compound V_2Te_2O [3]. In this contribution I will discuss our soft-chemical synthesis of a new titanium oxytelluride, Ti_2Te_2O , and its intercalation reactions with alkali metals in liquid ammonia.

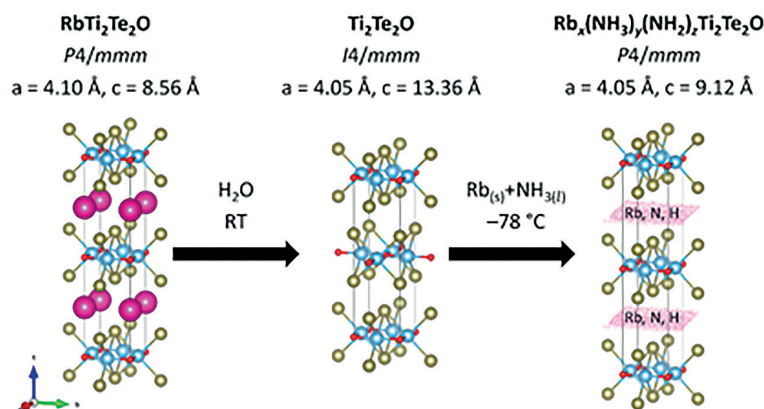


Figure: Schematic showing the topochemical reactions of $RbTi_2Te_2O$ (left) to form Ti_2Te_2O (middle) and then $A_x(NH_3)_y(NH_2)_zTi_2Te_2O$ where $A = K/Rb/Cs$ (right).

References

- [1] H. Kageyama, K. Hayashi, K. Maeda, J. P. Attfield, Z. Hiroi, J. M. Rondinelli, K. R. Poeppelmeier, *Nature Communications*, **9**, 772 (2018)
- [2] B. C. Sheath, X. Xu, P. Manuel, J. Hadermann, M. Batuk, J. O’Sullivan, R. S. Bonilla, S. J. Clarke, *Inorganic Chemistry*, **61**, 12373–12385 (2022)
- [3] A. Ablimit, Y.-L. Sun, E.-J. Cheng, Y.-B. Liu, S.-Q. Wu, H. Jiang, Z. Ren, S. Li, G.-H. Cao, *Inorganic Chemistry*, **57**, 14617–14623 (2018)

Acknowledgments

This work was supported by the UK Engineering and Physical Sciences Research Council (EP/T027991/1).

Thermal transformations and cation redistribution on $A_2B_2O_6$ oxides

K. Ji¹, E. Solana-Madruga^{1,2}, M. A. Patino³, Y. Shimakawa^{3*}, J. P. Attfield^{1*}

¹ Centre for Science at Extreme Conditions (CSEC), School of Chemistry, University of Edinburgh, Mayfield Road, Edinburgh, EH9 3FD UK;

² Dpto. Q. Inorgánica, Universidad Complutense de Madrid, Avda. Complutense sn, 28040 Madrid, Spain;

³ Institute for Chemical Research, Kyoto University, Uji, Kyoto, 611-0011 Japan;

* *The corresponding author e-mail:* j.p.attfield@ed.ac.uk; shimak@scl.kyoto-u.ac.jp

Keywords: high pressure; solid state oxide; cation ordering; structural transformation; powder diffraction

Cation ordering in solids is important for controlling physical properties and leads to ilmenite ($FeTiO_3$) and $LiNbO_3$ type derivatives of the corundum structure, with ferroelectricity resulting from breaking of inversion symmetry in the latter. [1] Co_2InSbO_6 recovered from high pressure has a new, ordered- $R32 A_2B_2O_6$ variant of the corundum structure. Co_2InSbO_6 is also remarkable for showing two cation redistributions, to $(Co_{0.5}In_{0.5})_2CoSbO_6$ and then Co_2InSbO_6 variants of the ordered- $LiNbO_3 A_2B_2O_6$ structure on heating. The cation distributions change magnetic properties as the final ordered- $LiNbO_3$ product has a sharp ferrimagnetic transition unlike the initial ordered- $R32$ phase. [2] Structural transformation can lead physical properties changes as well. Thermal transformations of double perovskites to ordered corundum can be achieved in solid solutions $Mn_{2-x}Co_xScSbO_6$, allowing magnetic properties changing from glassy state to ferrimagnetic state. [3] Future syntheses of metastable $A_2B_2O_6$ derivatives at pressure are likely to reveal other cation-redistribution or structural transformation pathways, and may enable $A_2B_2O_6$ materials with more flexible properties to be discovered.

References

- [1] A. M. Arevalo-Lopez and J. P. Attfield, *Phys. Rev. B.*, **88**, 104416 (2013)
- [2] K. Ji, E. Solana-Madruga, M. A. Patino, Y. Shimakawa and J. P. Attfield, *Angew. Chem. Int. Ed.*, **61**, e202203062 (2022)
- [3] K. Ji, F. D. Romero, Y. Shimakawa and J. P. Attfield, in preparation.

Acknowledgments

This work was partly supported by Grants-in-Aid for Scientific Research (Nos. 19H05823, 20H00397, and 20K20547) and by a grant for the International Collaborative Research Program of Institute for Chemical Research in Kyoto University from MEXT of Japan. This work was also supported by the JSPS Core-to-Core Program (A) Advanced Research Networks. We acknowledge EPSRC also for financial support.

Photoluminescence properties of nanocrystalline multicomponent garnet $\text{Gd}_3\text{Sc}_x\text{Ga}_{5-x}\text{O}_{12}$ doped with Er^{3+}

T. Netolický¹, L. Benes², S. Slang³, B. Frumarova³, J. Oswald⁴, T. Wagner^{1,3}

¹ Department of General and Inorganic Chemistry, Faculty of Chemical Technology, University of Pardubice, Studentska 573, 53210 Pardubice, Czech Republic;

² Joint Laboratory of Solid State Chemistry, Faculty of Chemical Technology, University of Pardubice, Studentska 95, 53210 Pardubice, Czech Republic;

³ Center of Materials and Nanotechnologies, Faculty of Chemical Technology, University of Pardubice, Cs. Legii 565, 530 02 Pardubice, Czech Republic;

⁴ Institute of Physics of the Czech Academy of Sciences, Cukrovarnicka 10, 162 00 Prague 6, Czech Republic

* The corresponding author e-mail: tomas.netolicky2@student.upce.cz

Keywords: nanocrystals; garnet structure; $\text{Gd}_3\text{Sc}_x\text{Ga}_{5-x}\text{O}_{12}$; X-ray diffraction; optical properties; photoluminescence

Nanocrystalline oxides of composition $\text{Gd}_3\text{Sc}_x\text{Ga}_{5-x}\text{O}_{12}$ ($x = 0 - 2$) belong to the family of materials with garnet-related structure. Although nanocrystalline $\text{Gd}_3\text{Ga}_5\text{O}_{12}$ garnet doped with Er^{3+} has been intensively studied with emphasis on the luminescence properties [1], the reports about luminescence properties of Er^{3+} -doped $\text{Gd}_3\text{Sc}_x\text{Ga}_{5-x}\text{O}_{12}$ garnets are missing yet. The use of Sc^{3+} as another component of the studied garnets may be found beneficial. It has been reported that in e.g. Er^{3+} -doped Y_2O_3 nanocrystals [2], the addition of Sc^{3+} leads to improvement of the luminescence properties due to a symmetry modification.

Nanocrystals of composition $\text{Gd}_3\text{Sc}_x\text{Ga}_{5-x}\text{O}_{12}$ ($x = 0, 0.5, 1, 1.5$ and 2) doped with 0.5 at.% Er^{3+} were prepared by sol-gel combustion synthesis using citric acid as chelation agent. Structure, morphology and chemical composition of the annealed powders were studied by X-ray diffraction, ATR-FTIR spectroscopy and by scanning electron microscope with Energy-dispersive X-ray spectrometer. The measurement of steady-state and time-dependent Stokes and anti-Stokes (upconversion) emission spectra was carried out using photoluminescence spectroscopy with 980 nm laser diode excitation.

References

- [1] F. Vetrone, J.-C. Boyer, J. A. Capobianco, A. Speghini, M. Bettinelli, *J. Phys. Chem. B*, **107**, 10747–10752 (2003)
- [2] Y. Wang, X. Wang, Y. Mao, J. A. Dorman, *J. Phys. Chem. C*, **126**, 11715–11722 (2022)

Acknowledgments

The authors thank for financial support from the grant of the Ministry of Education, Youth and Sports of Czech Republic (LM2018103), the European Regional Development Fund-Project “Modernization and upgrade of the CEMNAT” (No.CZ.02.1.01/0.0/0.0/16_013/0001829), the project NANOMAT CZ.02.1.01/0.0/0.0/17_048/0007376 and the project of Faculty of Chemical Technology, University of Pardubice „Excellent teams“ 2020.

Borosulfates – silicate analogue anions with the potential to stabilize polycations

J. Bruns

University of Cologne, GreinstraÙe 6, 50939 Cologne

* The corresponding author e-mail: j.bruns@uni-koeln.de

Keywords: crystal structure; borosulfate; gold; synthesis; super acid

The anionic substructures of borosulfates are similar to those found for silicates and consist of vertex-connected (BO_4) - and (SO_4) -tetrahedra [1]. Thereby, not only B-O-S bonds can form but also S-O-S and B-O-B bonds, as for example in $(\text{I}_4)[\text{B}(\text{S}_2\text{O}_7)_2]$ [2] and $\text{Sr}[\text{B}_3\text{O}(\text{SO}_4)_4(\text{SO}_4\text{H})]$ [3]. Charge compensation is typically achieved by metal cations.^[1] However, recently it was possible to crystallize homo- and even heteropolycations with the anion $[\text{B}(\text{S}_2\text{O}_7)_2]^-$. The $(\text{I}_4)^{2+}$ cation has been found in the structure of $(\text{I}_4)[\text{B}(\text{S}_2\text{O}_7)_2]$ [2]. This cation typically forms under strongly oxidizing conditions and in the presence of weakly coordinating anions.^[4] Even more astonishing is the stabilization of the heteropolycations in $[\text{Au}_3\text{Cl}_4][\text{B}(\text{S}_2\text{O}_7)_2]$ and $[\text{Au}_2\text{Cl}_4][\text{B}(\text{S}_2\text{O}_7)_2](\text{SO}_3)$ [5]. According to quantum chemical calculations the latter is a one-dimensional metal, which has been confirmed by polarization microscopy [5].

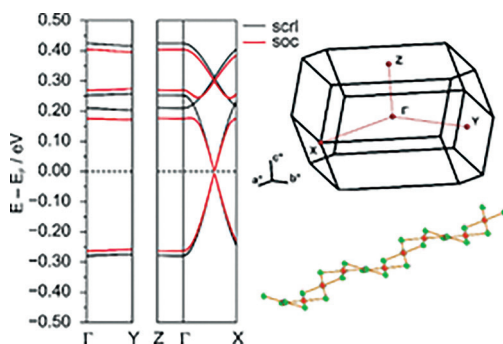


Figure: Heteropolycationic substructure of $[\text{Au}_2\text{Cl}_4][\text{B}(\text{S}_2\text{O}_7)_2](\text{SO}_3)$ and selected parts of the band structure together with the first Brillouin zone.^[5]

References

- [1] J. Bruns, H. A. Höpfe, M. Daub, H. Hillebrecht, *Chem. Eur. J.* 26, 7966–7980 (2020).
- [2] D. van Gerven, S. Sutorius, J. Bruns, M. S. Wickleder, *ChemistryOpen*, e202200122 (2022).
- [3] L. C. Pasqualini, H. Huppertz, M. Je, H. Choi, J. Bruns, *Angew. Chem.*, 133, 19892–19896 (2021); *Angew. Chem. Int. Ed.* 60, 19740–19743 (2021).
- [4] R. Faggiani, R. J. Gillespie, R. Kapoor, C. J. L. Lock, J. E. Vekris, *Inorg. Chem.* 27, 4350–4355 (1988).
- [5] S. Sutorius, D. van Gerven, S. Olthof, B. Rasche, J. Bruns, *Chem. Eur. J.*, e202200004 (2022).

Characterisation of Rh⁴⁺ oxides, an unusual case of pyrochlore stabilisation under high pressure, high temperature synthesis conditions

S. D. Injac^{1,2}, B. Mullens³, F. Denis Romero², M. Avdeev^{3,4}, C. Barnett³, A. K. L. Yuen³, B. J. Kennedy³, Y. Shimakawa²

¹ Centre for Science at Extreme Conditions, School of Chemistry, University of Edinburgh, Edinburgh, EH9 3FJ, Scotland, United Kingdom;

² Institute for Chemical Research, Kyoto University, Gokasho, Uji, Kyoto 611-0011, Japan;

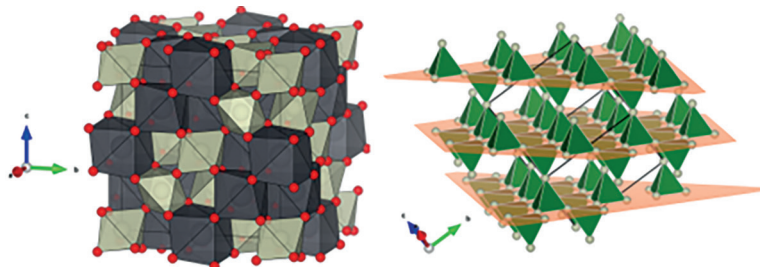
³ School of Chemistry, University of Sydney, Sydney 2006, NSW, Australia;

⁴ Australian Centre for Neutron Scattering, ANSTO, Lucas Heights, 2234, NSW, Australia

* The corresponding author e-mail: sean.injac@ed.ac.uk

Keywords: high pressure synthesis; pyrochlore; rhodium oxide; magnetic frustration; quantum magnet

The two pyrochlore oxides Pb₂Rh₂O₇ and Y₂Rh₂O₇ were synthesized using high pressure, high temperature techniques at 19 GPa and 8 GPa respectively. Both oxides' physical properties and catalytic activities were investigated. Structurally, both compounds were determined to crystallise in space group $Fm\bar{3}m$ with no observed oxygen vacancies. In both oxides effectively identical Rh-O bond lengths of 1.987 Å and BVS of 4.2 confirm a Rh⁴⁺ oxidation state. Y₂Rh₂O₇ represents an unusual case of the lower density (6.356 g/cm³) pyrochlore structure being stabilised under high pressure conditions, while the analogous, higher density (7.031 g/cm³) perovskite YRhO₃ is stabilised by synthesis under ambient pressure conditions. High pressure acts to stabilise the Rh⁴⁺ state, through the immense oxidising potential of HPHT techniques. The Rh⁴⁺ state results in a $S = \frac{1}{2}$ magnetic ground state. Magnetisation measurements suggest strong AFM coupling in Y₂Rh₂O₇, long range AFM order is however not observed due to the geometric frustration of the pyrochlore lattice. Specific heat and resistivity measurements indicate a large electronic contribution to heat capacity with a Wilson ratio of 4.78(11) being calculated, suggesting strong electron localisation. Resistivity measurements show a temperature dependence indicating semiconductivity, with a narrow band gap of 50 meV being determined. Overall, these results are similar to that reported for the metallic non-metal FeCrAs and other bad metals.[1,2] Physical property measurements for Pb₂Rh₂O₇ indicate a metallic ground state. This is consistent with similar Pb₂M₂O₇ oxides where $M = \text{Ru, Ir, Os}$. [3]



References

- [1] A. M. Hallas, A. Z. Sharma, C. Mauws, et al, npj. Quantum Materials, 4(1), 9 (2019)
- [2] J. G. Rau, H-Y Kee, Phys. Rev. B, 84, 104448, (2011)
- [3] M. A. Subramanian, et al, Progress in Solid State Chem., 15(2), 55-143, (1983)

Alkali metal oxide mercurides with isolated mercuride anions

L. Nusser¹, S. Feldl¹, C. Hoch^{1*}

¹ University of Munich (LMU), Department of Chemistry, Butenandtstraße 5-13, 81377 Munich, Germany

* The corresponding author e-mail: constantin.hoch@uni-muenchen.de

Keywords: mercuride anions; alkali metals; double salts; band structure; crystal structure

Mercuride anions are not stable against oxidation and can only be stabilised in solids with high enough lattice energy to account for their thermodynamic instability. [1] We present a series of compounds in which the first reported isolated mercuride anions are present together with oxide anions octahedrally coordinated by Cs cations. The ionic bonding is illustrated by the presence of band gaps at the Fermi level according to calculations of the electronic structures. In $A_{18}Hg_8O_6$, [2] A_8Hg_8O ($A = Rb, Cs$) and $Cs_{58}[Hg_8]_6O_{12}$, $[Hg_8]^{6-}$ anions in the shape of only marginally distorted cubes occur. In $Cs_{14}Hg_{12}O_4$, the anion $[Hg_{12}]^{6-}$ has the shape of two face-sharing cubes and is considerably distorted. Some of the mercurides show interesting structural similarities with thal- lides of the same composition. [3] The direct comparison shows how relativistic contributions can explain the observed structural distortions.

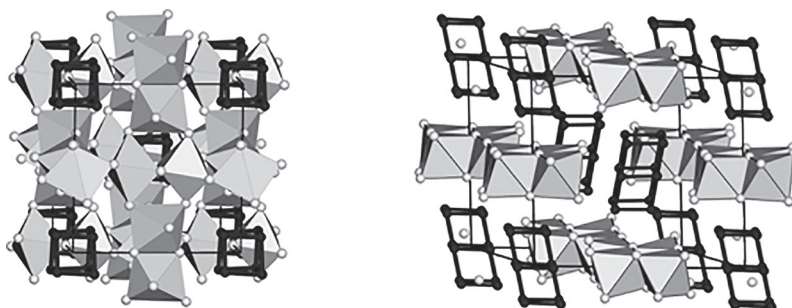


Figure 1: Left: crystal structure of $Cs_{18}Hg_8O_6$ with $[Cs_6O]$ polyhedra in grey and $[Hg_8]_6^-$ anions in black; right: crystal structure of $Cs_{14}Hg_{12}O_4$ with $[Cs_6O]$ polyhedra in grey and $[Hg_{12}]_6^-$ anions in black.

References

- [1] J. H. Simons, R. P. Seward, *J. Chem. Phys.* **6**, 790-794 (1938).
- [2] L. Nusser, T. Hohl, F. Tambornino, C. Hoch, *Z. Anorg. Allg. Chem.* **648**, e202100389 (2022).
- [3] a) A. Karpov, M. Jansen, *Chem. Comm.* **2006**, 1706-1708 (2006); b) A. Karpov, M. Jansen, *Angew. Chem. Int. Ed.* **44**, 7639-7643 (2005); c) U. Wedig, V. Saltykov, J. Nuss, M. Jansen, *J. Am. Chem. Soc.* **35**, 2458-12463 (2010)

Acknowledgments

This work was supported by Deutsche Forschungsgemeinschaft (Project number 513247541.).

Synthesis and characterization of a novel oxychloride, SrTe₂FeO₆Cl

L82

J. A. Sannes¹, B. Gonano¹, Ø. S. Fjellvåg^{2,3}, S. Kumar^{1,4}, O. Nilsen¹, M. Valldor¹

¹ Centre for Materials Science and Nanotechnology (SMN), Department of Chemistry, University of Oslo, Sem Sælands vei 26, N-0371 Oslo, Norway;

² Department for Hydrogen Technology, Institute for Energy Technology, NO-2027 Kjeller, Norway;

³ Laboratory for Neutron Scattering and Imaging, Paul Scherrer Institute, Forschungsstrasse 111, Villigen PSI, 5232, Switzerland;

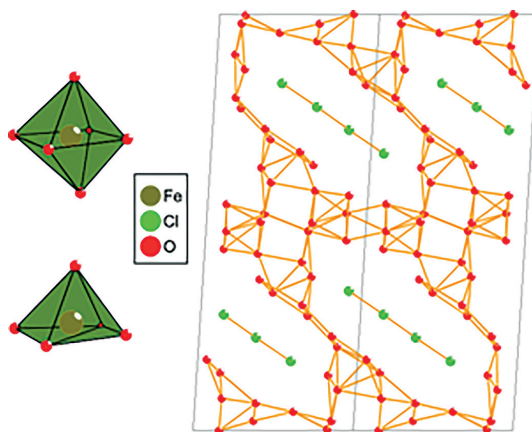
⁴ Present address: Elektro group, Justervesenet, Fetveien 99, N-2007 Kjeller, Norway

The corresponding author e-mail: j.a.sannes@kjemi.uio.no (+47 22859097)

Keywords: mixed-anion compounds; oxychloride; solid-state synthesis; neutron diffraction; anion-superstructure

Mixed anion compounds have gained a lot of attention in recent times, providing the material scientist with yet another way of fine tuning properties by introducing multiple anions [1].

In this work, a relatively new way of chemically designing low dimensional mixed-anion crystal structures has been applied, leading to the discovery of a novel oxychloride, SrTe₂FeO₆Cl. An almost x-ray pure sample have been synthesized and has been investigated by pXRD, SEM/EDX, magnetic susceptibility, specific heat and neutron diffraction. From the susceptibility measurement and neutron diffraction it is clear that the sample is antiferromagnetically ordered in its ground-state. The crystal structure reveals homoleptic coordinated iron, and a low dimensional anion superstructure consisting of 1D “square” chains of chlorine surrounded by an oxygen network.



References

- [1] Kageyama, H., Hayashi, K., Maeda, K., Attfield, J. P., Hiroi, Z., Rondinelli, J. M., Poeppelmeier, K. R. Expanding frontiers in materials chemistry and physics with multiple anions. *Nat Commun* **2018**, 9 (1), 772-15 DOI: 10.1038/s41467-018-02838-4.

Acknowledgments

This work was supported by the Norwegian Research Council (NFR) through project 301711.

The absence of expected paramagnetic behaviour in $\text{Ba}_6\text{Fe}_2\text{Te}_3\text{S}_7$

E. H. Frøen¹, P. Adler², M. Valldor¹

¹ Centre for Materials Science and Nanotechnology (SMN), Department of Chemistry, University of Oslo, Sem Sælands vei 26, N-0371 Oslo, Norway;

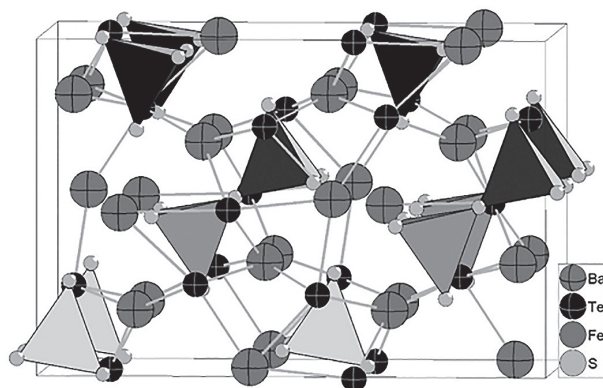
² Max-Planck-Institute for Chemical Physics of Solids, Nöthnitzer Straße 40, 01187 Dresden, Germany

The corresponding author e-mail: e.h.froen@smn.uio.no

Keywords: bichalcogenides; crystal structure; magnetism; mössbauer spectroscopy; dft

In the search for new inorganic materials, oxides, along with other monoanionic materials, have received the bulk all of scientific attention over the years. Multi-anionic compounds have received comparatively little attention. As such, the phase diagrams of multi-anionic species remains largely unexplored today, despite the field of multi-anionic compounds showing great promise for new chemistry. [1]

Here, a novel bichalcogenide, $\text{Ba}_6\text{Fe}_2\text{Te}_3\text{S}_7$, its synthesis and properties are shown. Exhibiting an original crystal structure with iron sulfide tetrahedra arranged in a vertex-sharing dimeric coordination, it would be expected to observe paramagnetic behavior a high temperatures, due to very low electric conductivity. $\text{Ba}_6\text{Fe}_2\text{Te}_3\text{S}_7$, however, remains essentially nonmagnetic in response to applied magnetic fields. Mössbauer spectroscopy and DFT analysis are employed to further understand the magnetic nature of this anomalous behavior.



References

[1] M. Valldor. *Inorganics* 2016, 4, 23.

Acknowledgments

This work was supported by the Norwegian Research Council (NFR) through project 301711.

Oxides as Pt catchment materials in the ammonia oxidation process – methodology and mechanistic insight

J. Hessevik¹, A. S. Fjellvåg¹, O. Iveland¹, C. S. Carlsen¹, H. Sønsteby¹, T. By², J. Skjelstad², D. Waller³, H. Fjellvåg¹, A. O. Sjøstad¹

¹ Department of Chemistry, Centre for Materials Science and Nanotechnology, University of Oslo, N-0318 Oslo, Norway;

² K. A. Rasmussen, N-2316 Hamar, Norway.

³ Yara International ASA, Yara Technology Centre, N-3936 Porsgrunn

* The corresponding author e-mail: juliehes@kjemi.uio.no

Keywords: platinum catchment; LaNiO₃; perovskite; thin films; diffusion; mechanism

One of the key steps in the production of nitrogen based inorganic fertilizers utilizes a Pt-Rh catalytic gauze (typically 95:5 wt.%) to give high yields of NO in the ammonia oxidation process (800–950 °C and P = 1–12 bar) [1]. This reaction is highly exothermic ($\Delta H^\circ = -908$ kJ/mol) and leads to losses of Pt and Rh as PtO₂(g) and RhO₂(g), respectively. The most common technology utilized today for recovering PtO₂ from the gas stream is to apply Pd-Ni (95:5 wt.%) catchment gauzes. However, there is a simultaneous loss of Pd from the catchment gauze, which makes the cost-benefit of the current Pt catchment process less beneficial. An alternative catchment material based on oxides would significantly lower operational costs.

The catchment of Pt by oxides provides a good basis for Pt recovery and recycling. However, a suitable oxide should at the same time not possess any negative catalytic activity with respect to the NO_x gases in question. A number of oxides are identified as suitable candidates. For one such oxide, LaNiO₃, we observed that Pt catchment takes place through a gradual increase of Pt content from LaNiO₃ via rhombohedral LaNi_{1-x}Pt_xO₃ (R-3c, $x \leq 0.075$) solid solution and thereafter via La₂Ni_{2-2x}Pt_{2x}O₆ (P2₁/n, $0.20 \leq x < 0.50$) until the fully ordered double perovskite La₂NiPtO₆ ($x = 0.50$) is formed [2]. The following overall reaction is suggested:



In order to design an optimized and efficient oxide for Pt catchment, it is essential to have good mechanistic insight into how the oxide captures Pt from the gas stream and transform into a Pt holding oxide like La₂NiPtO₆. Insight to surface reactions, nucleation and diffusion aspects are obtained from exploring thin films as model materials, e.g. LaNiO₃ thin films as grown by Atomic Layer Deposition that thereafter are subjected to PtO₂ gas streams. Characterization data were obtained by means of SEM, AFM, TEM, PXRD and XPS investigations.

References

- [1] M. Warner, *University of Sydney* (2013), Retrieved from <http://hdl.handle.net/2123/9426>.
- [2] J. Hessevik, A. S. Fjellvåg, O. Iveland, T. By, J. Skjelstad, D. Waller, H. Fjellvåg, A. O. Sjøstad, *Mater. Today Commun.* **33** (2022).

Acknowledgments

This work has been carried out as part of the center “iCSI – industrial Catalysis, Science and Innovation” (Research Council of Norway; project no. 237922).

Probing for dynamics in a strongly frustrated magnet

L. Kubíčková, A. K. Weber, M. Panthöfer, A. Möller*

Department of Chemistry, Johannes Gutenberg University Mainz, Duesbergweg 10-14, 55128 Mainz, Germany

* The corresponding author e-mail: angela.moeller@uni-mainz.de

Keywords: competing interactions; ^{57}Fe Mössbauer spectroscopy; magnetic properties; specific-heat data; langbeinite-type compounds; solid-state synthesis

The langbeinite-type of compounds, $A_2M_2(TO_4)_3$, where A mostly represents alkali metals, M transition metals and $T = \text{S, Mo, Se, Cr, or W}$, crystallize in the acentric polar space group $P2_13$. In particular, the sulfates of this family have been extensively studied in the past since several of them undergo ferroelectric or ferroelastic structural phase transitions [1]. More recently, those members involving magnetic M^{2+} ions have attracted attention due to their fascinating magnetic behavior arising from competing magnetic interactions and some have been classified as spin-liquid candidates, $\text{K}_2\text{Ni}_2(\text{SO}_4)_3$ [2] or $\text{KSrFe}_2(\text{PO}_4)_3$ [3].

The absence of long-range magnetic order in these highly frustrated magnetic langbeinite type of compounds has inspired us to investigate $\text{Cs}_2\text{Fe}_2(\text{MoO}_4)_3$ as a model compound, which features Fe^{2+} ions in trigonal ligand field. In contrast to the rigid units and *Pearson* hard cations (K^+) involved in the ferroelectric/ferroelastic phase transitions of sulfates, the softer bridging the $[\text{FeO}_6]$ -units along with the chemically softer Cs^+ -cation facilitate dynamics in this case. We will present insights from magnetic and thermodynamic data in a combination with the local probe of ^{57}Fe Mössbauer spectroscopy. By comparing our results with earlier studies involving langbeinite-type sulfates, distinct differences are unravelled. Most importantly, we will propose a dynamic scenario in an attempt to address the highly degenerate ground state in this frustrated magnet [4].

References

- [1] T. Hikita et al., *Journal of the Physical Society of Japan*, **65**, 1293–1296 (1996)
- [2] I. Živković et al., *Physical Review Letters*, **127**, 157204 (2021)
- [3] K. Boya et al., *APL Materials*, **10**, 101103 (2022)
- [4] L. Kubíčková, A. K. Weber, M. Panthöfer, A. Möller, *in preparation* (2023)

Acknowledgments

This work has received funding from the European Union's Research and Innovation Program Horizon Europe under the Marie Skłodowska-Curie grant agreement No. 101066568. The support from the Deutsche Forschungsgemeinschaft (DFG, German Research Foundation) under the projects 443703006 – CRC 1487 and 442589410 is gratefully acknowledged.

Chemical pressure driving phase transition and morphology in Eu³⁺-doped KY₃F₁₀: An experimental and theoretical insight

P. Serna-Gallén¹, S. C. S. Lemos², L. Gracia^{2,3}, E. O. Gomes², H. Beltrán-Mir¹, E. Cordoncillo¹, J. Andrés²

¹ Departamento de Química Inorgánica y Orgánica, Universitat Jaume I, 12071 Castelló de la Plana (Spain);

² Departamento de Química Física y Analítica, Universitat Jaume I, 12071 Castelló de la Plana (Spain);

³ Department of Physical Chemistry, University of Valencia (UV), 46100 Burjassot (Spain)

* The corresponding author e-mail: pserna@uji.es

Keywords: phase transitions; europium; chemical pressure; fluorides; surface

The complex fluoride KY₃F₁₀ and its Ln³⁺-doped counterparts have devoted a lot of attention due to a broad range of technological applications. Quite intriguing, though, only studies comprising the common α -phase of this structure can be found in the literature, neglecting the δ -phase discovered in 2000 by Le Berre *et al.* [1], a gap which has been filled by some contributions of the present authors [2,3]. Continuing with the aim of the synthesis and characterization of these polymorphs involving Ln³⁺-doping processes, in the present work Eu³⁺-doped KY₃F₁₀ materials were synthesized by a coprecipitation method. At lower Eu³⁺ doping concentration (until 10%) the δ -phase was obtained and increasing the doping concentration a mixture of α/δ phases was formed. In addition, first principles calculations, at the density functional theory (DFT) level, have been performed to disclose the mechanism of the phase transition between α/δ induced by the pressure, and morphology transformation.

The theoretical results indicated that α -phase is more stable than the δ and the study of phase transition induced by pressure depicted that the $\alpha \rightarrow \delta$ phase transition involves a volume expansion, thus requiring temperature to occur. Therefore, the observed experimentally $\delta \rightarrow \alpha$ transition (which involves a volume contraction provoked by the Eu³⁺ doping process) exhibits the behavior of a positive (chemical) pressure emerging along the doping process [4].

The electronic analysis indicates that local distortion greatly affects the Eu-F hybridization in δ -phase structure, which could culminate with the destabilization of this phase, allowing the α -KY₃F₁₀ formation. Additionally, the presence of Eu³⁺ stabilize the (111) surface at the morphology, which is characteristic in the SEM images. There is a morphological transformation from nanospheres toward the formation of mainly octahedra, also truncated octahedra, and cubes. A robust model is presented to match the theoretical and experimental morphologies, improving the understanding of reaction paths connecting them.

References

- [1] F. Le Berre, *et al. J. Mater. Chem.*, **10**, 2578–2586 (2000)
- [2] P. Serna-Gallén, *et al. J. Mater. Res. Technol.*, **15**, 6940–6946 (2021)
- [3] P. Serna-Gallén, *et al. Ultrason. Sonochem.*, **87**, 106059 (2022)
- [4] E. O. Gomes *et al. J. Phys. Chem. Lett.*, **13**, 9883–9888 (2022)

Part V

POSTERS

18th European
Conference
on Solid State
Chemistry

Nitridooxorhenate and -technetate anions $[MO_3N]^{2-}$ (M = Tc, Re) from reactions in highly alkaline media

D. Badea¹, E. Strub², J. Bruns^{1*}

¹ University of Cologne, Greinstrasse 6, 50939 Cologne, Germany;

² University of Cologne, Zulpicher Strasse 25, 50674 Cologne, Germany

* The corresponding author e-mail: j.bruns@uni-koeln.de

Keywords: hydroflux; oxoanion; technetium; rhenium; x-ray; xafs; magnetochemistry

When comparing the number of crystallographically characterized group 7 element oxides, significant differences can be observed. It turns out that compounds of manganese are described intensively, whereas the number of both ternary technetium and rhenium oxides is small. Considering potassium as second cation basically only pertechnetate and perrhenate are known, whereas a large variety of manganese compounds has been reported for this system [1].

Herein, the redox chemistry of technetium and rhenium in highly alkaline media was investigated. The resulting compounds contain the anions $[MO_3N]^{2-}$ (M = Tc, Re) [2]. All obtained samples have been investigated by single crystal X-ray diffraction for the first time. The $[TcO_3N]^{2-}$ anion in $Ba[TcO_3N]$ exhibits one short and three long metal-ligand bonds, which hints to a localized Tc-N bond (**Fig.**) [2]. Furthermore, $Ba[TcO_3N]$ was investigated in more detail by XAFS, Raman spectroscopy and magnetochemical measurements. Quantum chemical calculations corroborate the findings.[2]

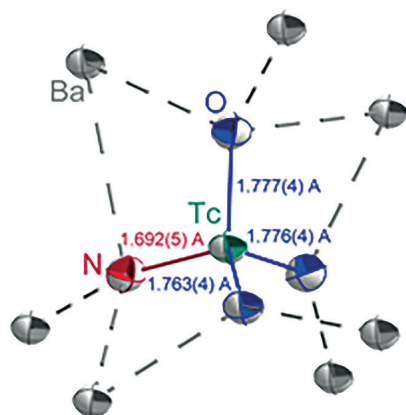


Figure:
Extended asymmetric unit of $Ba[TcO_3N]$. [2]

References

- [1] a) B. Krebs, K.-D. Hasse, *Acta Crystallogr.*, **B32**, 1334–1337 (1976); b) R. C. L. Mooney, *Phys. Rev.*, **37**, 1306–1310 (1931); c) M. Jansen, F. M. Chang, R. Hoppe, *Z. Anorg. Allg. Chem.*, **490**, 101–110 (1982); d) G. J. Palenik, *Inorg. Chem.*, **6**, 507–511 (1967); e) E. Seipp, R. Hoppe, *Z. Anorg. Allg. Chem.*, **530**, 117–126 (1985); f) J. Nuss, P. L. V. K. Dasari, M. Jansen, *Z. Anorg. Allg. Chem.*, **641**, 316–321 (2015); g) G. Brachtel, R. Hoppe, *Z. Anorg. Allg. Chem.*, **446**, 64–76 (1978); h) J. Nuss, R. K. Kremer, M. Jansen, *Z. Anorg. Allg. Chem.*, **644**, 1715–1720 (2018); i) J. Morrow, *Acta Crystallogr.*, **13**, 443–445 (1960).
- [2] D. Badea, K. Dardenne, R. Polly, J. Rothe, K. Meerholz, M. Hanrath, M. Reimer, J. Neudörfel, E. Strub, J. Bruns, *Chem. - Eur. J.*, e202201738 (2022).

Ternary alkali metal thallides ATl (A = K/Rb, Cs/Rb)

V. F. Schwinghammer¹, S. Gärtner^{1,2*}

¹ Department of Inorganic Chemistry University of Regensburg, Universitätsstr. 31, 93053 Regensburg (Germany);

² Department for X-Ray Structure Analysis, Central Analytics University of Regensburg, Universitätsstr. 31, 93053 Regensburg (Germany);

* The corresponding author e-mail: Stefanie.Gaertner@ur.de, phone: +49 94 1 943 4446

Keywords: thallium; indium; alkali metals; zintl ions; single crystal X-Ray analysis

The combination of an electropositive element, such as alkali metals, with thallium, leads to a large number of compounds in which this group 13 element is present in a formally negative oxidation state. The thallium substructures reach from three-dimensional networks, two-dimensional layers, or isolated clusters. This depends on the alkali metal to thallium ratio $A:Tl$. Despite the high variety of compounds, there are still some binary compounds A_xTl_y ($A = Na-Cs$) missing [1].

At the $A:Tl$ ratio 1:1 RbTl has not yet been reported. Binary approaches from high temperature solid state techniques did not yet result in the desired product. Additionally, experiments according to Zintl's low temperature approach in liquid ammonia ($TlX + 2 Rb$; $X = Cl, Br, I, BF_4, PF_6$) were prepared, which also did not result in RbTl [2]. Therefore, several ternary compositions of K/Rb and Cs/Rb have been prepared via high temperature route and analyzed by single crystal X-ray structure analysis to approximate RbTl. Those approaches resulted in the first mixed alkali metal thallides ATl. Mixed K/Rb thallides crystallize in the orthorhombic KTI type structure (space group $Cmce$) [3]. Contrary to the ternary compounds in the KTI type structure, mixtures of Cs and Rb did not crystallize in the CsTI type structure (space group $Fddd$) [4]. Instead, the new compound $Cs_{0.58}Rb_{0.42}Tl$ crystallizes in the monoclinic space group $C2/c$. In both ternary variants, distorted Tl_6^{6-} octahedra form the Tl substructure. Three to six alkali metal cations are located on symmetrically inequivalent, mixed occupied positions and compensate the sixfold negative charge of the clusters.

References

- [1] S. Gärtner, *Crystals*, **10**, 1013 (2020).
- [2] E. Zintl, W. Dullenkopf, *Z. phys. Chem.*, **B16**, 195–205 (1932).
- [3] Z. C. Dong, J. D. Corbett, *J. Am. Chem. Soc.*, **115**, 11299–11303 (1993).
- [4] Z. C. Dong, J. D. Corbett, *Inorg. Chem.*, **35**, 2301–2306 (1996).

Acknowledgments

This research was funded by a research grant of the German Science Foundation (DFG): GA2504/1-1

Solution combustion synthesis of thermodynamically metastable oxide-phosphates with rutile- and anatase-related structures

S. Früchtnicht*, M. Weber, R. Glaum

Institut für Anorganische Chemie, Rheinische Friedrich-Wilhelms-Universität Bonn,
Gerhard-Domagk-Straße 1, 53121 Bonn (Germany)

* The corresponding author e-mail: s6svfrue@uni-bonn.de

Keywords: solution combustion synthesis; metastable solid; oxide-phosphate, defect structure

Solution combustion synthesis (SCS) has been established as a versatile tool for materials synthesis [1]. By avoiding sintering processes, access to powders with particular nanostructure, high specific surface, and high chemical reactivity has become possible. Gaining access to thermodynamically metastable solids by SCS was until recently not in the focus of research. Therefore, discovery of multinary tungsten oxide-phosphates with P_4O_{10} content of up to 50 mol% and ReO_3/WO_3 related XRPD pattern was rather unexpected [2]. Thus obtained materials are promising catalysts for selective oxidation of short chain hydrocarbons [3]. These results triggered our search for (transition)metal oxide-phosphates with crystal structures related to rutile (slightly corrugated hcp of O^{2-}) and anatase (ccp of O^{2-}).

We are reporting the first oxide-phosphates with rutile- and anatase-type structures. $(Sn_{0.8}Cr_{0.1}P_{0.1})O_2$ was obtained by SCS and subsequent annealing of the combustion product with stepwise rising temperature in air ($T_{max} = 900$ °C). Its XRPD pattern can be fully assigned based on the tetragonal cell of rutile-type SnO_2 ($a = 4.737$ Å, $c = 3.185$ Å) however, with slightly different lattice parameters $a = 4.732(2)$ Å, $c = 3.174(3)$ Å. EDX analysis confirmed a homogeneous element distribution. Above 1000 °C $(Sn_{0.8}Cr_{0.1}P_{0.1})O_2$ is decomposed to Cr_2O_3 and SnO_2 , the later containing a small amount of phosphorus. Decomposition of $(Sn_{0.6}Cr_{0.2}P_{0.2})O_2$ leads to Cr_2O_3 , SnO_2 and SnP_2O_7 .

Anatase-type $(Ti_{0.8}Cr_{0.1}P_{0.1})O_2$ was obtained by a similar procedure (SCS, $T_{max} = 700$ °C) with tetragonal unit cell parameters $a = 3.791(2)$ Å, $c = 9.491(7)$ Å differing slightly from those of anatase-type TiO_2 ($a = 3.785$ Å, $c = 9.514$ Å). Thermal decomposition above 800 °C leads to $Cr^{III}_4Ti^{IV}_{27}O_{24}(PO_4)_{24}$ and TiO_2 (rutile-type, possibly containing small amounts of Cr_2O_3).

Details on further thermodynamically metastable oxide-phosphates related to rutile $\{(Sn_{0.8}In_{0.1}P_{0.1})O_2, (Sn_{0.8}Mn^{II}_{0.1}P_{0.1})O_{1.95}, (Sn_{0.6}Mn^{II}_{0.2}P_{0.2})O_{1.90}\}$ or anatase $\{(Ti_{0.6}Cr_{0.2}P_{0.2})O_2, (Ti_{0.8}In_{0.1}P_{0.1})O_2\}$ will be reported together with the results of structure modelling providing insights into the substitution mechanism.

References

- [1] A. Varma et al., *Chem. Rev.* **116**, 14493–14586 (2016).
- [2] S. C. Roy, PhD Thesis, University of Bonn (2015).
- [3] a) C. A. Welcker-Niewoudt et al., Patent DE102016007628A1 (2016) b) A. Karbstein et al., *Eur. J. Inorg. Chem.* **15** 1459–1469 (2021).

Acknowledgments

Fruitful discussions with Dr. F. Rosowski (BasCat Berlin) and Prof. S. A. Schunk (hte GmbH, Heidelberg) as well as partial funding of this work by BASF (Ludwigshafen) are gratefully acknowledged.

Ferroelectric properties on $\text{Ba}_{0.975}\text{Ln}_{0.017}(\text{Zr}_x\text{Ti}_{0.95-x})\text{Sn}_{0.0503}$ materials

P04

K. Taibi¹, S. Zemouri-Smail¹, A. Lahmar²

¹ LCT, Faculty of Chemistry, U.S.T.H.B., BP32, Al Alia, 16111, Algiers, Algeria,

² L. P. M. C., University of Picardy, Amiens Cedex 1, France

* The corresponding author e-mail: kamel-taibi.dz@gmail.com

Keywords: ferroelectric; properties; lead-free; materials; relaxor; rare earth

Ferroelectric materials are renowned for their various industrial and technological applications [1,2]. Among these, perovskite-type ferroelectric materials stood out as the most promising candidates for the fabrication of electronic components. Unfortunately, most of these materials are lead-based, such as $\text{PbMg}_{1/3}\text{Nb}_{2/3}\text{O}_3$ (PMN), $\text{PbSc}_{1/2}\text{Nb}_{1/2}\text{O}_3$ (PSN), $\text{PbZr}_x\text{Ti}_{1-x}\text{O}_3$ (PZT)... etc. Taking into account the risks pretended by lead compounds on health and the environment, recent universal legislation has been adopted concerning the use of toxic materials [3]. Therefore, the search for lead-free materials has become an alternative attracting the intention of many researchers. In this regard, the compound BaTiO_3 is the best-known prototype of classical (or conventional) ferroelectric materials characterized by a ferroelectric (tetragonal)-paraelectric (cubic) phase transition that occurs at 120°C (far from room temperature) thus limiting the applications of such materials. In order to overcome this drawback, various substitutions have been tested on the Ti and/or Ba sites of the BaTiO_3 material. In this purpose, we report the results obtained simultaneously by aliovalent ($\text{Ba}^{2+}\text{-Ln}^{3+}$) and isovalent ($\text{Ti}^{4+}\text{-Zr}^{4+}\text{-Sn}^{4+}$) substitutions within the lead-free solid solution of complex formula $\text{Ba}_{0.975}\text{Ln}_{0.017}(\text{Zr}_x\text{Ti}_{0.95-x})\text{Sn}_{0.05}\text{O}_3$ (denoted $\text{BLnZ100}_x\text{TS}$) with $\text{Ln} = \text{La, Eu, Ho}$ and $x = 0.05; 0.20$.

All the compositions were prepared using the high temperature solid-state process. The calcination as well as the sintering of the samples were carried out respectively at 1180 °C and 1400 °C. X-ray diffraction analysis at room temperature as well as Raman spectroscopy analyses revealed a perovskite-like phase. The influence of temperature and frequency on the real relative permittivity and dielectric losses revealed a classical or relaxor ferroelectric behavior depending on the zirconium content. On the other hand, it turns out that classical ferroelectric materials exhibit quadratic symmetry while relaxors are distinguished by cubic symmetry. Physical and structural models [4] corroborate this correlation. From an application point of view, some compositions exhibit maximum real relative permittivities near room temperature and seem to be promising candidates to replace the lead-based materials currently used in industry.

References

- [1] N. Setter, D. Damjanović, L. Eng, G. Fox, S. Gevorgian, S. Hong, A. Kingon, H. Kohlstedt, N. Y. Park, G. B. Stephenson, I. Stolitchnov, A. K. TagansteV, D. V. Taylor, T. Yamada, S. Streiffer, *J. Appl. Phys.*, **100**, 051606 (2006).
- [2] J. F. Scott, *Science*, **315**, 954 (2007)
- [3] Directive 2011/65/EU of the European Parliament and of the Council of 8 June 2011 on the Restriction of the Use of Certain Hazardous Substances in Electrical and Electronic Equipment Text with EEA Relevance (2011).
- [4] L. E. Cross, Relaxor ferroelectrics an overview, *Ferroelectrics*, **151**, 305 (1994)

Electrocrystallisation of ternary amalgams

D. Kraut¹, C. Hoch^{1*}

¹ University of Munich (LMU), Department of Chemistry, Butenandtstraße 5-13, 81377 Munich, Germany

* The corresponding author e-mail: constantin.hoch@uni-muenchen.de

Keywords: electrocrystallisation; amalgams; polar metals; ternary; sodium; potassium; mercury

Mercury-rich amalgams of electropositive metals are suitable model systems for the investigation of polar metals. The combination of ionic, covalent, and metallic bonding is typical for polar intermetallics and results in ‘bad metal behaviour’. This term expresses the physical properties resulting from low concentration of free charge carriers together with very small mean free path lengths. It allows for exotic combinations of properties which play a role in thermoelectrics, data storage materials and others.

The number of mercury-rich amalgams is scarce. This is due to the preparational difficulty of high reaction enthalpies and low decomposition temperatures. Isothermal electrocrystallisation has shown to be a successful method in overcoming these problems. [1-3] Whereas a thermochemical approach relies on the composition of the starting materials and variation of the temperature, isothermal electrocrystallisation changes composition over time by reduction of the electropositive component out of solution into a Hg cathode. The high overvoltage of the reduction potentials for alkali metals on a mercury cathode prefers the formation of amalgam, which is also used technically in the amalgam process. With electrocrystallisation formation of amalgams can be achieved under mild reaction conditions as fast as within one hour. The rate of crystallisation can be precisely controlled through the electrode potentials and the electric current applied. [4] The difficulty in producing ternary amalgams with two different electropositive metals consists in ensuring the simultaneous cathodic deposition of two metals. This can be achieved by adjusting the respective Nernst potentials via choosing suitable concentrations.

We show this procedure on the example of the first ternary amalgam synthesised by electrochemical deposition of Na and K from their iodides in DMF solution to yield a ternary sodium-potassium amalgam belonging to the Ag₁₄Gd₅₄ structure family (single crystal structure refinement, hexagonal, space group *P6*, $a = 39.547(5)$ Å, $c = 9.6777(12)$ Å, $Z = 9$).

References

- [1] F. Tambornino, J. Sappl, F. Pultar, T. M. Cong, S. Hübner, T. Gifftaler, C. Hoch, . *Inorg. Chem.*, **55**, 11551–11559 (2016)
- [2] C. Hoch, A. Simon, *Angew. Chem.*, **124**, 3316–3319 (2012)
- [3] F. Tambornino, C. Hoch, *J. Alloys Compd.*, **618**, 299–304 (2015)
- [4] J. Garche, C. Dyer, P. Moseley, Z. Ogumi, D. Rand, B. Scrosati, *Encyclopedia of Electrochemical Power Sources*, **1** (2009)

Acknowledgments

This work was supported by Deutsche Forschungsgemeinschaft (Project number 429690805).

Cs₂O as a strong oxidiser – a new synthetic route towards oxometalates

I. Zaytseva¹, C. Hoch^{1*}

¹ University of Munich (LMU), Department of Chemistry, Butenandtstraße 5-13 (D), 81377 Munich, Germany

* The corresponding author e-mail: constantin.hoch@uni-muenchen.de

Keywords: oxometalates; redox; caesium oxide; synthesis route; Ellingham; thermodynamics

There are several known ways for synthesising caesium oxometalates, e.g. via decomposition of caesium salts, by the azide nitrate route,[1] or, most commonly, from reaction with caesium oxides.[2-5] Most of those use transition metal oxides as starting material and need high reaction temperatures.

However, reactions of pure caesium oxide with elemental transition metals also result in caesium metalates at much lower temperatures. This was first observed for the reaction of caesium oxide with tantalum at 300 °C, yielding Cs₃TaO₄ and elemental caesium. Obviously, Cs⁺ in Cs₂O takes the role of a strong oxidising agent.

This counter-intuitive reaction is easily explained by Ellingham diagrams[6], which are commonly used in metallurgy and stability calculations.[7] They chart the thermodynamic stability of metal oxides ΔG^0 dependent on the partial pressure of oxygen against the temperature.[8] Therefore, a metal oxide with higher ΔG^0 can be reduced by any of the more stable oxides with lower ΔG^0 . The steep gradient of the Cs₂O line explains the unusual reaction of tantalum and suggests further possible syntheses of new caesium-rich metalates.

Until now, reactions of transition metals or lanthanides with Cs₂O (4:1, 650 °C) have resulted in several new compounds: Cs₃M^VO₄ ($M = V$, [9] Nb, Ta) in K₃NO₄ structure type; Cs₄M^I-VO₄ ($M = Ti, Zr$, [2] Hf, Ce) in Cs₃PO₄ and Cs₃ZrO₄ structure types; Cs₃M^OO₂ ($M = Cu, Ni, Co$) in Cs₃AuO₂ structure type; Cs₂Ce^{IV}O₃, Cs₁₄Sc^{III}O₁₃ in K₁₄Fe₄O₁₃ structure type; as well as reported oxometalates and suboxometalates: Cs₇Cr₂^{IV/VO}₈, [10] Cs₆Si₃^{IV}O₉, [3] Cs₆Mn₂^{III}O₆, [1] Cs₆Fe₂^{II}O₅, [4] Cs₄Zn^{II}O₃, [5] Cs₉M^{III}O₄ [11] ($M = Fe, In, Al$) in Cs₉InO₄ structure type. Further reactions of transition metals and main group elements are being investigated.

References

- [1] J. Nuss, R. K. Kremer, G. S. Thakur, M. Jansen, *Z. Anorg. Allg. Chem.*, **645**, 50–56 (2019)
- [2] T.-M. Chen, J. D. Corbett, *Z. Anorg. Allg. Chem.*, **553**, 50–56 (1950)
- [3] C. Hoch, C. Röhr, *Z. Naturforsch. B*, **56**, 423–430 (2001)
- [4] H. P. Müller, R. Hoppe, *Z. Anorg. Allg. Chem.*, **619**, 193–201 (1993)
- [5] C. Hoch, *Z. Naturforsch. B*, **66**, 1248–1249 (2011)
- [6] H. J. T. Ellingham, *J. Soc. Chem. Ind.*, **63**, 125 (1944)
- [7] T. B. Lindemer, T.M. Besmann, C.E. Johnson, *J. Nucl. Mater.*, **100**, 178–226 (1981)
- [8] T. B. Reed, *Free Energy of Formation of Binary Compounds*, MIT Press, Cambridge, MA (1972)
- [9] C. Hoch, C.Z. Solano, *Z. Kristallogr. Suppl.*, **39**, 92 (2019)
- [10] J. Bender, A. Wohlfart, C. Hoch, *Z. Naturforsch. B*, **65**, 1416–1426 (2010)
- [11] C. Hoch, J. Bender, A. Simon, *Angew. Chem. Int. Ed.*, **48**, 2415–2417 (2009)

Acknowledgments

IZ acknowledges support by DFG under grant number 444769550.

Novel representatives of the structure type Na_7RbTl_4 with the lighter homologue indium

M. Janesch¹, S. Gärtner²

¹ Department of Inorganic Chemistry University of Regensburg, Universitätsstr. 31, 93053 Regensburg (Germany);

² Department for X-Ray Structure Analysis, Central Analytics University of Regensburg, Universitätsstr. 31, 93105 Regensburg (Germany);

* The corresponding author e-mail: Stefanie.Gaertner@ur.de, Tel.: +49 941 943 4446

Keywords: indium; alkali metals; Zintl ions; single crystal X-Ray analysis

Indium in its formally positive oxidation states finds many applications in contemporary and emerging technology, such as in displays of various kinds, solar cells, electrochromic devices and heatable glass. There it is mostly present as ITO (indium tin oxide), which can be coated as a thin film with optical transparency and electrical conductivity.

In contrast, the investigation of indium in its formally negative oxidation states is not yet that sophisticated. To realize these formally negative oxidation states in solid state materials, the combination of electropositive elements like alkali metals with the triel is necessary. In this context it was recently shown for the heavier homologue thallium, that the role of the alkali metals goes far beyond simple charge balancing but can realize (novel) anionic substructures. [1,2]

In the electron poor part of the $A:\text{In}$ ($A = \text{Na}, \text{K}, \text{Rb}, \text{Cs}$) system only NaIn and Na_2In are known so far. In NaIn the Na- and the In-atoms form a diamond-like substructure whereas in Na_2In isolated $[\text{In}_4]^{8-}$ -clusters are present. These two alkali metal indies are isostructural to the heavier homologues NaTl [3] and Na_2Tl [4]. In this analogy it was possible to synthesize $\text{Na}_7\text{K-In}_4$ ($a = 16.3429(4) \text{ \AA}$, $b = 16.3388(3) \text{ \AA}$, $c = 11.3096(3) \text{ \AA}$), which is isostructural to the structure type Na_7RbTl_4 . [2] Here, the orthorhombic space group of the binary Na_2Tr ($C222_1$) changed in the ternary materials Na_7ATr_4 ($A = \text{K}, \text{Rb} \ \& \ \text{Tr} = \text{In}, \text{Tl}$) to the orthorhombic space group $Pbam$. The stacking sequence for the $[\text{In}_4]^{8-}$ -tetrahedra (ABAB) in the binary Na_2In can be derived from the hexagonal closed packing (hcp), which is reasonable as the space group $C222_1$ is a subgroup of $P6_3/mmc$. With the incorporation of the bigger alkali metal potassium the stacking sequence of the $[\text{In}_4]^{8-}$ -tetrahedra changes to ABCABC, which is related to the cubic closed packing (ccp). This also changes the coordination sphere of the isolated $[\text{In}_4]^{8-}$ -clusters. Whereas in Na_2In 23 sodium atoms are arranged around a tetrahedron in the ternary Na_7KIn_4 only 21 alkali metals are observed surrounding $[\text{In}_4]^{8-}$.

References

- [1] S. Gärtner, *Crystals*, **10**, 1013 (2020)
- [2] V. F. Schwinghammer, M. Janesch, N. Korber, S. Gärtner, *ZAAC*, e202200332 (2022)
- [3] E. Zintl, W. Dullenkopf, (1932)
- [4] D. A. Hansen, J. F. Smith, *Acta Cryst.*, **22**, 836 (2022)

Acknowledgments

This research was funded by the Promotionsanschubstipendium of the Frauenförderung of the University of Regensburg.

High-pressure Synthesis of Alkaline Metal Niobates with Tetragonal Tungsten Bronze-type Structure

P08

K. Murase¹, T. Sato¹, A. Yamamoto^{1*}, K. Sugiyama²

¹ Graduate school of Sci. Eng. Shibaura Ins. Tech., 337-8570, Saitama, Japan

² Ins. Mat. Res., Tohoku Univ., 980-8501, Sendai, Japan.

* The corresponding author e-mail: ayako@shibaura-it.ac.jp

Keywords: high-pressure synthesis; tetragonal tungsten bronze-type; alkaline metal niobate; ferroelectrics

Several alkaline metal niobates, *e.g.* LiNbO₃, NaNbO₃, and KNbO₃, show ferroelectricity by the displacement of Nb from the ideal position in NbO₆ octahedra. In the K-Nb-O system, not only KNbO₃ perovskite but also K₆Nb_{10.8}O₃₀ tetragonal tungsten bronze (TTB, cf. **Fig. 1a**) show ferroelectricity [1].

To induce stronger lattice distortion that leads to higher ferroelectricity, we prepared Rb substitutions of K-Nb-O by the high-pressure method. This method should be effective in shrinking the relatively large ionic size of Rb⁺ ($r = 1.72\text{\AA}$, cf. $r = 1.64\text{\AA}$ in K⁺).

We obtained both RbNbO₃ perovskite (another presentation in this conference) and Rb_{6-x}Nb_{10+y}H_zO₃₀ TTB those diffraction pattern is similar to the ambient phase of K₆Nb_{10.8}O₃₀ (**Fig. 1b**). Here, we report the phase stability, crystal structure and physical properties of Rb-Nb-O TTB phase. The structure of the TTB phase was determined by the single-crystal X-ray diffraction analysis, suggesting the deficiency in Rb, excess in Nb, and existence of H, that could be notated in Rb_{6-x}Nb_{10+y}H_zO₃₀. We also prepared (K, Rb)-Nb-O and (K, Rb, Li)-Nb-O phases by the high-pressure method, and the TTB structure looks stable by adding Li. Details will be reported in the presentation.

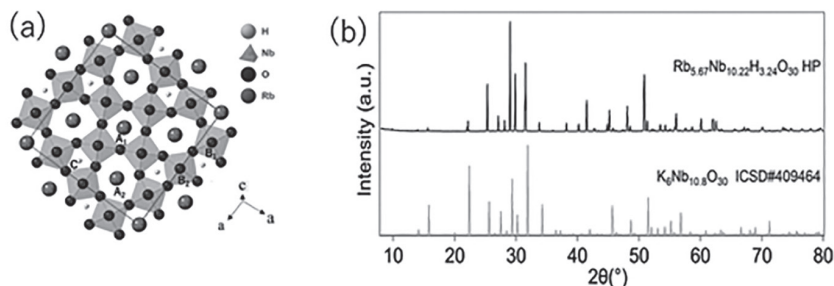


Figure 1: (a) Crystal structure model of TTB-type Rb_{6-x}Nb_{10+y}H_zO₃₀ (b) XRD patterns of high pressure(HP) phase of Rb_{6-x}Nb_{10+y}H_zO₃₀ and K₆Nb_{10.8}O₃₀

References

- [1] P. Becker, P. Held, *Z. Kristallogr.* NCS, 215, 319–320 (2000).

Acknowledgments

This work was supported by the Kazuchika Okura Memorial Foundation, Japan, and GIMRT program (202112-RDKGE-0008) of Institute of Materials Research, Tohoku University, Japan.

Anion redox in lithium main-group metal oxides

Z. Chen¹, S. Mahato¹, X. M. De Irujo Labalde¹, M. Hayward¹

¹ Department of Chemistry, University of Oxford, Inorganic Chemistry Laboratory, OX1 3QR *

* The corresponding author e-mail: zizhen.chen@chem.ox.ac.uk

Keywords: Li-ion cathode materials; energy storage; topochemical anion-redox; main-group oxides

Cathode materials for lithium-ion batteries have been intensively studied, with a focus on the use of transition-metal redox states to store energy¹. However, many of the transition-metals which are widely used in cathodes materials are scarce or expensive, if not both, so there is a strong motivation to explore other redox couples in cathode materials.

Recently, we have observed that lithium can be chemically extracted from main-group oxides which contain no oxidizable transition-metal cations. These observations suggest extensive anion-redox chemistry is occurring. The structures and redox chemistry of a series of these phases (LiEO_x) will be described.

References

- [1] S. Booth, A. Nedoma, N. Anthonisamy, P. Baker, R. Boston, H. Bronstein, S. Clarke, E. Cussen, V. Daramalla, M. De Volder, S. E. Dutton, V. Falkowski, N. Fleck, H. Geddes, N. Gollapally, A. Goodwin, J. Griffin, A. Haworth, M. Hayward, S. Hull, B. Inkson, B. Johnston, Z. Lu, J. MacManus-Driessell, X. Martínez De Irujo Labalde, I. McClelland, K. McCombie, B. Murdock, D. Nayak, S. Park, G. Pérez, C. Pickard, L. Piper, H. Playford, S. Price, D. Scanlon, J. Stallard, N. Tapia-Ruiz, A. West, L. Wheatcroft, M. Wilson, L. Zhang, X. Zhi, B. Zhu, and S. Cussen, *APL Materials* **9**, 109201 (2021)

Acknowledgements

This work was supported by the Dept. of Chemistry, University of Oxford.

Synthesis and characterisation of lanthanum zirconate as a candidate filler material for polymer derived ceramic coatings

P. N. Moghaddam¹, M. Parchovianský¹, I. Parchovianská¹, A. Pakseresht¹

¹ FunGlass, Alexander Dubček University of Trenčín, Študentská 2, 911 50 Trenčín

* The corresponding author e-mail: parisa.moghaddam@tnuni.sk

Keywords: solid state synthesis; lanthanum zirconate; polymer derived ceramics; thermal stability; differential scanning calorimetry

Polymer derived ceramics (PDCs) is an appropriate material for preparing protective coatings due to their excellent oxidation and corrosion resistance at elevated temperatures [1]. However, the primary challenge of this approach is the remarkable shrinkage during polymer-to-ceramic conversion. One way to compensate for high volume shrinkage is to add suitable filler particles in the coating slurry. In addition, fillers can be utilized to adjust and improve the thermal and structural stability of PDC coatings. In this work, $\text{La}_2\text{Zr}_2\text{O}_7$ (LZ) powder has been selected as a promising filler material for PDC coatings because of its excellent thermal stability, high melting point (2300 °C), and low thermal conductivity [2]. For this purpose, LZ ceramic powder was synthesized by high temperature solid state reaction (SSR) using commercial La_2O_3 and ZrO_2 oxides. The synthesized LZ powder was heat-treated at 1400 °C for 6 h and some properties, such as powder morphology, chemical composition, crystal structure and thermal stability, were investigated after high temperature treatment. A single pyrochlore phase of $\text{La}_2\text{Zr}_2\text{O}_7$ was detected by X-ray diffraction analysis (XRD) after annealing at 1400 °C. Scanning electron microscopy (SEM) of synthesized powder illustrated homogenous dispersion, sphere-like shape and nanoscale particle size of the powder. The thermal behaviour and phase stability of the LZ powder were studied by differential scanning calorimetry (DSC) in the temperature range of 25 °C–1300 °C. The endothermic and exothermic peaks were not presented in the tested temperature range, proving the significant phase stability of $\text{La}_2\text{Zr}_2\text{O}_7$.

References

- [1] Q. Wen, Z. Yu, R. Riedel, *Progress in Materials Science*, **109**, 100623 (2020).
- [2] J. Zhang, X. Guo, Y. G. Jung, L. Li, & J. Knapp, *Surface and Coatings Technology*, **323**, 18-29 (2017).

Acknowledgments

This paper was created in the frame of the project Centre for Functional and Surface Functionalised Glass (CEGLASS), ITMS code 313011R453, operational program Research and innovation, co-funded from European Regional Development Fund. This work is a part of dissemination activities of project FunGlass. This project has received funding from the European Union's Horizon 2020 research and innovation programme under grant agreement No 739566. The authors also gratefully acknowledge the financial support from the project VEGA no. 1/0171/21.

Investigation of structure and luminescence properties of bismuth-based coordination polymers with N-donor ligands

K. V. Borysova¹, J. R. Sorg², E. A. Mikhalyova¹, K. Müller-Buschbaum^{1,2}

¹ Institute of Inorganic and Analytical Chemistry, Justus-Liebig-University Giessen, Heinrich-Buff-Ring 17, 35392 Giessen, Germany;

² Institute of Inorganic Chemistry, Julius-Maximilians-University Würzburg, Am Hubland, 97074 Würzburg, Germany

* The corresponding author e-mail: Kateryna.Borysova@anorg.chemie.uni-giessen.de

Keywords: bismuth; bismuth halides; N-donor ligands; triazine derivatives; 4-cyanopyridine; coordination polymers; melt synthesis; luminescence; charge transfer

Coordination compounds and polymers (CPs) based on bismuth are attracting wide attention due to their low toxicity and a wide range of potential applications [1].

Relatively recent works have been dedicated to the study of the luminescence properties of such compounds [2], as well as reported possibility of their doping with trivalent lanthanides ions, which are the basis of emissive materials [3]. Hence, this clearly demonstrates the prospects for research in this area.

In this work coordination polymers (CPs) of bismuth halides (chloride or bromide) with N-donor ligands, such as 4-cyanopyridine and triazine derivatives are presented.

All compounds were prepared by melt synthesis utilizing a reagent in molten form under reduced pressure and inert conditions.

According to single-crystal X-ray diffraction data, CPs with a 4-cyanopyridine ligand are one-dimensional structures connected by halide bridges. Compounds with triazine derivatives form network structures of two-dimensional coordination polymers.

For all coordination compounds presented, the luminescence properties were determined by photoluminescence spectroscopy at 77K and room temperature. Bismuth CPs with chloride and bromide ligands with 4-cyanopyridine emit in the blue-green region of the visible spectrum. The luminescence of these CPs result from ligand-to-metal and metal-to-ligand charge-transfer processes. The difference in position of the maxima in both emission and excitation spectra can be explained by the influence of different halide anions, as described in previous studies [2].

Coordination compounds with triazine derivatives have similar luminescence properties with abovementioned dependencies.

References

- [1] R. Mohan, *Nat. Chem.*, **2**, 336–336 (2010)
- [2] J. R. Sorg, T. Wehner, P. R. Matthes, R. Sure, S. Grimme, J. Heine, K. Müller-Buschbaum, *Dalton Trans.*, **47**, 7669–768 (2018)
- [3] J. Heine, T. Wehner, R. Bertermann, A. Steffen, K. Müller-Buschbaum, *Inorg. Chem.*, **53**, 7197–7203 (2014)

Acknowledgments

The authors gratefully acknowledge the Deutsche Forschungsgemeinschaft for funding of the project MU-1562/16-1 and the Fonds der Chemischen Industrie (FCI) for a PhD scholarship for Jens Sorg.

Tin-Boroxines-Based Inorganic-Organic Macrocycles: Synthesis, Characterization and Hydrophobicity

P12

M. Novák¹, M. Bouška², Š. Podzimek³, R. Jambor⁴

¹ Institute of Chemistry and Technology of Macromolecular Materials, Faculty of Chemical Technology, University of Pardubice, Studentská 573, 53210 Pardubice, Czech Republic;

² Department of Graphics Arts and Photophysics, Faculty of Chemical Technology, University of Pardubice, Studentská 573, 53210 Pardubice, Czech Republic;

³ Synpo, Ltd., S.K. Neumannova 1316, 53207 Pardubice, Czech Republic;

⁴ Department of General and Inorganic Chemistry, Faculty of Chemical Technology, University of Pardubice, Studentská 573, 53210 Pardubice, Czech Republic

* The corresponding author e-mail: miroslav.novak@upce.cz

Keywords: tin; boroxine; metal-organic framework; hydrophobicity; thin layer

Recently, a great attention has been focused on the development of hydrophobic coatings. In addition to the traditional materials such as silanes and silicones, inorganic-organic hybrid materials that combine the mechanical properties and the thermal stability of the inorganic component with the flexibility, ductility and processability of the organic component are currently being studied.

Recently, we have reported the synthesis of N→M intramolecularly coordinated tin-boroxines (SnBOs) having the central six membered ring SnB₂O₃. [1] Advantage of suggested SnBOs is their facile synthesis, so variety of functional groups may be easily introduced and some functional groups may be even further modified. Our preliminary tests demonstrated that peripheral CH = O formyl group reacts easily with an amine RNH₂ affording a Schiff base.

Based on this study, we report here the synthesis SnBOs-based macrocycles by Schiff-coupling of appropriate L(Ph)Sn(O₃B₂(4-CH = O-C₆H₄)₂), where L = {2,6-(Me₂NCH₂)-C₆H₃}⁻, with various diamines such as 1,4-benzenediamine, ethylenediamine or amine-terminated siloxanes. The synthesized materials were used for the preparation of thin layer on the silicon wafer by the spin-coating method. The surfaces of layers were studied using IR, SEM to check the morphologies of the layers and also by energy-dispersive X-ray EDX to determined thickness, the refractive index and to prove the presence of main group metals in the thin films. Finally, the hydrophobicity of surfaces was determined using contact angle measurements of water droplet.

References

- [1] B. Mairychová, I. V. Kityk, A. Maciag, F. Bureš, M. Klikar, A. Růžička, L. Dostál, R. Jambor. *Inorg. Chem.* **55**, 15 (2016); b) M. Kořenková, B. Mairychová, A. Růžička, R. Jambor, L. Dostál, *Dalton Trans.*, 43, 7096 (2014); c) Y. Milasheuskaya, J. Schwarz, L. Dostál, Z. Růžičková, M. Bouška, Z. Olmrová Zmrhalová, T. Syrový, R. Jambor, *Dalton Trans.*, **50**, 18164 (2021).

Acknowledgments

This work was supported by the Czech Science Foundation (23-06548S).

High-Pressure Synthesis of SmSi_3

T. Neziraj¹, S. Wirth¹, Y. Grin¹, U. Schwarz¹

¹ Max-Planck Institut für Chemische Physik fester Stoffe, Nöthnitzer Str. 40, 01187 Dresden

* The corresponding author e-mail: schwarz@cpfs.mpg.de

Keywords: high pressure; silicon; samarium; van Vleck paramagnetism; antiferromagnetic ordering

The semiconducting elements silicon or germanium form a rich variety of binary phases and new structural patterns with rare-earth metals when high pressure is applied for synthesis [1-3]. The high-pressure phases often show unique silicon arrangements with unusual coordination numbers and environments [4]. Often, the enhanced coordination in the covalent partial structure gives rise to novel bonding behavior that frequently goes beyond classical 8-N scenarios. According to the Sm-Si phase diagram, synthesis at ambient pressure yields SmSi_{2-x} as the silicon-richest phase. In an effort to realize an increased number of Si-Si contacts, silicon-rich phases need to be synthesized at high-pressure and then quenched. In this study, we describe the high-pressure and high-temperature synthesis of the new compound SmSi_3 , as well as report the crystal structure and magnetic properties.

The metastable binary samarium trisilicide is obtained at a pressure of 9.5 GPa and a temperature of 1100 K. At ambient pressure, the compound decomposes exothermally at approximately 650 K into Si and SmSi_{2-x} . Single crystal data refinements reveal that the crystal structure of the compound is isotopic to that of YbSi_3 [5].

The magnetic susceptibility $\chi(T) = M/H$ of polycrystalline sample SmSi_3 measured in an external field of 0.5 T between 1.8 and 350 K, indicates van Vleck-type paramagnetic behavior and antiferromagnetic ordering at very low temperatures (Fig. 1). Fits to the magnetic data show a small effective magnetic moment (μ_{eff}) at low T.

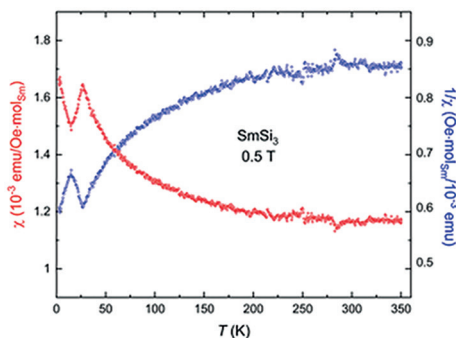


Figure 1:
Magnetic susceptibility
of SmSi_3 vs temperature.

References

- [1] U. Schwarz, A. Wosylus, H. Rosner, W. Schnelle, A. Ormeci, K. Meier, A. Baranov, M. Nicklas, S. Leipe, C. J. Müller, Yu. Grin, *J. Am. Chem. Soc.*, 134, 13558–13561 (2012).
- [2] T. Nishikawa, H. Fukuoka, K. Inumaru, *Inorg. Chem.*, 54, 7433–7437 (2015).
- [3] T. Neziraj, K. Meier-Kirchner, W. Schnelle, S. Wirth, Yu. Grin, U. Schwarz, *Z. Naturforsch. B*, 4-5, 323-329 (2022).
- [4] J. M. Hübner, W. Carrillo-Cabrera, Yu. Prots, M. Bobnar U. Schwarz, Yu. Grin, *Angew. Chem. Int Ed.*, 58, 12914-12918 (2019).
- [5] A. Wosylus, Yu. Prots, U. Schwarz, *Z. Kristallogr.*, 226, 295-296 (2011).

Mixed-metal monophosphate tungsten bronzes containing divalent transition metal ions (M^{II} : Fe, Co, Ni) and tungsten(VI)

L. K. Aymans*, R. Glaum

Institut für Anorganische Chemie, Rheinische Friedrich-Wilhelms-Universität Bonn, Gerhard-Domagk-Straße 1, 53121 Bonn (Germany)

* The corresponding author e-mail: s6lkschm@uni-bonn.de

Keywords: MPTB; mixed-valency; solid state synthesis; MMCT; metastable solids

RAVEAU and co-workers discovered in 1981 the first monophosphate tungsten bronze (MPTB) $W_8P_4O_{32}$ [1]. The formula might be re-written as $(WO_3)_{2m}(PO_2)_4$ ($m = 4$) to emphasize the width of ReO_3/WO_3 -like layers separated by phosphate groups. Since then the family of mixed-valent tungsten phosphate bronzes has been extended with more and more complex compositions (see reviews [2,3]). However, only recently the possibility for substitution of W^{5+} in the MPTBs by appropriate mixed-metal combinations was discovered (e.g. $(M^{III}_{1/3}W^{VI}_{2/3})OPO_4$ with M^{III} : V, Cr, Fe, Mo, instead of W^VOPO_4 [4]; $(M^{III}_{4/3}W^{VI}_{20/3})O_{24}(PO_2)_4$ with M^{III} : V, Cr, Fe, Rh, Ir [5,6] instead of $W_8O_{24}(PO_2)_4$ [1]) The discovery of these so-called mixed-metal monophosphate tungsten bronzes (mm-MPTBs) led to a whole new family of catalyst materials for selective oxidation of short-chain hydrocarbons [7]. Here we report on synthesis and characterization of oxide-phosphates $(M^{II}W^{VI}_7)O_{24}(PO_2)_4$ (M^{II} : Fe, Co, Ni) with substitution of W^V by $(M^{II}_{1/4}W^{VI}_{3/8})$ in the MPTB at $m = 4$.

Powders of $(Ni^{II}W^{VI}_7)O_{24}(PO_2)_4$ (light-green) and $(Co^{II}W^{VI}_7)O_{24}(PO_2)_4$ (dark-brown) were obtained via solution combustion synthesis [8] followed by annealing of the combustion product in air with stepwise rising temperature ($T_{max} = 800$ °C for the nickel and 700 °C for the Co compound). Pale turquoise powders of the precursor of nominal composition “ $Fe^{III}_{2/3}W^{VI}_7O_{24}(PO_2)_4$ ” (SCS in air, 800 °C) were reduced by iron in sealed silica ampoules at 800 °C yielding dark-blue $(Fe^{II}W^{VI}_7)O_{24}(PO_2)_4$, due to a strong MMCT transition $Fe^{2+} \rightarrow W^{6+}$. Crystals of $(Ni^{II}W^{VI}_7)O_{24}(PO_2)_4$ suitable for SXRD analysis were obtained by chemical vapour transport (900 \rightarrow 700 °C, transport agent Cl_2). $(Ni^{II}W^{VI}_7)O_{24}(PO_2)_4$ shows in contrast to the orthorhombic symmetry of the pure MPTB a minute monoclinic distortion. Its crystal structure refinement ($P2_1$, $Z = 1$, $a = 6.5021(3)$ Å, $b = 5.2255(2)$ Å, $c = 17.3855(7)$ Å, $\beta = 90.162(3)^\circ$, $R1 = 0.0517$, $wR2 = 0.157$, 1896 params., 123 variables) confirmed the anticipated ratio Ni/W and shows mixed occupancy Ni/W only for the two metal sites coordinated by one phosphate group (plus five oxide ions). In contrast, the two metal sites coordinated to three PO_4 tetrahedra (plus three O^{2-}) are occupied exclusively by W. Details on synthesis, crystallographic characterization and optical spectra of the new mm-MPTBs will be reported.

References

- [1] J. P. Giroult et al., *Acta Crystallogr.* **B37**, 2139–2142 (1981).
- [2] C. Hess et al., *Solid State Comm.* **104**, 663–668 (1997).
- [3] P. Roussel et al., *Acta Crystallogr.* **B57**, 603–632 (2001).
- [4] S. C. Roy et al., *Z. Naturforsch.* **B71**, 543–552 (2016).
- [5] S. C. Roy, PhD Thesis, University of Bonn (2015).
- [6] A. Karbstein et al., *Eur. J. Inorg. Chem.* 1459–1469 (2021).
- [7] R. Machado et al., *ACS Catalysis* (2022). <https://doi.org/10.1021/acscatal.2c02645>.
- [8] a) A. Varma et al., *Chem. Rev.* **116**, 14493–14586 (2016); b) K. C. Patil et al., in *Chemistry of nano-crystalline oxide materials*, World Scientific, Singapore, vol. 1, pp. 42–60 (2008).

Amino acid crystals as high-performance, eco-friendly structural health monitors

K. Hari¹, S. Bhattacharya², S. Guerin^{1,2*}

¹ Department of Physics, Bernal Institute, University of Limerick;

² SSPC, SFI Research Centre for Pharmaceuticals, Bernal Institute, University of Limerick

* *The corresponding author e-mail: sarah.guerin@ul.ie*

Keywords: piezoelectric materials; amino acids; polycrystalline films; structural health monitoring; crystallisation

Amino acids are the simplest biological units and are inexpensive and easy to crystallise and demonstrate measurable piezoelectricity in single crystal and polycrystalline forms [1,3,4]. The piezoelectric voltages produced under an applied force are inversely proportional to the dielectric constant of the material and so even ‘weak’ organic piezoelectrics [2] can generate large voltages in response to strain.

Recently, we have experimentally validated flexible glycine-based sensors for pipe leak detection and monitoring in real-time, for a variety of flow rates and leak sizes using a custom fluid test rig developed for the validation of PVDF patches [5]. This is the first time that glycine crystals have been grown and characterised as a high-concentration, polycrystalline aggregate for piezoelectric sensing [6]. However, a key limitation is that the piezoelectric response of the film was less than that of glycine single crystals due to the random orientation of glycine crystallites.

In this work, we will investigate and optimise different parameters to modulate the piezoelectric response and increase the detection sensitivity and voltage output of amino acid-based piezoelectric devices and characterise using various techniques. The study will highlight the use of low-dielectric, non-centrosymmetric biomolecular crystal films for monitoring built infra-structure systems by showing how reliably and sustainably they may be used as sensors for pipe structural health monitoring applications.

References

- [1] Vijayan, N.; Rajasekaran, S.; Bhagavannarayana, G.; Ramesh Babu, R.; Gopalakrishnan, R.; Palani-chamy, M.; Ramasamy, P., Growth and characterization of nonlinear optical amino acid single crystal: L-alanine. *Crystal growth & design* 2006, 6 (11), 2441–2445.
- [2] Panda, P.; Sahoo, B., PZT to lead free piezo ceramics: a review. *Ferroelectrics* 2015, 474 (1), 128–143.
- [3] Kumar, R. A.; Vizhi, R. E.; Vijayan, N.; Babu, D. R., Structural, dielectric and piezoelectric properties of nonlinear optical γ -glycine single crystals. *Physica B: Condensed Matter* 2011, 406 (13), 2594–2600.
- [4] Guerin, S.; Tofail, S. A.; Thompson, D., Longitudinal Piezoelectricity in Orthorhombic Amino Acid Crystal Films. *Crystal Growth & Design* 2018, 18 (9), 4844–4848.
- [5] Okosun, F.; Cahill, P.; Hazra, B.; Pakrashi, V., Vibration-based leak detection and monitoring of water pipes using output-only piezoelectric sensors. *The European Physical Journal Special Topics* 2019, 228 (7), 1659–1675.
- [6] Okosun, F.; Guerin, S.; Celikin, M.; Pakrashi, V., Flexible amino acid-based energy harvesting for structural health monitoring of water pipes. *Cell Reports Physical Science* 2021, 2 (5), 100434.

Acknowledgments

This research is funded by Science Foundation Ireland under award 21/PATH-S/9627.

High temperature magnetic ordering in new quadruple perovskites $\text{Sr}_4\text{NaM}_3\text{O}_{12}$ ($\text{M} = \text{Ru}$ and Os)

P16

G. S. Thakur^{1,2*}, T. Doert¹, T. Hansen³, E. Osmic⁴, W. Schnelle⁵, T. Herrmannsdörfer⁴, M. Ruck^{1*}

¹ Faculty of Chemistry and Food Chemistry, Technical University, Bergstr. 66, 01069 Dresden, Germany;

² Würzburg–Dresden Cluster of Excellence 'ct.qmat';

³ Institut Laue-Langevin, 71 avenue des Martyrs, 38000 Grenoble, France;

⁴ High Field Magnetic Laboratory Dresden (HLD-EMFL), Helmholtz Center Dresden-Rossendorf, D-01328 Dresden, Germany, Max-Planck-Institute for Chemical Physics of Solids, Nöthnitzerstr. 40, 01187 Dresden, Germany

* The corresponding author e-mail: gohil_singh.thakur@tu-dresden.de, Michael.ruck@tu-dresden.de

Keywords: magnetism; ordered perovskites; high-temperature ordering; $4d/5d$ oxides; exchange bias

Magnetism is technologically most important functional property arising from electron interactions. $4d$ and $5d$ systems show strong SOC effects which results in interesting physical properties like Mott insulation and ferromagnetism, metal-insulator transition and superconductivity. [1-4] However, correlated magnetism is less common in these systems due to small Coulomb parameters (U) and large bandwidths (W) leading to stronger hybridization between the metal d orbitals and the O $2p$ orbitals. In fact, among the $4d$ -oxide systems, mostly those containing Ru exhibit long-range ordered magnetism. [2,5,6] Among $5d$ systems, Os oxides have shown to exhibit high magnetic ordering temperatures. [7,8] Here we present, two new isostructural compounds of the series $\text{Sr}_4\text{NaM}_3\text{O}_{12}$ ($\text{M} = \text{Ru}$ and Os) which crystallize in a regular perovskite structure with only corner-sharing connectivity and 1:3 ordering of Na and M atoms on the B-sites. The Ru compound shows long range AFM ordering near room temperature ($T_N \sim 270$ K). The Os compound is ferri-magnetic in nature with a high T_C of 337 K. More interestingly, a giant exchange bias like shift of ~ 3.75 T accompanied by a large coercivity of upto 4.3 T is observed. Both the compounds are semiconductors.

References

- [1] Y. Maeno, H. Hashimoto et al, *Nature* **372**, 532–534 (1994).
- [2] A. Callaghan, C. W. Moeller and R. Ward, *Inorg. Chem.* **5**, 1572–1576 (1966).
- [3] Y. G. Shi, Y. F. Guo, S. Yu, et al, *Phys. Rev. B* **80**, 161104 (2009).
- [4] B. J. Kim, H. Ohsumi, T. Komesu, S. Sakai et al, *Science* **323**, 1329 (2009).
- [5] C. I. Hiley, D. O. Scanlon, A. A. Sokol, et al, *Phys. Rev. B* **92**, 104413 (2015).
- [6] W. Schnelle, B. E. Prasad, C. Felser, *Phys. Rev. B* **103**, 214413(2021).
- [7] G. S. Thakur, T. Doert, W. Schnelle and M. Jansen, *Cryst. Growth Des.* **2**, 2459–2464 (2021).
- [8] G. S. Thakur, T. C. Hansen, W. Schnelle et al, *Chem. Mater.* **34**, 4741–4750 (2022).

Effect of concentration of conductive polymers in zinc-pigmented epoxy-ester based anticorrosive coatings

Y. Raycha, M. Kohl, A. Kalendová

Faculty of Chemical Technology, University of Pardubice,
Studentská 573, CZ-532 10 Pardubice, Czech Republic

* The corresponding author e-mail: yash.raycha@student.upce.cz

Keywords: anticorrosive pigment; conductive polymer; polyaniline; zinc; corrosion

Zinc-containing organic coatings are frequently employed to preserve metals, especially steel constructions. For both financial and environmental reasons, it is sought after to find ways to lower the zinc concentration of coating materials. The concentration of zinc put into the coating composition determines how well a zinc coating performs in terms of protecting metal. Cathodic protection and barrier protection mechanisms of zinc pigment provide corrosion prevention, but sufficient zinc dose must be maintained. This work focuses on creating extremely effective zinc coatings for good anticorrosion protection and mechanical performance because lower zinc dosages are insufficient to achieve cathodic protection and much higher concentrations create pores in the film that influence corrosion. [1-3] The goal of the current work is to investigate how zinc powder and conductive polymers affect the effectiveness of epoxy-ester resin-based anticorrosive coatings. Nontoxicity, high stability, electric conductivity, and redox potential are advantages of conductive polymers. [4] Physical-chemical techniques were used to create and characterize the polyaniline salts. Organic coverings with zinc content and containing the polyaniline salts were then produced. In order to evaluate the coatings' mechanical and corrosion resistance, they underwent accelerated corrosion tests as well as mechanical tests. By using linear polarization, the organic coatings' resistance to corrosion was also investigated. The findings of mechanical testing, accelerated corrosion tests, and linear polarization studies show that the type of polyaniline salts and the pigment volume concentration have an impact on the properties of organic coatings. The crucial discovery is that the usage of polyaniline salts in zinc-containing coatings was advantageous.

References

- [1] Z. Li, H. Bi, C.E. Weinell, G. Ravenni, L. Benedini, K. Dam-Johansen, *Progress in Organic Coatings*, **178** 107477 (2023).
- [2] A. Meroufel, S. Touzain, *Progress in Organic Coatings*, **59(3)** 197–205 (2007).
- [3] Y. Li, G. Ravenni, H. Bi, C.E. Weinell, B. Ulusoy, Z. Zhang, K. Dam-Johansen, *Progress in Organic Coatings*, **158** 106351 (2021).
- [4] J.W. Schultze, H. Karabulut, *Electrochimica Acta*, **50** 1739–1745 (2005).

Acknowledgments

Authors appreciate financial support from grant LM2023037 from the Ministry of Education, Youth and Sports of the Czech Republic.

Oligothiophene dendron-modified CdS nanoparticles and their optical properties

P18

A. Yoshida², R. Nozawa², Y. Sakagami⁴, M. Matsubara^{2,3}, A. Mori⁴, A. Muramatsu^{1,2}, K. Kanie^{1,2}

¹ SRIS, Tohoku University, Sendai City, Miyagi 980-8577, Japan;

² IMRAM, Tohoku University, Sendai City, Miyagi 980-8577, Japan;

³ National Institute of Technology, Sendai College, Natori City, Miyagi, 981-1239, Japan;

⁴ Graduate school of Engineering, Kobe University, Kobe City, Hyogo, 657-8501, Japan.

* The corresponding author e-mail: kanie@tohoku.ac.jp

Keywords: organic-inorganic hybrid materials; quantum dots; nanoparticles; dendron; optical materials

Quantum dots (QDs) are semiconductor nanoparticles showing unique tunable photoluminescence (PL) which depends on their particle size and interaction between close packed QDs. In our previous study, [1] liquid crystalline (LC) dendron-modified CdS QDs were developed. The QDs form a self-assembled structure and show a unique optical property. Among organic soft matters, an oligothiophene dendron is one of the hyper-branched dendritic organic semiconductor molecules having π -conjugated oligothiophene moieties to show controllable emission property depending on the length of the oligothiophene. In this paper, oligothiophene dendron-modified CdS QDs was synthesized to develop new functional optical materials based on an interaction between QDs and oligothiophenes.

Two types of CdS QDs were synthesized by a complex pyrolysis method as follows. Cadmium stearate, 1,1,3,3-tetramethyl thiourea, and 1-dodecanethioul (DT) were dissolved in *n*-octyl ether. The mixture was heated at 150 °C for 2 hours and at 230 °C for 3 hours. After centrifugation, DT-modified QDs (**Q**) were obtained. Oligothiophene dendron [2] (**7T**)-modified CdS QDs (**DQ**) were also prepared in the presence of equimolar **7T** and DT by the similar procedure. **Fig. 1** shows transmission electron microscopy (TEM) images of **Q** and **DQ**. The sizes of **Q** and **DQ** were 4.0 ± 0.4 and 4.2 ± 0.6 nm, respectively. **Fig. 2** exhibits the PL spectra of QDs and **7T** in toluene. **Q** showed two PL peaks at 449 and 587 nm derived from band-edge and defect-state emission, respectively. On the other hand, **DQ** showed one PL peak at the same wavelength of PL peak of **7T**. The disappearance of PL of QDs core indicates that the excitation energy was transferred from QDs to dendrons.

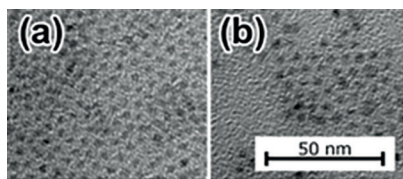
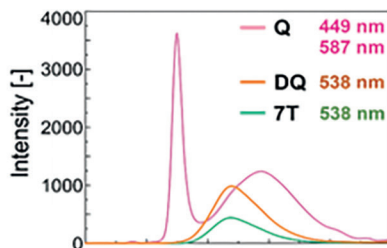


Fig. 1: TEM images of (a) **Q** and (b) **DQ**.

Fig. 2: PL spectra of QDs and **7T**. The peak positions are also listed.



References

- [1] K. Kanie, *et al. Chem.*, **2017**, 2, 860–876.
- [2] A. Mori, *et al. Chem. Eur. J.* **2013**, 19, 1658–1665.

Synthesis and characterization of glass and crystalline compositions in the $(\text{Na}_2\text{Se})_x(\text{As}_2\text{Se}_3)_{1-x}$ chalcogenide system

A. Sammoury^{1,3}, M. Kassem¹, M. Bokova¹, T. Hamieh², J. Toufaily³, E. Bychkov¹

¹ Université du Littoral Côte d'Opale, Laboratoire de Physico-Chimie de l'Atmosphère (LPCA), 189A Avenue Maurice Schumann, 59140 Dunkerque, France;

² Faculty of Science and Engineering, Maastricht University, 6200 MD, Maastricht, The Netherland;

³ Laboratory of Applied Studies for Sustainable Development and Renewable Energy (LEADDER), EDST, Lebanese University, Hariri Campus, Hadath, Lebanon

* *The corresponding author e-mail:* ali.sammoury@univ-littoral.fr; mohamad.kassem@univ-littoral.fr

Keywords: chalcogenide glass; XRD; DSC; conductivity; ball-milling; Raman

There is an enduring enigma surrounding the dissimilarities in ionic conductivity between glasses and crystals with the same chemical composition. In most cases, vitreous alloys display greater ionic conductivity, indicating that there must be variations in structural patterns between the two forms. Superionic sodium crystal conductors have three-dimensional tunnels, allowing for rapid ion migration through an unobstructed space around lattice-forming polyhedral, e.g. PX_4 or SbX_4 tetrahedra ($X = \text{S}, \text{Se}$), that possess additional cationic vacancies. In contrast, the functional characteristics of sodium vitreous alloys are heavily influenced by the order present in the glass network at short- and intermediate-ranges, which provide the foundation for preferential conduction pathways and facilitates the high ionic mobility. In this regard, $\text{Na}_2\text{Se}-\text{As}_2\text{Se}_3$ binaries serve as a valuable model to investigate this enigma because in addition to binary end members, i.e., monoclinic As_2Se_3 and face-centred cubic Na_2Se , it possesses two ternary crystalline compositions, namely orthorhombic NaAsSe_2 and cubic Na_3AsSe_3 with distinct network topology.

Chalcogenide glasses in the quasi-binary $(\text{Na}_2\text{Se})_x(\text{As}_2\text{Se}_3)_{1-x}$, $0.0 \leq x \leq 0.4$, system were synthesized using melt quenching technique and the fundamental properties were studied using a variety of technical tools, e.g. XRD, density and DSC measurements, d.c. conductivity measurements and Raman spectroscopy. XRD patterns show that the compositions are amorphous in the domain, $0 \leq x \leq 0.3$. The $x = 0.4$ composition corresponds to orthorhombic NaAsSe_2 crystal, space group Pbca . With increasing Na_2Se content, the density, d , and the glass transition temperature, T_g , decrease. The later indicates reduced network connectivity. The room-temperature conductivity, σ_{298} , for the $(\text{Na}_2\text{Se})_x(\text{As}_2\text{Se}_3)_{1-x}$ samples, increases by two orders of magnitude, from $\sim 10^{-13} \text{ S cm}^{-1}$ ($x = 0.0$) to $\sim 10^{-11} \text{ S cm}^{-1}$ ($x = 0.3$). The mechanical milling (MM) technique was used to further extend the vitreous domain and the obtained glass-ceramic $\text{MM}-(\text{Na}_2\text{Se})_{0.4}(\text{As}_2\text{Se}_3)_{0.6}$ composition displays $\sigma_{298} = 4 \times 10^{-8} \text{ S cm}^{-1}$, i.e., higher by four orders of magnitude comparing to its crystalline counterpart. Raman spectroscopy measurements recorded different vibrational modes between glass compositions and c - NaAsSe_2 sample.

Influence of twill fabric topography on bloodstain pattern shape

P20

S. Brnada¹, A. Kalazic^{1*}

¹ University of Zagreb Faculty of Textile Technology, Prilaz baruna Filipovića 28a
HR-10000 Zagreb, email: sbrnada@ttf.unizg.hr

* The corresponding author e-mail: ana.kalazic@ttf.unizg.hr

Keywords: twill weave; bloodstain patterns; topography; forensic

At a crime scene, forensic scientists analyse the event by finding physical evidence to help evaluate potential scenarios. Analysing of bloodstains on clothing can be complex work and often requires experimentation and extensive experience. For this reason, care should be taken when interpreting blood samples. In the case of fabrics woven in twill weave, a so-called “*canals with islands*” structure was observed. In this paper, the influence of the diagonally structured woven fabric in the twill weave on the distribution of liquid and its final shape inclination will be examined.

The binary image shows a distributed liquid drop on the diagonally structured fabric surface in a twill 1/3 weave. When the drop spread over the surface, the distribution of the stain in diagonal channels occurred. Given that the tested fabric has a lower hydrophilic character, the distribution of the stain was intense in the directions of the diagonals, and the final shape of the stain had an elliptical, twisted shape, as can be seen from the parameters in **Tab. 1**: Major axis of fitted ellipse angle and Feret angle.

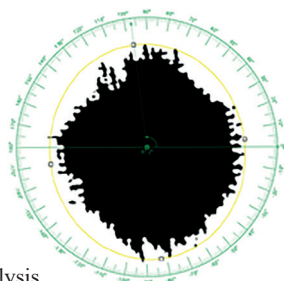


Figure 1:
Image analysis

Table 1: Shape inclination descriptors

Fit ellipse parameters	Major axis, mm	5,430
	Minor axis, mm	4,810
	Major axis angle, °	97,163
Feret parameters	Feret max, mm	5,720
	Feret angle, °	81,459

References

- [1] Michielsen, S., Taylor, M., Parekh, N., & Ji, F. Bloodstain patterns on textile surfaces: a fundamental analysis. *National Institute of Justice, US Department of Justice*. (2015)
- [2] S. Brnada, T. Pušić, T. Dekanić, & S. Kovačević, Impact of Fabric Construction on Adsorption and Spreading of Liquid Contaminations. *Materials*, 15(6), 1998. (2022)

Acknowledgments

This work has been supported by the European Union from the European Regional Development Fund under the project KK.01.2.1.02.0064 Development of multifunctional nonflammable fabric for dual use.

Assessing the local structure and quantifying defects in $\text{Ca}_4\text{Fe}_9\text{O}_{17}$ combining STEM and FAULTS

J. Oró-Solé¹, J. Serrano-Sevillano², J. Gázquez¹, C. Frontera¹, A. P. Black¹, M. Casas-Cabanas², M. Rosa Palacín¹

¹ Institut de Ciència de Materials de Barcelona, ICMA-B-CSIC, Campus UAB, 08193 Bellaterra, Catalonia, Spain;

² Centro de Investigación Cooperativa de Energías Alternativas (CIC energiGUNE), Basque Research and Technology Alliance (BRTA), Parque Tecnológico de Alava, Albert Einstein 48, 01510 Vitoria-Gasteiz, Spain

* The corresponding author e-mail: jserrano@cicenergigune.com, rosa.palacin@icmab.es

Keywords: stacking faults, HR-STEM, FAULTS software, $\text{Ca}_4\text{Fe}_9\text{O}_{17}$

Defects in crystalline structures play a vital role in their properties, so their proper characterization is essential to understanding and improving the behaviour of the materials. In this work, their presence in $\text{Ca}_4\text{Fe}_9\text{O}_{17}$ has been analysed. Its structure exhibits three different iron coordination topologies and can be described as layers of corner-sharing FeO_5 bipyramids stacked along the c axis together with layers of edge-sharing FeO_6 octahedra, both being linked by FeO_4 tetrahedra. Structural refinement using the Rietveld method in X-ray and neutron powder diffraction data was not possible due to significant mismatches between the observed and calculated integrated intensities for several peaks which was tentatively attributed to the presence of stacking faults induced by the fact that the relative position of the FeO_4 tetrahedra generates three possible stacking directions.

Selected area electron diffraction (SAED) and high-resolution scanning transmission electron microscopy (HR-STEM) images confirm the presence of a significant amount of local defects in the material, which is consistent with experimental and simulated SAED patterns. The FAULTS software enabled a successful refinement of the structure from both X-ray and neutron diffraction data when considering a high concentration of planar defects, conferred by the existence of three possible stacking directions in the crystal structure, all of them confined in the basal plane.

Besides giving methodological insights into the investigation of defective compounds, the work reported here provides independent and complementary validation of the FAULTS approach via complementary techniques and hence nicely illustrates the capabilities of this program.

References

- [1] M. Casas-Cabanas, J. Rodríguez-Carvajal, J. Canales-Vázquez, Y. Laligant, P. Lacorre, M.R. Palacín. *J. Power Sources*, **174**, 414–420 (2007)
- [2] M. Casas-Cabanas, J. Rikarte-Ormazabal, M. Reynaud, J. Rodríguez Carvajal. *FAULTS manual*, <https://cicenergigune.com/en/faults>
- [3] J. Serrano-Sevillano, J. Oró-Solé, J. Gázquez, C. Frontera, A. P. Black, M. Casas-Cabanas, M. R. Palacín, *Inorganic Chemistry Frontiers*, **9**, 6425–6430 (2022)

Resonant properties of polycrystalline biomolecular assemblies

T. E. Ryan¹, S. Guerin²

¹ Department of Physics and Bernal Institute, University of Limerick, Castletroy, Limerick, V94T9PX, Republic of Ireland.

² Synthesis of Solid State Pharmaceutical Centre, University of Limerick, Castletroy, Limerick, V94T9PX, Republic of Ireland.

* The corresponding author e-mail: tara.e.ryan@ul.ie

Keywords: piezoelectric, polycrystalline, resonant properties, eco-friendly, amino acids

Piezoelectric materials, ubiquitous in modern day technologies, are commonly exploited as resonators- often used to keep track of time, to provide a stable clock signal for digital integrated circuits, and to stabilize frequencies for radio transmitters and receivers. As such there exist many characterisation techniques to study the converse piezoelectric effect, whereby an electrical signal is passed through the sample to induce internal strain or vibration. As we move away from toxic conventional piezoceramics, our group's research focuses on the design and development of polycrystalline biomolecules for these applications. However no research currently exists on the resonance properties of polycrystalline biomolecular assemblies, such as their resonance frequencies or electromechanical coupling constants.

We will present the first such data on simple amino acid-based piezoelectric device components, as well as discussing the necessary developments in electromechanical characterisation that need to occur for efficient metrology of non-conventional piezoelectrics. The nanoscale chemistry that gives rise to this macroscopic actuation can be used to guide the chemical synthesis and crystallisation of future eco-friendly piezoelectric resonators.

References

- [1] Guerin, Sarah, Syed AM Tofail, and Damien Thompson. "Organic piezoelectric materials: milestones and potential." *NPG Asia Materials* 11, no. 1 (2019): 1–5.
- [2] Casadei, Filippo, et al. "Piezoelectric resonator arrays for tunable acoustic waveguides and metamaterials." *Journal of Applied Physics* 112.6 (2012): 064902.
- [3] Guerin, Sarah, Aimee Stapleton, Drahomir Chovan, Rabah Mouras, Matthew Gleeson, Cian McKeown, Mohamed Radzi Noor et al. "Control of piezoelectricity in amino acids by supramolecular packing." *Nature materials* 17, no. 2 (2018): 180–186.
- [4] Jiang, Chengming, Qikun Li, Jijie Huang, Sheng Bi, Ruonan Ji, and Qinglei Guo. "Single-layer MoS₂ mechanical resonant piezo-sensors with high mass sensitivity." *ACS Applied Materials & Interfaces* 12, no. 37 (2020): 41991–41998.

Acknowledgments

This work was supported by The European Research Council.

Polysulfide in-situ characterization with 3D electron diffraction for Lithium-Sulfur batteries

S. Rahimi, A. Hajizadeh, J. Hadermann

¹ Electron microscopy for material science (EMAT), Department of Physics, University of Antwerp, Antwerpen 2020, Belgium

* The corresponding author e-mail: loke.hadermann@uantwerpen.be

Keywords: sulfur; 3DED; in-situ electron microscopy; structure solution; structure refinement

Sulfur is known for its high specific capacity (1675 mAh/g) as the cathode material in Lithium-sulfur batteries (LSBs). [1] The transformation of the sulfur structure during cycling is important for its lifetime capacity. In LSBs, the limitation is the shuttling effect where different polysulfides (S_n , $n=1,2,\dots,8$) are (re)produced during the oxidation reaction of sulfur with lithium, and dissolve in the electrolyte. [2] As a consequence, sulfur will deposit on the lithium anode and cause capacity loss since the cathode material is consumed in each cycle. In literature, many studies are trying to prevent this effect, but details about the crystal structure of different species during the shuttling have remained unclear. [3]

There are single-crystal XRD datasets for a few forms of polysulfides in the ICSD database [4-7] which have been measured ex-situ. In the real situation, it is not practical to grow large crystals that are suitable for single-crystal XRD during the reaction. But, electron diffraction is more efficient for small crystals. Also, thanks to the progress in in-situ facilities developed for TEM [8], sulfur can be studied in a gas or liquid cell. Therefore, it is possible to study the crystal structure of polysulfides either in the stable phase (conventional powders in a gas cell) or during a reaction for less stable phases (intermediate species in a liquid nanoreactor).

In this work, for the first time, the crystal structure of the sulfur S_8 phase has been studied under a protective atmosphere with the 3D electron diffraction (3DED) method and the structure has been solved successfully. Although the geometry of the holder tip and the nano-reactor limit the tilting range, merging several datasets from different particles was used as a complementary technique to add more completeness to the imported data for solving the structure.

References

- [1] Shi, K., Lin, Y., Li, J., Xiong, Z., Liao, J., Liu, Q. (2022) *Ind. Eng. Chem. Res.*, **61**(6), 2502–2510.
- [2] Huang, J. Q., Zhang, Q., Peng, H. J., Liu, X. Y., Qian, W. Z., Wei, F. (2014) *Energy Environ. Sci.*, **7**, 347–353.
- [3] Huang, Y., et al. (2022) *Adv. Sci.*, **9**(12), 2106004.
- [4] Pawley, G.S. & Rinaldi, R.P. (1972) *Acta Crystallographica B*, **28**, 3605–3609.
- [5] Templeton, L. K., Templeton, D., H., Zalkin, A. (1976) *Inorg. Chem.*, **15**(8), 1999–2001.
- [6] Steudel, R., Bergemann, K., Buschmann, J., Luger, P. (1996) *Inorg. Chem.*, **35**, 2184–2188.
- [7] Gromilov, S.A., Piryazev, D.A., Egorov, N.B., Akimov, D.V. (2016) *J. Str. Chem.*, **57**(8), 1663–1666.
- [8] Karakulina, O. M., Demortière, A., Dachraoui, W., Abakumov, A. M., Hadermann, J. (2018) *Nano Lett.*, **18**(10), 6286–6291.

In-situ 3D ED to study the structural transformation of NMC during electrochemical reactions

P24

A. Hajizadeh¹, S. Rahimi¹, J. Hadermann¹

¹ EMAT, University of Antwerp, Groenenborgerlaan 171, B-2020 Belgium

* The corresponding author e-mail: loke.hadermann@uantwerpen.be

Keywords: battery; electron microscopy; *in-situ*; electron diffraction; NMC; crystallography

Recently, 3D electron diffraction (3D ED) has been employed *in situ* to show the structural transformation of nanomaterials during phase transformations upon reactions such as heating and oxidizing and reducing reactions [1-2]. 3D ED is widely used to study the crystal structure of functional nanomaterials that are too small to study with X-ray or neutron single crystal diffraction. When it comes to *in situ* studies of materials with 3D ED, several challenges should be taken into account. In the presence of the liquid, the quality of the data will be decreased because of scattering by the liquid, large inelastic scattering and reactions between the beam and the liquid. In literature, the crystal structure transformation of LiFePO₄ upon charging *in situ* in liquid was studied by decreasing the liquid thickness using the beam shower method [1]. However, this method cannot be employed to study the structure transformations across several cycles as it changes the properties of the electrolyte dramatically.

Here, we used a low dose method to acquire data on Li_{1.2}Ni_{0.13}Mn_{0.54}Co_{0.13}O₂ in the liquid environment with 3D ED without drastically changing the electrolyte properties. We will discuss the method in brief, the challenges to perform electrochemical measurements along with 3D ED, the results from the *in-situ* transformation of NMC, and the further application of this method for rechargeable batteries.

References

- [1] O. Karakulina, A. Demortière, W. Dachraoui, A. Abakumov, and J. Hadermann. *Nano letters*, **18**, 6286-6291 (2018).
- [2] M. Batuk, D. Vandemeulebroucke, M. Ceretti, W. Paulus, and J. Hadermann. *J. Mater. Chem. A*, **11**, 213-220, (2023)

Acknowledgments

This work was Funded by the European Union's Horizon 2020 research and innovation programme under the Marie Skłodowska Curie grant agreement No 956099.

Bloodstain pattern analysis using shape descriptors

A. Kalazic¹, S. Brnada*

¹ University of Zagreb Faculty of Textile Technology, Prilaz baruna Filipovića 28a HR-10000 Zagreb, email: ana.kalazic@ttf.unizg.hr

* The corresponding author e-mail: snjezana.brnada@ttf.unizg.hr

Keywords: bloodstain; plain weave; forensic; shape descriptors; droplet distribution

Bloodstain pattern analysis provides significant information about the actual event at the crime scene. Analyzing the shape of bloodstains is one of the key methods in forensics that allows the forensic expert not only to reconstruct a violent crime, but also to develop technical arguments to confirm or refute statements made in the courtroom. The shape of blood stain samples on woven textiles are unpredictable due to the different raw material composition and the different morphological characteristics of the woven surface. In this paper, the new method will be applied and interpretation of the blood stain shape will be performed using shape descriptors in the analysis of the image of bloodstain pattern on plain weave woven fabric.

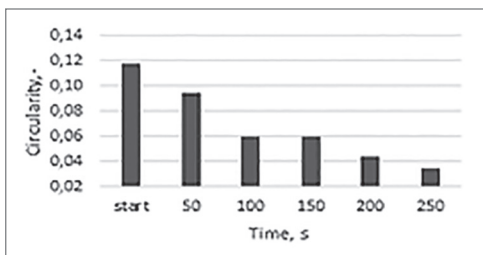


Figure 1: Circularity parameter

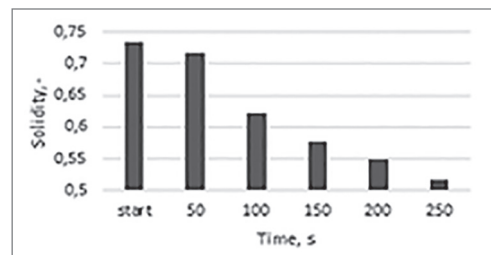


Figure 2: Solidity parameter

For the analysis, a cotton fabric in plain weave was used, with a warp and weft density of 20 threads/cm, on which one drop of colored liquid was applied. The droplet distribution was analyzed after every 50 s until the droplet stopped spreading. Circularity and solidity parameters were used as shape descriptors in order to establish the amount of ray shape distribution on the surface of the woven, considering that the droplet was distributed capillary along the length of the yarn. The Fig.1 and Fig. 2 shows that the circularity and solidity parameters are reduced by the spread of the ray shape pattern, which confirms the effectiveness of this type of analysis on blood pattern shape analysis.

References

- [1] Michielsen, S., Taylor, M., Parekh, N., & Ji, F. Bloodstain patterns on textile surfaces: a fundamental analysis. *National Institute of Justice, US Department of Justice*. (2015)
- [2] Calvimontes, A., Hasan, M. M. B., and Dutschk, V., Effects of Topographic Structure on Wettability of Differently Woven Fabrics, “Woven Fabric Engineering”, book edited by Polona Dobnik Dubrovski, 71–92 (2010)

Acknowledgments

This work has been supported by the European Union from the European Regional Development Fund under the project KK.01.2.1.02.0064 Development of multifunctional nonflammable fabric for dual use.

The effects of alkali metal intercalation on the structure and superconductivity of Niobium Selenide

P26

K. Steele^{1*}, S. J. Clarke¹

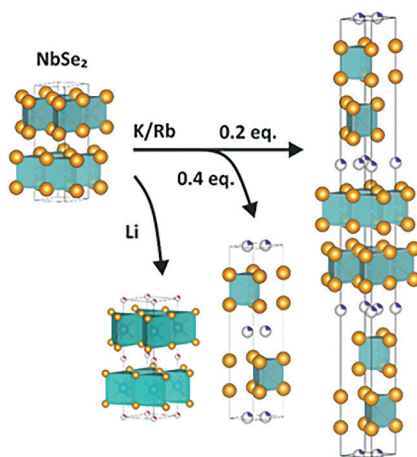
¹ Department of Chemistry, University of Oxford, South Parks Road, Oxford, OX1 3QR, UK

* The corresponding author e-mail: katherine.steele2@stcatz.ox.ac.uk

Keywords: intercalation; niobium selenide; layered materials; superconductivity; staged compounds

In this work, alkali metal intercalated niobium selenide species were synthesised using soft chemical and high temperature methods. These compounds were analysed using x-ray diffraction and magnetometry.

Niobium Selenide is a layered member of the transition metal dichalcogenide family, which displays structural polymorphism. The room temperature stable 2H form has a charge density wave transition at 33.5K and a superconducting transition at 7K. Upon intercalation, superconductivity is suppressed and structural changes occur. The intercalated phases show structural complexity dependant on the identity and amount of the alkali metal intercalated and the synthetic route, some forming unusual staged phases, where alkali metal occupies only some interlayer spaces. The composition-structure-property relationships of these phases will be described.



References

- [1] D. E. Moncton, J. D. Axe, F. J. Disalvo, *Phys. Rev. B*, **16**, 801–819 (1977)
- [2] R. C. Morris, R. Bhandari, R. V. Coleman, *Phys. Rev. B*, **5**, 895 (1972)
- [3] X. Fan, H. X. Chen, J. Deng, X. N. Sun, L. L. Zhao, L. Chen, S. F. Jin, G. Wang, X. L. Chen, *Inorg Chem*, **58**, 7564–7570 (2019)
- [4] X. Fan, H. X. Chen, L. L. Zhao, S. F. Jin, G. Wang, *Solid State Commun*, **297**, 6–10 (2019)

Acknowledgments

Funding from the EPSRC Centre for Doctoral Training in Inorganic Chemistry for Future Manufacturing (OxICFM), EP/S023828/1.

Discovery of superconductivity in Nb_4SiSb_2 with a V_4SiSb_2 -type structure and implications of interstitial doping on its physical properties^[1]

M. D. Balestra^{1,2}, **O. Atanov**³, **O. Blacque**², **R. Lefèvre**², **Y. H. Ng**³, **R. Lortz**³, **F. O. von Rohr**^{1,2}

¹ Department of Quantum Matter Physics, University of Geneva, CH-1211 Geneva, Switzerland;

² Department of Chemistry, University of Zürich, CH-8057 Zürich, Switzerland;

³ Department of Physics, The Hong Kong University of Science and Technology, Clear Water Bay Kowloon, Hong Kong

* *The corresponding author e-mail:* manuele.balestra@unige.ch

Keywords: interstitial doping; superconductivity; intermetallic compounds; V_4SiSb_2 -type structure; physical properties manipulation

We report on the discovery, structural analysis, and the physical properties of the heretofore unknown compound Nb_4SiSb_2 , crystallizing in the Nb_4SiSb_2 -type structure. Nb_4SiSb_2 undergoes a superconducting transition with a critical temperature of $T_c \approx 1.59$ K in the resistivity as well as in the discontinuity in specific heat. Nb_4SiSb_2 further features unoccupied sites on the $4b$ position, which can be partially occupied by either Cu, Pd, or Pt. Insertion of mentioned electron donors into the void positions of the parent compound, result in a lowered superconducting transition temperature. The low temperature resistivity measurements show transitions to superconductivity at $T_c \approx 1.16$ K for $\text{Nb}_4\text{Cu}_{0.2}\text{SiSb}_2$, $T_c \approx 0.76$ K for $\text{Nb}_4\text{Pd}_{0.2}\text{SiSb}_2$ and $T_c \approx 0.84$ K for $\text{Nb}_4\text{Pt}_{0.14}\text{SiSb}_2$.

References

- [1] M. D. Balestra, O. Atanov, O. Blacque, R. Lefèvre, Y. H. Ng, R. Lortz, and F. O. von Rohr, *J. Mater. Chem. C*, **10**, 11703–11709 (2022)

Selective ion transport of catalytic hybrid aerofilm Li-S batteries

P28

C. Senthil¹, S. S. Kim¹, H. S. Kim¹, J. W. Hong¹, H. Y. Jung^{1*}

¹ Department of Energy Engineering, Gyeongsang National University, 33 Dongjin-ro, Jinju-si, 52725, South Korea

* The corresponding author e-mail: hyjung@gnu.ac.kr

Keywords: Li-S battery; hybrid aerofilm; sulfide; ion transport; long-life

Realistic prospects of high-energy and compact lithium-sulfur (Li-S) batteries promising as next-generation energy storages are hindered by their poor cycle life and severe self-discharge impelled through the polysulfide dissolution. Here, we report a feasible strategy to effectively suppress polysulfide and selectively control ion transport by applying a new-type ultralight aerofilm membrane for practical Li-S batteries. Catalytic hybrid aerofilm interlayer (HAI) consisting of sulfonated tetrafluoroethylene and manganese dioxide nanowires suffices physical shield and sieve polysulfides through sulphophilicity polymer within the gaps of manganese dioxide layers, while also imparting chemical anchoring and catalysis of Mn-O. Such cooperative synergistic effects of the hybrid aerofilm interlayer for the Li-S cells enable the realization of a high discharge capacity of 1189 mAh/g at the end of the 500th cycle with a capacity retention of over 92.3%, which is a 671% improvement over sulfur battery with NO interlayer. Moreover, the aerofilm interlayer provides Li-dendritic growth inhibition and self-discharge prevention to retain the cycle life and safety of the device. This study presents a forward-looking strategy for developing an ultralight-compact and high-power Li-S battery [1].

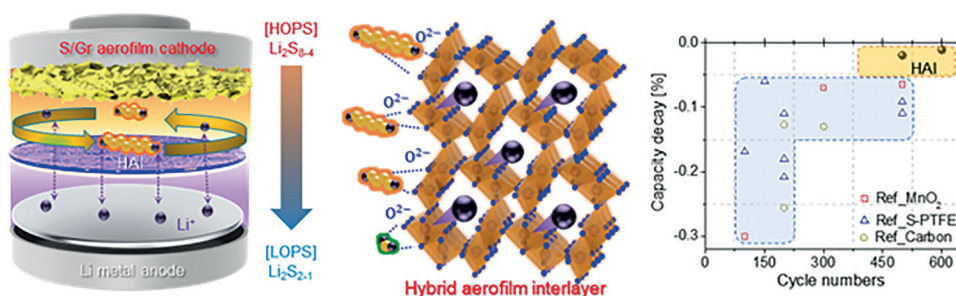


Figure: Schematic illustration and specific capacity comparison of ultralight Li-S battery

References

- [1] D. W. Kim, C. Senthil, S. M. Jung, S. Kim, H. S. Kim, J. W. Hong, J. H. Ahn, H. Y. Jung, *Energy Storage Materials*, **47**, 472–481 (2022)

Acknowledgments

This research was supported by the National Research Foundation of Korea (NRF) funded by the Ministry of Education (2021R111A3A04034294) and the Ministry of Science and ICT (2021R1A4A1030318). Also, this research was supported by Brain Pool program funded by the Ministry of Science and ICT through the National Research Foundation of Korea (NRF-2021H1D3A2A02039346, 2022H1D3A2A02081640).

Solid-state electrolytes for Na-ion batteries: exploring the synergy between metal-organic frameworks and ionic liquids

A. Mirandona-Olaeta^{1,2}, E. Goikolea¹, S. Lanceros-Mendez^{2,3}, A. Fidalgo-Marijuan^{1,2}, I. Ruiz de Larramendi¹

¹ Departamento de Química Orgánica e Inorgánica, Facultad de Ciencia y Tecnología, Universidad del País Vasco/Euskal Herriko Unibertsitatea (UPV/EHU), 48940 Leioa, Spain;

² BCMaterials, Basque Center for Materials, Applications and Nanostructures, UPV/EHU Science Park, 48940, Leioa, Spain;

³ Ikerbasque, Basque Foundation for Science, Bilbao, Spain

* The corresponding author e-mail: idoia.ruizdelarramendi@ehu.eus

Keywords: metal-organic framework; ionic liquid; solid-state electrolyte; battery; sodium

The intermittent nature of renewable energy sources such as solar or wind causes a high demand for energy storage systems. In this context, lithium-ion batteries (LIBs) comprise the majority of the electrochemical energy storage market, although problems arising from the use of lithium (such as its limited abundance and the increasing cost of lithium resources) have driven the exploration of alternative systems such as sodium-ion batteries (NIBs). Both systems, LIBs and NIBs, conventionally use liquid-based organic electrolytes that carry safety problems. For this reason, the next generation of metal-ion batteries will be based on the use of solid electrolytes (solid-state batteries), since they prevent the leaks, do not require volatile solvents and adapt easily to temperature changes due to their high thermal stability. [1] In addition, these solid electrolytes are compatible with the use of Li or Na metal anodes, providing a significant increase in both volumetric and gravimetric energy density. This work focuses on combating two of the main challenges related to the implementation of solid electrolytes in metal-ion batteries: low ionic conductivity and the formation of inefficient electrode-electrolyte interfaces. A family of hybrid electrolytes produced from the combination of metal-organic frameworks (MOFs) with ionic liquids (ILs) is developed. The robustness of the MOFs inhibits the growth of dendrites, while the IL facilitates ionic mobility and favour better contact at the electrode-electrolyte interfaces. In this work, Zn-MOF-74 has been selected due to the dimension of the channels ($10.3 \times 5.5 \text{ \AA}^2$), which are optimal for introducing different amounts of sodium-enriched [EMIm][TFSI] ILs. In addition, Zn-MOF-74 presents a fast and simple synthesis method, easily reproducible on a larger scale, and is environmentally friendly. The solid electrolyte developed exhibits an ionic conductivity of $4 \cdot 10^{-4} \text{ S cm}^{-1}$ at 20 °C. This value supports the starting hypothesis, according to which the metal cations (Na^+) move through the periodically well-organized channels of the MOF, allowing a more homogeneous and orderly deposition/release of the sodium in charge/discharge processes.

References

[1] M. Urgoiti-Rodríguez et al., *Front. Chem.*, **10**, 995063 (2022)

Acknowledgments

This work was supported by Ministerio de Ciencia, Innovación y Universidades (PID 2019-107468RB-C21) and Gobierno Vasco/Eusko Jaurlaritza under the ELKARTEK program and Basque University System Research Groups (IT1546-22).

Understanding Fe-cation migration in $\text{LiFe}_{2-x}\text{In}_x\text{SbO}_6$ Cathode Materials

X. Martinez de Irujo-Labalde^{1*}, S. Mahato¹, M. Hayward¹

¹ Inorganic Chemistry Laboratory, Department of Chemistry, University of Oxford, South Parks Road, OX1 3QR, United Kingdom

* The corresponding author e-mail: xabimart@ucl.ac.uk

Keywords: sustainable li-ion cathodes; energy storage; electrochemistry; topochemical reactions, crystal structure

Li-ion batteries have transformed daily life by acting as energy dense, rechargeable power sources for a wide range of electronic devices. As part of the UK Faraday Institute FutureCat project [1] we are investigating a range of new lithium-ion battery cathode materials for application in all-electric vehicles. In addition to the normal requirements of maximizing energy density and power output, as part of this project we are also trying to move away from cobalt-based materials due to their poor environmental impacts; we have focused on materials containing earth-abundant elements, with a particular emphasis on iron-based materials. Most of the iron, in particular, Fe^{3+} materials, that have been investigated to-date suffer from a capacity loss after long term cycling, although a good performance can be achieved for the first cycle [2]. This capacity loss is generally attributed to the easy migration of Fe^{3+} between different coordination sites. To get more insight into these issues, we are currently investigating a novel Fe-based system, $\text{LiFe}_{2-x}\text{In}_x\text{SbO}_6$ [3].

In the present work, we have performed a detailed structural characterization of the different members of the solid solution, as well as their electrochemical properties. Additionally, we have performed Li (de)intercalation procedures on these phases through different topochemical approaches to yield lithiated and delithiated materials. Based on these results, we will discuss the implications of partial substitution of Fe by In over the electrochemical performance of these Fe-based materials.

References

- [1] <https://futurecat.ac.uk/>
- [2] J. Li, J. Li, J. Luo, L. Wang, X. He. *Int. J. Electrochem. Sci.*, **6**, 1550–1561 (2011)
- [3] Martinez de Irujo-Labalde, H. Grievson, J.M. Mortimer, S. Booth, A. Scrimshire, P. Bingham, E. Suard, S. Cussen, M. Hayward. *Chem. Mater.*, **35**, 1, 337–346 (2022)

Acknowledgments

This work was supported by FutureCat project (Faraday Institution).

Synthesis of low-pt-based electrocatalyst derived from porous MOF-808(Zr)-NH₂ nanoparticles towards oxygen reduction reaction

T. M. Pham¹, J. Kim^{1,*}

¹ Department of Chemical Engineering, Kyung Hee University, Yongin-si, Republic of Korea

* The corresponding author e-mail: jkim21@khu.ac.kr

Keywords: Pt-N-C; MOF-808(Zr); low Pt loading; oxygen reduction reaction; PEMFC

The high cost and poor durability are the main problems preventing the wide application of the commercial 20 wt% Pt/C catalyst in oxygen reduction reaction (ORR). Hence, lowering the percentage of Pt as well as boosting the stability of electrocatalysts are highly desirable. In this research, the active Pt-N-C catalyst with ultrasmall amount of Pt was synthesized from the porous MOF-808(Zr)-NH₂ nanoparticles. By simple Pt impregnation into MOF particles followed by carbonization, the Pt-N-C with a uniform octahedral morphology was obtained, showing the large surface area and mesoporous structure. The high ORR activity of the nanostructured Pt-N-C catalyst was demonstrated by the electrochemical analysis, which revealed the high half-wave potential, onset potential as well as the limited current density in both acidic and alkaline environments. Furthermore, as-synthesized low-Pt-content catalysts exhibited a 4-electron pathway of ORR with very low peroxide yield. In particular, the durability tests showed that the Pt-N-C catalyst achieved high stability, which was better than the commercial 20 wt% Pt/C catalyst. Therefore, this study provides a promising strategy for reducing the amount of precious Pt metal and improving the long-term stability for of the ORR performance.

Upcycling Lithium Titanate (LTO) anodes into the next generation of high power Ti Doped Nb₂O₅ Anodes (TNO)

A. J. Green^{1,2}, **E. H. Driscoll**^{1,2}, **P. R. Slater**^{1,2}

¹ School of Chemistry, University of Birmingham, Birmingham B15 2TT, U.K;

² The Faraday Institution, Harwell Science and Innovation Campus, Didcot OX11 0RA, U.K

* The corresponding author e-mail: ajg119@student.bham.ac.uk

Keywords: lithium titanate; anode; lithium ion; high power; niobates

The growth and popularity of Lithium-ion batteries (LIBs) has been increasing since the drive for ‘net zero’ was announced by numerous countries around the world. This demand will ultimately put stress on existing natural resources resulting in the inevitable need to recycle these LIBs to preserve the valuable metals inside these batteries. High power anodes are an important area in the field of LIBs, that is increasing in popularity, due to the increased safety and their ability to charge and discharge at fast rates, which is essential for high power applications (e.g. drones, motorsports, power tools, HEV). Lithium titanate (LTO) has been used in commercial high power batteries, however, LTO has many limitations, including a low theoretical capacity and low energy density due to its high operating voltage (1.55 V Vs Li+/Li) [1]. With these drawbacks there has been a rising interest in niobate anodes as the next generation of high power anodes. These anodes have a Wadsley-Roth structure that contain corner-sharing distorted octahedra which form ReO₃- like channels that facilitates fast Li⁺ ion diffusivity. Within the structure there are crystallographic shear planes, created by edge-sharing octahedra, which enhances the stability of the structure [2,3]. Given the fact that these Wadsley Roth phases have started to supersede LTO as the anode in high power batteries, we have been investigating the possibility to upcycle spent LTO anodes into Wadsley Roth Ti-Nb-O anodes. We illustrate a route to this, along with associated Li recovery.

References

- [1] M. M. Thackeray and K. Amine, *Nat. Energy*, 6, 683 (2021).
- [2] C. P. Koçer, K. J. Griffith, C. P. Grey, A. Morris *J. Am. Chem. Soc.* 141, 15121-15134 (2019).
- [3] Y. Lakhdar, H. Geary, M. Houck, D. Gastol, A. Groombridge, P. R. Slater, E. Kendrick, *ACS Applied Energy Materials*, 5, 11229-11240 (2022).

Acknowledgments

We would like to thank the Faraday Institution for funding.

Investigation of electrochemical properties of Zn-ion batteries based on ZnMo_6S_8 cathodes

Y. Wang¹, A. Y. Ganin^{1*}

¹ School of Chemistry, University of Glasgow, Glasgow G12 8QQ, UK

* The corresponding author e-mail: Alexey.Ganin@glasgow.ac.uk

Keywords: energy storage; zinc ion battery; chevrel phase compound; cathode material; intercalation

The production of lithium-ion batteries (LIBs) relies on availability of scarce resources such as lithium ore. Therefore, LIBs should be reserved for high power density applications (such as portable devices and electric vehicles) rather than employed in stationary applications (such as for example, the storage of excess renewable energy). In the context of stationary devices, less power dense but cheap in production and recycling, aqueous zinc ion batteries (AZIBs) may provide a better alternative to LIBs [1]. However, better understanding is required of AZIBs. Studies of well-defined intercalation system similar in behavior to Li-ion cathodes are essential for a better understanding of how to build an improved AZIB systems.

In this work, we focused on $\text{Mo}_6\text{S}_8 - \text{ZnMo}_6\text{S}_8$ system which shows charge – discharge curves consistent with an intercalation behaviour [2,3]. ZnMo_6S_8 was synthesized directly from the elements by heating stoichiometric amounts of elements in sealed ampoules at 1050 °C. In comparison, Mo_6S_8 was prepared by deintercalation of Cu from $\text{Cu}_2\text{Mo}_6\text{S}_8$ with 1 M $\text{Fe}(\text{NO}_3)_3$ in water. After the targeted phases and composition were confirmed by PXRD and EDX, the materials were tested in two electrode system using 1 M ZnSO_4 in water as electrolyte and Zn as counter electrode. The cycling voltammetry (CV) measurements showed two distinct peaks consistent with a reversible intercalation and deintercalation of only one zinc in the host materials. The galvanostatic charge discharge (GCD) tests showed flat plateaus which were in accordance with the CV curves. Finally, we discuss the difference in electrochemical performance of Mo_6S_8 and ZnMo_6S_8 to elucidate the intercalation mechanism and provide some future strategies for the optimization of AZIBs.

References

- [1] M. Song et al. *Adv. Funct. Mater.* 28, 1802564 (2018)
- [2] Y. Cheng et al. *ACS Appl. Mater. Interfaces* 8, 22, 13673–13677 (2016)
- [3] M. Chae et al., *Inorg. Chem.* 55, 7, 3294–3301 (2016)

Crystal Chemistry of Argyrodite type Li-ion conductors

P34

D. Shanbhag¹, J. Auvergniot², V. Viallet¹, C. Masquelier^{1*}

¹ LRCS, UMR CNRS #7314, Université de Picardie Jules Verne, 80039 Amiens Cedex, France;

² Umicore, Broekstraat 31/Rue du Marais, B-1000 Brussels, Belgium

* The corresponding author e-mail: christian.masquelier@u-picardie.fr

Keywords: ASSB, Argyrodite, sulfide solid electrolyte, ionic conductivity, moisture stability

Fast-ion conductors are crucial for the development of all-solid-state batteries (ASSBs), foreseen as next-generation energy storage devices. Lithium-containing solid electrolytes of the argyrodite structural family $(\text{Li}^+)_6(\text{PS}_4)_3\text{S}^{2-}\text{X}^-$ ($\text{X} = \text{Cl}, \text{Br}, \text{I}$) are a promising class of sulfide based lithium ionic conductors owing to their high ionic conductivity and ductility [1]. The high-temperature polymorph of these materials crystallizes into tetrahedrally close-packed anion lattice in the cubic space group and exhibits X^-/S^{2-} site disorder which has a direct correlation with high lithium ion conductivities. However, this class of materials still presents several shortcomings such as low moisture stability, interfacial reactivity with lithium metal anode and instability to high voltage cathodes. These challenges can be overcome by fine-tuning the argyrodite composition *via* wide range of cationic and/or anionic substitutions and by systematically engineering the X^-/S^{2-} site disorder through modification of the synthesis conditions [2-3].

From this perspective, we have examined the compositional space of cation/anion substituted argyrodites and the influence of chemical substitution on the crystal structure and ion transport properties. In this work, we optimized the synthesis conditions (ball-milling, annealing, quenching, ...) to find the optimal balance between crystallite size and site disorder so as to get the best ionic conductivity. Additionally, we focused on investigating and understanding how substitutions might affect the moisture stability and Li metal compatibility and thereby making argyrodites an ideal class of solid electrolyte for finding practical applications in ASSBs.

References

- [1] H. J. Deiseroth *et al.*, *Angewandte. Chemie - Int. Ed.*, vol. 47, no. 4, pp. 755–758, 2008
- [2] S. Ohno *et al.*, *Chemistry of Materials*, vol. 31, no. 13, pp. 4936–4944, 2019,
- [3] A. Gautam *et al.* *Advanced Energy Materials*. 2021, 11, 2003369

Acknowledgments

This work is a part of Ph.D thesis which is supported by UMICORE, Belgium.

Boosting the electrochemical performance of TNO anode material through structural and compositional modifications

E. García-González^{1*}, A. Solana-Bello², F. García-Alvarado³

¹ Departamento de Química Inorgánica, Universidad Complutense (Madrid);

² Departamento de Química y Bioquímica, Universidad San Pablo-CEU (Madrid)

* The corresponding author e-mail: esterg@ucom.es

Keywords: TiNb₂O₇; Wadsley-Roth; anode-material; Li-ion batteries; ultra-fast charge

The Wadsley-Roth TiNb₂O₇ block phase has recently emerged as a promising anode material for Li-ion batteries and a motivating alternative to Li₄Ti₅O₁₄ spinel [1]. Its redox chemistry accounts for a large theoretical capacity (387,7 mAh/g) and minimizes dendrites/SEI formation and the structural characteristics provide robustness and stability as well as 2D structural channels for a good rate capability of the material. These properties, however, are overshadowed by the low electronic conductivity and poor diffusion kinetics of Li. Various strategies have been used to surpass these shortcomings, among them doping with heteroatoms with the aim of improving electronic conductivity through charge compensation or reducing particle size, through the synthesis process, to reduce the lithium diffusion pathway. In this work, we present preliminary results on the impact of two different approaches on the electrochemical activity of TiNb₂O₇.

In order to favor the kinetics of Li intercalation/deintercalation, we have performed the partial isovalent substitution of Ti by Zr in the series Ti_{1-x}Zr_xNb₂O₇ (x = 0 – 0.5). The beneficial effect of the presence of Zr reaches its maximum in the interval x = 0.1– 0.2, limit composition of the solid solution, with a capacity of 300 mAh/g. Higher Zr contents cause the formation of Ti₂Nb₁₀O₂₇ as secondary phase, to the detriment of the specific capacity of the materials. Ongoing microstructural characterization by means of HR-STEM will allow to correlate the local effect of the presence of Zr in the structure with the macroscopic response of the material.

On the other hand, oxygen vacancies creation is a simple way of modifying electronic properties. In this work we attempted the synthesis of reduced TiNb₂O_{7-x} by using different controlled reductive atmospheres. Partial reduction keeping the block structure led in all cases to very low concentrations of vacancies, 0.1–0.3%, concentration close to 1% onwards, is associated with the formation of the TiNb₂O₆ rutile phase, which is a unique phase for 14.3% vacancies. Preliminary characterization show a significant increase of capacity (200 mAh/g) with respect to TiNbO₄ [2]. Interestingly, EELs spectra show the reduction of Nb⁵⁺ to Nb⁴⁺ and the presence of mixed Ti⁴⁺/Ti³⁺ related to the charge storage capacity.

References

- [1] Han, J.-T., Huang, Y.-H., Goodenough, J. B., *Chem. Mater.* **23**, 2027 (2011)
- [2] J. Lee, H. Kwak, S. Bak, G. Lee, S. Hong, M. Abbas, J. Bang, *Chem. Mater.* **34**, 854 (2022)

Acknowledgments

Authors acknowledge MICINN/AEI/10.13039/501100011033 for funding the Projects PID2019-106662RB-C41 and PID2019-106662RB-C44.

Fe-substituted LiTi_2O_4 ramsdellite as electrode material in lithium batteries

P. Díaz-Carrasco¹, A. Kuhn¹, N. Menéndez², F. García-Alvarado¹

¹ Departamento de Química y Bioquímica, Facultad de Farmacia, Universidad San Pablo-CEU, CEU Universities, Urbanización Montepríncipe, 28668 Boadilla del Monte, Madrid, Spain;

² Departamento de Química Física Aplicada, Facultad de Ciencias, Universidad Autónoma de Madrid, 28049 Madrid, Spain

* The corresponding author e-mail: pcarrasco.fcex@ceu.es

Keywords: solid-state structures; lithium titanate; ramsdellite; negative electrode material; lithium battery; ⁵⁷Fe Mössbauer spectroscopy

Titanium oxides and titanates have been widely investigated as negative electrode materials for lithium-ion batteries and some of them successfully commercialized. Among titanates, ramsdellite LiTi_2O_4 exhibits an interesting electrochemical behavior in both lithium insertion and extraction reactions due to the presence of a mixed transition metal oxidation state ($\text{LiTi}^{4+}\text{Ti}^{3+}\text{O}_4$). Replacement of Ti^{3+} by other transition metals as V^{3+} and Cr^{3+} has been researched to get a dual electrode [1-2].

In this work, Ti/Fe substitution of the ramsdellite compound LiTi_2O_4 has been performed yielding electrode materials with general stoichiometry $\text{LiFe}_x\text{Ti}_{2-x}\text{O}_4$, prepared by the ceramic method up to 1300 °C. Samples with $0 \leq x \leq 0.5$ resulted in well crystallized orthorhombic ramsdellite phases, space group *Pbnm*, while samples with $x > 0.5$ formed spinel, space group *Fd-3m*, as revealed by powder X-ray diffraction.

The ramsdellites were further investigated with X-EDS microanalysis, ⁵⁷Fe Mössbauer spectroscopy and lithium (de-)intercalation. This allowed to get a full insight into the Ti/Fe substitution mechanism, which turned out to be rather more complex than a predicted simple M^{3+} isovalent substitution, with participation of $\text{Fe}^{3+}/\text{Fe}^{2+}$ and $\text{Ti}^{4+}/\text{Ti}^{3+}$. Upon testing against lithium in the low voltage range (*ocv*-1 V), ramsdellite with low Ti/Fe substitution $\text{LiFe}_{0.125}\text{Ti}_{1.875}\text{O}_4$ outperformed undoped LiTi_2O_4 electrochemically, by delivering a 1st cycle capacity of 180 mAh g^{-1} at C/30 (5.3 mA g^{-1}) stabilized at 140 mAh g^{-1} upon cycling, compared to 120 and 80 mAh g^{-1} , respectively in LiTi_2O_4 . Two active redox pairs, $\text{Ti}^{4+/3+}$ and $\text{Fe}^{3+/2+}$, a high lithium diffusion coefficient and better electrical properties due to the presence of metallic iron, boosting farther electronic conductivity in $\text{LiFe}_{0.125}\text{Ti}_{1.875}\text{O}_4$, allow a noticeable capacity of 71 mAh g^{-1} still to be held at a high current of 2C (320 mA g^{-1}). In the high voltage range (*ocv*-4V), $\text{LiFe}_{0.125}\text{Ti}_{1.875}\text{O}_4$ also outmatched electrochemically higher Fe-substituted ramsdellites, which are characterized by important irreversible capacity ascribed to unavailability of $\text{Fe}^{3+}/\text{Fe}^{4+}$ redox couple and electrolyte decomposition.

References

- [1] J. C. Pérez-Flores, M. Hoelzel, F. García-Alvarado, A. Kuhn, *ChemPhysChem*, **17**, 10621069 (2016)
- [2] A. Kuhn, M. Martin, F. García-Alvarado, *Z. Anorg. Allg. Chem.*, **634**, 880886 (2008)

Acknowledgments

We thank MCIN/AEI/10.13039/501100011033 for funding the project “PID2019-106662RB-C41”. Financial support from Universidad San Pablo is also acknowledged.

Fabrication and characterization of Cu, Zn-doped $\text{Li}_4\text{Ti}_5\text{O}_{12}$ anode nanomaterials for energy conversion applications

J. Dhairat, B. A. Albiss*, A. Bozeyya

Nanotechnology Institute, Jordan University of Science and Technology, 22110, Irbid, Jordan

* The corresponding author e-mail: baalbiss@just.edu.jo

Keywords: anode material; lithium titanate; lithium-ion batteries; doping; energy storage

Copper and Zinc doped Lithium titanates $\text{Li}_{4-x}\text{Cu}_x\text{Ti}_{5-x}\text{ZnO}_{12}$ (CZ-LTO) were successfully prepared as anode materials by sol-gel method. The concentration of dopants ($x = \text{Cu}^{2+}, \text{Zn}^{2+}$) was varied from $x = 0.03$ to 0.14 to find the optimal concentration with ideal electrical properties. The effect of using different carbon-based materials on the kinetic feature of all prepared anodes was examined, which showed that the Li^+ distribution in the anode raised significantly when CB was used in preparing the electrode. The phase structure and morphology were characterized by X-ray diffraction (XRD), scanning electronic microscope (SEM) and Fourier Transform Infrared (FTIR). The XRD analysis revealed that the spinel-type LTO was obtained and the two dopants, Cu^{2+} and Zn^{2+} , inserted in the LTO structure effectively causing no significant changes in the phase structure and the crystallinity. SEM images exhibited that all prepared powders had comparable size particles distributed from 88 – 120 nm. The electrochemical properties were tested using Potentiostat Galvanostat.

Alloy nanowire arrays with controlled compositions templated by block copolymers

P38

O. Burg¹, R. Shenhar^{1*}

¹ Institute of Chemistry and the Center for Nanoscience and Nanotechnology, The Hebrew University of Jerusalem, Jerusalem 9190401, Israel.

* The corresponding author e-mail: roys@huji.ac.il, phone +972-2-6586272

Keywords: block copolymers; nanowires; bimetallic structures; thin films; alloys

Metallic nanowire arrays are promising components for nanotechnology thanks to their directional, continuous, longitudinal structure. Nanowires made from alloys of two or more metals are beneficial for certain applications such as catalysis and magnetism. The alloy composition influences the properties of the nanowires, and certain metal ratios show improved properties compared to those of their individual constituents. Yet, creating these nanowire arrays requires enhanced control over their composition and organization. This requirement may be answered by using block copolymer films, which provide three advantages: (a) they exhibit periodic arrays with typical periodicities of a few tens of nanometers; (b) the domains could be aligned using patterned substrates; (c) selective impregnation of the films with metal precursors and subsequent plasma treatment affords metallic nanowire arrays that are organized in a periodic fashion.

In this work, we use block copolymer films to create arrays of alloy nanowires with controlled compositions. We achieve this control by studying how different impregnation parameters affect the amount of metal in the nanowires and the metal ratio in alloys. Namely, impregnating with palladium precursors, followed by platinum precursors for different durations, shows how one metal increases over the other, and the rate of metal precursor replacement in the film. Additionally, impregnating with a mixture of palladium and platinum precursors in different ratios gives different Pd-Pt alloys, and elucidates the affinity of each metal to the film. These experiments give an understanding of the interaction between the metal precursors and the polymer film and lay a foundation for fabricating alloy nanowires with controlled compositions.

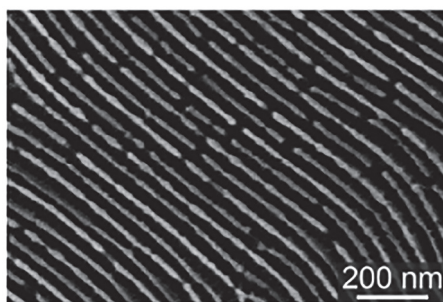


Figure: SEM image of a nanowire array made with a block copolymer template, with alternating arrangement of PdPt alloy nanowires and pure palladium nanowires [1].

References

- [1] O. Burg, R. A. Sanguramath, E. Michman, N. Eren, I. Popov, R. Shenhar, *Soft Matter*, **17**, 9937–9943 (2021)

Local structure insight into hydrogen evolution reaction with bimetal nanocatalysts

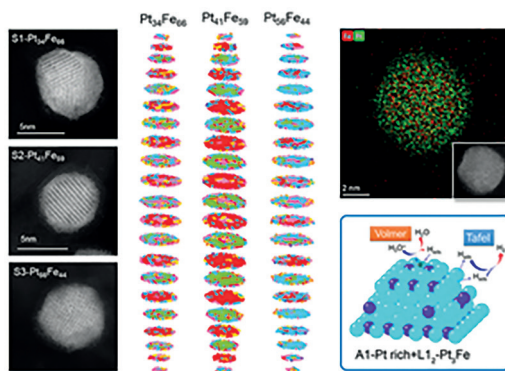
Q. Li¹, X. Xing¹

¹ Institute of Solid State Chemistry, University of Science and Technology Beijing, Beijing 100083, China.

* The corresponding author e-mail: qiangli@ustb.edu.cn, xing@ustb.edu.cn

Keywords: local structure; pair distribution function; reverse monte carlo; hydrogen evolution reaction catalysts; bimetallic alloy

The revelation of the atomic 3D structure of sub-5 nm bimetal nanocatalysts challenges the limitations of conventional methods. Notably, the identification of the cooperative relationship between the active sites and nearby coordination environment during catalytic reactions depends on the stereo distribution of local phases and chemical composition within a short range. As a model nanocatalyst in our investigation, we studied the ordered PtFe bimetals in hydrogen evolution reactions (HER). By combining pair distribution functions with reverse Monte Carlo, local-range phase symmetry, chemical composition, and atom distribution were determined. The segregation of local phase segments as disordered Pt-rich A1 and Pt₃Fe L1₂ phases can be attributed to the marked improvement of HER activity and stability in Pt₅₆Fe₄₄. Following the etching of the outermost-surface Fe, the remaining disordered segregation offered a large number of active Pt sites for discharge and electrochemical desorption reactions. It resulted in local-bonding Pt pairs that made it easier for adsorbed hydrogen atoms to recombine. The current research will provide structural insight into the local range for bimetal nanocatalysts and be valuable for the creation of new, low-cost nanocatalysts.



References

- [1] Qiang Li, He Zhu and Xianran Xing* et al, *J. Am. Chem. Soc.*, **144**, 20298–20305 (2022).
- [2] Qiang Li, Yang Ren and Xianran Xing* et al, *Natl. Sci. Rev.*, **9**, nwac053 (2022)
- [3] Qiang Li, He Zhu and Xianran Xing* et al, *Inorg. Chem.*, **57**, 10494-10497 (2018)

Acknowledgments

This work was supported by the National Natural Science Foundation of China (22090042, 21731001 and 22175018).

Impact of Surfactant-Assisted Downsizing to Luminescent nanoMOFs on Morphological and Photophysical Properties

M. Maxeiner¹, L. Wittig¹, A. Sedykh¹, T. Kasper¹, K. MüllerBuschbaum¹

¹ Institute of Inorganic and Analytical Chemistry, Justus-Liebig-University Giessen, HeinrichBuffRing 17, 35392 Giessen (Germany)

* The corresponding author e-mail: moritz.maxeiner@anorg.chemie.unigiessen.de

Keywords: nanomaterials; MOF; surfactant; luminescence; lanthanide; morphology

Throughout the last two decades, metal organic frameworks (MOFs) have been extensively studied because of their capability of incorporating molecules and ions into the pores of the 3D crystal structure. Optical sensors, optoelectronic or medical applications are highly interesting applications of luminescent MOFs. The sensitizer effect of organic linkers makes lanthanides remarkable phosphors besides other advantages. [1]

This work approaches the question if downsizing to nanometer range (^NMOF) has an impact on the performance of MOFs. Therefore, nanosized ^NLn-bdc, ^NDUT 5(Ln) and ^NMOF 253(Ln) (Ln = Eu, Tb) have been synthesized by a surfactant approach and investigated regarding their morphological and photophysical properties. Insertion of lanthanides was carried out by either *in situ* synthesis or post impregnation.

In principle, ^NMOFs achieve a better dispersibility and stability in dispersions by having a homogenous small particle size and size distribution. The above-mentioned ^NMOFs were examined using dynamic light scattering and scanning electron microscopy and show narrow particle size distributions of 20–60 nm. Miniaturized crystals (i.e., a few unit cells) lead to a reduction of crystallinity and long-range order within the crystal. As a consequence, reflections in powder diffractometry become broader for all three ^NMOFs in accordance with the nanoscale of the crystallites. [2]

Moreover, ^NTb-bdc exhibits an excellent quantum yield of 78%, despite the additional surfactant content leading to an additional broad absorption band at 400–600 nm recorded by UV-Vis diffuse reflectance spectroscopy. Depending on the ^NMOF and lanthanide, the energy transfer processes can be even more efficient. Furthermore, excitation and emission photoluminescence spectra endorse the phenomenon of improved energy transfer efficiency.

The ^NMOFs discussed exhibit morphological properties as well as photophysical results that make them highly interesting for further investigation for the potential optical applications mentioned above.

References

- [1] R. Freund, O. Zaremba, G. Arnauts, R. Ameloot, G. Skorupskii, M. Dincă, A. Bavykina, J. Gascon, A. Ejsmont, J. Goscińska, M. Kalmutzki, U. Lächelt, E. Ploetz, C. S. Diercks, S. Wuttke, *Angew. Chemie - Int. Ed.*, **60**, 23975–24001 (2021).
- [2] M. J. Neufeld, H. Winter, M. R. Landry, A. M. Goforth, S. Khan, G. Pratz, C. Sun, *ACS Appl. Mater. Interfaces*, **12**, 26943–26954 (2020).

Acknowledgments

This work is generously funded by the Deutsche Forschungsgemeinschaft (DFG) within the project MU-1562/13-1.

Hydrophobic materials based on heteroboroxines

R. Jambor^{1*}, M. Srb¹, M. Novák¹

¹ Department of General and Inorganic Chemistry, Faculty of Chemistry and Technology, University of Pardubice, Studentská 95, Pardubice, 53002, Czech Republic

* The corresponding author e-mail: roman.jambor@upce.cz

Keywords: hydrophobicity; heteroboroxines; polymers; spin coating

Probably the most widely used hydrophobic compounds reducing the surface energy are fluorocarbons represented by poly(tetrafluoroethylene). Despite very good hydrophobic properties, fluorocarbons show certain limits, especially price and hazardous behavior on the environment. Thus, research of fluorine-free materials for a hydrophobic coating is actual. Accordingly, several alternative routes using non-fluorinated compounds were proposed such as long alkyl chains, long-chain fatty acids, organosilanes, polysiloxanes (especially polydimethylsiloxane PDMS) or polymers with combined chemistry.¹ However, these non-fluorinated compounds often do not exhibit such good hydrophobic properties as fluorinated materials. For this reason, these materials are used in the combination with various additives, which can both further reduce the surface energy but also create a suitable roughness of the solid substrate. Here we report the synthesis of N→M intramolecularly coordinated heteroboroxines (HBO) having the central six membered ring MB₂O₃, where M is Ga or Sn.² The main advantage of the HBO is their solubility in organic solvents or polymers, which allows an easy preparation of thin layers containing the HBOs by printing or spin coating. New HBOs were tested as additives in already known polymer matrices and finally, the resulting thin layers were tested as suitable hydrophobic materials.

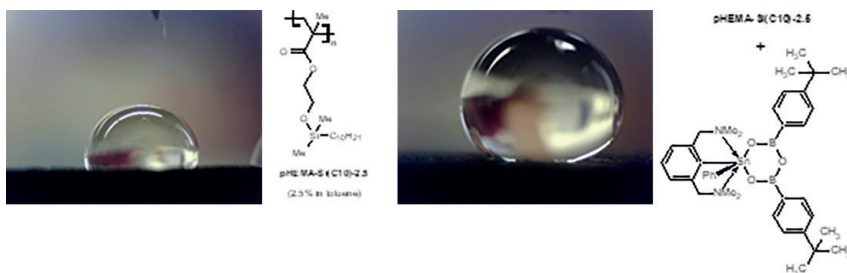


Figure 1: The photos of water droplet on PE coated with silanized polyacrylate (left) and on PE coated with silanized polyacrylate in combination with stannaboroxine (right).

References

- [1] Z. Shi, I. Wyman, G. Liu, H. Hu, H. Zou, J. Hu, *Polymer*, **54**, 6406–6412 (2013)
- [2] X. Yin, C. Sun, B. Zhang, Y. Song, N. Wang, L. Zhu, B. Zhu., *Chem. Eng. J.*, **330**, 202–212 (2017)
- [3] A. B. López, J. C. de la Cal, J. M. Asua, *Polymer*, **124**, 12–21 (2017)
- [4] Y. Milasheuskaya, J. Schwarz, L. Dostál, Z. Růžičková, M. Bouška, Z. Olmrová Zmrhalová, T. Syrový, R. Jambor, *Dalton Trans.*, **50**, 18164–18172 (2021)

Acknowledgments

This work was supported by the Czech Science Foundation (GA23-06548S).

Preparation of GeTe nanoparticles by low temperature synthetic method

P42

M. Bouška¹, Y. Milasheuskaya², R. Jambor², P. Němec¹

¹ Department of Graphic Arts and Photophysics, Faculty of Chemical Technology, University of Pardubice, Studentská 573, 53210 Pardubice, Czech Republic;

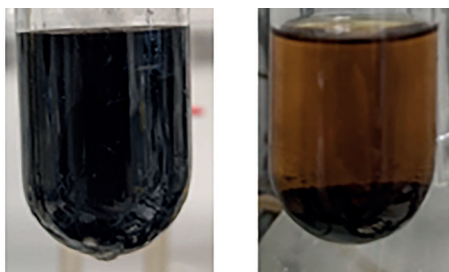
² Department of General and Inorganic Chemistry, Faculty of Chemical Technology, University of Pardubice, Studentská 573, 53210 Pardubice, Czech Republic

* The corresponding author e-mail: marek.bouska@upce.cz

Keywords: nanoparticles; GeTe; organometallic precursors; XRD; SEM EDX; DLS

Synthesis of tellurium-based materials via chemical synthesis is usually based on the reduction of the tellurium source (for example Na_2TeO_3 or TeCl_4) [1] together with (semi)metallic source (GeI_2 or SnCl_2) [2] at the elevated temperatures (above 150 °C) for several hours. There are also reports showing that similar procedure in the presence of second metallic source (for example InCl_3 , $\text{In}(\text{NO}_3)_3$) or even the metallic nanoparticles (NPs) may provide doped telluride materials [3]. The presence of NPs with various diameters gives the possibility to control the dimensions of nanostructures of tellurium-based materials [4]. Contrary, the reports of chemical synthesis at room temperatures are in fact unknown.

The aim of this work is preparation of GeTe nanoparticles by low temperature synthetic method by the help new organometallic precursors. Different preparation methods and characterization GeTe nanoparticles will be discussed. The characterization of prepared nanomaterial was performed on the basis of scanning electron microscopy with energy-dispersive X-ray analysis, X-ray diffraction, Raman spectroscopy and dynamic light scattering.



References

- [1] R. Biswas, P. Deb, S. Das, *Opt. Mater.* 47, 586–588 (2015).
- [2] M. R. Buck, I.T. Sines, R.E. Schaak, *Chem. Mat.*, 22(10) 3236–3240 (2010)
- [3] K. Kadel, L. Kumari, X. Wang, W. Li, J. Y. Huang, P. P. Provencio, *Nanoscale Res. Lett.*, 9(1), 227 (2014).
- [4] S. Atherton, B. Steele, S. Sasaki, *Crystals*, 7(3) (2017).

Acknowledgments

The financial support of the Czech Science Foundation under the project No. 22-07635S is greatly acknowledged.

High-spin vs low-spin Ni²⁺ ions in highly distended octahedral environments: Sr₂NiO₂Cu₂Se₂, Sr₂NiO₂Cu₂S₂ and the solid solution Sr₂NiO₂Cu₂(Se_{1-x}S_x)₂

R. D. Smyth¹, J. N. Blandy^{1,2}, Z. Yu¹, S. Liu^{1,3}, C. V. Topping⁴, S. J. Cassidy^a, C. F. Smura¹, D. N. Woodruff¹, P. Manuel⁵, C. L. Bull^{5,6}, N. P. Funnell⁵, J. E. McGrady¹, S. J. Clarke^{1*}

¹ Department of Chemistry, University of Oxford, Inorganic Chemistry Laboratory, South Parks Road, Oxford OX1 3QR, UK;

² Diamond Light Source Ltd., Harwell Science and Innovation Campus, Didcot OX11 0DE, UK;

³ College of Chemistry and Chemical Engineering, Anhui University, Hefei 230601, Peoples Republic of China;

⁴ Department of Physics, University of Oxford, Clarendon Laboratory, Parks Road, Oxford OX1 3PU, UK;

⁵ ISIS Facility, Rutherford Appleton Laboratory Harwell Oxford, Didcot, OX1 10QX, UK;

⁶ School of Chemistry, The University of Edinburgh, King's Buildings, David Brewster Road, Edinburgh EH9 3FJ, UK

* The corresponding author e-mail: simon.clarke@chem.ox.ac.uk

Keywords: nickel; mixed-anion; antiferromagnetic ordering; oxide chalcogenide; spin-state

Sr₂NiO₂Cu₂Se₂, comprising alternating [Sr₂NiO₂]²⁺ and [Cu₂Se₂]²⁻ layers, is reported. Powder neutron diffraction shows that the Ni²⁺ ions, which are in a highly distended NiO₄Se₂ environment with D_{4h} symmetry, adopt a high-spin configuration and carry localised magnetic moments which order antiferromagnetically below ≈160 K in a $\sqrt{2}a \times \sqrt{2}a \times 2c$ expansion of the nuclear cell with an ordered moment of 1.31(2) μ_B per Ni²⁺ ion. The adoption of the high spin configuration for this d⁸ cation in a pseudo-square planar ligand field is supported by consideration of the experimental bond lengths and the results of Density Functional Theory (DFT) calculations. This is in contrast to the sulfide analogue Sr₂NiO₂Cu₂S₂, which according to both experiment and DFT calculations has a much more distended ligand field more consistent with a low spin configuration, which is commonly found for square planar Ni²⁺ and supported by the fact that there is no evidence for a magnetic moment on the Ni²⁺ ions. Examination of the solid solution Sr₂NiO₂Cu₂(Se_{1-x}S_x)₂ shows direct evidence from the evolution of the crystal structure and the magnetic ordering for the transition from high-spin selenide-rich compounds to low-spin sulfide-rich compounds. Close consideration of the experimental and computed Ni coordination environments and subtle changes in the Ni coordination environment as a function of temperature in addition to transitions evident in the transport properties and magnetic susceptibilities in both the end members, Sr₂NiO₂Cu₂Se₂ and Sr₂NiO₂Cu₂S₂, suggest that simple high-spin and low-spin models for Ni²⁺ may not be entirely appropriate and point to further complexities in these compounds.

Acknowledgments

This work was supported by the UK EPSRC (Grants EP/P018874/1, EP/R042594/1, EP/T027991/1 and EP/M020517/1), ISIS pulsed neutron and muon source (DOI: 10.5286/ISIS.E.RB2000047, 10.5286/ISIS.E.RB1620080 and 10.5286/ISIS.E.RB2000252), Diamond Light Source Ltd (EE13284, EE18786 and CY25166) and the ESRF (CH-5335).

Complex magnetic ordering of the mixed-valent layered iron oxychalcogenides $\text{Ca}_2\text{Fe}_{2.6}\text{O}_3\text{S}_{2-x}\text{Se}_x$ ($x = 0, 0.5, 1, 1.5$)

A. Gillette¹, B. Sheath¹, S. J. Clarke¹

¹ Department of Chemistry, University of Oxford, Inorganic Chemistry Laboratory,
South Parks Road, OX1 3QR, U.K.

* The corresponding author email: simon.clarke@chem.ox.ac.uk

Keywords: mixed-valent; magnetic ordering; neutron scattering; layered oxychalcogenides

The oxychalcogenides $\text{Ca}_2\text{Fe}_{2.6}\text{O}_3\text{S}_{2-x}\text{Se}_x$ ($0 \leq x \leq 1$) (originally reported by Zhang et. al. in 2016^[1]) are mixed-valent compounds of Fe^{2+} and Fe^{3+} cations in FeO_2 and Fe_2O square layers, which are anti-types one another, separated by calcium chalcogenide slabs. The Fe_2O layers are Fe-deficient and as the Se content increases, the iron/vacancy ordering is suppressed within these layers. The results of neutron and synchrotron X-ray powder diffraction experiments which reveal the complex magnetic ordering and subtle structural features of these compounds both as functions of temperature and of composition will be described along with preliminary analysis of further related compounds.

References

[1] H. Zhang et al. *J. Phys.: Condens. Matter.* **28**, 145701 (2016)

Acknowledgments

We thank: the Canterbury Institute (registered charity no. 1186234) for funding to support the studies of ANG; the Institut Laue-Langevin (ILL) and the Diamond Light Source Ltd for the award of beam time.

Tuning magnetism and superconductivity in transition metal chalcogenides as a function of composition

L. Taskesen*¹, S. J. Clarke¹

¹ Department of Chemistry, University of Oxford, South Parks Rd, Oxford, OX1 3QR, UK.

* *The corresponding author email: ludmila.babicova@chem.ox.ac.uk*

Keywords: chalcogenides; ferromagnetism; antiferromagnetism; superconductivity; X-ray diffraction

The discovery of high-temperature superconductivity in La(O,F)FeAs has sparked renewed interest in intermetallics bearing the square anti-fluorite layers of M_2X_2 (M = transition metal, X = pnictide or chalcogenide), since this is where superconductivity is believed to occur. [1] The tetragonal FeSe, composed of anti-fluorite layers of Fe_2Se_2 , has been found to be superconducting at 8K. [2] Upon insertion of an alkali metal into this structure, a new phase – AFe_2Se_2 – emerges, with an increased superconducting transition temperature of 30K. [3] AFe_2Se_2 belongs to the 122 family of iron-based superconductors, adapting a versatile $ThCr_2Si_2$ -type structure, which has been known to demonstrate diverse magnetic phenomena.^[4,5] In this research, we are exploring the magnetic regions of nickel and cobalt-based 122 phases, which adapt the $ThCr_2Si_2$ -type structure. The solid solutions of $KNi_{2-x}Co_xSe_2$ and $RbNi_{2-x}Co_xSe_2$ are both particularly interesting in terms of the magnetic states present in the members of their respective members; KNi_2Se_2 is superconducting, while KCo_2Se_2 is ferromagnetic, and the newly reported middle member – $KNiCoSe_2$ – shows antiferromagnetic behaviour. $RbNi_2Se_2$ is a new, unreported phase and is an antiferromagnet, while $RbNiCoSe_2$ and $RbCo_2Se_2$ are both ferromagnets. Therefore, our study shows the tuning of magnetism as a function of composition across the solid solution series of $KNi_{2-x}Co_xSe_2$ and $RbNi_{2-x}Co_xSe_2$.

References

- [1] M. Shatruk, *Solid State Chem. Soc.*, **272**, 198–209 (2019)
- [2] G. Zhou et al., *Appl. Phys. Lett.*, **108**, 16432–16442 (2016)
- [3] J. R. Neilson, T. M. McQueen, A. Llobet, J. Wen, M. R. Suchomel, *Phys. Rev. B - Condens. Matter Mater. Phys.*, **87**, 1–11 (2013)
- [4] H. Lei et al., *J. Phys. Condens. Matter*, **26**, 184505 (2014)
- [5] P. Zhang, H. F. Zhai, *Condens. Matter*, **2**, 1–14 (2017)

Acknowledgments

This work is supported by EPSRC Centre for Doctoral Training for Future Manufacturing (OxICFM), EP/S023828/1.

Lattice dynamics of $\text{Cs}_2[\text{Mo}_2\text{O}_7]\cdot\text{CsX}$ ($X = \text{Cl}, \text{Br}, \text{I}$)

A. K. Weber¹, K. Denisova², P. Lemmens², A. Möller^{1*}

¹ Department of Chemistry, Johannes Gutenberg University, Duesbergweg 10-14, 55128 Mainz, Germany;

² IPKM, TU Braunschweig, Mendelssohnsstr. 3, 38106 Braunschweig, Germany

* The corresponding author e-mail: angela.moeller@uni-mainz.de

Keywords: Raman spectroscopy; lattice dynamics; thermal analysis; x-ray diffraction; solid-state synthesis

Members of the $A_2[\text{Mo}_2\text{O}_7]\cdot AX$ family of compounds with $A = \text{K}, \text{Rb}, \text{Cs}$ and $X = \text{Cl}, \text{Br}, \text{I}$, can be prepared from reacting $A_2\text{MoO}_4$ with MoO_3 in alkaline metal halide fluxes [1]. The isotopic compounds crystallize in the space group $P6_3/mmc$. The crystal structure consists of isolated $[\text{Mo}_2\text{O}_7]^{2-}$ units centered in a hetero-honeycomb layer. An interesting feature of these multi-anionic compounds is the pyromolybdate anion in a rare D_{3h} symmetry. Here, we present the assignment of lattice modes as a function of X for the Cs-series based on polarized single-crystal Raman spectra. In order to distinguish those modes representative of the two crystallographically independent alkaline metal sites, we include the $\text{Rb}_2[\text{Mo}_2\text{O}_7]\cdot\text{RbCl}$ and $\text{KCs}[\text{Mo}_2\text{O}_7]\cdot\text{CsCl}$ derivatives.

The focus of this study extends to explore the stiffness of the two dissimilar structural anionic entities by temperature dependent Raman scattering experiments. We show the increase in energy for the fundamental $[\text{Mo}_2\text{O}_7]^{2-}$ stretching modes with decreasing temperature, while in contrast the in-plane modes related to the halide-part of the structure soften. Furthermore, intriguing insights into the interplay of the hetero-honeycomb layer on the symmetry reduction of the pyromolybdate will be discussed.

References

- [1] A. K. Weber, M. Panthöfer, and A. Möller, *Inorg. Chem.* **61**, 10108 (2022).

Novel oxochloridoselenites(IV) with cuban-derived structural motives

M. A. Bonnin¹, C. Feldmann^{1*}

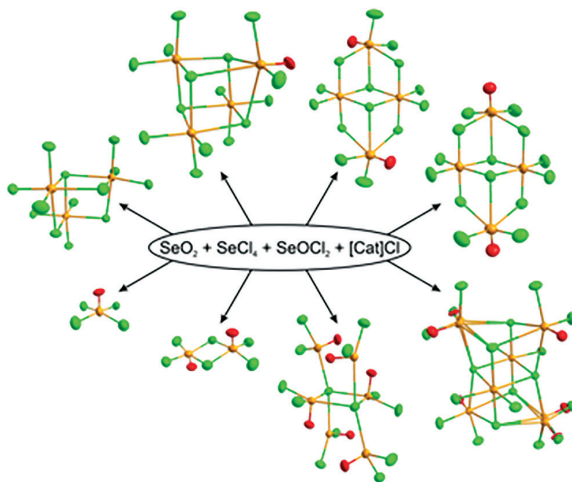
¹ Karlsruhe Institute of Technology, Engesserstr. 15, 76131 Karlsruhe

* The corresponding author e-mail: claus.feldmann@kit.edu

Keywords: oxochloridoselenites(IV); ionic liquid; synthesis near room temperature; crystal structure; cuban-derived structural motives

Metal oxides often require high temperatures or polar solvents for reactions due to their ionic bonding and high lattice energy. However, high temperatures typically lead to the most stable product and prevent the formation of novel metastable compounds. Selenium dioxide is a promising starting material, possessing certain covalent bonding components and less high lattice energy than most metal oxides, while not being a molecular compound. Since polar solvents often form coordination compounds with metal oxides in order to dissolve them, we used an Ionic Liquid as solvent [1].

Here, we present the novel oxochloridoselenites $[\text{BMIm}][\text{Se}_4\text{Cl}_{15}\text{O}]$ **1**, $[\text{BMIm}]_2[\text{Se}_4\text{Cl}_{14}\text{O}_2]$ **2**, $[\text{BMPyr}]_2[\text{Se}_4\text{Cl}_{14}\text{O}_2]$ **3**, $[\text{BMPyr}]_2[\text{Se}_6\text{Cl}_{18}\text{O}_4]$ **4** and $[\text{BMPyr}]_2[\text{Se}_6\text{Cl}_{14}\text{O}_6]$ **5** ($[\text{BMIm}] = 1\text{-butyl-3-methylimidazolium}$; $[\text{BMPyr}] = 1\text{-butyl-1-methylpyrrolidinium}$). **1–4** were obtained by the reaction of SeO_2 , SeCl_4 , (AlCl_3) and $[\text{BMIm}]\text{Cl}$ or $[\text{BMPyr}]\text{Cl}$ at 60–80°C. **1–4** consist of oxochloridoselenites, whose structures are derived from the tetrameric cubane-like $[\text{SeCl}_4]_4$, which shows stepwise degradation in the presence of Lewis bases (SeO_2). Depending on the stoichiometry and temperature, one to four SeCl_2O units are bound to edge-linked $[\text{SeCl}_6]^{2-}$ octahedra, which remained from the degradation of $[\text{SeCl}_4]_4$. The addition of SeOCl_2 to the reactants (SeO_2 , SeCl_4 , $[\text{BMPyr}]\text{Cl}$) at room temperature leads to **5** with an anionic structure, which consists of an edge-linked square pyramidal $[\text{Se}_2\text{Cl}_6\text{O}_2]^{2-}$ unit with SeCl_2O units bound to the bridging chlorine. All compounds were characterized by single crystal X-ray diffraction as well as X-ray powder diffraction, infrared spectroscopy and thermal analysis [2].



References

- [1] A. R. West, *Solid State Chemistry and Its Applications*, Wiley, Chichester (2015).
 [2] M. A. Bonnin, C. Feldmann, *in preparation*.

Acknowledgments

The authors acknowledge the Deutsche Forschungsgemeinschaft (DFG) for funding within the project "Crown-Ether-Coordination-Compounds with Unusual Structural and Optical Properties/Crown I (FE 911/14-1)".

Wurtzite-Type Be_2PN_3 - a new and hard-type material

P48

G. Krach¹, M. Pointner¹, K. Witthaut¹, W. Schnick^{1*}

¹ Department of Chemistry, Ludwig-Maximilians-University Munich,
Butenandtstraße 5–13, 81377 Munich (Germany)

* The corresponding author e-mail: wolfgang.schnick@cup.uni-muenchen.de

Keywords: nitrides; HP/HT-synthesis; beryllium; hard type materials; TEM; DFT calculations

Beryllium nitrides are known for their high incompressibility and hardness. One example is the ultra-incompressible spinel modification of BeP_2N_4 with a bulk modulus of 325(8) GPa [1,2]. The synthesis of hard and low density materials is a favourable aim in the field of current nitride research.

In this contribution, we report about the high-pressure high-temperature synthesis of the novel wurtzite-type Be_2PN_3 and its characterization by means of PXRD, TEM, UV-VIS spectroscopy and FTIR. Moreover, we present DFT-calculations examining the elastic properties.

Be_2PN_3 was synthesized by the reaction of stoichiometric amounts of Be_3N_2 and P_3N_5 in a HP-/HT approach at 9 GPa and 1500 °C in a large volume press.

The crystal structure ($Cmc2_1$ (no. 36), $Z = 4$, $a = 8.4524(2)$, $b = 4.8812(1)$, $c = 4.57422(9)$ Å) was solved and refined based on powder X-ray diffraction data and confirmed by tilt series measured with a transmission electron microscope as well as FTIR spectroscopy.

The wurtzite-analogue structure is built up of all corner sharing PN_4 - and BeN_4 -tetrahedra resulting in a coordination description of $\text{Be}_2^{[4]}\text{P}^{[4]}\text{N}_3$ [4]. The tetrahedra form *dreier* rings [3]. In each layer PN_4 -tetrahedra are surrounded by six BeN_4 -tetrahedra. The N atoms possess two different coordination environments: N1 is surrounded by three Be atoms and one P atom, whereas N2 is surrounded by two Be and two P atoms.

Elastic properties were calculated with the Vienna Ab initio Simulation Package (VASP). Considering the results for Bulk- and Shear-Modulus a Vickers hardness of ca. 28 GPa was determined. Wurtzite-type Be_2PN_3 is expected to be harder than SiC and WC (both 25 GPa) and is in the same range with WB_2 (28 GPa) or VC (29 GPa) [4].

References

- [1] F. J. Pucher, S. R. Römer, F. W. Karau, W. Schnick, *Chem. Eur. J.* **2010**, *16*, 7208.
- [2] S. Vogel, M. Bykov, E. Bykova, S. Wendl, S. D. Kloß, A. Pakhomova, N. Dubrovinskaja, L. Dubrovinsky, W. Schnick, *Angew. Chem.* **2020**, *132*, 2752; *Angew. Chem. Int. Ed.* **2020**, *59*, 2730.
- [3] F. Liebau, *Structural Chemistry of Silicates*, Springer, Berlin, **1985**.
- [4] Friedrich, B. Winkler, E. A. Juarez-Arellano, L. Bayarjargal, *Materials* **2011**, *4*, 1648–1692.

Acknowledgments

Financial support by the Friedrich-Naumann-Foundation for a PhD fellowship for G.K. is gratefully acknowledged.

Ionic-liquid-based synthesis of Ge_3N_4 nanoparticles

F. Jung^{1*}, C. Feldmann¹

¹ Institute for Inorganic chemistry, Karlsruhe Institute of Technology, Engesserstraße 15, 76131 Karlsruhe, Germany

* The corresponding author e-mail: felix.jung@kit.edu

Keywords: germanium nitride; ionic liquid; nanomaterial; semiconductor; photoluminescence

With the discovery of GaN as a luminescent compound in blue-light emitting diodes (LEDs), nitride-based semiconductors received considerable attention despite their often demanding synthesis. [1] By reducing the particle size to few nanometers, the optical properties of semiconductors can be tuned due to quantum confinement, but their higher surface area and associated reactivity also increase the risk of hydrolysis. By adaptation of the synthesis route for GaN nanoparticles employed by Gaiser *et al.* [2], Ge_3N_4 nanoparticles were prepared in a liquid-phase synthesis for the first time.

For this purpose, $\text{Ge}(\text{NH})_2$ was synthesized by reaction of GeI_4 with KNH_2 in liquid NH_3 . The imide was suspended in $[\text{Bu}_3\text{MeN}][\text{NTf}_2]$, a room-temperature ionic liquid, and subsequently heated to 290 °C for 1 h for crystallization. Washing with acetonitrile and subsequent drying under reduced pressure yielded Ge_3N_4 as a colorless powder.

Successful decomposition of $\text{Ge}(\text{NH})_2$ to Ge_3N_4 was confirmed by infrared spectroscopy (IR), elemental analysis and energy-dispersive X-ray spectroscopy (EDXS). Powder X-ray diffraction (PXRD) and high resolution transmission electron microscopy (HRTEM) showed overall low crystallinity, but indicated the presence of crystalline Ge_3N_4 particles with a mean diameter of 4.7 ± 1.2 nm. A direct optical band gap of 4.1 eV was determined by UV-Vis spectroscopy, and the obtained powder showed green fluorescence with a broad emission peak centered around 540 nm. [4] A photoluminescence quantum yield of 14 ± 1 % was measured for the obtained Ge_3N_4 nanoparticles.

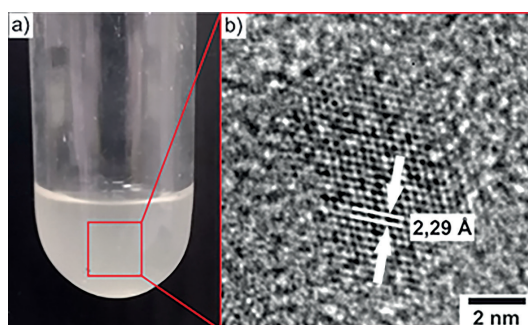


Figure: a) Suspension of washed Ge_3N_4 nanoparticles in acetonitrile and b) HRTEM image of a Ge_3N_4 nanoparticle showing lattice fringes. The measured lattice fringe spacing of 2.29 Å corresponds to $d(202)$ of $\alpha\text{-Ge}_3\text{N}_4$. [3]

References

- [1] S. C. Jain, M. Willander, J. Narayan, R. V. Overstraeten, *J. Appl. Phys.*, **87**, 965–1006 (2000)
- [2] H. F. Gaiser, R. Popescu, D. Gerthsen, C. Feldmann, *Chem. Comm.*, **56**, 2312–2315 (2020)
- [3] S. N. Ruddlesden, P. Popper, *Acta Cryst.*, **11**, 465–468 (1958)
- [4] F. Jung, R. Popescu, D. Gerthsen, C. Feldmann, *in preparation*

Structural influence of lone pairs in GeP_2N_4 , a germanium(ii) nitridophosphate

S. J. Ambach¹, C. Somers², T. de Boer², L. Eisenburger¹, A. Moewes², W. Schnick¹

¹ University of Munich (LMU), Department of Chemistry, Butenandtstraße 5-13, D-81377 Munich, Germany;

² University of Saskatchewan, Department of Physics and Engineering Physics, 116 Science Place, Saskatoon, Saskatchewan, S7N 5E2 Canada

* The corresponding author e-mail: wolfgang.schnick@uni-muenchen.de

Keywords: germanium; high-pressure; lone pair; nitridophosphates; solid-state structures

Owing to their widespread properties, nitridophosphates are of high interest in current research. Explorative high-pressure high-temperature investigations yielded various compounds with stoichiometry MP_2N_4 ($M = \text{Be}, \text{Ca}, \text{Sr}, \text{Ba}, \text{Mn}, \text{Cd}$), which are discussed as ultra-hard or luminescent materials, when doped with Eu^{2+} . [1]

Here, we report the first germanium nitridophosphate, GeP_2N_4 , synthesized from Ge_3N_4 and P_3N_5 at 6 GPa and 800 °C. [2] The structure was determined by single-crystal X-ray diffraction and confirmed as main constituent in corresponding samples by Rietveld refinement. Further characterization was done by energy-dispersive X-ray spectroscopy, density functional theory calculations, IR and NMR spectroscopy. The highly condensed network of PN_4 -tetrahedra and GeN_3 trigonal pyramids shows a strong structural divergence to other MP_2N_4 compounds, which is attributed to the stereochemical influence of the lone pair of Ge^{2+} . Thus, the formal exchange of alkaline earth cations with Ge^{2+} may open access to various compounds with literature-known stoichiometry, however, new structures and properties.

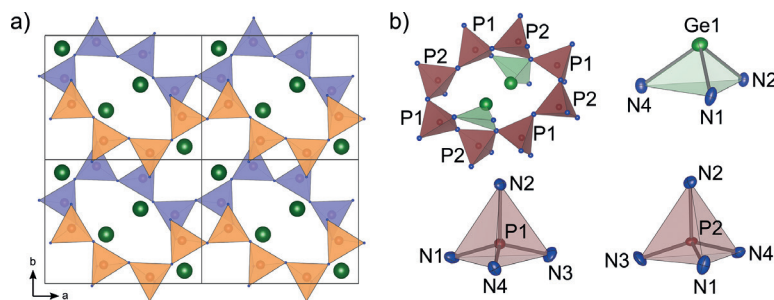


Figure 1: a) Structure of GeP_2N_4 consisting of undulated chains of PN_4 tetrahedra (blue, orange) and Ge^{2+} ions (green). b) Polyhedra of the GeP_2N_4 structure.

References

- [1] F. J. Pucher, A. Marchuk, P. J. Schmidt, D. Wiechert, W. Schnick, *Chem. Eur. J.*, **21**, 6443-6448 (2015)
- [2] S. J. Ambach, C. Somers, T. de Boer, A. Moewes, W. Schnick, *Angew. Chem. Int. Ed.*, **62**, e202215393 (2023)

Acknowledgments

This work was supported by the Deutsche Forschungsgemeinschaft (project SCHN 377/18). Support by the Natural Sciences and Engineering Research Council of Canada, the Canada Research Chair program, the Compute Canada and the Plato computing cluster at the University of Saskatchewan is gratefully acknowledged.

Ca₅AsSb(NH)₂ – a cation-deficient Antiperovskite with A-site ordering

T. Chau¹, S. Rudel¹, D. Han¹, F. Wolf¹, T. Bein¹, H. Ebert¹, W. Schnick¹

¹ Department of Chemistry, Ludwig-Maximilians-University Munich, Butenandtstraße 5–13, 81377 Munich, Germany

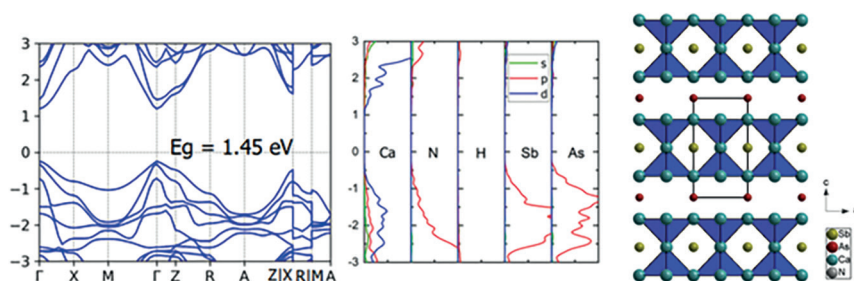
* The corresponding author e-mail: wolfgang.schnick@uni-muenchen.de

Keywords: perovskite; photovoltaic; lead-free; ammonothermal; DFT-calculations

Inorganic antiperovskites with the formula X_3AN ($X = \text{Ba}, \text{Sr}, \text{Ca}, \text{Mg}$; $A = \text{As}, \text{Sb}$) have recently been reported to exhibit excellent optoelectronic properties like small carrier effective masses, suitable direct bandgaps, high optical absorption coefficients as well as allowed optical transitions at band edges. These properties can be tuned depending on the X and A site. Extending the composition to quaternary antiperovskites ($X_6AA'N_2$) enables the enlargement of the theoretical maximum solar cell efficiencies to above 29%. [1-2]

Here we report on the ammonothermal synthesis of Ca₅AsSb(NH)₂. The compound crystallizes in the tetragonal space group $P4/mmm$. Its crystal structure was solved and refined by scXRD leading to an X/A which could be also confirmed by SEM-EDX measurements. Further investigations were carried out using powder X-ray diffraction, UV/Vis-spectroscopy and density functional theory calculations.

The new imide compound feature a distorted square-pyramidal coordination geometry around the imide-group (Ca₅NH). The structure shows layers of Ca²⁺ vacancies with an alternating As³⁺ and Sb³⁺ coordination along the A -site. Due to the alternating orientation of the imide-groups and the introduced vacancies, two different A -site coordination can be observed namely a Ca₈As-cube and a Ca₁₂Sb-cuboctahedra. The photovoltaic-related properties are currently being investigated.



References

- [1] D. Han, C.Feng, M.-H. Du, T. Zhang, S. Wang, G. Tang, T. Bein, H. Ebert *J. Am. Chem. Soc.* 2021, **143**, 12369–12379.
- [2] Y. Mochizuki, H.-J. Sung, A. Takahashi, Y. Kumagai, F. Oba *Phys. Rev. Mater.* 2020, **4**, 044601-1–14.

Morin transition in β -Fe₂SeO

N. Qureshi¹, R. Morrow², S. Eltoukhy², V. Grinenko^{3,4}, Y. A. Onykiienko³, D. S. Inosov³, M. Valldor⁵

¹ Institute Laue Langevin, 71 Ave Martyrs, CS 20156, F-38042 Grenoble 9, France;

² Leibniz Institute for Solid State and Materials Research IFW Dresden, Helmholtzstraße 20, D-01069 Dresden, Germany;

³ Institute for Solid State and Materials Physics, TU Dresden, Haeckelstraße 3, D-01069 Dresden, Germany;

⁴ Tsung-Dao Lee Institute, Shanghai Jiao Tong University, Pudong, 201210 Shanghai, China; ⁵ Chemistry Department, Centre for Material Science & Nanotechnology SMN, University of Oslo, Sem Sælands vei 26, N-0315 Oslo, Norway

* The corresponding author e-mail: b.m.valldor@kjemi.uio.no, phone: +47-22855676

Keywords: bichalcogenide; anti-perovskite; chiral structure; magnetism; neutron diffraction

Bichalcogenides offer a particularly versatile multi-anion chemistry [1]. Through a chemical reaction in a salt melt it was possible to obtain two different modifications of compound Fe₂SeO, which can be described as a 1/3 metal-vacant anti-perovskite structure [2]. The high-temperature modification, β -Fe₂SeO, is described in the chiral, non-centrosymmetric space group *P*31, which is promising for magnetic investigations due to possible magneto-electric couplings.

Despite a difficult synthesis and an obvious meta-stability of β -Fe₂SeO, it was possible to obtain a relatively pure polycrystalline sample by reaction in a salt flux, so that an extensive investigation, including neutron diffraction and thermodynamics, could be performed.

Thermodynamic and magnetic data reveal two magnetic phase transitions. In the temperature range 105–80 K, the magnetic state can be described as a canted antiferromagnet. However, an abrupt change in magnetism is observed at 79 K, below which a collinear antiferromagnetic state evolves. The most obvious difference between the magnetic states is a spin-flop, where the spins reorient themselves about 90 degrees within a very narrow temperature range. This type of phase change is known in literature as a Morin transition, which is very rare, and was first observed for Fe³⁺ in α -Fe₂O₃ (hematite) [3], but in β -Fe₂SeO iron is +2; As the Morin transition is accompanied by strong, competing magnetic interactions and a significant magneto-electric coupling, the question is: are Heisenberg-like spins really necessary to have observable magneto-electric effects?

References

- [1] M. Valldor, *Inorganics*, **4**, 23 (2016), <https://doi.org/10.3390/inorganics4030023>
- [2] M. Valldor, T. Wright, A. Fitch, Yu. Prots, *Angew. Chem. Int. Ed.*, **55**, 9380–9383 (2016)
- [3] I. E. Dzialoshinskii, *Soviet Phys. JETP*, **5**, 1259 (1957)

Acknowledgments

This work is supported by the Norwegian Research Council (NFR) through project 301711, and by the German Science Foundation (DFG) through SFB1143.

Electron-Electron and Electron-Phonon Interactions in van-der-Waals compounds: MOX , $M = \text{Sc, Ti, V, Fe}$ and $X = \text{Cl, Br}$

F. Predelli¹, F. Büscher¹, P. Lemmens^{1*}, V. P. Gnezdilov², Yu. G. Pashkevich³, T. N. Shevtsova³, S. Berinskat⁴, A. Möller⁴

¹ IPKM, TU Braunschweig, Mendelssohnsstr. 3, 38106 Braunschweig, Germany;

² B. Verkin Institute for Low Temperature Physics and Engineering of NASU, 47 Nauky Ave., Kharkiv, 61103 Ukraine;

³ Donetsk Institute for Physics & Engineering named after O. O. Galkin (Donetsk PhysTech) of NASU, 46 Nauki ave. Kyiv, 03028 Ukraine;

⁴ Department of Chemistry, Johannes Gutenberg University, Duesbergweg 10-14, 55128 Mainz, Germany

* *The corresponding author e-mail:* p.lemmens@tu-bs.de

Keywords: Raman spectroscopy; lattice dynamics; DFT-calculations; group theory; phase transitions; mixed anions

The isostructural series of compounds, MOX , $M = \text{Sc, Ti, V, Fe}$, and $X = \text{Cl, Br}$, have been recently reevaluated as quasi-2D vdW materials with a surprising variety of structural and electronic properties, from both fundamental as well as applied point of view. In our systematic study, we compare MOX compositions with various electron configurations and different halides in order to pinpoint effects of electron-electron and electron-phonon interactions effecting the dynamic lattice properties. For this instance, we performed synthesis, structure refinement, Raman scattering, and lattice dynamic and band structure calculations. We present systematic as well as specific dependencies of the optical phonon frequencies on lattice parameters of individual metal cations. Most noticeable are rather anisotropic anharmonicities, i.e. phonon softenings and line-width anomalies, for those displacements that concern out-of-plane M-O vibrations.

Acknowledgments

Work supported by DFG GrK 1952/2, Metrology for Complex Nanosystems—NanoMet, and DFG EXC-2123 QuantumFrontiers - 390837967.

Intercalation chemistry of excitonic insulator candidate Ta_2NiSe_5

P54

P. A. Hyde^{1*}, J. Cen², S. J. Cassidy¹, N. H. Rees¹, P. Holdship³, R. I. Smith⁴, D. O. Scanlon², S. J. Clarke¹

^a Department of Chemistry, University of Oxford, Inorganic Chemistry Laboratory, 5 Parks Road, Oxford, OX1 3QR, UK;

^b Department of Chemistry, University College London, 20 Gordon Street, London, WC1H 0AJ, UK;

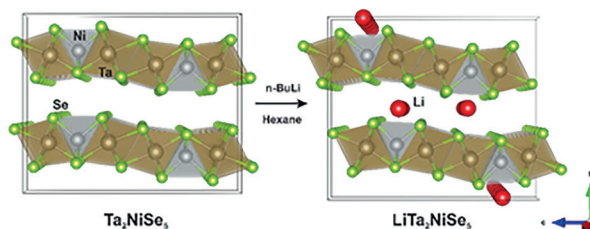
^c Department of Earth Sciences, University of Oxford, South Parks Road, Oxford, OX1 3AN, UK;

^d ISIS Facility, Rutherford Appleton Laboratory, Chilton, Didcot, Oxon, OX11 0QX, UK

* The corresponding author email: penny.hyde@chem.ox.ac.uk

Keywords: intercalation; excitonic insulator; Ta_2NiSe_5 ; narrow band-gap semiconductor; layered chalcogenides

A new reduced phase derived from the excitonic insulator candidate Ta_2NiSe_5 has been successfully synthesised via the intercalation of lithium. $\text{LiTa}_2\text{NiSe}_5$ crystallises in orthorhombic space group $Pmnb$ (No. 62) with lattice parameters $a = 3.50247(3)$ Å, $b = 13.4053(4)$ Å, $c = 15.7396(2)$ Å, $Z = 4$, with an increase of unit cell volume by 5.44(1)% compared to Ta_2NiSe_5 . Significant rearrangement of the Ta-Ni-Se layers is observed, in particular a very significant relative displacement of the layers compared to the parent phase.



Neutron diffraction experiments and computational analysis confirm Li occupies a distorted triangular prismatic site formed by Se atoms of adjacent Ta_2NiSe_5 layers with an average Li-Se bond length of 2.724(2) Å. Intercalation suppresses the distortion to monoclinic symmetry that occurs in Ta_2NiSe_5 at 328 K, which is believed to be driven by the formation of an excitonic insulating state. Magnetometry data shows that the reduced phase has a smaller diamagnetic susceptibility than Ta_2NiSe_5 , due to the enhancement of the temperature independent Pauli paramagnetism. This is consistent with an increased density of states at the Fermi level caused by the injection of electrons during intercalation.

References

- [1] S. A. Sunshine, J. A. Ibers, *Inorg. Chem.* **24**, 3611–3614 (1985)
- [2] F. J. Di Salvo, *et al.*, *J. Less-Common Met.*, **116**, 51-61 (1986)

Acknowledgments

We thank: the UK EPSRC (EP/T027991/1, EP/R042594/1) and the Leverhulme Trust (RPG-2018-377) for funding; the ISIS pulsed neutron and muon source (RB1990078), and the Diamond Light Source Ltd (EE18786 and CY25166) for the award of beam time.

Functionalisation of $\text{CaAl}_2\text{O}_4:\text{Eu}^{2+}, \text{Nd}^{3+}$ phosphors with Fe_3O_4 magnetic nanoparticles

S. T. Tsantis¹, G. Kastrinaki², V. Zaspalis^{2,3}, C. Sarafidis⁴, C. Chatzidoukas³, S. N. Yannopoulos^{1,*}

¹ FORTH-ICE/HT, Stadiou Str. Platani Achaïas, Rio-Patras, Greece;

² LIM, CERTH, 57001, Thessaloniki;

³ Department of Chemical Engineering, Aristotle University of Thessaloniki, 54124, Thessaloniki;

⁴ Department of Physics, Aristotle University of Thessaloniki, 54124, Thessaloniki

* The corresponding author e-mail: sny@iceht.forth.gr

Keywords: long persistent luminescent materials; calcium aluminate doped phosphors; Eu^{2+} emission; magnetic nanoparticles

Long persistent luminescent materials can store energy in excited states after proper illumination and release slowly this energy by emitting at a different wavelength for long time after ceasing excitation [1]. While persistent luminescent materials (PLM) are known for centuries, a breakthrough advance in the field took place in mid-1990s, when co-doping of $\text{SrAl}_2\text{O}_4:\text{Eu}^{2+}$ with Dy^{3+} not only gave rise to increased brightness but also led to prolonged afterglow duration [2]. Among the most studied PLMs are those that belong to the inorganic matrix family MAl_2O_4 ($\text{M} = \text{Ca}, \text{Sr}$) doped with rare earths ions. Crystals of this family doped with Eu^{2+} are phosphors exhibiting strong broad band emission characteristic to the Eu^{2+} ion in the blue/green visible range under UV-excitation (~ 365 nm). For $\text{CaAl}_2\text{O}_4:\text{Eu}^{2+}$ the emission band centered at 440 arises from transitions between the $^8\text{S}_{7/2}$ ($4f^7$) ground state and the crystal field components of the excited $4f^65d^1$ configuration of the Eu^{2+} ion. Such materials find applications in toy decoration, road marking and signage, safety and bio-imaging and so on [1]. However, more challenging applications that pertain to the usage of a light source into liquid media, for example in photodynamic therapy, demand multifunctionality. The materials need to possess not only proper luminescence properties (duration, emission wavelength etc.) but also bear hard magnetism in order to be easily manipulated in liquid media.

In this work we report the successful functionalisation of $\text{CaAl}_2\text{O}_4:\text{Eu}^{2+}, \text{Nd}^{3+}$ (CAO) persistent phosphor with Fe_3O_4 magnetic nanoparticles (MNPs) and the study of the optical properties (luminescence, afterglow) of the composite material. Various extents of loading of Fe_3O_4 MNPs were explored and their optical properties were evaluated. Our preliminary results show that the ratio of CAO/ Fe_3O_4 plays important role in the afterglow and decay time of the composite compound but the optical behavior (emission, afterglow) of $\text{CaAl}_2\text{O}_4:\text{Eu}^{2+}, \text{Nd}^{3+}@ \text{Fe}_3\text{O}_4$ is highly retained.

References

- [1] D. Poleman, D. Van der Heggen, E. Cosaert, P. F. Smet, *J. Appl. Phys.* **128**, 240903 (2020).
 [2] T. Matsuzawa, Y. Aoki, N. Takeuchi, Y. Murayama, *J. Electroch. Soc.* **143**, 2670 (1996).

Acknowledgments

This research has been co-financed by the European Union and Greek national funds through the Operational Program Competitiveness, Entrepreneurship and Innovation, under the call RESEARCH-CREATE-INNOVATE (project code: T2EDK-02279 “Human nutrition, animal and fish feeding on microalgae derived products through sustainable photosynthetic autotrophic cultures”).

Transition metal doping strategy for the reversible anion redox process

P56

A. Wang¹, Z. Chen¹, M. Hayward¹

¹ Department of Chemistry, University of Oxford, Inorganic Chemistry Laboratory, OX1 3QR

* The corresponding author e-mail: anni.wang@chem.ox.ac.uk

Keywords: anion redox; Li-ion cathode materials; topochemical reaction; electrochemistry; crystal structure

The increasing dependence on lithium-ion batteries for energy storage calls for continual improvements in the performance of cathode materials, the majority of which rely solely on cationic redox of transition-metal ions for driving the electrochemical reactions. But recently, anionic redox has been placed as great hope as it leads to a near-doubling of capacity [1]. Thus, efficiently utilizing such process have been a new research hotspot.

Previous work has proved that $\text{Li}_2\text{TiTeO}_6$ [2] could chemically intercalate and deintercalate lithium ions. Considering both Ti and Te are at their highest oxidation state, which should strongly disfavour further oxidation, the redox reaction should actually arise from oxygen in the system. But such oxygen redox is irreversible in electrochemical processes, due to the sluggish kinetics and unstable intermediates. Based on this, transition metals with various oxidation states has been introduced into the $\text{Li}_2\text{TiTeO}_6$ structure, aiming to regulate the charge transfer of oxygen, finally stabilizing the anion redox process and achieving reversible electrochemistry behaviour. Until now $\text{Li}_2\text{Ti}_{(1-x)}\text{Mn}_x\text{TeO}_6$ samples have been prepared and chemically and electrochemically lithiated and delithiated. The structure evolution, different oxygen oxidation states and the effect of Mn doping have been monitored and analysed via XRD, SXRD, O K-edge (XAS), and titration measurements.

References

- [1] R. A. House et al., *Nat Energy*. **6**, 781–789 (2021)
- [2] J. Choynet et al., *Journal of Solid State Chemistry*. **82.2**, 272–278 (1989)

Acknowledgments

This work was supported by the FutureCat project (The Faraday Institution) and the Clarendon fund scholarship.

Part VI

LIST OF PARTICIPANTS

18th European
Conference
on Solid State
Chemistry

A

Adam Jean-Luc	CNRS-Université Rennes, France
Albert Barbara	University of Duisburg-Essen, Germany
Amano Patino Midori	CNRS - DR13, Montpellier, France
Ambach Sebastian	University of Munich, Germany
Arevalo-Lopez Angel M.	CNRS-SCTD, Vandoeuvre-Les-Nancy, France
Arnold Donna	University of Kent, Canterbury, United Kingdom
Attfield John Paul	University of Edinburgh, United Kingdom
Aymans Lea Katharina	University of Bonn, Germany

B

Badea Desiree	University of Cologne, Germany
Balestra Manuele	University of Geneva, Switzerland
Benincasa Louise	ICMCB/CNRS, Bordeaux, France
Bocarsly Joshua	University of Cambridge, United Kingdom
Bonnin Maxime	Karlsruher Institute of Technology, Germany
Borysova Kateryna	Justus Liebig University Giessen, Germany
Bouška Marek	University of Pardubice, Czechia
Bouzek Karel	University of Chemistry and Technology, Prague, Czechia
Bouzková Darina	CONCREA, s.r.o., Kladno, Czechia
Branda Snježana	University of Zagreb, Croatia
Brown Alex	University of Sydney, Australia
Bruns Jörn	University of Cologne, Germany
Burg Ofer	Hebrew University of Jerusalem, Israel

C

Chau Thanh Giang	University of Munich, Germany
Chavhan Madhav Prabhakar	University of Ostrava, Czechia
Chen Zizhen	University of Oxford, United Kingdom
Cheong Jun Young	University of Bayreuth, Germany
Clark Lucy	University of Birmingham, United Kingdom
Clarke Simon	University of Oxford, United Kingdom
Clemens Oliver	University of Stuttgart, Germany
Cohen Carmel	Hebrew University of Jerusalem, Rishon Lezion, Israel
Cordoncillo Eloísa	Jaume I University, Castelló de la Plana, Spain

D

Djafri Elias	University of Kent, Canterbury, United Kingdom
Doert Thomas	Technical University Dresden, Germany
Dong Bo	University of Birmingham, United Kingdom
Dragomir Mirela	Jožef Stefan Institute, Ljubljana, Slovenia

E

Eickmeier Katharina	RWTH Aachen University, Germany
---------------------	---------------------------------

F

Feldmann Claus	Karlsruhe Institute of Technology, Germany
Frøen Emil	University of Oslo, Norway
Früchticht Svenja	University Bonn, Germany
Fuertes Amparo	Institute of Materials Science of Barcelona, Spain

G

Ganin Alexey	University of Glasgow, United Kingdom
Garcia-Alvarado Flaviano	Universidad CEU San Pablo, Madrid, Spain
García-González Ester	Complutense University, Madrid, Spain
García-Martín Susana	Complutense University, Madrid, Spain
Gaudin Etienne	CNRS, ICMCB UMR5026, Pessac, France
Gawryluk Dariusz Jakub	Paul Scherrer Institut, Villigen, Switzerland
Gillette Alexis	University of Oxford, United Kingdom
Giri Souvik	University of Oxford, United Kingdom
Glaum Robert	Rheinische-Friedrich-Wilhelms-Universität, Bonn, Germany
Green Alex	University of Birmingham, United Kingdom
Gregory Duncan	University of Glasgow, United Kingdom
Guignard Marie	Institute of Condensed Matter Chemistry, Pessac, France
Guiot Florentine	Institut des Sciences chimiques de Rennes, France

H

Hadermann Joke	University of Antwerp, Belgium
Hajizadeh Amirhossein	University of Antwerp, Belgium
Hari Krishna	University of Limerick, Ireland
Hartmann Thomas	STOE & Cie GmbH, Darmstadt, Germany
Helmer Fjellvag	University of Oslo, Norway
Hessevik Julie	University of Oslo, Norway
Hitchings Thomas	University of Kent, Canterbury, United Kingdom
Hoch Constantin	Ludwig-Maximilians-Universität München, Germany
Honč Jiří	Tescan Orsay Holding, a.s., Czechia
Höppe Henning	University of Augsburg, Germany
Horák Jakub	Měřicí technika Morava s. r. o., Czechia
Hrabovsky Jan	Charles University, Prague, Czechia
Hrbek Tomáš	Charles University, Prague, Czechia
Hyde Penny	University of Oxford, United Kingdom

I

Injac Sean	University of Edinburgh, United Kingdom
Isobe Masahiko	Max Planck Institute for Solid State Research, Stuttgart, Germany

J

Jambor Roman	University of Pardubice, Czechia
Janek Jürgen	Justus-Liebig University Giessen, Germany
Janesch Melissa	University of Regensburg, Germany
Ji Kunlang	University of Edinburgh, United Kingdom
Jiang Jianwen	National University of Singapore, Singapore
Johrendt Dirk	Ludwig-Maximilians-Universität München, Germany
Jones Robert	Forschungszentrum Jülich, Germany
Jung Felix	Karlsruhe Institute of Technology, Germany
Jung Hyun Young	Gyeongsang National University, Jinju, South Korea

K

Kalazić Ana	University of Zagreb, Croatia
Kanazawa Yuzuki	Tohoku University, Sendai, Japan
Kano Junya	Tohoku University, Sendai, Japan
Kanie Kiyoshi,	Tohoku University, Japan

Karppinen Maarit	Aalto University, Espoo, Finland
Kelly Nicola	University of Oxford, United Kingdom
Khalakhan Ivan	Charles University, Prague, Czechia
Kim Jinsoo	Kyung Hee University, Yongin-si, South Korea
Klásterecký Michal	Tescan Orsay Holding, a.s., Czechia
Kochetkova Ekaterina	Leibniz IFW Dresden, Germany
Krach Georg	Ludwig-Maximilians-Universität München, Germany
Kraut Daniel	Ludwig-Maximilians-Universität München, Germany
Kubíčková Lenka	Johannes Gutenberg University Mainz, Germany
Kuhn Alois	Universidad CEU San Pablo, Madrid, Spain
Kumari Geetu	University of Limerick, Ireland
Kůš Peter	Charles University, Prague, Czechia

L

Lee Jet-Sing	Nature Portfolio, United Kingdom
Lemmens Peter	Technische Universität Braunschweig, Germany
Lemos Samantha	Jaume I University, Castellón de la Plana, Spain
Li Qiang	University of Science and Technology Beijing, China
Ling Chris	University of Sydney, Australia
Lonkar Sunil	Technology Innovation Institute, Abu Dhabi, United Arab Emirates
Lonsdale James	University of Kent, Canterbury, United Kingdom
Lopez Paz Sara	University of Geneva, Switzerland
Louhibi Hamza	Sidi Mohamed Ben Abdellah University, Fez, Morocco

M

Mahato Suraj	University of Oxford, United Kingdom
Maignan Antoine	CNRS, Caen, France
Marvan Petr	Malvern Panalytical B. V. Branch, Prague, Czechia
Matvija Peter	Charles University, Prague, Czechia
Maxeiner Moritz	Justus Liebig University Giessen, Germany
Mclaughlin Abbie	University of Aberdeen, United Kingdom
Mentré Olivier	CNRS-UCCS, Villeneuve d'Ascq, France
Meyer Thomas	CEA Grenoble, France
Milton Michael	University of Edinburgh, United Kingdom
Möller Angela	Johannes Gutenberg-University Mainz, Germany
Müller-Buschbaum Klaus	Justus-Liebig University Giessen, Germany
Mumba Mpanga Eunice	Institut Charles Gerhardt Montpellier, France
Muramatsu Atsushi	Tohoku University, Sendai, Japan
Murase Kimitoshi	Shibaura Institute of technology, Machida, Japan
Müssig Stephan	Friedrich-Alexander-Universität Erlangen-Nürnberg, Germany
Mustonen Otto	University of Birmingham, United Kingdom

N

Naghadian Moghaddam Parisa	FunGlass – Centre for Functional and Surface Functionalized Glass, Trenčín, Slovakia
Nénerth Gwilherm	Malvern Panalytical, Almelo, Netherlands
Netolický Tomáš	University of Pardubice, Czechia
Neziraj Teuta	Max Planck Institute for Chemical Physics of Solids, Dresden, Germany
Nimoh Hicham	Rheinische Friedrich-Wilhelms Universität Bonn, Germany
Novák Miroslav	University of Pardubice, Czechia

O

Orava Jiří	J. E. Purkyně University, Ústí nad Labem, Czechia
Oró Judith	ICMAB-CSIC, Bellaterra, Spain
Orolín Jakub	Měřicí technika Morava s. r. o., Zastávka, Czechia
Ovchinnikov Alexander	Technical University Dresden, Germany

P

Palacin M. Rosa	ICMAB-CSIC, Bellaterra, Spain
Perween Shama	University of Stuttgart, Stuttgart, Germany
Petrik Marek	Philipps University of Marburg, Germany
Plokhikh Igor	Paul Scherrer Institute, Villigen, Switzerland
Portehault David	CNRS-Sorbonne Université, Paris, France
Powell Anthony	University of Reading, United Kingdom

R

Rahimi Sepideh	University of Antwerp, Belgium
Rasche Bertold	University of Cologne, Germany
Raycha Yash	University of Pardubice, Czechia
Rodriguez Pereira Jhonatan	University of Pardubice, Czechia
Rojas-Hernandez Rocio E	Tallinn University of Technology, Estonia
Ruck Michael	Technical University Dresden, Germany
Ruiz de Larramendi Idoia	Universidad del País Vasco, Leioa, Spain
Ryan Tara	University of Limerick, Ireland

S

Sahlberg Martin	Uppsala University, Sweden
Sammoury Ali	Université du Littoral Côte d'Opale, Dunkerque, France
Samsonova Ekaterina	University of Pardubice, Czechia
Sannes Johnny	University of Oslo, Norway
Sarkar Antara	University of Stuttgart, Germany
Sayed Farheen	University of Cambridge, United Kingdom
Sederholm Linda	Aalto University, Vanda, Finland
Sedláčková Leona	CONCREA, s.r.o., Czechia
Sedmidubský David	University of Chemistry and Technology, Prague, Czechia
Serna-Gallén Pablo	Jaume I University, Castellón de la Plana, Spain
Shahzad Anjum	University of Stuttgart, Germany
Shanbhag Dhanush	Laboratoire de Réactivité et Chimie des Solides, Amiens, France
Shtender Vitalii	Uppsala University, Sweden
Schwinghammer Vanessa	University of Regensburg, Germany
Siddiqui Kafeel Ahmad	National Institute of technology Raipur, India
Slater Peter	University of Birmingham, United Kingdom
Smyth Robert	University of Oxford, United Kingdom
Solana-Madruga Elena	Universidad Complutense de Madrid, Spain
Steele Katie	University of Oxford, United Kingdom
Steinberg Simon	RWTH Aachen University, Germany
Střížik Lukáš	University of Pardubice, Czechia
Suský Jakub	University of Pardubice, Czechia
Šibav Lia	Jožef Stefan Institute, Ljubljana, Slovenia

T

Taskesen Ludmila	University of Oxford, United Kingdom
Thakur Gohil	Technical University Dresden, Germany
Tomar Ritu	University of Bonn, Germany
Tron Artur	AIT Austrian Institute of Technology GmbH, Vienna, Austria
Turgunbajew Erich	University of Augsburg, Germany

V

Vaidya Shefali	Czech Technical University in Prague, Czechia
Valldor Martin	University of Oslo, Norway
Vlček Miroslav	University of Pardubice, Czechia
von Rohr Fabian	University of Geneva, Switzerland
Vorokhta Mykhailo	Charles University, Prague, Czechia
Vradman Leonid	NRCN, Israel
Vrazel Martin	University of Pardubice, Czechia

W

Wagner Tomas	University of Pardubice, Czechia
Wagnerova Valerie	University of Pardubice, Czechia
Wang Anni	University of Oxford, United Kingdom
Wang Yuanshen	University of Glasgow, United Kingdom
Weber Anna Katharina	Johannes Gutenberg-University Mainz, Germany
Wessels Vivien	University of Augsburg, Germany

X

Xie Xianxian	Charles University, Prague, Czechia
Xing Xianran	University of Science and Technology Beijing, China

Y

Yamamoto Ayako	Shibaura Institute of Technology, Saitama, Japan
Yannopoulos Spyros	FORTH/ICE-HT and University of Patras, Greece
Yörük Emre	Institute of Physics of the Czech Academy of Science, Prague, Czechia
Yoshida Akari	Tohoku University, Sendai, Japan

Z

Zaytseva Irina	University of Munich, Germany
Zupancic Maja	Technobis Crystallization Systems, Alkmaar, Netherlands
zur Loye Hans-Conrad	University of South Carolina, Columbia, USA

Part VII

AUTHOR INDEX

18th European
Conference
on Solid State
Chemistry

A			
Adam, Jean-Luc	IL 07	Blacque, Olivier	P 27
Adler, Peter	L 83	Blandy, Jack	P 43
Aicher, Julian	L 70	Bocarsly, Joshua	L 56
Alabd, Khaled	L 50	Bokova, Maria	P 19
Albiss, Borhan	P 37	Bonnin, Maxime	P 47
Allan, Phoebe	L 21	Booth, Samuel	L 23
Allen, David	L 01	Bordet, Pierre	L 37
Allison, Morgan	L 14	Borysova, K.	P 11
Amano, Patino Midori	IL 11	Boukerma, Kada	L 75
Ambach, Sebastian	P 50	Boussard-Pledel, Catherine	IL 07
Amoroso, Jake	L 57	Bouška, Marek	P 12, P 42
Andres, Juan	L 67, L 86	Bouzek, Karel	IL 03
Aoki, Takeshi	L 64	Bozey, Ayat	P 37
Arcon, Denis	L 30	Brand, Helen	L 39
Arevalo-Lopez, Angel	L 29, L 42	Branda, Snježana	P 25
Arnold, Donna	L 46, L 53, L 71	Bräuninger, Sascha	L 14
Arthur, Haffner	L 70	Brázda, Petr	L 48
Assis, Marcelo	L 67	Bredow, Thomas	L 45
Atanov, Omargeldi	P 27	Brnada, Snjezana	P 20
Attfield, Paul	L 06, L 77	Brown, Alex	L 39
Autran, Pierre-Olivier	IL 14	Bruns, Jörn	L 79, P 01
Auvergniot, Jeremie	P 34	Budáč, Daniel	IL 03
Avdeev, Max	L 39, L 80	Buchner, Gwendolyn	L 69
Aymans, Lea Katharina	P 14	Büchner, Bernd	L 14
B		Bures, Filip	L 47
Badea, Desiree	P 01	Burg, Ofer	P 38
Baillieul, Marion	L 75	Busa, Chiara	L 16
Baker, Peter	L 27	Büscher, Florian	P 53
Balestra, Manuele	P 27	By, Thomas	L 84
Bardet, Michel	L 07	Bychkov, Eugene	P 19
Barnett, Chris	L 80	C	
Baron, Marzena	IL 14	Cabaj, Malgorzata Katarzyna	L 48
Basa, Anna	L 25	Cairns, Andrew	L 01
Batuk, Maria	PL 05	Can, Fabien	L 50
Beecham - Lonsdale, James	L 46	Cano, Andrés	L 29
Bein, Thomas	P 51	Carda, Michal	IL 03
Belak, Vivod Matic	L 13	Carlsen, Cathinka Scheele	L 84
Beltrán-Mir, H.	L 86	Casas-Cabanas, Montserrat	P 21
Beneš, Ludvík	L 34, L 78	Casati, Nicola	L 15
Benincasa, Louise	L 73	Cassidy, Simon	L 63, P 43, P 54
Berinskat, Stefanie	P 53	Castells-Gil, Javier	L 21
Berthelot, Romain	L 61	Castro, Laurent	L 24
Besmann, Theodore	L 57	Cen, Jiayi	P 54
Beutl, Alexander	L 05	Ceretti, Monica	IL 11
Bhattacharya, Suman	P 15	Cervellino, Antonio	L 15
Bion, Nicolas	L 50	Chang, Joon Ha	IL 10
Black, Ashley	P 21	Charrier, Joel	L 75
		Charvot, Jaroslav	L 47

Chau, Thanh	P 51	Driscoll, Laura	L 21
Chavhan, Madhav P.	L 09	Drnec, Jakub	IL 15, L 22
Chen, Yuqi	L 10	Duarte, Angelica	L 25
Chen, Zizhen	P 09, P 56	Duttine, Mathieu	L 73
Cheong, Jun Young	IL 10	Dutton, Siân	L 56
Cibin, Giannantonio	L 63		
Clark, Lucy	IL 04	E	
Clarke, Simon	L 63, L 76, P 26, P 43, P 44, P 45, P 54	Ebert, Hubert	P 51
		Eisenburger, Lucien	P 50
Claus, Feldmann	L 74	Ejaz, Ammara	L 68
Colin, Claire	L 58	Eltoukhy, Samar	P 52
Cordoncillo, Eloisa	L 67, L 86	Emge, Steffen	L 44
Corredor, Laura Teresa	L 28	Evans, Ivanna	L 39
Courson, Rémi	L 75		
Courtois, Xavier	L 50	F	
Croisé, Charlotte	L 50	Fan, Zeyu	L 37
Cussen, Edmund	L 27	Fateeva, Alexandra	L 37
Černošková, Eva	L 32	Feldl, Sofia	L 81
		Feldmann, Claus	P 47, P 49
D		Fernandez Lozano, Jose F	L 40
Daniel, Kraut	P 05	Fidalgo-Marijuan, Arkaitz	P 29
de Boer, Tristan	P 50	Fjellvåg, Øystein	L 82
De Irujo Labalde, Xabier Martinez	L 23	Fjellvåg, Asbjørn Slagtern	L 84
de Rolland Dalon, Edouard	IL 14	Fjellvåg, Helmer	L 84
De Vito, Eric	L 07	Forsberg, Kerstin	L 58
Deason, Travis	L 57	Frederich, Nadia	IL 11
Defoy, Emile	IL 14	Frøen, Emil	L 83
Delmas, Claude	L 24	Frontera, Carlos	P 21
Demessence, Aude	L 37	Früchtnicht, Svenja	P 03
Denis Romero, Fabio	L 80	Frumarová, Božena	L 34, L 78
Denisova, Ksenia	P 46	Fuertes, Amparo	PL 06
Desevedavy, Frederic	L 36		
Dey, Sunita	L 44, L 63	G	
Dhairat, Joman	P 37	Galvão, Yara	L 67
Diaz-Carrasco, Pilar	L 25, P 36	Ganin, Alexey	L 17, P 33
Díez-Gómez, Virginia	L 26	Garcia Nunez, Carlos	L 68
Ding, Lei	L 58	Garcia-Alvarado, Flaviano	L 25, L 26, P 35, P 36
Dinhová, Thu Ngan	IL 02, IL 09	García-González, Ester	P 35
DiPrete, David	L 57	García-Martín, Susana	L 02
Dirk, Johrendt	L 70	Gärtner, Stefanie	P 02, P 07
Djafari, Elias	L 71	Gaudin, Etienne	L 50
Dluhoš, Jiří	L 65	Gawryluk, Dariusz Jakub	L 54
Doert, Thomas	L 72, P 16	Gázquez, Jaume	P 21
Domen, Kazunari	L 59	Gholam, Saleh	PL 05
Dong, Bo	L 21	Ghoridi, Anissa	IL 14
Dorcet, Vincent	L 35	Gibbs, Alexandra	L 27
Dragomir, Mirela	L 13, L 30	Gibson, Des	L 68
Driscoll, Elizabeth	L 18, P 32	Gillette, Alexis	P 44
		Giri, Souvik	L 63
		Glaum, Robert	L 29, P 03, P 14

Gnezdilov, Vladimir	P 53	Inosov, Dmytro	P 52
Goikolea, Eider	P 29	Isaeva, Anna	L 28
Gomes, E. O.	L 86	Ismail, Raïssa	L 75
Gonano, Bruno	L 82	Isobe, Masahiko	L 12
Gouveia, Amanda	L 67	Iveland, Oskar	L 84
Gracia, Lourdes	L 67, L 86		
Green, Alex	L 18, P 32	J	
Gregory, Duncan	PL 03	Jacquet, Quentin	L 44
Grey, Clare	L 44, L 56, L 63	Jagličić, Zvonko	L 13, L 30
Grin, Yuri	P 13	Jambor, Roman	P 12, P 41, P 42
Grinenko, Vadim	P 52	Janek, Jürgen	PL 02
Groszewicz, Pedro	L 44	Janesch, Melissa	P 07
Guerin, Sarah	P 15, P 22	Ji, Kunlang	L 77
Guguchia, Zurab	L 15	Jiang, Jianwen	PL 01
Guignard, Marie	L 24, L 73	Jones, Robert O.	PL 04
Guilmeau, Emmanuel	L 35	Jung, Hyun Young	P 28
Guiot, Florentine	L 35	Jung, Felix	P 49
Guselnikova, Olga	L 17		
Gutel, Thibaut	L 07	K	
		Kaban, Ivan	L 38
H		Kalazic, Ana	P 20, P 25
Hadermann, Joke	PL 05, P 23, P 24	Kalendová, Andréa	P 17
Hajizadeh, Amirhossein	PL 05, P 23, P 24	Kanazawa, Yuzuki	L 59
Hamieh, Tayssir	P 19	Kanie, Kiyoshi	L 59, L 60, P 18
Hämmer, Matthias	L 69	Kano, Junya	L 51
Han, Dan	P 51	Kaper, Helena	IL 11
Hansen, Thomas	P 16	Karppinen, Maarit	IL 01, L 04
Hari, Krishna	P 15	Kasper, Thomas	P 40
Hayward, Michael	L 23, P 09, P 30, P 56	Kassem, Mohamad	P 19
Herrmannsdoerfer, Thomas	P 16	Kawamata, Toru	L 03
Hessevik, Julie	L 84	Kelly, Nicola	L 76
Hines, Adrian	L 57	Kendrick, Emma	L 21
Hitchings, Thomas	L 01	Kennedy, Brendan	L 80
Hoelzel, Markus	L 26	Khadiev, Azat	L 72
Hoch, Constantin	L 81, P 05, P 06	Khalakhan, Ivan	IL 05
Holdship, Philip	P 54	Khalyavin, Dmitry	L 42
Honč, Jiří	L 65	Kim, Jinsoo	P 31
Höppe, Henning	L 69	King, Graham	L 13, L 30
Horák, Jakub	L 49	Klauss, Hans-Henning	L 14
Horiike, Satoshi	L 37	Knotek, Petr	L 32
Hornfeck, Wolfgang	L 08	Kny, Anna	L 45
Hrabovsky, Jan	L 36, L 64	Kobayashi, Hiroki	L 60
Hrbek, Tomáš	IL 15, L 22	Koblar, Maja	L 30
Hussainova, Irina	L 40	Kocer, Can	L 44
Hyde, Penny	P 54	Kohl, Miroslav	P 17
		Kochetkova, Ekaterina	L 28
I		Krach, Georg	P 48
Ibrahim, Maya	IL 11	Kubičková, Lenka	L 85
Igoa Saldaña, Fernando	IL 14	Kuhn, Alois	L 25, L 26, P 36
Injac, Sean	L 80	Kumar, Susmit	L 82

Kushimoto, Kizuku	L 51	McPhillips, Holly	L 53
Kúš, Peter	IL 15, L 22	Menéndez, Nieves	P 36
Kutálek, Petr	L 32	Mentré, Olivier	L 29, L 33, L 42, L 71
L			
Lahmar, Abdelilah	P 04	Meyer, Thomas	L 07
Lanceros-Mendez, Senentxu	P 29	Mikhalyova, E. A.	P 11
Lawrence, Gaynor	L 41	Milasheuskaya, Yaraslava	P 42
Lefèvre, Robin	P 27	Miloš, Vojtěch	IL 03
Lemmens, Peter	P 46, P 53	Milton, Michael	L 06
Lemoine, Pierric	L 35	Mirandona-Olaeta, Alexander	P 29
Lemos, Samantha	L 67, L 86	Mirolo, Marta	IL 15, L 22
Li, Qiang	L 66, P 39	Moewes, Alexander	P 50
Lima, Renata	L 67	Möller, Angela	L 85, P 46, P 53
Ling, Chris	L 14, L 39	Mori, Atsunori	P 18
Liu, Shuai	P 43	Morpurgo, Alberto F.	L 15
Longo, Elson	L 67	Morris, Andrew	L 44
Lonkar, Sunil	L 16	Morrow, Ryan	P 52
Lopez, Nuria	L 17	Mullens, Bryce	L 80
López-Paz, Sara A.	L 15	Müller-Buschbaum, Klaus	L 52, P 11, P 40
Lortz, Rolf	P 27	Mumba Mpanga, Eunice	L 61
Loulergue, Patrick	L 75	Muramatsu, Atsushi	L 59, L 60, P 18
Lozinšek, Matic	L 13	Murase, Kimitoshi	L 03, P 08
Lu, Ziyu	P 43	Müssig, Stephan	L 19
Luetkens, Hubertus	L 15	Mustonen, Otto	L 27
M			
Macak, Jan	L 47	Naghadian Moghaddam, Parisa	P 10
Magusin, Pieter	L 44	Nazabal, Virginie	L 75
Mahato, Suraj	L 23, P 09, P 30	Nedumkulam, Hridya	IL 15, L 22
Maki, Sachiko	L 60	Němec, Petr	L 75, P 42
Malaman, Bernard	L 35	Nénert, Gwilherm	L 58
Mandel, Karl	L 19	Netolicky, Tomas	L 78
Mangin-Thro, Lucile	L 27	Netzsch, Philip	L 69
Manjón-Sanz, Alicia	L 39	Neumann, Iuliiia	L 10
Manuel, Pascal	L 06, P 43	Neziraj, Teuta	P 13
Manzanarez, Hervé	L 07	Ng, Yat Hei	P 27
Marín-Gamero, Rafael	L 02	Nilsen, Ola	L 82
Martens, Isaac	IL 15	Nimoh, Hicham	L 29
Martínez de Irujo-Labalde, Xabier	L 02, P 09, P 30	Ninomiya, Kakeru	L 60
Masquelier, Christian	P 34	Nishibori, Maiko	L 60
Matolín, Vladimír	L 22	Novák, Miroslav	P 12, P 41
Matolínová, Iva	IL 02, IL 09, IL 15, L 22	Nowak, Lukas	L 36
Matsubara, Masaki	L 59, L 60, P 18	Nozawa, Ryosuke	P 18
Matvija, Peter	IL 02, IL 09	Nusser, Lukas	L 81
Maxeiner, Moritz	P 40	O	
Mcgrady, John	P 43	O'Keefe, Chris	L 44
Mclaughlin, Abbie	L 41	Onykienko, Yevhen	P 52
		Orava, Jiri	L 38
		Oró-Solé, Judith	P 21

Osmic, Ena	P 16	Rodriguez Pereira, Jhonatan	L 47
Osuga, Ryota	L 59, L 60	Rojas-Hernandez, Rocio E	L 40
Oswald, Jiri	L 36, L 78	Rubio-Marcos, Fernando	L 40
Otoničar, Mojca	L 30	Ruck, Michael	L 20, L 62, L 72, P 16
Oveysipoor, Shiva	IL 02	Rudel, Stefan	P 51
Ovchinnikov, Alexander	L 20	Ruiz de Larramendi, Idoia	P 29
P		Ryan, Tara	P 22
Paidar, Martin	IL 03	S	
Pakseresht, Amirhossein	P 10	Sahlberg, Martin	IL 12
Palacín, M. Rosa	P 21	Sahoo, Manaswini	L 28
Palatinus, Lukas	L 48	Saïbi, Valentin	L 24
Panthöfer, Martin	L 85	Saines, Paul	L 01
Parchovianská, Ivana	P 10	Sakagami, Yuma	P 18
Parchovianský, Milan	P 10	Sammoury, Ali	P 19
Pashkevich, Yurii	P 53	Samsonova, Ekaterina	L 32
Patino, Midori	L 77	Sannes, Johnny	L 82
Paulus, Werner	IL 11	Sanz, Jesús	L 26
Pérez-Flores, Juan Carlos	L 26	Sasaki, Shunsuke	L 63
Petrik, Marek	L 08	Sato, Takeru	P 08
Pham, Toan Minh	P 31	Sayed, Farheen	L 44
Pchálek, František	IL 02	Scanlon, David	P 54
Pienack, Nicole	L 72	Sederholm, Linda	L 04
Piliai, Lesia	IL 02, IL 09	Sedykh, Alexander	P 40
Plokhikh, Igor	L 31	Séné, Amandine	IL 14
Podzimek, Štěpán	P 12	Serna-Gallén, Pablo	L 86
Pointner, Monika	P 48	Serrano-Sevillano, Jon	P 21
Pomjakushin, Vladimir Y.	L 15	Seuffert, Marcel	L 52
Poppe, Romy	PL 05	Shanbhag, Dhanush	P 34
Portehault, David	IL 14	Sheath, Bradley	P 44
Powell, Anthony	IL 13	Shenhar, Roy	P 38
Predelli, Fabian	P 53	Shevtsova, Tanya	P 53
Prestipino, Carmelo	L 35	Shimakawa, Yuichi	L 77, L 80
Prokop, Vit	L 64	Shtender, Vitalii	L 55
Pughe, Charlotte	L 27	Schnelle, Walter	P 16
Puphal, Pascal	L 12	Schnick, Wolfgang	P 48, P 50, P 51
Q		Schwarz, Jiří	L 32
Quintelier, Matthias	PL 05	Schwarz, Ulrich	P 13
Qureshi, Navid	P 52	Schweitzer, Thierry	L 35
R		Schwinghammer, Vanessa	P 02
Rahimi, Sepideh	PL 05, P 23, P 24	Siddiqui, Kafeel Ahmad	L 43
Ramos-Perez, Silvia	L 46, L 53	Sihem, Smail-Zemouri	P 04
Rasche, Bertold	L 10	Simpson, Struan	L 41
Raycha, Yash	P 17	Sjåstad, Anja Olafsen	L 84
Rees, Nick	P 54	Skjelstad, Johan	L 84
Reichstein, Jakob	L 19	Slang, Stanislav	L 78
Renier, Olivier	L 28	Slater, Peter	L 18, L 21, P 32
Ribeiro, Lara	L 67	Smektala, Frederic	L 36
Rodríguez, Miquel	L 22		

Smith, Ron	P 54		
Smuda, Matthias	L 72		
Smura, Catherine	P 43		
Smyth, Robert	P 43		
Sobrados, Isabel	L 26		
Söhnel, Tilo	L 14		
Sokolowski, Moritz	L 45		
Solana-Bello, Andrés	P 35		
Solana-Madruga, Elena	IL 08, L 77		
Somers, Cody	P 50		
Song, Yang	IL 14		
Sønsteby, Henrik	L 84		
Sorg, J. R.	P 11		
Srb, Michael	P 41		
Steele, Katherine	P 26		
Strizik, Lukas	L 34, L 36, L 64		
Ströh, Jonas	L 72		
Strub, Erik	P 01		
Sugiyama, Kasumisa	L 03, P 08		
Sugiyama, Issei	L 24		
Suchomel, Matthew	L 73		
Sui, Tan	L65		
Sun, Youyi	L 17		
Sun, Yonghao	L 38		
Suresh, Ashwin	L 48		
Suský, Jakub	L 34		
Svoboda, Roman	L 34		
Szymczyk, Anthony	L 75		
Šamořil, Tomáš	L65		
Šibav, Lia	L 30		
Šlang, Stanislav	L 34		
Šmíd, Břetislav	IL 02		
T			
Taibi, Kamel	P 04		
Takagi, Hidenori	L 12		
Tanaka, Ginpei	L 60		
Taskesen, Ludmila	P 45		
Tencé, Sophie	L 50		
Terraschke, Huayna	L 72		
Thakur, Gohil	P 16		
Thiaudière, Dominique	IL 14		
Tisdale, Hunter	L 57		
Tomar, Ritu	L 45		
Topping, Craig	P 43		
Toufaily, Joumana	P 19		
Troles, Johann	IL 07		
Tron, Artur	L 05		
Turgunbajew, Erich	L 69		
U			
Urones-Garrote, Esteban	L 02		
V			
Vaidya, Shefali	L 37		
Valldor, Martin	L 82, L 83, P 52		
Vandemeulebroucke, Daphne	PL 05		
Veis, Martin	L 36		
Vella, Joseph	L 14		
Veselska, Oleksandra	L 37		
Viallet, Virginie	P 34		
Villesuzanne, Antoine	L 50		
von Rohr, Fabian O.	IL 06, L 15, P 27		
Vorokhta, Mykhailo	IL 02, IL 09		
Vrážel, Martin	L 75		
W			
Waggstaff, Oliver	L 39		
Wágner, Tomáš	L 34, L 36, L 64, L 78		
Walker, cHelen	L 27		
Waller, David	L 84		
Wang, Yuanshen	P 33		
Wang, Anni	P 56		
Weber, Anna Katharina	L 85, P 46		
Weber, Markus	P 03		
Wehner, Tobias	L 52		
Weippert, Valentin	L 70		
Wildman, Eve	L 41		
Wintzheimer, Susanne	L 19		
Wirth, Steffen	P 13		
Witteveen, Catherine	L 15		
Witthaut, Kristian	L 70, P 48		
Wittig, Lea	P 40		
Wolf, Florian	P 51		
Wurmehl, Sabine	L 14		
X			
Xie, Xianxian	L 11		
Xing, Xianran	L 66, P 39		
Y			
Yabushita, Mzuho	L 60		
Yamamoto, Ayako	L 03, L 04, P 08		
Yang, Minjun	L 10		
Yannopoulos, Spyros	P 55		
Yao, XF	L65		
Yaresko, Alexander	L 27		
Yörük, Emre	L 48		
Yoshida, Akari	P 18		
Yuen, Alex	L 80		

Z

Zaytseva, Irina
Zazpe, Raul
Zhadan, Antonii

P 06
L 47
L 37

Zhang, Xiang-Hua
Zhou, Yecheng
Zhu, Pengcheng
zur Loye, Hans-Conrad

IL 07
L 17
L 21
L 57

SUNDAY July 9, 2023		MONDAY July 10, 2023		TUESDAY July 11, 2023		WEDNESDAY July 12, 2023	
		Session I	Session II	Session I	Session II	Session I	Session II
09:00–10:00		PL02 Janek		PL04 Jones		PL06 Fuertes	
		IL03 Bouzek L05 Tron	IL04 Clark L06 Milton	IL07 Adam L32 Samsonova	IL08 Solana-Madruga L33 Mentré	IL12 Sahlberg L57 zur Loye	IL13 Powell L58 Néneret
10:00–11:00		CB	CB	CB	CB	CB	CB
11:00–12:00		L07 Meyer	L12 Isobe	L34 Susky	L39 Bown	L59 Kanazawa	L64 Strizik
		L08 Petrik	L13 Dragomir	L35 Guiot	L40 Rojas-Hernandez	L60 Muramatsu	L65 Honč
		L09 Chavhan	L14 Ling	L36 Hrabovsky	L41 McLaughlin	L61 Mumba-Mipanga	L66 Xing
		L10 Rasche	L15 López-Paz	L37 Vaidya	L42 Arévalo-López	L62 Ruck	L67 Lemos
12:00–13:00		L11 Xie	L16 Lonkar	L38 Orava	L43 Siddiqui	L63 Giri	L68 Ejaz
13:00–14:00		Lunch	Lunch	Lunch	Lunch	Lunch	Lunch
14:00–15:00		PL03 Gregory		PL05 Hadermann		IL14 Portehault	
		IL05 Khaiakhan	IL06 von Rohr	IL09 Vorokhta	IL11 Amamo Patino	L69 Höpfe	IL15 Kus
		L17 Ganin	L19 Müssig	IL10 Cheong	L45 Tomar	L70 Johrendt	L73 Benincasa
		L18 Slatter	L20 Ovchinnikov	L44 Sayed	L46 Beecham-Lonsdale	L71 Djafrí	L74 Feldmann
15:00–16:00		CB	CB	CB	CB	L72 Doert	L75 Vrazel
		L21 Dong	L27 Muustonen	L47 Rodriguez-Pereira	L52 Müller-Buschbaum	L76 Kelly	L76 Kelly
		L22 Hrbek	L28 Kochetkova	L48 Yörük	L53 Arnold	CB	CB
16:00–17:00	Opening	L23 Mahato	L29 Nimoh	L49 Horak	L54 Gawryluk	L77 Ji	L82 Sannes
	PL01 Jiang	L24 Guignard	L30 Šibav	L50 Gaudin	L55 Shtender	L78 Netolicky	L83 Frøen
	IL01 Karpinen	L25 García-Alvarado	L31 Plokhikh	L51 Kano	L56 Bocarsly	L79 Bruns	L84 Hessevik
17:00–18:00	IL02 Matvija	L26 Kuhn				L80 Injac	L85 Kubičková
	Welcome Drink					L81 Hoch	L86 Serna-Gallén
18:00–19:00	L01 Hitchings					Closing Ceremony	
	L02 García-Martín	Poster Session I	Poster Session II				
	L03 Yamamoto						
19:00–20:00	L04 Sederholm						



ECSSC 2023

ISBN 978-80-7560-466-8